

ALMA MATER STUDIORUM · UNIVERSITÀ DI BOLOGNA

Scuola di Scienze
Corso di Laurea Magistrale in Fisica

ENTANGLEMENT ENTROPY IN 1-D QUANTUM SPIN CHAINS

Relatore:
Prof. Francesco Ravanini

Presentata da:
David Palazzo

Correlatori:
Prof.ssa Elisa Ercolessi
Dott. Fabio Franchini

Sessione II
Anno Accademico 2013/2014

Abstract

In questa tesi abbiamo studiato il comportamento delle entropie di Entanglement e dello spettro di Entanglement nel modello XYZ attraverso delle simulazioni numeriche. Le formule per le entropie di Von Neumann e di Renyi nel caso di una catena bipartita infinita esistevano già, ma mancavano ancora dei test numerici dettagliati. Inoltre, rispetto alla formula per l'Entropia di Entanglement di J. Cardy e P. Calabrese per sistemi non critici, tali relazioni presentano delle correzioni che non hanno ancora una spiegazione analitica: i risultati delle simulazioni numeriche ne hanno confermato la presenza. Abbiamo inoltre testato l'ipotesi che lo Schmidt Gap sia proporzionale a uno dei parametri d'ordine della teoria, e infine abbiamo simulato numericamente l'andamento delle Entropie e dello spettro di Entanglement in funzione della lunghezza della catena di spin. Ciò è stato possibile solo introducendo dei campi magnetici "ad hoc" nella catena, con la proprietà che l'andamento delle suddette quantità varia a seconda di come vengono disposti tali campi. Abbiamo quindi discusso i vari risultati ottenuti.

Contents

1	Statistical Mechanics	11
1.1	Towards a field theory	11
1.2	The renormalization group	14
1.2.1	Conformal invariance	18
2	Conformal field theory	21
2.1	Basic hypothesis	21
2.2	Classical Conformal invariance	22
2.2.1	Definition of conformal transformation	22
2.2.2	Global and local conformal transformations	24
2.2.3	The Stress Tensor	27
2.3	Quantum conformal invariance	28
2.3.1	Conformal Ward identity	29
2.3.2	The central charge	31
2.3.3	CFT on a cylinder	32
2.3.4	Correlation functions	34
2.4	Quantization of a CFT	35
2.4.1	Radial quantization	35
2.4.2	The Virasoro algebra	37
2.4.3	The Hilbert space	38
2.4.4	Verma modules and Kac table	40
2.5	CFT on a torus: modular invariance	44
2.6	Out of the critical point	48
2.6.1	Conformal Perturbation Theory	49
2.6.2	The Callan-Symanzik equation	51
2.6.3	Zamolodchikov's c theorem	54
3	Entanglement entropy in 1-D quantum chains	57
3.1	The path integral approach	57
3.1.1	The case of a single interval	59
3.1.2	The case of n disjoint intervals	64
3.2	Entanglement Entropy in a non critical model	64
3.3	Corrections to Entanglement Entropy	66
3.3.1	Corrections to Scaling	67

Contents

3.3.2	Correction for gapped systems	72
3.3.3	Parity effects in gapless spin chains	74
3.4	The Corner Transfer Matrix method	74
3.5	The XYZ model	78
3.5.1	The definition of the model	78
3.5.2	Von Neumann and Renyi entropies	80
3.5.3	The essential critical points	83
3.5.4	Unusual corrections to the entanglement entropy	86
3.6	The entanglement spectrum	89
3.6.1	ES and critical exponents	89
3.6.2	ES for the XY model	91
4	Numerical simulations	95
4.1	Entanglement spectrum for the XYZ model	95
4.2	Check of known results	96
4.3	The Essential critical point	100
4.3.1	Lines of constant l	101
4.3.2	Circles surrounding the essential critical point	105
4.4	Study of the Schmidt gap	107
4.5	Studying the FSS of the entanglement spectrum	111
4.6	Conclusions and outlook	120
A	Entanglement	121
A.1	EPR paradox and Bell inequality	122
A.2	Reduced density matrices	124
A.3	Schmidt decomposition	125
A.4	Information theory and Shannon entropy	126
A.5	Measuring the entanglement	128
A.5.1	The Von Neumann entropy	128
A.5.2	The Renyi entropies	131
B	Corner Transfer Matrix	133
B.1	Definitions	133
B.2	The eight vertex model	138
C	Numerical data	143
C.1	The DMRG algorithm	143
C.1.1	Density-Matrix approach	143
C.1.2	Density-Matrix algorithm	145
C.1.3	The DMRG program	146
C.2	Simulations for constant l	147
C.3	Simulations around the circles	148
	Bibliography	171

Introduction

Entanglement, firstly recognized in 1935 by Schrödinger, is one of the most striking evidence of the quantum behaviour of nature: it represents the fact that parts of a system can influence each other instantaneously. At first sight it seemed that Entanglement was in contrast with Einstein's principle of Relativity, because nothing can move faster than light. But afterwards it was shown that these physical facts are compatible, since two systems can send informations about their status only through channels which involve devices necessarily slower than light.

Much effort has been devoted to a quantitative understanding of Entanglement. For subsystems of pure states, a list of reasonable requirements for a measure of Entanglement led to the definitions of the Von Neumann and the Renyi entropies, which deal with bipartite systems. For mixed states, and for multipartite systems, a satisfactory way to measure Entanglement is still missing.

While, at the beginning, Entanglement was considered as a simple interesting effect arising from the laws of Quantum Mechanics, it is only in the last years that the interest for this phenomenon flourished again, mainly due to Quantum Information. It is believed that an entangled state, such as for Qubits, can be used to store information and to construct logical gates. The amount of information stored by such a quantum system would be potentially infinite, in contrast with the classical way to store memory through bits, and the logical operations between Qubits are expected to work much faster than nowadays computers.

Other important applications of Entanglement arised in General Relativity for the study of black holes, and in Statistical Mechanics. First of all, Von Neumann entropy coincides, for pure systems, with the thermodynamical Entropy of a quantum system. Moreover, Entanglement is related to quantum phase transitions, since it diverges at critical points. A deeper analysis of the Entanglement entropy in the space of parameters reveals further important properties of a quantum system, such as the presence of what are called essential singularities.

In this work we will focus on $1-d$ quantum spin chains. One dimensional quantum systems have been deeply investigated in about the last 70 years, for several reasons. They are strongly interacting (collisions can never be

ignored), and the role of quantum statistics is somehow special: two particles can exchange their position only if they interact. Moreover, most of higher dimensional systems can't still be solved, but nevertheless 1- d quantum chains can give some insights on the behaviour of 3- d analogous systems, such as the Ising model. More recently, Entanglement of 1- d systems at criticality has been connected to the classes of universality of these systems through their central charge, thanks to the use of Conformal Field Theories.

The definition of Von Neumann entropy involves what is called the Entanglement Spectrum (ES), which is the spectra of the reduced density matrix of a subsystem. The ES is also a very important feature, since it is believed that it can describe the thermodynamics of statistical systems. As an example, in [14] is presented the ansatz that the Schmidt Gap (that is the difference between the two largest values of the ES) scales as some order parameter of the theory: this implies that studying the Schmidt gap we should recover the critical exponents of the theory.

In this thesis we focus on the XYZ model. We present in detail the results obtained from numerical simulations performed on this model, for different sizes of the spin chain. Furthermore, we give some analytical results about the Entanglement Spectrum, which are tested numerically. Formulas for the Von Neumann and Renyi entropies already exist in the case of an infinite bipartite system (see [21]) but exhaustive numerical checks of these relations were still lacking. Furthermore, these formulas contain corrections to the Von Neumann entropy, arising near the critical XXZ chain, that are not explained by the corrections described by Cardy, Calabrese and Peschel in [12], obtained using a quantum field approach. Numerical simulations should help to understand if these unusual corrections are indeed present in the model, and eventually a theoretical description of these will be needed. Nonetheless, an analytic description of the entropies, and of the Entanglement Spectrum, for finite size of the system still need to be found.

This thesis has the following structure:

Chapter 1 We justify, in the context of statistical systems at criticality, the use of Lagrangians which are invariant under scale transformations of the coordinates: this leads to the concept of Conformal Field Theories (CFTs). Furthermore, we give a glance at the Renormalization Group, which is at the core for the subdivision of statistical models into classes of universality.

Chapter 2 In the first part we present a summary of Conformal Field Theories. Then we describe field theories which are perturbation of CFTs, thus representing statistical system out of criticality.

Chapter 3 In this chapter we firstly discuss how to compute bipartite entanglement concerning one dimensional statistical models, for both the cases at criticality and out of criticality. An introduction to the concept of Entanglement and how this can be measured is presented in Appendix A. Then we show the "corner transfer matrix" (CTM) method (a definition of CTMs is in Appendix B), which serves to evaluate Von Neumann and Renyi entropies for infinitely large spin chains, splitted in two half-infinite parts. Finally, we present the XYZ model, and a brief discussion on the computation of the Entanglement Spectrum for some selected systems.

Chapter 4 Here we present all the work performed on the XYZ model. First we derive a formula for the Entanglement Spectrum of this model, in the thermodynamical limit. Then we discuss all the numerical simulations performed, concerning Von Neumann entropies and the Entanglement Spectrum, first for infinite systems, and then for finite systems as a function of their size. In Appendix C we report the numerical data, as well as a description of the DMRG algorithm, which is at the basis of the C++ program used to perform the numerical simulations.

Contents

Chapter 1

Statistical Mechanics

This chapter is devoted to a review of some basic concepts about statistical systems at criticality, that is at a second order phase transition.

1.1 Towards a field theory

Suppose we have a 2-dimensional classical statistical spin system, described by the hamiltonian $H(\{\sigma_i\})$ and the partition function:

$$Z = \sum_{\sigma_i} e^{-\beta H(\{\sigma_i\})} \quad (1.1)$$

This determines all the thermodynamics of the model, which can be derived from the Helmholtz free energy $F = \log Z$ (see e.g. [25]).

Let's use the "operatorial form" for a classical model. If the lattice has N columns, and M rows labelled by a (integer) parameter τ , then we take as a 'state' the spin configuration of all the N sites in row τ , denoted by $|\sigma(\tau)\rangle$. Most of the models are described by an Hamiltonian which can be splitted in contributions that involve only 2 adjacent lines (or otherwise are equivalent to models of this kind):

$$H(\{\sigma_i\}) = \sum_{\tau} H(\{\sigma(\tau)\}, \{\sigma(\tau + 1)\}) \quad (1.2)$$

We define the *transfer matrix* as an operator acting on the space of spin states $|\sigma(\tau)\rangle$, whose matrix elements are:

$$\langle \sigma(\tau) | T | \sigma(\tau') \rangle = \sum_{\tau''=\tau}^{\tau'} e^{H(\tau'', \tau''+1)} \quad (1.3)$$

If we use open boundary conditions, where the boundaries are associated to $|\sigma(1)\rangle$ and $|\sigma(M)\rangle$, the partition function can be written as:

$$\begin{aligned}
 Z &= \sum_{i=2, \dots, M-1}^{\sigma_i} \langle \sigma(1) | T | \sigma(2) \rangle \langle \sigma(2) | T | \sigma(3) \rangle \dots \langle \sigma(M-1) | T | \sigma(M) \rangle \\
 &= \langle \sigma_1 | T^M | \sigma_M \rangle
 \end{aligned}
 \tag{1.4}$$

Comparing this expression to

$$\langle x_b, t_b | e^{-\frac{i}{\hbar} \tilde{H}(t_b - t_a)} | x_a, t_a \rangle
 \tag{1.5}$$

which gives the transition amplitude between two space-time points (x_a, t_a) and (x_b, t_b) , we can then interpret T as an euclidean evolution operator:

$$T = e^{-\tau \tilde{H}}
 \tag{1.6}$$

This defines the one dimensional *quantum Hamiltonian* \tilde{H} associated to our classical model. One way to obtain \tilde{H} is the hamiltonian limit procedure, descibed e.g. in [24]. As an example, associated to the 2-dimensional Ising model

$$H(\{\sigma_k\}) = -J \sum_{i \text{ nn } j} \sigma_i \sigma_j - h \sum_i \sigma_i
 \tag{1.7}$$

we have the one dimensional quantum Hamiltonian:

$$\tilde{H} = - \sum_{a=1}^n [\tilde{\sigma}_1(a) + \lambda \tilde{\sigma}_3(a) \tilde{\sigma}_3(a+1)]$$

where the $\tilde{\sigma}_i$ are the Pauli matrices.

This reasoning can be easily extended between d -dimensional statistical models and $(d-1)$ -dimensional quantum models. It's importance lays on the fact that we can focus in all generality only on classical models.

In the following we will always work with classical systems in $d = 2$ dimensions. Let's remind the definition of the correlation functions of a set of observables $\{O_i(x_j)\}$:

$$\langle O(x_1) O(x_2) \dots O(x_n) \rangle = \frac{1}{Z} \sum_{\sigma_k} O_1(x_1) O_2(x_2) \dots O_n(x_n) e^{-\beta H(\{\sigma_k\})}
 \tag{1.8}$$

where the O_i take their value on the lattice, whose points are labelled with x_i . This gives us a measure on how, say, the values of $O_1(x_1), \dots, O_{n-1}(x_{n-1})$ influence the value of $O_n(x_n)$. Clearly, if the value of the observable in x_i does not influence the value of the observable in x_j , $\forall x_i, x_j$, we expect the correlation function to assume the value $\langle O_1(x_1) \rangle \langle O_2(x_2) \rangle \dots \langle O_n(x_n) \rangle$.

It is known (see e.g. [25]) that, for $T \neq T_c$ and $r \equiv |i - j| \rightarrow \infty$ the two-point correlation function of two spins has the following behaviour:

$$G(r) \equiv \langle \sigma_i \sigma_j \rangle - \langle \sigma_i \rangle \langle \sigma_j \rangle \underset{r \rightarrow \infty}{\approx} e^{-\frac{r}{\xi}},
 \tag{1.9}$$

where d is the spatial dimension of the system. This defines one of the main quantities of a statistical model, the *correlation length* ξ . We can roughly say that, for $r < \xi$, the spins are correlated: this means that they tend to assume the *same value*. And if $r > \xi$, they are not. So ξ gives us a measure of the statistical fluctuations in the system. This doesn't mean that all the spins within a range of ξ have all the same value: it better means we can find clusters of spins of all dimensions, and the widest ones have a diameter approximately long ξ .

Moreover, if $T = T_c$, the correlation length diverges and it can be shown that:

$$G(r) = \frac{1}{r^\eta} \quad (1.10)$$

where the exponent η is the *anomalous dimension*, which in two dimensions must be $\neq 0$ to avoid the unphysical behaviour $G(r) \propto \log(r)$, for $r \gg \xi$. Now, if $\xi \rightarrow \infty$, the spatial dimension of spin clusters can be very huge compared to the lattice spacing a , so we can assume that σ_i does not vary "appreciably" in a very little portion of space: we can then substitute the *discrete* variable σ_i with a *continuous* one $\phi(x)$, which is indeed a *field*, and write our main object, the partition function, as:

$$Z = \sum_{\sigma_i} e^{-\beta H(\{\sigma_i\})} \rightarrow \int \mathcal{D}\phi(x) e^{-S[\phi]} \quad (1.11)$$

The correlation functions will change accordingly from:

$$\langle \sigma_1 \sigma_2 \dots \sigma_n \rangle = \sum_k \sigma_1 \sigma_2 \dots \sigma_n e^{-\beta H(\{\sigma_k\})} \quad (1.12)$$

to

$$\langle \phi(x_1) \phi(x_2) \dots \phi(x_n) \rangle = \int \mathcal{D}\phi(x) \phi(x_1) \phi(x_2) \dots \phi(x_n) e^{-S[\phi]} \quad (1.13)$$

We further require the action to be invariant under rotation and translation of the system: this, in two dimensions, corresponds to Lorentz invariance in the Minkowsky space (after a Wick rotation $t \rightarrow -i\beta$), so we are dealing with a relativistically invariant quantum field theory. But in what follows we will always work in the *Euclidean space*. For example, to the Ising model (1.7), it corresponds (see *e.g.* [26]) the Field Theory with action:

$$S = \frac{1}{2} \int d^2x \left[(\partial_\mu \varphi(x))^2 + m^2 \varphi^2(x) + \frac{\lambda}{4} \varphi^4(x) + \dots \right] \quad (1.14)$$

where $\varphi(x)$ is the continuum version of σ_i . As we shall see later, these requirements for the action are not enough to describe a system *at criticality*: we'll need to impose conformal invariance as well, as we shall see later.



Figure 1.1: A system at criticality looks the same if we apply a magnification or a de-magnification. The two figures represents the same system with different magifications.

We conclude the section with a last remark. The fields we are considering take values on the points of the lattice, and the statement $\xi \rightarrow \infty$ is somehow equivalent to say that $a \rightarrow 0$, where a is the spacing lattice. When we deal with a field theory, the roled played by *space* and *time* are different, but in a $2D$ (two dimensional) lattice both spatial dimensions are completely equivalent: this means that we can choose the "spatial direction" and the "time direction" as we prefer. Consider for example a infinite $2D$ strip, whose width is L . If we take the time direction across the strip, then we have a field theory extended in an infinite $1D$ space dimension, living a finite amount of time. If otherwise we take t to be along the strip, we have a field theory defined on a finite space, but whose time extention is infinite.

1.2 The renormalization group

When we study a statistical model at a second order phase transition, which happens for $\xi \rightarrow \infty$, it will always have the same "shape", no matter at which scale we observe it (see fig 1.1): we will refer to this situation as a "critical point" of the system. This means that the system can be described in the same way, indipendently on the scale we choose to study it.

This naive intuition can be rigorously formalized in a branch of statistical physics known as *renormalization group* (RG). The aim of renormalization group theory is, roughly speaking, to describe how a system changes under a dilation of the lattice: we can obtain lots of physical results with this approach, such as all the critical exponents of a statistical system, and so on. We will study some applications in the next sections. The topic is very wide: we refer to *e.g.* [5] for further details.

When we talk about a dilation $a \rightarrow ba$ of the lattice, through a dilation factor $b > 1$, we do not simply dilate everything, otherwise the system will always remain the same. From now on, we will use field theories to describe classical systems (as in section 1.1): suppose, for example, that our classical

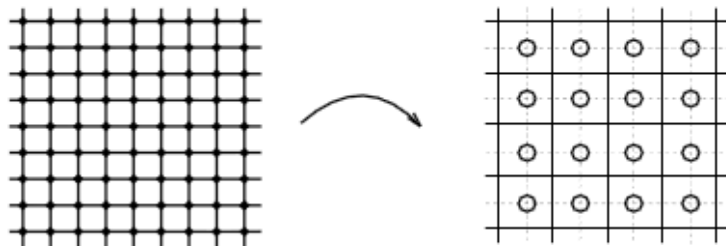


Figure 1.2: The renormalization group transformation.

system is described by the action:

$$S = \int d^2x \left[\frac{1}{2} (\partial_\mu \varphi(x))^2 + g_1 \varphi(x) + \frac{g_2}{2} \varphi(x)^2 + \dots + \frac{g_n}{n!} \varphi(x)^n + \dots \right] \quad (1.15)$$

The parameters $\{g_i\}$ are called *coupling constants*, and we will refer to them simply as g . A renormalization group transformation consists in a reduction of the degrees of freedom of the system. Since the concept is clearer with a figure on hand, refer to fig. 1.2. Start from a given lattice, where each spin σ_i is situated at the center of a face \mathcal{B}_i whose side has length a . Then, *enbody* all the faces that lie in a bigger face of side length ba , and call this block of spins \mathcal{B}' . The new lattice is built by these bigger faces \mathcal{B}'_j , and its spacing is now ba . We need a rule that gives new spins σ'_j at the center of each \mathcal{B}'_j . An example is the *majority rule*: we can take the value of the new spin to be

$$\sigma'_j = A \sum_{i \in \mathcal{B}'_j} \sigma_i \quad (1.16)$$

where the constant A ensures that σ'_j may only take the values ± 1 , and we sum over all the old spins in \mathcal{B}'_j . This transformation simulates the de-magnification of an object: if we look at this object from a larger distance, we lose the resolution of some of its details. In the same fashion, after a RG transformation on a lattice, we will lose the details, say, over the spins in the block \mathcal{B}' , and we will only be able to discern a sort of "mean" of these spins, which we call σ'_i . It is important to notice that applying this transformation to the lattice the action doesn't change, but since we are modifying the spins arrangement it will be characterized by new coupling constants g' . These are fixed by the requirement:

$$\boxed{Z(g, \{\sigma_i\}) = Z(g', \{\sigma'_i\})} \quad (1.17)$$

This means that a de-magnification of a system doesn't change its physics, so the partition function must be invariant. Now, after we obtained the new lattice, we can perform many other RG transformations: if the system is huge enough, the g then describe a curve on what is called the manifold \mathcal{M} of the coupling constants. This is the *renormalization group flow* of the coupling constants, and a limit of this procedure usually exists.

1. Statistical Mechanics

If a system is in its critical point, that is $\xi \rightarrow \infty$, its description doesn't change at all if we perform a RG transformation, so we expect that $g = g'$. This is a *fixed point* of the theory, usually denoted as g^* . Indeed, if we require $g = g'$ for a RG transformation, it can be shown that either $\xi = \infty$ or $\xi = 0$. In the following, we will always deal with critical fixed points.

To a change $a \rightarrow ba$ of the lattice spacing it corresponds a coordinate dilatation:

$$x \rightarrow x' = b^{-1}x \quad (1.18)$$

and this means that at criticality the action is invariant under a dilation of coordinates, that is it doesn't change its form at all.

Let's then put ourselves in the neighbour of a (critical) fixed point, and denote with δg_a the change of a coupling constant under RG. Then:

$$\delta g'_a = \mathcal{K}_{ab} \delta g_b \quad (1.19)$$

Denoting with $\lambda^i \equiv b^{y_i}$ the eigenvalues of \mathcal{K} , and with Δ^i its left eigenvectors, let's define the *scaling variables* (or scaling fields) as

$$u_i \equiv \sum_a \Delta_a^i \delta g_a = \sum_a \Delta_a (g_a - g_a^*) \quad (1.20)$$

These transform, under RG, as:

$$u'_i = \lambda^i u_i = b^{y_i} u_i \quad (1.21)$$

and if we start from a fixed point, we will always have $u_i \equiv 0$ by definition. Depending on the sign of y_i (supposing it's real for simplicity), we have the following cases:

- $y_i > 0$. u_i is said to be a *relevant variable*, and repeated application of RG transformations moves it away from the fixed point value $u_i = 0$.
- $y_i < 0$. u_i is a *irrelevant variable*, and a RG flow moves it towards the fixed point.
- $y_i = 0$. u_i is a *marginal variable*, and its value never changes under RG.

We define the *scaling fields* (or scaling operators) ϕ_i to be the fields coupled to u_i . Since these scaling variables depend on $\{g_a\}$, the ϕ_i are particular combinations of the fields φ_a coupled to g_a (see (1.15)), such that:

$$\sum_i u_i \phi_i(x) = \sum_a (g_a - g_a^*) \varphi_a \quad (1.22)$$

So, in the vicinity of a fixed point g^* we can write:

$$S = S^* + \sum_i u_i \int d^2x \phi_i(x) \quad (1.23)$$

From this equation, it is clear that the ϕ_i will have the same character of their coupling constants: fields coupled to relevant variables will push the action out from S^* , and so on. We will refer to them simply as relevant, irrelevant and marginal fields respectively.

If a fixed point is perturbed by irrelevant operators, we still have $\xi = \infty$: this defines a surface in the manifold \mathcal{M} , called the *critical surface*. If a point lies on this surface, it will always reach a fixed point under RG flow, independently on its initial position. This important fact is the origin of the universal behaviour of the critical phenomena: hamiltonians (or actions as in our case) that differ only by irrelevant scaling fields give rise to the same *critical behaviour*. In other words, these action describe systems that all look the same under a sufficient de-magnification.

Now, we want to describe systems at criticality, that is systems at some fixed points. Since the ϕ_i are all the fields of the theory, we want to study how they change under dilation at these points. Consider the Ising model, whose relevant scaling variables are (see [5]):

$$t = \frac{T - T_c}{T_c} \quad h = \frac{B}{k_B T} \quad (1.24)$$

Actually, in the nearest-neighbour Ising model these are the only variables. They are associated to the energy density operator $\epsilon(|i - j|) = \sigma_i \sigma_j$ (with i and j nearest neighbours) and to the spin operator σ_i respectively. It will be useful in the following to let these scaling variables depend on the points of the lattice: for example, we will have $h(i)$, corresponding to a term in the classical Hamiltonian $\sum_i h(i) \sigma_i$. Let's denote the field theory versions of these operators as $\phi_t(x)$ and $\phi_h(x)$. Under a RG transformation $a \rightarrow ba$ of the lattice, the scaling variables change as (see (1.21)):

$$\begin{cases} t' = b^{y_t} t \\ h' = b^{y_h} h \end{cases}$$

If we want the physical description of the system to be invariant, we must require

$$Z(t, \phi_t, h, \phi_h) = Z(t', \phi'_t, h', \phi'_h) \quad (1.25)$$

To describe the change of ϕ_t and ϕ_h at the fixed point, we need to study the change under RG of the correlation functions, and it's useful to evaluate these objects away from criticality first. Using the definition of $\langle \phi_h(x) \rangle_{t,h}$ we have:

$$\begin{aligned} \langle \phi_h(x) \rangle_{t,h} &\equiv \frac{1}{NZ(t,h)} \frac{\partial Z(t,h)}{\partial h(x)} \\ &= b^{y_h - d} \langle \phi'_h(x') \rangle_{t',h'} \end{aligned} \quad (1.26)$$

Notice that, after the RG transformation, the field $\phi_h(x)$ undergoes a *global* transformation $\phi_h(x) \rightarrow \phi'_h(x')$. Similarly, the two-point correlation function of the spin operator

$$G_\sigma(x_1 - x_2, t, h) = \frac{1}{N^2 Z(t, h)} \frac{\partial^2 Z(t, h)}{\partial h(x_1) \partial h(x_2)}$$

(where we have implemented translational invariance) transform as:

$$G_h(x_1 - x_2, t, h, S) = b^{2y_h - 2d} G_h\left((x_1 - x_2)', b^{y_t} t, b^{y_h} h, S'\right). \quad (1.27)$$

where S is the action corresponding to a given magnification of the system. It is clear that this procedure generalizes to higher correlation functions. Anyway, if we put ourselves on the fixed point, we have:

$$\langle \phi_h(x_1) \phi_h(x_2) \rangle = b^{2y_h - 2d} \langle \phi_h(x'_1) \phi_h(x'_2) \rangle \quad (1.28)$$

This suggests that the field $\phi_h(x)$, at criticality, transforms under a coordinate dilation as:

$$\phi_h(x) = b^{-x_h} \phi_h(x') \quad (1.29)$$

where

$$x_h = d - y_h \quad (1.30)$$

is the *scaling dimension* of $\phi(x)$. But it can be shown (see [17]) that, if the action remains invariant under a certain transformation of coordinates and fields, then a correlation function of a set of fields $\{\varphi_i(x)\}$ satisfy:

$$\langle \varphi_1(x'_1) \dots \varphi_n(x'_n) \rangle = \langle \varphi'_1(x'_1) \dots \varphi'_n(x'_n) \rangle \quad (1.31)$$

So the actual transformation of the fields is given by:

$$\boxed{\phi'_h(x') = b^{x_h} \phi(x)} \quad (1.32)$$

The same reasoning holds for $\phi_t(x)$: denoting $x_t = d - y_t$, we have:

$$\phi'_t(x') = b^{x_t} \phi_t(x) \quad (1.33)$$

1.2.1 Conformal invariance

We can generalize the reasoning of the previous section. Suppose we have a theory whose scaling fields are $\{\phi_i\}$. It can be shown that any correlation function of such fields transform, under RG at criticality, as:

$$\langle \phi_1(x_1) \dots \phi_n(x_n) \rangle = \prod_i b^{-x_i} \langle \phi'_1(x'_1) \dots \phi'_n(x'_n) \rangle \quad (1.34)$$

where we defined the scaling dimensions $x_i \equiv d - y_i$. If we further implement rotation and translation invariance of the whole system, and we consider spinless fields for simplicity, we can generalize (1.34) as:

$$\langle \phi_1(x_1) \dots \phi_n(x_n) \rangle = \prod_i \mathcal{J}(x_i)^{x_i/2} \langle \phi'_1(x'_1) \dots \phi'_n(x'_n) \rangle \quad (1.35)$$

where

$$\mathcal{J}(x) = \left| \frac{\partial x'}{\partial x} \right| \quad (1.36)$$

is the Jacobian of the coordinate transformation considered. Equation (1.35) is correct since it implies that the correlation functions are always invariant under translations and rotations, and it reduces to (1.34) for dilations. The fields then change as:

$$\phi'_i(x') = \left| \frac{\partial x'}{\partial x} \right|^{-x_i/2} \phi_i(x) \quad (1.37)$$

Now, we want to show, at least heuristically, that there is still another class of transformations leaving the system unchanged: this is the *conformal invariance*, and we'll see in chapter 2 that it follows from the invariance of the system under translations, rotations and dilations. These transformations require the parameter b of the dilation to depend on the space point of the lattice, that is $b \rightarrow b(x)$ and:

$$x \rightarrow x' = b(x)x \quad (1.38)$$

(here we define the dilation parameter to be b^{-1} instead of b). We have to suppose that the Hamiltonian of the classical system doesn't involve long range interactions, that is, the field theory description only involves *local fields*. If this is so, since at the critical point $\xi \rightarrow \infty$, we expect that the long range correlations between parts of the systems are not originating from the Hamiltonian parameters. Even if H has anisotropic interactions, these will only play a marginal role, and we expect the system to be translational and rotational invariant. Now, suppose we make local dilations in our system. We know the system has a global dilation invariance, but if $b(x)$ doesn't vary appreciably, it's like we are performing dilation sufficient wide portions of our system: thanks to the short range interactions, our system will be invariant anyway. We will give a rigorous definition of conformal invariance in the next chapter, we will study its implications on systems at criticality. Here we just wanted to give the idea that at criticality another kind of symmetry exists, so to justify the rather formal developments of the following chapters.

Chapter 2

Conformal field theory

In this chapter we review the basic concepts of conformal field theory (CFT). The first five sections are devoted to field theories that describe systems at criticality, that is CFT in a strict sense, while in section 2.6 we deal with systems out of criticality.

2.1 Basic hypothesis

The construction of a conformal field theory is completely different from the lagrangian formalism usually developed in quantum field theories. There, one solves the equations of motion, and derivev the fundamental fields as the most general solution of these equations. Notice that this can be done only in the non-interacting case, which is the only solvable one. Here, instead, we won't introduce any Lagrangian, but we assume the existence of a basis of *local fields* $\{\phi_i(x)\}$, even in the interacting case. These fields must be local, since we pointed out that conformal invariance is only possible for short range interactions. Furthermore, we assume that they are eigenvectors of the dilation operator (see equation (1.29)), that is:

$$\phi_i(x) = \lambda^{x_i} \phi(\lambda x) \tag{2.1}$$

where x_i is the scaling dimension of $\phi(x)$, and $x \rightarrow \lambda x$. All other fields, such as $\phi_i^3(x)$ or $(\partial_\mu \phi_i(x))^2$, can be expressed as a linear combination of this basis.

Our task is to understand how many such basis fields are present in a theory, and how they transform under conformal transformations, defined in the next section. This will be enough, at least in principle, to compute all the possible correlation functions, which are the only measurable quantities: this means that we have solved the theory.

The hypothesis of locality of the fields allows us to evaluate a product of two fields $A(x_1)B(x_2)$. In fact, if $x_1 \rightarrow x_2$ it is natural to assume that this product behaves in a local way, so it can be expanded in the basis of local

2. Conformal field theory

fields:

$$A(x_1)B(x_2) = \sum_k \beta(x_1, x_2)\phi_k(x_2) \quad (2.2)$$

This defines the *operator product expansion* (OPE) of two fields. Anyway, since any field can be expanded in terms of the basis fields $\{\phi_i(x)\}$, the OPE we really need to know is:

$$\phi_i(x_1)\phi_j(x_2) = \sum_k C_{ij}^k(x_1, x_2)\phi_k(x_2) \quad (2.3)$$

It is important to bear in mind that (2.2) holds only in a *weak sense*. If

$$\langle A(z)X \rangle = \langle B(z)X \rangle \quad (2.4)$$

for all possible combination of fields, then we have $A(z) = B(z)$, an equality that only holds in correlation functions, otherwise it gives rise to inconsistencies (see [26]). Thus, if we want for example to know the correlation function

$$\langle \phi_1(x_1)\phi_2(x_2)\phi_3(x_3)\phi_4(x_4) \rangle \quad (2.5)$$

we need to perform

$$\phi_1(x_1)\phi_2(x_2) = \sum_i C_{12}^i(x_1, x_2)\phi_i(x_2),$$

then

$$\phi_3(x_3)\phi_4(x_4) = \sum_k C_{34}^k(x_3, x_4)\phi_k(x_4),$$

and at least the OPE between the resulting fields $\phi_i(x_2)\phi_k(x_4)$. This is one way how we can obtain all the correlation functions. We refer to [17] for the difficult task of computing the quantities $C_{jk}^i(x_a, x_b)$.

2.2 Classical Conformal invariance

In chapter 1 we gave an intuition about the existence of a new symmetry called conformal invariance. Here the approach is formal, and we will always suppose that our scaling operators $\phi_i(x)$ takes their value on a manifold parametrized by coordinates x^μ (from now on we will remove the symbol of vector from the coordinates). This manifold is not always the simple \mathbb{R}^2 plane, and we'll see that its curvature plays an important role.

2.2.1 Definition of conformal transformation

A conformal transformation (CT) is defined as an invertible mapping $x \rightarrow x'$, such that the metric tensor $g_{\mu\nu}(x)$ is invariant up to a scale:

$$g'_{\mu\nu}(x') = \Lambda(x)g_{\mu\nu}(x) \quad (2.6)$$

2.2. Classical Conformal invariance

The set of all these invertible transformation forms a *group*, and has the Poincaré group as a subgroup. The epithet "conformal" is due to the property of these transformation to leave unchanged the angle between two curves crossing each other in some point. If we perform an infinitesimal coordinate transformation $x^\mu \rightarrow x'^\mu = x^\mu + \epsilon^\mu(x)$, the metric tensor change as:

$$g_{\mu\nu} \rightarrow g_{\mu\nu} - (\partial_\mu \epsilon_\nu + \partial_\nu \epsilon_\mu) \quad (2.7)$$

Imposing conformal invariance we end up with:

$$\partial_\mu \epsilon_\nu + \partial_\nu \epsilon_\mu = (1 - \Lambda(x))g_{\mu\nu} \quad (2.8)$$

where the factor $f(x) \equiv (1 - \Lambda(x))$ is obtained by taking the trace on both sides of this last equation:

$$f(x) = \frac{2}{d} \partial_\rho \epsilon^\rho \quad (2.9)$$

Suppose now that $g_{\mu\nu} = \eta_{\mu\nu}$, where $\eta_{\mu\nu}$ is the metric of a flat euclidean space. This condition is not restrictive, since the finite transformations will be in tensorial form. Working on (2.8), we end up with

$$\begin{cases} (2-d)\partial_\mu \partial_\nu f(x) = \eta_{\mu\nu} \square f(x) \\ (d-1)\square f(x) = 0 \end{cases} \quad (2.10)$$

We just mention that in the case $d \geq 3$ we have the constraint $\partial_\mu \partial_\nu f(x) = 0$, which implies, from (2.9):

$$\epsilon_\mu = a_\mu + b_{\mu\nu} x^\nu + c_{\mu\nu\rho} x^\nu x^\rho \quad (2.11)$$

that is, ϵ_μ is at most quadratic in the coordinates. Clearly, a_μ refers to an infinitesimal translation, while $b_{\mu\nu}$ is connected to infinitesimal rotation and dilation, since from (2.8) it follows that $b_{\mu\nu} = \alpha \eta_{\mu\nu} + m_{\mu\nu}$ with $m_{\mu\nu} = -m_{\nu\mu}$. The main novelty is represented by the term $c_{\mu\nu\rho}$, which introduces a new transformation we can apply to a system at criticality, leaving it unchanged. This is the *special conformal transformation*:

$$x'^\mu = \frac{x^\mu - b^\mu x^2}{1 - 2b^\mu x_\mu + b^2 x^2} \quad b_\mu = \frac{1}{d} c_{\sigma\mu}^\sigma \quad (2.12)$$

Let's turn to the case we want to study, that is $d = 2$. From (2.10), we see that there are infinite independent transformations satisfying the condition of conformal transformation. To be more specific, consider again equation (2.6). We label the coordinates in a different way, that is we study the conformal transformation $z^\mu \rightarrow w^\mu(z)$, with $z^\mu \equiv (z^0, z^1)$. We then require that:

$$g'_{\mu\nu}(w) = \left(\frac{\partial w^\mu}{\partial z^\alpha} \right) \left(\frac{\partial w^\nu}{\partial z^\beta} \right) g_{\mu\nu}(z) \propto g_{\mu\nu}(z) \quad (2.13)$$

2. Conformal field theory

If again we set $g_{\mu\nu}(z) = \eta_{\mu\nu}$, we arrive at the two couple of constraint:

$$\frac{\partial w^1}{\partial z^0} = \frac{\partial w^0}{\partial z^1}, \quad \frac{\partial w^0}{\partial z^0} = -\frac{\partial w^1}{\partial z^1} \quad (2.14)$$

which are nothing but the *Cauchy-Riemann equations* for holomorphic functions. It is then natural to change to complex coordinates:

$$\begin{cases} z = z^0 + iz^1 \\ \bar{z} = z^0 - iz^1 \end{cases} \quad (2.15)$$

Notice that this can be considered as a real coordinate transformation, from (z^0, z^1) to (z, \bar{z}) , where the metric in the complex coordinates system is:

$$g_{\mu\nu} = \begin{pmatrix} 0 & \frac{1}{2} \\ \frac{1}{2} & 0 \end{pmatrix} \quad g^{\mu\nu} = \begin{pmatrix} 0 & 2 \\ 2 & 0 \end{pmatrix} \quad (2.16)$$

All the tensor equations we are going to express are then valid in both coordinate systems.

The Cauchy-Riemann equations can be rewritten as:

$$\partial_{\bar{z}} w(z, \bar{z}) = 0 \quad (2.17)$$

where $\partial_{\bar{z}} = \frac{\partial}{\partial \bar{z}}$. Their solution is then simply any function that doesn't depend on \bar{z} , that is any holomorphic function $w(z)$. For the component \bar{w} we have a similar constraint:

$$\partial_z \bar{w}(z, \bar{z}) = 0 \quad (2.18)$$

and it follows that $\bar{w} = \bar{w}(\bar{z})$ is any possible antiholomorphic function.

2.2.2 Global and local conformal transformations

We must bear in mind that a set of transformations form a *group* if they are invertible and if they map the complex plane onto itself: this last requirement ensures that the transformations are all of the same kind. We know that representation theory holds for any set of transformation which forms a group, so in principle it would be useful to recover a group. Clearly, the constraints (2.14) are of a local type: they don't necessary impose a transformation to be defined everywhere and be invertible. We then must distinguish between *global* conformal transformation, which form the conformal group, and *local* conformal transformations, which are not defined everywhere and may not be invertible. It can be shown that the set of all global CT is given by the maps:

$$f(z) = \frac{az + b}{cz + d} \quad ad - bc = 1 \quad (2.19)$$

Each of these maps is in one-to-one correspondence with a matrix

$$A = \begin{pmatrix} a & b \\ c & d \end{pmatrix} \quad (2.20)$$

and the group of global CT is then isomorphic to the group of complex invertible 2×2 matrix with unit determinant, which in turn is isomorphic to the Lorentz group in four dimensions $SO(3,1)$. This means that the global CT group is characterized by 6 parameters. Indeed, it is known that a map of the form (2.19) is completely determined by successive applications of:

- translations:

$$z' = z + a \quad a \in \mathbb{C}$$

- rotations:

$$z' = e^{i\theta} z \quad \theta \in \mathbb{R}$$

- dilations:

$$z' = \lambda z \quad \lambda \in \mathbb{R}$$

- special conformal transformations:

$$z' = \frac{z}{1 + bz} \quad b \in \mathbb{C}$$

More in general, the conformal group in d dimensions is isomorphic to $SO(d+1,1)$, since their generators share the same algebra (see [17]).

Let's now turn to the discussion of local CT, which form the local conformal group. We want to find the generators G_a of this "group", and we remind that these are defined by a local transformation on the fields, with infinitesimal parameters ω_a

$$\delta\Phi(x) = \Phi'(x) - \Phi(x) \equiv -i\omega_a G_a \Phi(x) \quad (2.21)$$

We need the Laurent expansion of the infinitesimal transformation, that is

$$\epsilon(z) = z' - z = \sum_{-\infty}^{\infty} c_n z^{n+1} \quad (2.22)$$

If we consider a spinless and scalar field ϕ , such that $\phi'(z', \bar{z}') = \phi(z, \bar{z})$, we have:

$$\begin{aligned} \phi'(z, \bar{z}) - \phi(z, \bar{z}) &= -\epsilon(z)\partial\phi(z, \bar{z}) - \bar{\epsilon}(\bar{z})\bar{\partial}\phi(z, \bar{z}) \\ &= \sum_n \left(c_n l_n \phi(z, \bar{z}) + \bar{c}_n \bar{l}_n \phi(z, \bar{z}) \right) \end{aligned} \quad (2.23)$$

We argue from this equation that the generators are

$$l_n = -z^{n+1}\partial_z \quad \bar{l}_n = -\bar{z}^{n+1}\partial_{\bar{z}} \quad (2.24)$$

and they obey what is called the Witt algebra:

$$\begin{cases} [l_n, l_m] = (n - m)l_{n+m} \\ [\bar{l}_n, \bar{l}_m] = (n - m)\bar{l}_{n+m} \\ [l_n, \bar{l}_m] = 0 \end{cases} \quad (2.25)$$

2. Conformal field theory

which is a direct sum of two infinite dimensional isomorphic algebras. Notice that we have an *infinite number* of generators for the local case, which would imply an infinite number of conserved charges. We expect that the global CT group subalgebra is composed by six elements, since this is the number of conserved charges. This can be seen by requiring the regularity of (2.23) at 0 and ∞ . Indeed, the two vector fields

$$v(z) = - \sum_n a_n z^{n+1} \partial_z \quad w(z) = \sum_n a_n \left(-\frac{1}{y}\right)^{n-1} \partial_y \quad (2.26)$$

are regular in the neighbours of 0 and ∞ respectively, provided $n \geq -1$ and $n \leq q$. So, the algebra of the global CT group is formed by the generators of

1. translations on the complex plane $z' = z + a$:

$$l_{-1} = -\partial_z$$

2. scale transformations $z' = \lambda z$ and rotations $z' = e^{-i\theta} z$:

$$l_0 = -z\partial_z$$

3. special conformal transformations $z' = z/(1 + bz)$:

$$l_1 = -z^2\partial_z$$

and their complex conjugated $\bar{l}_{-1}, \bar{l}_0, \bar{l}_1$. We have thus discussed how classical fields change under CT, and we defined the classical generators l_n, \bar{l}_n for these transformations.

Let's go back to equation (1.37) for the change of the fields under a change of coordinates. We remind that, under a dilation $x \rightarrow \lambda x$ of the coordinates of a system at criticality, we have for a scaling field:

$$\phi'(\lambda x) = \lambda^{-x} \phi(x) \quad (2.27)$$

Now, the elicity of a field Φ is a quantity \mathcal{E} such that, if the coordinates transform as $x'^\mu = \exp(i\theta) x^\mu$, the field changes as $\Phi' = \exp(i\mathcal{E}\theta) \Phi$. Here, in the same fashion, we define the *conformal spin* s such that, under a rotation $z \rightarrow z \exp(i\theta)$, we have:

$$\phi'(e^{i\theta} z, e^{-i\theta} \bar{z}) = e^{-is\theta} \phi(z, \bar{z}) \quad (2.28)$$

We can then state that a scaling field change as:

$$\phi'(\lambda z, \bar{\lambda} \bar{z}) = \lambda^{-\Delta} \bar{\lambda}^{-\bar{\Delta}} \phi(z, \bar{z}) \quad (2.29)$$

This embodies the cases of rotations $\lambda = \exp(i\theta)$ and dilations $\lambda = b$ (see equation (2.27)), provided we have:

$$\begin{cases} x = \Delta + \bar{\Delta} \\ s = \Delta - \bar{\Delta} \end{cases} \quad (2.30)$$

The quantities $(\Delta, \bar{\Delta})$ are the *holomorphic conformal dimensions*, or complex scaling dimensions, or simply conformal dimensions of the fields ϕ , and are the only quantities that characterize completely the behaviour of a field under coordinate transformations, as we shall see. The case $\lambda \in \mathbb{C}$ is a combined rotation and scale transformation.

We can now say which fields are *relevant*. Suppose a field $\phi(z, \bar{z})$ has conformal dimensions (Δ, Δ) for simplicity (it is a scalar field) and is coupled to a certain scaling variable u . In the action we will have the term

$$u \int dz d\bar{z} \phi(z, \bar{z}) \quad (2.31)$$

Under the coordinate transformation $z' = z/b$, the field has scaling dimension $x \equiv \Delta + \bar{\Delta} = 2\Delta$, while the term $dz d\bar{z}$ scales as b^{-2} . If we require the action to remain invariant under conformal transformations then u must scale as $b^{2(1-\Delta)}$. This means that a scalar field is relevant only if its conformal dimension satisfy:

$$\boxed{\Delta < 1} \quad (2.32)$$

2.2.3 The Stress Tensor

We know from Nother's theorem that to each continuous coordinate transformation under which the action remains invariant, there corresponds a conserved current. From translational invariance, we have that the conserved current is the stress tensor (or energy-momentum tensor) $T^{\mu\nu}$, which satisfies the continuity equation

$$\partial_\mu T^{\mu\nu} = 0 \quad (2.33)$$

This tensor is really important: if a system is translationan invariant, then under an *arbitrary* infinitesimal coordinate transformation $x^\mu \rightarrow x^\mu + \epsilon^\mu$ the action changes as

$$\delta S = \int d^2x T^{\mu\nu}(x) \partial_\mu \epsilon_\nu(x) \quad (2.34)$$

If furthermore we require rotational and scale invariance of the system, then (2.34) implies $T^{\mu\nu} = T^{\nu\mu}$ and $T^\mu_\mu = 0$. We use the first property to write:

$$\delta S = \int d^2x T^{\mu\nu}(x) \left(\partial_\mu \epsilon_\nu(x) + \partial_\nu \epsilon_\mu(x) \right) \quad (2.35)$$

2. Conformal field theory

and thanks to (2.8), we can write this as:

$$\delta S = \frac{1}{2} \int d^2x T_\mu^\mu \partial_\rho \epsilon^\rho \quad (2.36)$$

Since $T^{\mu\nu}$ is traceless, we have that $\delta S = 0$ automatically for conformal transformations of the kind (2.8). This is *Polyakov's theorem*: if a system has translational, rotational and scale invariance, then it automatically satisfy conformal invariance.

We can write the stress tensor in complex coordinates as well. Let's then define the components:

$$T_{zz} \equiv T(z, \bar{z}) = \frac{1}{4}(T_{00} - T_{11} + 2iT_{01}) \quad (2.37a)$$

$$T_{\bar{z}\bar{z}} \equiv \bar{T}(z, \bar{z}) = \frac{1}{4}(T_{00} - T_{11} - 2iT_{01}) \quad (2.37b)$$

$$T_{z\bar{z}} = T_{\bar{z}z} \equiv \frac{1}{4}\Theta(z, \bar{z}) = \frac{1}{4}(T_{00} + T_{11}) = \frac{1}{4}T_\mu^\mu \quad (2.37c)$$

Equation (2.33) can then be written as:

$$\begin{cases} \partial_{\bar{z}}T(z, \bar{z}) + \frac{1}{4}\partial_z\Theta(z, \bar{z}) = 0 \\ \partial_z\bar{T}(z, \bar{z}) + \frac{1}{4}\partial_{\bar{z}}\Theta(z, \bar{z}) = 0 \end{cases} \quad (2.38)$$

Notice that, thanks to conformal invariance, we have $\Theta(z, \bar{z}) = 0$, so $T(z, \bar{z}) \equiv T(z)$ and $\bar{T}(z, \bar{z}) \equiv \bar{T}(\bar{z})$: these are called the holomorphic and antiholomorphic part of the stress tensor.

2.3 Quantum conformal invariance

When we deal with the quantum theory of an action invariant under conformal transformations, we may not rely anymore on some classical results. What we can do is study the variation of *correlation functions* under coordinate transformations. Using path integrals, we have the definition:

$$\langle \phi_1(z_1, \bar{z}_1) \dots \phi_n(z_n, \bar{z}_n) \rangle = \frac{1}{Z} \int \mathcal{D}\Phi \phi_1(z_1, \bar{z}_1) \dots \phi_n(z_n, \bar{z}_n) e^{-S[\Phi]} \quad (2.39)$$

where Φ is a fundamental field. Here $-S[\Phi]$ is the classical action, and the path integral approach allows us to use some classical arguments, for example the relations derived for the variation of S under coordinate transformations.

If we make an infinitesimal conformal transformation $z \rightarrow z' = z + \alpha(z)$, we expect that:

$$\delta \langle \phi_1(z_1, \bar{z}_1) \dots \phi_n(z_n, \bar{z}_n) \rangle = 0 \quad (2.40)$$

that is, the *local* variation of a correlation functions is zero (see eq. (1.31)): indeed, a coordinate transformation should not change the description of a physical system (see eq. (1.31)). The variation on $1/Z$ gives rise to a term including $\langle T_{\mu\nu} \rangle$, but we know that, at criticality, this value is zero (as we shall see). We then have:

$$\sum_i \langle \phi_1(z_1, \bar{z}_1) \dots \delta\phi_i(z_i, \bar{z}_i) \dots \phi_n(z_n, \bar{z}_n) \rangle = \langle (\delta S) \phi_1(z_1, \bar{z}_1) \dots \phi_n(z_n, \bar{z}_n) \rangle \quad (2.41)$$

We leave the expression of δS undeveloped, for the moment. This is our starting point for the next section.

2.3.1 Conformal Ward identity

Suppose we want to study the variation of a correlation function, defined by (2.39), under an infinitesimal conformal transformation $z \rightarrow z' = z + \alpha(z)$. We are going to perform this change of coordinates *only* in a region C that contains the points (z_i, \bar{z}_i) , and in the remaining we leave the coordinates unchanged: $z' = z$. We then expect a change of the action along the curve C , given by (2.34). If we perform some integrations by parts, and turn to complex coordinates, we end with (see *e.g.* [6]):

$$\delta S = \frac{1}{2\pi i} \oint_C \alpha(z) T(z) dz - \frac{1}{2\pi i} \oint_C \bar{\alpha}(\bar{z}) \bar{T}(\bar{z}) d\bar{z} \quad (2.42)$$

If we put this expression into (2.41), we have:

$$\begin{aligned} \sum_i \langle \phi_1(z_1, \bar{z}_1) \dots \delta\phi_i(z_i, \bar{z}_i) \dots \phi_n(z_n, \bar{z}_n) \rangle \\ = \frac{1}{2\pi i} \oint_C \alpha(z) \langle T(z) \phi_1(z_1, \bar{z}_1) \dots \phi_n(z_n, \bar{z}_n) \rangle dz + \text{c.c.} \end{aligned} \quad (2.43)$$

Now, remind that for a scaling field the relation (2.29) holds. If we perform a transformation such that $\alpha(z) = \lambda(z - z_1)$ where $\lambda \in \mathbb{C}$, then $\delta\phi_1 = (\Delta_1\lambda + \bar{\Delta}_1\bar{\lambda})\phi_1$, and if we vary only ϕ_1 we end with:

$$\begin{aligned} \frac{1}{2\pi i} \oint_C (z - z_1) \langle T(z) \phi_1(z_1, \bar{z}_1), \dots, \phi_n(z_n, \bar{z}_n) \rangle dz \\ = \Delta_1 \langle \phi_1(z_1, \bar{z}_1), \dots, \phi_n(z_n, \bar{z}_n) \rangle \end{aligned} \quad (2.44)$$

This is not, strictly speaking, correct since all the fields must vary, but suppose we can do such an operation. If otherwise we perform a translation, then $\alpha = \text{const}$ and $\delta\phi_i \propto \partial_{z_i}\phi_i$. Varying again only ϕ_1 , we obtain:

$$\begin{aligned} \frac{1}{2\pi i} \oint_C \langle T(z) \phi_1(z_1, \bar{z}_1), \dots, \phi_n(z_n, \bar{z}_n) \rangle dz \\ = \partial_{z_1} \langle \phi_1(z_1, \bar{z}_1), \dots, \phi_n(z_n, \bar{z}_n) \rangle \end{aligned} \quad (2.45)$$

2. Conformal field theory

Since we are integrating over a close contour, we can apply the theorem of residues to the OPE between $T(z)$ and $\phi_1(z_1)$. We then gain informations about two singular terms of this OPE, and in general of the OPE between $T(z)$ and $\phi_i(z_i)$, that is:

$$T(z)\phi_i(z_i, \bar{z}_i) = O((z - z_i)^{-3}) + \frac{\Delta_i}{(z - z_i)^2}\phi_i(z_i, \bar{z}_i) + \frac{1}{z - z_i}\partial_{z_i}\phi_i(z_i, \bar{z}_i) + \text{reg.} \quad (2.46)$$

We define the *primary fields* as those fields such that the term $O((z - z_i)^{-3})$ is absent in (2.46). We then have:

$$\begin{aligned} & \langle T(z)\phi_1(z_1, \bar{z}_1) \dots \phi_n(z_n, \bar{z}_n) \rangle \\ &= \sum_j \left(\frac{\Delta_j}{(z - z_j)^2} + \frac{1}{z - z_j}\partial_{z_j} \right) \langle \phi_1(z_1, \bar{z}_1) \dots \phi_n(z_n, \bar{z}_n) \rangle \end{aligned} \quad (2.47)$$

and this is the *conformal Ward identity* for primary fields. We derived this relation using the holomorphic part of the stress tensor: the identity concerning $\bar{T}(\bar{z})$ is similar, and we simply have to make the substitutions $T(z) \rightarrow \bar{T}(\bar{z})$ and $\Delta_i \rightarrow \bar{\Delta}_i$. If, at last, we put the OPE just obtained in (2.43), we must have, for consistency:

$$\delta\phi_i(z_i, \bar{z}_i) = -(\Delta_i\partial_{z_i}\alpha(z_i) + \alpha(z_i)\partial_{z_i})\phi_i(z_i, \bar{z}_i) + \text{c.c.} \quad (2.48)$$

which integrated gives the transformation law for primary fields:

$$\boxed{\phi'(z', \bar{z}') = \left(\frac{dz'}{dz}\right)^{-\Delta} \left(\frac{d\bar{z}'}{d\bar{z}}\right)^{-\bar{\Delta}} \phi(z, \bar{z})} \quad (2.49)$$

Notice that from (2.47) we can infer the conformal dimensions of $T(z)$. For this purpose, we must study the behaviour of this equation under a scale transformation $z \rightarrow \lambda z$ and under a rotation $z \rightarrow \exp(i\theta)z$. Notice that the conformal dimensions of the coordinates z and \bar{z} are $(-1, 0)$ and $(0, -1)$ respectively. If now we require that both sides of (2.47) have the same conformal dimensions, we get:

$$T(z) : \begin{cases} \Delta = 2 \\ \bar{\Delta} = 0 \end{cases} \quad \bar{T}(\bar{z}) : \begin{cases} \Delta = 0 \\ \bar{\Delta} = 2 \end{cases} \quad (2.50)$$

A last comment is in order. If in (2.43) we consider the variation of one field, we obtain that the variation of an arbitrary field $\phi(z, \bar{z})$ is (in a weak sense):

$$\delta\phi(z, \bar{z}) = \oint_z d\zeta \alpha(\zeta)T(\zeta)\phi(z, \bar{z}) \quad (2.51)$$

where \oint_z is for a contour integral containing the point z .

2.3.2 The central charge

We now want to calculate the OPE $T(z)T(w)$, which has dimension $(4, 0)$ from (2.50). This fixes its general form:

$$T(z)T(w) = \frac{c/2}{(z-w)^4} + \frac{J(w)}{(z-w)^3} + \frac{Q(w)}{(z-w)^2} + \frac{R(w)}{(z-w)} + \text{reg.} \quad (2.52)$$

where $c/2$ is a constant (it can't have any dimensions for consistency). We can expand in Taylor series the functions comparing in this OPE, for example:

$$J(z) = J(w) + (z-w)\partial_w J(w) + \frac{1}{2}(z-w)^2\partial_w^2 J(w) + \dots \quad (2.53)$$

Since $T(z)T(w) = T(w)T(z)$, we have the constraints

$$J(w) = 0 \quad R(w) = \frac{1}{2}\partial_w Q(w) \quad (2.54)$$

and so:

$$T(z)T(w) = \frac{c/2}{(z-w)^4} + \frac{Q(w)}{(z-w)^2} + \frac{(1/2)\partial_w Q(w)}{z-w} \quad (2.55)$$

Now, $Q(z)$ has the same conformal dimensions of $T(z)$, and the OPE $Q(z)Q(w)$ has the same form of $T(z)T(w)$:

$$Q(z)Q(w) = \frac{c/2}{(z-w)^4} + \frac{R(w)}{(z-w)^2} + \frac{(1/2)\partial_w R(w)}{z-w} \quad (2.56)$$

where again $R(w)$ has the same dimensions of $Q(w)$ and $T(w)$. These all belong to the space of fields with conformal dimensions $(2, 0)$. If we suppose that the only fields belonging to this class are stress tensors, then we can redefine $T(w)$ as being the sum of all these, apart for a multiplicative factor: so we set $Q(w) = kT(w)$ in (2.55). We can calculate k in the case $c = 0$: $T(w)$ is then a primary field by definition (see (2.46)), and its variation is given by (2.48). Under an infinitesimal dilation $z' - z = \epsilon z$ we have (see (2.51)):

$$\delta T(z) = \epsilon \oint_z d\zeta \zeta T(\zeta)T(z) \quad (2.57)$$

We now just need to integrate this by parts and use the theorem of residues. Since $\Delta = 2$ for $T(w)$, this fixes $k = 2$, and at last we obtain:

$$T(z)T(w) = \frac{c/2}{(z-w)^4} + \frac{2T(w)}{(z-w)^2} + \frac{\partial_w T(w)}{z-w} \quad (2.58)$$

The constant c is very important in the context of CFT, and is called the *central charge*.

2. Conformal field theory

If $c \neq 0$, then $T(w)$ is not a primary field anymore, and its variation is given by, using again (2.51):

$$\delta T(z) = 2(\partial_z \alpha)T(z) + \alpha(z)\partial_z T(z) + \frac{c}{12}\partial_z^3 \alpha(z) \quad (2.59)$$

We state without demonstration that if we integrate this variation we end up ([17]) with the transformation law for the stress tensor under a coordinate conformal transformation $z \rightarrow w(z)$:

$$T'(w) = \left(\frac{dw}{dz}\right)^{-2} \left(T(z) - \frac{c}{12}\{w; z\}\right) \quad (2.60)$$

where we have introduced the Schwartzian derivative

$$\{w, z\} = \frac{d^3 w/dz^3}{dw/dz} - \frac{3}{2} \left(\frac{d^2 w/dz^2}{dw/dz}\right)^2$$

2.3.3 CFT on a cylinder

Here we want to give an example of the role played by the central charge. Let's start from a CFT living on the complex plane, and map it on a cylinder of circumference L via the transformation:

$$z \rightarrow w = \frac{L}{2\pi} \log z \quad (2.61)$$

From the point of view of statistical mechanics, we are going from a classical 2 dimensional system defined on the plane to a system defined on a strip, where periodic boundary conditions are imposed. These systems are in the same class of universality, since they are linked by a conformal transformation.

Using (2.60), the stress tensor on the cylinder is given by:

$$T_{\text{cyl.}}(w) = \left(\frac{2\pi}{L}\right)^2 \left[T_{\text{plane}}(z)z^2 - \frac{c}{24}\right] \quad (2.62)$$

We'll see that $\langle T_{\text{plane}}(z) \rangle = 0$ when we quantize the theory through the operator formalism. This implies:

$$\langle T_{\text{cyl.}}(w) \rangle = -\frac{c\pi^2}{6L^2} \quad (2.63)$$

Since $T_\mu^\mu = 0$, it follows from equations (2.38) that

$$\langle T_{\text{cyl.}}^{00} \rangle = \langle T_{zz} \rangle + \langle T_{\bar{z}\bar{z}} \rangle = -\frac{1}{\pi} \langle T_{\text{cyl.}} \rangle = \frac{\pi c}{6L^2} \quad (2.64)$$

where we redefined $T \rightarrow -2\pi T$ following [17]. Thus, if we introduce a finite length in the system, it will react through a non-zero vacuum energy density $\langle T_{\text{cyl.}}^{00} \rangle$ related to the central charge. This is similar to what happens in

the *Casimir effect*, where the vacuum energy density becomes finite due to a transformation of the global geometry.

Now, under a change of the metric tensor, the free energy $F = -\log Z$ varies accordingly to ([17]):

$$\delta F = -\frac{1}{2} \int d^2x \sqrt{g} \delta g_{\mu\nu} \langle T^{\mu\nu} \rangle \quad (2.65)$$

Let's apply an infinitesimal scaling of the circumference $L \rightarrow (1 + \epsilon)\delta L$, with $\epsilon = \delta L/L$. If the cylinder coordinates are $w = w^0 + iw^1$, where w^1 runs across the cylinder, then $w^1 \rightarrow (1 + \epsilon)w^1$, and (2.7) implies $\delta g_{\mu\nu} = -2\epsilon \delta_{\mu 0} \delta_{\nu 0}$. Using (2.64) the variation of the free energy on the cylinder is:

$$\delta F = \int dw^0 dw^1 \frac{\pi c}{6L^2} \frac{\delta L}{L} \quad (2.66)$$

Suppose the system has a free energy f_0 per unit area in the $L \rightarrow \infty$ limit. Then we have to change (2.66) as:

$$\delta F = \int dw^0 dw^1 \left(f_0 + \frac{\pi c}{6L^2} \right) \frac{\delta L}{L} \quad (2.67)$$

The integral over w^1 gives a factor L . We then have that the free energy per unit length of the cylinder F_L varies accordingly to:

$$\delta F_L = \left(f_0 + \frac{\pi c}{6L^2} \right) \delta L \quad (2.68)$$

from which it follows that:

$$F_L = f_0 L - \frac{\pi c}{6L} \quad (2.69)$$

This important relation describes the behaviour of the free energy density

$$f = f_0 - \frac{\pi c}{6L^2} \quad (2.70)$$

at order $O(L^{-3})$, and allows us to extract c for a given model. As we shall see, the central charge determines all the fields content of the theory. Consider for example the one dimensional quantum Hamiltonian:

$$H = -\frac{1}{2\eta} \sum_{n=1}^N \left[\frac{1+\eta}{2} \sigma_n^x \sigma_{n+1}^x + \frac{1-\eta}{2} \sigma_n^y \sigma_{n+1}^y + h \sigma_n^z \right] \quad (2.71)$$

This model is also known as the *XY model*, and it has a critical point at $|h_c| = 1$ (see *e.g.* [24]). Suppose that the sites are separated by unity (so that the spatial length of the system is $L = N$) and that the temporal extension is infinite. If $N \rightarrow \infty$ and $h = h_c$ the system is conformally invariant, and it can be shown that the free energy density has the behaviour:

$$f = -\frac{\pi}{2} \left(1 + \frac{\arccos \eta}{\eta \sqrt{1-\eta^2}} \right) - \frac{\pi}{12N^2} + O(N^{-4}) \quad (2.72)$$

From (2.70) we deduce that the central charge of the XY model is $c = \frac{1}{2}$.

2.3.4 Correlation functions

Global conformal invariance permits us to fix completely (apart for a constant) the form of the two and three points correlations functions for primary fields. To see this, let's turn back to real coordinates for a while, and consider spinless fields. We know that, thanks to (2.49) and to the fact that (see chapter 1)

$$\langle \phi_1(x_1) \dots \phi_n(x_n) \rangle = \langle \phi'_1(x_1) \dots \phi'_n(x_n) \rangle$$

the correlation functions have the property:

$$\langle \phi_1(y_1) \dots \phi_n(y_n) \rangle = \prod_i \left| \frac{\partial y'}{\partial y} \right|_{y=y_i}^{x_i/2} \langle \phi_1(y'_1) \dots \phi_n(y'_n) \rangle \quad (2.73)$$

(the exponents are scaling dimensions, and not coordinates). Consider the case of a two-point correlation function. Translational and rotational invariance require that

$$\langle \phi_1(y_1) \phi_2(y_2) \rangle = f(|y_1 - y_2|) \quad (2.74)$$

while under a dilation $y \rightarrow \lambda y$ we have

$$\langle \phi_1(y_1) \phi_2(y_2) \rangle = \lambda^{x_1+x_2} \langle \phi_1(\lambda y_1) \phi_2(\lambda y_2) \rangle \quad (2.75)$$

This implies that this correlation function assumes the form:

$$\langle \phi_1(y_1) \phi_2(y_2) \rangle = \frac{C_{12}}{|y_1 - y_2|^{x_1+x_2}} \quad (2.76)$$

We need at last to use special conformal transformations, defined by (2.12), and whose Jacobian turns out to be

$$\left| \frac{\partial y'}{\partial y} \right| = \frac{1}{(1 - 2b^\mu y_\mu + b^2 y^2)^2} \quad (2.77)$$

Using again (2.73), the two point correlation function of two spinless fields is

$$\langle \phi_1(y_1) \phi_2(y_2) \rangle = \begin{cases} \frac{C_{12}}{|y_1 - y_2|^{2x_1}} & \text{if } x_1 = x_2 \\ 0 & \text{if } x_1 \neq x_2 \end{cases} \quad (2.78)$$

For the correlator of two fields ϕ_i and ϕ_j we can set $C_{ij} = \delta_{ij}$ if we normalize the fields in a proper way. A similar reasoning fixes the form of the three point correlation function:

$$\langle \phi_1(y_1) \phi_2(y_2) \phi_3(x_3) \rangle = \frac{C_{123}}{y_{12}^{x_1+x_2-x_3} y_{23}^{x_2+x_3-x_1} y_{13}^{x_3+x_1-x_2}} \quad (2.79)$$

where we defined $y_{12} = y_1 - y_2$, and so on. Notice that the constant C_{123} remains free, and is not fixed by the normalization of the fields.

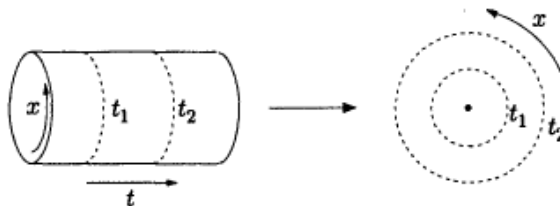


Figure 2.1: Mapping from the cylinder to the complex plane.

We may now turn to complex coordinates. At first sight, we simply need to substitute $y_{ij} \rightarrow (z_{ij}\bar{z}_{ij})^{1/2}$. But if we allow the fields to have non-zero spin, we must furthermore substitute x_i with Δ_i if it's the exponent of holomorphic coordinates, and with $\bar{\Delta}_i$ for antiholomorphic coordinates. In this way we recover the correct spin of the correlator. In conclusion, we have:

$$\langle \phi_1(z_1, \bar{z}_1)\phi_2(z_2, \bar{z}_2) \rangle = \frac{C_{12}}{(z_1 - z_2)^{2\Delta}(\bar{z}_1 - \bar{z}_2)^{2\bar{\Delta}}} \quad \text{if } \begin{cases} \Delta_1 = \Delta_2 \equiv \Delta \\ \bar{\Delta}_1 = \bar{\Delta}_2 \equiv \bar{\Delta} \end{cases} \quad (2.80)$$

and

$$\begin{aligned} \langle \phi_1(z_1, \bar{z}_1)\phi_2(z_2, \bar{z}_2)\phi_3(z_3, \bar{z}_3) \rangle &= C_{123} \frac{1}{z_{12}^{\Delta_1+\Delta_2-\Delta_3} z_{23}^{\Delta_2+\Delta_3-\Delta_1} z_{13}^{\Delta_3+\Delta_1-\Delta_2}} \\ &\times \frac{1}{\bar{z}_{12}^{\bar{\Delta}_1+\bar{\Delta}_2-\bar{\Delta}_3} \bar{z}_{23}^{\bar{\Delta}_2+\bar{\Delta}_3-\bar{\Delta}_1} \bar{z}_{13}^{\bar{\Delta}_3+\bar{\Delta}_1-\bar{\Delta}_2}} \end{aligned} \quad (2.81)$$

There are several methods to completely determine the n -points correlation functions, but they won't be discussed here: see [17] for details.

2.4 Quantization of a CFT

2.4.1 Radial quantization

Suppose we have a conformal field theory defined on the complex plane. We pointed out in chapter 1 that we could choose which direction we prefer for time and space. If for example the time direction t coincides with the real axis and the space direction x with the imaginary axis, we may denote our complex coordinates as

$$z = t + ix \quad (2.82)$$

Actually, when approaching the problem of quantizing a CFT it is typical to let all the points at a fixed time t lying on a circle centered at the origin, while the space direction runs over these circles. This choice leads to the so-called *radial quantization*.

If we want to implement radial quantization it's convenient to put ourselves in a infinite cylinder first, and then turn back to the complex plane. Each point

2. Conformal field theory

of the cylinder is labelled by $\zeta = t + ix$: t is running from $-\infty$ to ∞ , while x takes its value from 0 to L , with the identification $(t, 0) = (t, L)$. We can map the cylinder to the complex plane through the *conformal mapping* (see Fig. 2.1):

$$z = \exp\left(\frac{2\pi\zeta}{L}\right) \quad (2.83)$$

Let's now assume the existence of a vacuum $|0\rangle$, which is invariant under conformal transformations. Since a CFT is generally an interacting theory, we cannot simply apply the quantized version of a field $\hat{\phi}(z, \bar{z})$ to create a state at position (z, \bar{z}) . We need to define the asymptotic state

$$\phi_{\text{in}} = \lim_{t \rightarrow -\infty} \phi(x, t) \quad (2.84)$$

where we suppose that for $t \rightarrow -\infty$ the interactions are negligible. Notice that this is the same approach one uses to define quantum field theories in a curved space-time manifold. Then, in complex coordinates, our "in" state is:

$$|\phi_{\text{in}}\rangle = \lim_{z, \bar{z} \rightarrow 0} \phi(z, \bar{z}) |0\rangle \quad (2.85)$$

This definition, at first sight, is not very precise since we only specify at which time we quantize our field, without any reference to space points. But fortunately in radial quantization all the points such that $t \rightarrow -\infty$ degenerate to the origin $z = 0$ in the complex plane, and this justifies our definition: we are really defining a state at one point (of the complex plane).

If we want to define a scalar product between states, we need as well "out" states. Notice anyway the following important point. In Minkowsky coordinates, the Hermitian conjugation doesn't affect the coordinates, while in Euclidean space it does: the Euclidean time $\tau = it$ is reversed. This corresponds to the mapping $z \rightarrow 1/z^*$ in the plane (remember that time is first defined on the cylinder and then mapped on the complex plane). The definition of an "adjoint" operator is then:

$$[\phi(z, \bar{z})]^\dagger = \bar{z}^{-2\Delta} z^{-2\bar{\Delta}} \phi\left(\frac{1}{\bar{z}}, \frac{1}{z}\right) \quad (2.86)$$

We can justify the prefactors by demanding that

$$\langle \phi_{\text{out}} | \phi_{\text{in}} \rangle = \lim_{\substack{z, \bar{z} \rightarrow 0 \\ w, \bar{w} \rightarrow 0}} = \langle 0 | \phi(z, \bar{z})^\dagger \phi(w, \bar{w}) | 0 \rangle$$

is well defined and doesn't depend on the coordinates (see [17]).

The field $\phi(z, \bar{z})$ can be expanded in modes as:

$$\phi(z, \bar{z}) = \sum_{m \in \mathbb{Z}} \sum_{n \in \mathbb{Z}} z^{-m-\Delta} \bar{z}^{-n-\bar{\Delta}} \phi_{m,n} \quad (2.87)$$

Taking the adjoint of this expression, and comparing it with (2.86) we have $\phi_{m,n}^\dagger = \phi_{-m,-n}$. Furthermore, if the "in" and "out" states are to be well-defined, the vacuum must satisfy:

$$\phi_{m,n} |0\rangle = 0 \quad \text{for } m > -\Delta, n > -\bar{\Delta} \quad (2.88)$$

From now on, we will suppose that each field can be expressed as a product between a holomorphic and an antiholomorphic part, denoted $\phi(z)$ and $\bar{\phi}(\bar{z})$ respectively

$$\phi(z, \bar{z}) = \phi(z) \otimes \bar{\phi}(\bar{z}) \quad (2.89)$$

Their expansions are given by:

$$\phi(z) = \sum_{m \in \mathbb{Z}} z^{-m-\Delta} \phi_m \quad \bar{\phi}(\bar{z}) = \sum_{n \in \mathbb{Z}} \bar{z}^{-n-\bar{\Delta}} \bar{\phi}_n \quad (2.90)$$

and we'll say that the fields $\phi(z)$ and $\bar{\phi}(\bar{z})$ have conformal dimensions Δ and $\bar{\Delta}$ respectively.

2.4.2 The Virasoro algebra

In the correlation functions of a quantum theory, the fields must be time ordered, otherwise we will head for unphysical effects. Now, because of radial ordering, time ordering on the complex plane assumes the following form:

$$\mathcal{R} \phi_1(z) \phi_2(w) = \begin{cases} \phi_1(z) \phi_2(w) & \text{if } |z| > |w| \\ \phi_1(w) \phi_2(z) & \text{if } |z| < |w| \end{cases} \quad (2.91)$$

This allows us to relate OPE with commutation relations. Given two holomorphic fields $a(w)$ and $b(w)$, we define

$$A = \oint a(z) dz \quad (2.92)$$

where the integration is taken at fixed time, if there are no subscripts. Then, it can be shown that:

$$[A, b(w)] = \oint_w dz a(z) b(w) \quad (2.93)$$

If we now define the conformal charge as

$$Q_\epsilon = \frac{1}{2\pi i} \oint dz \epsilon(z) T(z) \quad (2.94)$$

(where in this case the contour is around the point w) it is clear that we can write (2.51) as:

$$\delta\phi(w) = -[Q_\epsilon, \phi(w)] \quad (2.95)$$

2. Conformal field theory

This means that Q_ϵ is the quantum generator of conformal transformations (see [17]). Let's perform a mode expansion of the stress tensor, that is:

$$T(z) = \sum_{n \in \mathbb{Z}} z^{-n-2} L_n \quad (2.96)$$

We remind that, if $z \rightarrow z' = z + \epsilon(z)$, we can write the infinitesimal change of coordinates as:

$$\epsilon(z) = \sum_{n \in \mathbb{Z}} z^{n+1} \epsilon_n \quad (2.97)$$

It follows that:

$$Q_\epsilon = \sum_{n \in \mathbb{Z}} \epsilon_n L_n \quad (2.98)$$

Then, the modes of the holomorphic and antiholomorphic parts of the stress tensors L_n and \bar{L}_n are the *quantum generators* of the conformal transformations, exactly like l_n are the classical generators. They satisfy the *Virasoro algebra*:

$$\begin{cases} [L_n, L_m] = (n-m)L_{n+m} + \frac{c}{12}n(n^2-1)\delta_{n+m,0} \\ [L_n, \bar{L}_m] = 0 \\ [\bar{L}_n, \bar{L}_m] = (n-m)\bar{L}_{n+m} + \frac{c}{12}n(n^2-1)\delta_{n+m,0} \end{cases} \quad (2.99)$$

Like in the classical case, we have that global conformal transformations are generated by L_{-1} , L_0 and L_1 . In particular, $L_0 + \bar{L}_0$ is the generator of the dilations $(z, \bar{z}) \rightarrow \lambda(z, \bar{z})$. But we are using radial quantization, so if we dilate a circle of constant time t we obtain a new circle corresponding to t' . This means that $L_0 + \bar{L}_0$ is indeed the generator of time translations, and is then proportional to the *Hamiltonian* of the system.

2.4.3 The Hilbert space

We now want to study the two spaces of states generated by L_n and \bar{L}_n respectively: the total Hilbert space is the direct sum of these. As a first task, we require the vacuum to be invariant for global conformal transformations: it must be annihilated by L_{-1} , L_0 and L_1 and their antiholomorphic counterparts. This is a subcondition of the requirement that $T(z)|0\rangle$ and $\bar{T}(\bar{z})|0\rangle$ should be well defined, which implies:

$$\begin{cases} L_n |0\rangle = 0 \\ \bar{L}_n |0\rangle = 0 \end{cases} \quad \text{for } n \geq -1 \quad (2.100)$$

Since $L_n^\dagger = L_{-n}$, we also have

$$\langle 0 | T(z) | 0 \rangle = \langle 0 | \bar{T}(\bar{z}) | 0 \rangle = 0 \quad (2.101)$$

Consider now a primary field with conformal dimensions $(\Delta, \bar{\Delta})$. It can be shown that the state

$$|\Delta, \bar{\Delta}\rangle \equiv \phi(0, 0) |0\rangle \quad (2.102)$$

is an eigenstate of the Hamiltonian, with eigenvalue proportional to $\Delta + \bar{\Delta}$:

$$L_0 |\Delta, \bar{\Delta}\rangle = \Delta |\Delta, \bar{\Delta}\rangle \quad \bar{L}_0 |\Delta, \bar{\Delta}\rangle = \bar{\Delta} |\Delta, \bar{\Delta}\rangle \quad (2.103)$$

This follows from (2.93): using the OPE between $T(w)$ and $\phi(z, \bar{z})$, we have

$$[L_n, \phi(z, \bar{z})] = \Delta(n+1) z^n \phi(z, \bar{z}) + z^{n+1} \partial_z \phi(z, \bar{z}) \quad (2.104)$$

which furthermore implies

$$\begin{cases} L_n |\Delta, \bar{\Delta}\rangle = 0 \\ \bar{L}_n |\Delta, \bar{\Delta}\rangle = 0 \end{cases} \quad \text{if } n > 0 \quad (2.105)$$

Now, the Virasoro algebra implies that

$$[L_0, L_{-m}] = mL_{-m} \quad (2.106)$$

This means that we can obtain *excited states* by simply applying operators L_{-m} with $m > 0$. An example of such states is

$$L_{-k_1} L_{-k_2} \dots L_{-k_n} |\Delta\rangle \quad (2.107)$$

where $1 \leq k_1 \leq \dots \leq k_n$ for convention. Notice that we consider only the Hilbert space spanned by holomorphic components of the fields.

$$|\Delta\rangle = \phi(0) |0\rangle$$

We mention that, in a typical quantum field theory, each Fock space is generated by applying on $|0\rangle$ the modes ϕ_m (defined by (2.90)) of a fundamental field, and the Hilbert space is the direct sum of these. Here, our approach is equivalent since, thanks to (see [17])

$$[L_0, \phi_m] = -m \phi_m \quad (2.108)$$

the modes ϕ_m and L_{-m} produce *the same effect* on a given state.

The states (2.107) are eigenstates of L_0 with eigenvalue $\Delta + \sum_i k_i$, and are called *descendants*. The set of all the states $|\Delta\rangle$ and their descendants constitutes a representation of the Virasoro algebra, which is called a *Verma Module*. We have as well a representation where the states of the "Fock space" are the fields themselves, and to every descendant we can associate a *descendant field*. To see this, consider the following descendant:

$$L_{-n} |h\rangle = L_{-n} \phi(0) |0\rangle = \frac{1}{2\pi i} \oint dz z^{1-n} T(z) \phi(0) |0\rangle \quad (2.109)$$

2. Conformal field theory

The descendant field associated to this state is then

$$\phi^{-n}(w) = \frac{1}{2\pi i} \oint_w dz \frac{1}{(z-w)^{n-1}} T(z) \phi(w) \quad (2.110)$$

and an arbitrary descendant field is given by the recursive relation:

$$\phi^{(-k_1, -k_2, \dots, -k_n)}(w) = \frac{1}{2\pi i} \oint_w dz (z-w)^{1-k_1} T(z) \phi^{(-k_2, \dots, -k_n)}(w) \quad (2.111)$$

By definition, all the descendant fields are *secondary fields*. From this last equation we can infer the conformal dimensions of $\phi^{(-k_1, -k_2, \dots, -k_n)}(w)$, which are $(\Delta + \sum_i k_i, \bar{\Delta} + \sum_i k_i)$. The set of a given primary field and all its descendants is called a *conformal family*, and we will denote it with $[\phi]$.

It's easy to obtain all the possible existing fields of a certain CFT. We start from the set of its primary fields $\{\phi_i(z, \bar{z})\}$: this can be infinite, and there can be fields with the same conformal dimensions. We then build all the secondary fields by simply performing integrals like (2.110). It's really important to realize that the scaling dimension of a scalar secondary field is always greater than 2, since by definition $k_i > 1$: it follows (see (2.32)) that the only relevant fields are primary fields. Since a theory has typically only a finite number of relevant fields (we have seen for example that the Ising model has 2 of these), we would like it to have a *finite number* of primary operators.

Furthermore, we require that all correlation functions must be positive, that is we require a theory to be *unitary*. We will deal with these issues in the next sections.

2.4.4 Verma modules and Kac table

The Fock space built up from a state $|\Delta\rangle \equiv \phi(0)|0\rangle$ is called a *Verma module*. The set of raising operators $\{L_{-n}\}$ can be applied to the highest weight states $|\Delta\rangle$ (the terminology derives from the representation theory of Lie algebras) to form a descendant state, which has the form:

$$L_{-k_1} L_{-k_2} \dots L_{-k_n} |0\rangle \quad (2.112)$$

This is an eigenvector of the "Hamiltonian" L_0 , with eigenvalue

$$\Delta' = \Delta + \sum_i k_i \equiv \Delta + N \quad (2.113)$$

N is called the *level* of a string operator. All the states with the same level form a subspace of eigenvectors with the same "energy" given by (2.113). The number of states $p(N)$ at a given level N is simply the number of partitions of the integer N . The generating functions of $p(N)$ is the *Euler function*:

$$\frac{1}{\varphi(q)} \equiv \prod_{n=1}^{\infty} \frac{1}{1-q^n} = \sum_{n=1}^{\infty} p(n) q^n \quad (2.114)$$

To see this, use the formula for a geometric series

$$\frac{1}{1 - q^n} = \sum_{n=0}^{\infty} q^n$$

and rearrange all terms. We can define a dual state by

$$(L_{-k_1} \dots L_{-k_n} |0\rangle)^\dagger \equiv \langle \Delta | L_{k_n} \dots L_{k_1} \quad (2.115)$$

which satisfies:

$$\langle \Delta | L_j = 0 \quad \text{if } j < 0 \quad (2.116)$$

The inner product between two states

$$L_{-k_1} \dots L_{-k_n} |\Delta\rangle \quad \text{and} \quad L_{-l_1} \dots L_{-l_m} |\Delta\rangle \quad (2.117)$$

is clearly

$$\langle \Delta | L_{k_n} \dots L_{k_1} L_{-l_1} \dots L_{-l_m} | \Delta \rangle \quad (2.118)$$

and can be evaluated using the Virasoro algebra. Furthermore, states belonging to different levels are orthogonal. If we denote with $V(c, \Delta)$ the Verma module generated by a field, with conformal dimension Δ , belonging to a theory with central charge c , then the Hilbert space of a given theory is the tensor product:

$$\sum_{\Delta, \bar{\Delta}} \mathcal{N}_{\Delta, \bar{\Delta}} V(c, \Delta) \otimes \bar{V}(c, \bar{\Delta}) \quad (2.119)$$

This means that a theory has the set primary fields $\{\phi_{\Delta, \bar{\Delta}}\}$ where each field $\phi_{\Delta, \bar{\Delta}}$ generates the space $V(c, \Delta) \otimes \bar{V}(c, \bar{\Delta})$, and a number of $\mathcal{N}_{\Delta, \bar{\Delta}}$ fields have the same conformal dimensions.

Now, it may happen that a Verma module $V(c, \Delta)$ is *reducible*. By this we mean that there is a subspace of $V(c, \Delta)$ which is itself a representation of the Virasoro algebra. This is so if there exists a vector $|\chi\rangle$ satisfying

$$L_n |\chi\rangle = 0 \quad \text{for } n > 0 \quad (2.120)$$

The vector $|\chi\rangle$ then behaves like a generic highest weight state (see equation (2.105)), thus we can build a Verma module V_χ included in $V(c, \Delta)$. Furthermore, it's clear that $|\chi\rangle$ is orthogonal to the whole Verma module, and in particular to itself: $|\chi\rangle$ is therefore a *null vector*. Thanks to this property it can be shown that all the descendants of $|\chi\rangle$ are orthogonal to the whole Verma module as well, and they all have zero norm.

If we want to recover an irreducible representation we need to identify states that differs only by a state of zero norm: this is equivalent to quotienting out the null submodule V_χ . We will call this irreducible representation $M(c, \Delta)$.

2. Conformal field theory

A representation $V(c, \Delta)$ is said to be *unitary* if all the states have positive norm. To understand when is this the case, we define the *Gram matrix* as the matrix of the inner products between all states of a Verma module:

$$M_{ij} = \langle i | j \rangle \quad (2.121)$$

This matrix is hermitian ($M^\dagger = M$) and block diagonal: denote with $M^{(l)}$ the block corresponding to the states at level l . Now, an arbitrary state $|a\rangle$ whose expansion is $|a\rangle = \sum_i a_i |i\rangle$ has norm

$$\langle a | a \rangle = a^\dagger M a = \sum_i \Lambda_i |b_i|^2 \quad (2.122)$$

where Λ_i are the eigenvalues of the Gram matrix M and $b = Ua$, where U is the matrix that diagonalizes M . It follows that a representation is unitary if all the eigenvalues of the Gram matrix are positive, and contains null vectors if one of these is zero. A way to understand when a representation is unitary is to study the determinant of the Gram matrix, which takes the name of *Kac determinant*, given by the following formula due to Kac:

$$\det M^{(l)} = \alpha_l \prod_{\substack{r,s \geq 1 \\ rs \leq l}} (\Delta - \Delta_{r,s}(c))^{p(l-rs)} \quad (2.123)$$

where α_l is a constant and $p(l-rs)$ is defined by (2.114). Using the Kac determinant one can show that representations with $c \geq 1$ and $\Delta \geq 0$ are all unitary, and for $c < 1$ unitarity is recovered for primary fields whose dimensions are given by one of the $\Delta_{r,s}(c)$ (see [17]).

Furthermore, this formula tells us that we have null vectors if the dimension of the primary field over which we construct $V(c, \Delta)$ is equal to some $\Delta_{r,s}(c)$. If this is the case, we denote our primary fields as $\phi_{(r,s)}$. The functions $\Delta_{r,s}(c)$ can be expressed in various ways. One of these is:

$$\begin{aligned} \Delta_{r,s}(c) &= \Delta_0 + \frac{1}{4}(r\alpha_+ + s\alpha_-)^2 \\ \Delta_0 &= \frac{1}{24}(c-1) \\ \alpha_\pm &= \frac{\sqrt{1-c} \pm \sqrt{25-c}}{\sqrt{24}} \end{aligned} \quad (2.124)$$

A very important fact is that the set of conformal families generated by $\{\phi_{(r,s)}\}$ closes under the operator algebra, which means that the OPE of two such fields can be expressed as a sum involving only the same kind of fields. This statement is made rigorous by the following relation:

$$\phi_{(r_1,s_1)} \times \phi_{(r_2,s_2)} = \sum_{\substack{k=r_1+r_2-1 \\ k=1+|r_1-r_2| \\ k+r_1+r_2=1 \pmod{2}}}^{k=r_1+r_2-1} \sum_{\substack{l=s_1+s_2-1 \\ l=1+|s_1-s_2| \\ l+s_1+s_2=1 \pmod{2}}} \phi_{(k,l)} \quad (2.125)$$

Table 2.1: The Kac table for the minimal model $\mathcal{M}(4, 3)$, with central charge $c = \frac{1}{2}$.

$\frac{1}{2}$	$\frac{1}{16}$	0
0	$\frac{1}{16}$	$\frac{1}{2}$

Formula (2.125) is an OPE (denoted by the symbol \times) written in a concise way. It states that only the primary fields with conformal dimensions $\Delta_{r,s}$ appearing in the sum on the r.h.s. contribute to the OPE $\phi_{(r_1,s_1)}\phi_{(r_2,s_2)}$. The coefficients are suppressed for clarity, and writing $\phi_{(k,l)}$ on the r.h.s. we mean that all the fields of its conformal family may contribute. We refer to [17] for the details of the demonstration. Notice that, in generality, we need an infinite number of conformal families to close the algebra.

Now, it can be shown that, if two coprime integers p and p' exist such that $p\alpha_- + p'\alpha_+ = 0$, we have the periodicity property

$$\Delta_{r,s} = \Delta_{r+p',s+p} \tag{2.126}$$

to which corresponds:

$$c = 1 - \frac{(p-p')^2}{pp'} \tag{2.127}$$

$$\Delta_{r,s} = \frac{(pr - p's)^2 - (p-p')^2}{4pp'}$$

This is a really important statement since in (2.125) we then only need a *finite number* of conformal families to close the algebra. That is, for such values of the parameters α_{\pm} we have a finite number of distinct primary fields $\phi_{(r,s)}$, where the subscripts are delimited by

$$\begin{cases} 1 \leq r < p' \\ 1 \leq s < p \end{cases} \tag{2.128}$$

Since from (2.127) it follows that

$$\Delta_{r,s} = \Delta_{p'-r,p-s} \tag{2.129}$$

we can identify the fields $\phi_{(r,s)}$ and $\phi_{(p'-r,p-s)}$. Then, the number of distinct primary fields of our theory is:

$$\frac{(p-1)(p'-1)}{2}$$

These are usually organized in what is called a *Kac table*, see for example table 2.1. In other words, if a theory has an infinite set of primary fields, we can restrict ourselves to the subset of conformal families generated by $\{\phi_{(r,s)}\}$,

2. Conformal field theory

with $\Delta_{r,s}$ given by (2.127): we will never need to use the other fields of the theory since (2.125) is enough to compute all the correlation functions between field belonging to the conformal families of $\{\phi_{(r,s)}\}$. The theories built up from $\{\phi_{(r,s)}\}$ are called *Minimal models*, and we'll refer to them as

$$\mathcal{M}(p', p)$$

Furthermore, we stated without demonstration that the representation involving such fields are *unitary*. But these, as we discussed at the end of section 2.4.3, are the requirements we demanded for a CFT to describe a statistical model. Then, we expect that all our models are described conformal field theories whose central charges is of the form (2.127). Since c depends on p , and p' , we then have that the central charge determines the field content of a theory (as we anticipated in section 2.3.3), and the dimensions $\Delta_{r,s}$ are delimited by

$$1 \leq r < p' \quad 1 \leq s < p \quad (2.130)$$

To give an example, consider the minimal model $\mathcal{M}(4, 3)$, with central charge $c = \frac{1}{2}$. This corresponds to $p = 4$ and $p' = 3$, so we'll have the three primary fields \mathbb{I} , $\phi_{(2,2)}$ and $\phi_{(2,1)}$, with conformal dimensions $\Delta_{1,1} = 0$, $\Delta_{2,2} = 1/16$ and $\Delta_{2,1} = 1/2$. If we consider scalar fields, then $\Delta = \bar{\Delta}$, and the two point correlation functions are, using (2.80):

$$\langle \phi_{(2,1)}(z, \bar{z}) \phi_{(2,1)}(0, 0) \rangle = \frac{1}{z^{1/8} \bar{z}^{1/8}} \quad \langle \phi_{(2,2)}(z, \bar{z}) \phi_{(2,2)}(0, 0) \rangle = \frac{1}{z \bar{z}} \quad (2.131)$$

Consider now the Ising model. We saw that this model has two relevant fields: the spin operator σ_i and the energy operator ϵ_i . It is known by exact solution that:

$$\langle \sigma_i \sigma_{i+n} \rangle = \frac{1}{|n|^{1/4}} \quad \langle \epsilon_i \epsilon_{i+n} \rangle = \frac{1}{|n|^2} \quad (2.132)$$

This strongly suggests that, since (2.132) and (2.131) are the same with $|n| = z\bar{z}$, the Ising model is described by scalar fields whose holomorphic and antiholomorphic parts belong to a $c = \frac{1}{2}$ conformal field theory.

To described other models, such as the three states Potts model, we will need fields with *spin*, but we won't develop this topic here, and we refer again to [17] for details.

2.5 CFT on a torus: modular invariance

In the last section we gave a hint on how to find all the primary (relevant) fields of a statistical system. Here, given a minimal model, we want to face the problem of *how many fields* are there with a same conformal dimensions, and *which fields* of the minimal model appear. This can be solved by requiring the modular invariance of a CFT defined on the torus.

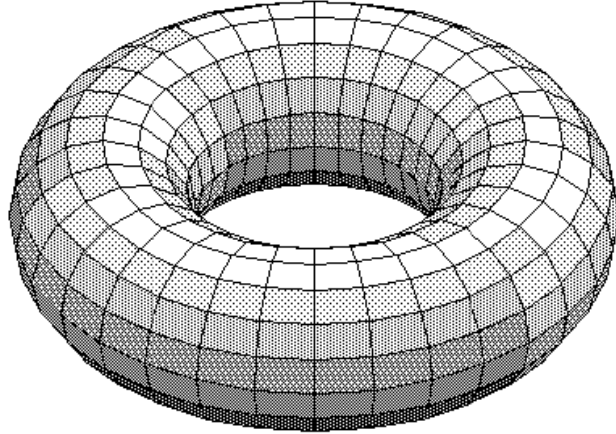


Figure 2.2: A torus.

A torus in complex coordinates may be defined as a complex plane with two periodic directions (see fig. 2.2), which we denote with ω_1 and ω_2 . It is characterized by the *modular parameter*

$$\tau = \frac{\omega_2}{\omega_1} \quad (2.133)$$

Let's compute the partition function of a CFT defined on a torus. This object must be invariant under translations by $\omega_{1,2}$. We define space and time directions running over the real and the imaginary axis respectively. Recall from chapter 1 that the partition function of a 2 dimensional classical system is:

$$Z = \langle \sigma_1 | T^M | \sigma_M \rangle \quad (2.134)$$

where M is the rows number of the lattice. Since we require periodic boundary conditions, from (1.4) we have that the partition functions is expressed as a trace:

$$Z = \text{Tr}(T^M) = \text{Tr}(e^{H_{\text{lattice}}}) \quad (2.135)$$

As we discussed in chapter 1, the transfer matrix acts like an evolution operator. But now we quantized our theory, and in a quantum theory the evolution operator has the form:

$$\exp (iaG)$$

We then suppose, roughly speaking, that the space of classical spin configuration $|\sigma\rangle$ is described by the states of the form (2.112), belonging to a representation of the Virasoro algebra. Here G is the generator of the translations: it corresponds to H for time translations, and P for space translations. It can be shown that the Hamiltonian and the momentum operator on the plane, using radial quantization, are given by:

$$H = \frac{2\pi}{L} \left(L_0 + \bar{L}_0 - \frac{c}{12} \right) \quad P = \frac{2\pi i}{L} (L_0 - \bar{L}_0) \quad (2.136)$$

2. Conformal field theory

We've already seen that the Hamiltonian is proportional to the combination of Virasoro generators $L_0 + \bar{L}_0$. The form of P can be justified by noting that $L_0 - \bar{L}_0$ generates the rotations in the complex plane, which are spatial translations in the view of radial quantization. If the classical lattice spacing is a , the evolution operator that translates the system parallel to the ω_2 direction is then:

$$\exp\left[-\frac{a}{|\omega_2|}(H \operatorname{Im}(\omega_2) - iP \operatorname{Re}(\omega_2))\right] \quad (2.137)$$

Suppose now that ω_1 is real and equal to L , which implies $|\omega_2| = Ma$. To compute the partition function, we need to take the trace of the operator (2.137) to the M -th power, which gives:

$$Z(\omega_1, \omega_2) = \operatorname{Tr}\left(\exp(H \operatorname{Im}(\omega_2) - iP \operatorname{Re}(\omega_2))\right) \quad (2.138)$$

If we now write $\operatorname{Re}(\omega_2)$ and $\operatorname{Im}(\omega_2)$ as functions of τ and $\bar{\tau}$, and define

$$q = \exp(2\pi i\tau) \quad \bar{q} = \exp(-2\pi i\bar{\tau}) \quad (2.139)$$

we can express the partition function as:

$$Z(\tau) = \operatorname{Tr}\left(q^{L_0 - c/24} \bar{q}^{\bar{L}_0 - c/24}\right) \quad (2.140)$$

Let's work with minimal models. As we saw in section 2.4.4, a certain theory is described by the Hilbert space

$$\mathcal{H} = \bigoplus_{(r,s),(t,u) \in E_{p,p'}} \mathcal{M}_{(r,s);(t,u)} M(c, \Delta_{r,s}) \otimes M(c, \bar{\Delta}_{t,u}) \quad (2.141)$$

where $E_{p,p'}$ is the domain of the couple of variables (r, s) and (t, u) . Notice that in general $(r, s) \neq (t, u)$: this allows the existence of fields with spins, that is whose left and right conformal dimensions are different. We can write (2.140) as:

$$Z(\tau) = \sum_{(r,s),(t,u) \in E_{p,p'}} \mathcal{M}_{(r,s);(t,u)} \chi_{r,s}(\tau) \bar{\chi}_{t,u}(\bar{\tau}) \quad (2.142)$$

The number $\mathcal{M}_{(r,s);(t,u)}$ denotes how many primary fields of the theory have the same conformal dimensions $(\Delta_{r,s}, \bar{\Delta}_{t,u})$. From another point of view, it describes how many times the tensor product $M(c, \Delta_{r,s}) \otimes M(c, \bar{\Delta}_{t,u})$ appears in the Hilbert space. Moreover, we define the *Virasoro characters* as:

$$\chi_{r,s}(\tau) = \operatorname{Tr}_{M(c, \Delta_{r,s})}(q^{L_0 - c/24}) = q^{\Delta - c/24} \sum_{n \geq 0} d(n) q^n \quad (2.143)$$

where $d(n)$ is the number of states at level n of the Virasoro representation built on the holomorphic field $\phi_{(r,s)}$. We can say, roughly speaking, that a Virasoro character counts how many states are there in a representation.

2.5. CFT on a torus: modular invariance

Now, the partition function on the torus must satisfy *modular invariance*. On the plane, we can always redefine the parameters $\omega_{1,2}$ as:

$$\begin{pmatrix} \omega'_1 \\ \omega'_2 \end{pmatrix} = \begin{pmatrix} a & b \\ c & d \end{pmatrix} \begin{pmatrix} \omega_1 \\ \omega_2 \end{pmatrix} \quad (2.144)$$

where $a, b, c, d \in \mathbb{Z}$. This is a modular transformation: it changes the periodicity directions on the plane, but since we only take integer combinations, the $\omega'_{1,2}$ describe the same torus of $\omega_{1,2}$. Equation (2.144) defines a matrix of integers. The inverse matrix must obviously be of the same form, and if we choose the convention $ad - bc = 1$ (which is not restrictive), these transformations form a group isomorphic to $SL(2, \mathbb{Z})$, the group of integer, invertible matrices with unit determinant. The modular parameter transforms as

$$\tau \rightarrow \frac{a\tau + b}{c\tau + d} \quad (2.145)$$

It can be shown that every modular transformation can be written as a product involving only the following transformations:

$$\mathcal{T} : \tau \rightarrow \tau + 1, \quad \mathcal{S} : \tau \rightarrow -\frac{1}{\tau} \quad (2.146)$$

described by the matrices

$$T = \begin{pmatrix} 1 & 1 \\ 0 & 1 \end{pmatrix} \quad S = \begin{pmatrix} 0 & 1 \\ -1 & 0 \end{pmatrix} \quad (2.147)$$

As a last step to construct partition functions invariant under modular transformations, we need to know how the Virasoro characters transform under \mathcal{T} and \mathcal{S} . It can be shown that:

$$\begin{aligned} \chi_{r,s}(\tau + 1) &= \sum_{(\rho,\sigma) \in E_{p,p'}} \mathcal{T}_{(r,s);(\rho,\sigma)} \chi_{\rho,\sigma}(\tau) \\ \mathcal{T}_{(r,s);(\rho,\sigma)} &= \delta_{r,\rho} \delta_{s,\sigma} \exp \left[2i\pi \left(\Delta_{r,s} - \frac{c}{24} \right) \right] \end{aligned} \quad (2.148)$$

and

$$\begin{aligned} \chi_{r,s} \left(-\frac{1}{\tau} \right) &= \sum_{(\rho,\sigma) \in E_{p,p'}} \mathcal{S}_{(r,s);(\rho,\sigma)} \chi_{\rho,\sigma}(\tau) \\ \mathcal{S}_{(r,s);(\rho,\sigma)} &= 2\sqrt{\frac{2}{pp'}} (-1)^{1+s\rho+r\sigma} \sin \left(\pi \frac{p}{p'} r \rho \right) \sin \left(\pi \frac{p'}{p} s \sigma \right) \end{aligned} \quad (2.149)$$

Let's now make some examples. Thanks to the unitarity of \mathcal{S} we have a first modular invariant partition function:

$$Z = \sum_{(r,s) \in E_{p,p'}} |\chi_{r,s}|^2 \quad (2.150)$$

2. Conformal field theory

which is said to be *diagonal*. Here we have only scalar fields, and all the fields of the minimal model appear, with no copies. Recall that the Ising model is described by scalar fields whose holomorphic components belong to $\mathcal{M}(4, 3)$ (see the Kac table 2.1). Then, the partition function of the Ising model defined on the torus is

$$Z = |\chi_{1,1}|^2 + |\chi_{2,1}|^2 + |\chi_{1,2}|^2 \quad (2.151)$$

Other examples of modular invariant partition functions can be found for $p'/2$ odd: the characters combination $\chi_{r,s} + \chi_{p'-r,s}$ is then invariant under \mathcal{S} and is multiplied by a phase under \mathcal{T} . This implies that the following diagonal combination

$$Z = \sum_{r \text{ odd}, s} |\chi_{r,s} + \chi_{p'-r,s}|^2 \quad (2.152)$$

is a modular invariant. A similar partition function can be constructed if $p/2$ is odd. These modular invariants, among others, are not arranged in a casual manner, but follow the so called *ADE classification*: see [17], [24] or [26] for details.

2.6 Out of the critical point

In the previous sections we dealt with CFT, which means that the statistical systems associated to a quantum field theory were all at criticality. We now want to describe these systems out of criticality, where conformal invariance doesn't hold anymore, maintaining the field theory approach. The idea is to start from a given action, which is conformal invariant, and then *perturb* it with some fields $\Phi_i(x)$:

$$S = S^{\text{CFT}} + \sum_{i=1}^n \lambda_i \int \Phi_i(x) d^2x \quad (2.153)$$

We know that, at the fixed point, the two-point correlation function of two primary fields behaves like:

$$G_i(r) \equiv \langle \phi_i(r) \phi_i(0) \rangle \simeq \frac{\delta_{ij}}{r^{2d_j}} \quad \text{for } r \rightarrow 0 \quad (2.154)$$

where d_j is the scaling dimension of the field ϕ_j . While the lattice spacing changes as $a \rightarrow ba$, the coupling constants g will flow in the scaling region, and in general there are two different physical scenarios associated to (2.153) (see [26]):

- The final point of the RG flow is also a fixed point to another conformal field theory. This means that our theory is described by S^{CFT} at the beginning of the flow (the ultraviolet region), while is described by another CFT action S^* at the end of the flow (the infrared region). We remind

that the ultraviolet region concerns with very short distances, while for the infrared region is the opposite. This means that, in the two regimes, the two-point correlation functions will have the following behaviour:

$$G_i(r) = \begin{cases} r^{-2d_i^{\text{uv}}}, & r \rightarrow 0 \\ r^{-2d_i^{\text{ir}}}, & r \rightarrow \infty \end{cases} \quad (2.155)$$

where $d_i^{\text{uv}} \neq d_i^{\text{ir}}$, because the two conformal field theories are different. We will see later how the central charges of the two theories are related.

- The final point of the RG flow is not a CFT anymore, and the system acquires a *finite* correlation length ξ : the infrared behaviour of the theory is ruled by a massive QFT. The two-point correlation functions now behave like:

$$G_i(r) = \begin{cases} r^{-2d_i^{\text{uv}}}, & r \rightarrow 0 \\ e^{-m_i r}, & r \rightarrow \infty \end{cases} \quad (2.156)$$

Here, $m_i = \xi^{-1}$ is the mass of the lightest particle that couples to ϕ_i .

2.6.1 Conformal Perturbation Theory

A quantum field theory is solved if we know all its correlation functions, that is all the measurable quantities. One of the main approach to deal with field theories out of the fixed point is the *conformal perturbation theory*. What one does is to consider a theory that is solvable, and perturb its action with some powers of the basic fields. In 4-dimensional QFT, the solvable theory is typically a free theory. Consider for example the $\lambda\phi^4$ theory, whose action is:

$$S = \int d^4x \left(\frac{1}{2}(\partial_\mu\phi)^2 + \frac{1}{2}m^2\phi^2 + \frac{\lambda}{4!}\phi^4 \right) \quad (2.157)$$

The correlation functions of this QFT are expressed as powers of λ , whose coefficients are correlation functions of the free theory, which in principle are all calculable. Here, instead, we start from the QFT at the *fixed point*, that is the CFT, and then perturb its action S^{CFT} , for example, with $\lambda \int \Phi(x) d^2x$. The correlation function of a set of observables A is then expressed as:

$$\begin{aligned} \langle A \rangle_\lambda &= \frac{1}{Z_\lambda} \left\langle A e^{-\lambda \int d^2x \Phi(x)} \right\rangle_0 \\ &= \frac{1}{Z_\lambda} \sum_{n=0}^{\infty} \frac{(-\lambda)^n}{n!} \int d^2x_1 \dots d^2x_n \langle A \phi(x_1) \dots \phi(x_n) \rangle_0 \end{aligned} \quad (2.158)$$

If $\lambda \rightarrow 0$, the theory is at its conformal point, so Φ must tend to some field of the set all the conformal families of the theory (this is valid also for more than

2. Conformal field theory

one coupling constant). Because the coefficients of λ^n are evaluated for $\lambda = 0$, we must perform the replacement $\Phi \rightarrow \phi$ in the correlation functions.

In general, S^{CFT} may be perturbed by more than one field, so in more generality we have:

$$S = S^{\text{CFT}} + \sum_i \lambda_i \int \Phi_i(x) d^2x \quad (2.159)$$

The coupling constants of the renormalization group theory must be adimensional, so these are truly given by:

$$g_i = \mu^{-d_\lambda} Z_{g_i} \lambda_i \quad (2.160)$$

where d_λ is the scaling dimension of λ , and Z_{g_i} describes the change of g under renormalization. This naturally introduces a *scale* μ , which is usually taken as the mass of the lightest particle:

$$\mu = D_i \lambda^{\frac{1}{2\epsilon_i}} \quad (2.161)$$

As a first condition on this action, we require that it's invariant under dilations, since theories belonging to the same RG flow are equivalent, which means that they have the same partition function $Z = \int \mathcal{D}\varphi \exp(-S[\varphi])$. Furthermore, we want this action to be invariant under rotation: this implies that Φ_i must be *scalar fields*. It is known (see for example [32]) that a QFT is renormalizable if all the coupling constant λ_i has a scaling dimension that satisfy $d_\lambda \geq 0$. If our perturbing fields are all *relevant*, then d_{λ_i} are all strictly positive, so our theories are of the super-renormalizable type: only a finite number of Feynman diagrams superficially diverges. In this case, the fields Φ_i must tend, in the limit $\lambda \rightarrow 0$, to *primary fields* ϕ_i of the CFT, more exactly to some scalar primary fields. If these have scalar dimension $x_i = 2\Delta_i$, for the action to be invariant under dilations we require $d_{\lambda_i} = 2 - 2\Delta_i$. The primary fields are the only fields of the CFT with $\Delta < 1$, so are the only ones that ensure $d_{\lambda_i} > 0$.

We now show that, under renormalization, the fields change as:

$$\Phi_i(x, g) \rightarrow \left(Z(g)^{-1/2} \right)_i^j \phi_j(x, g) \quad (2.162)$$

where ϕ_j are certain fields of the unperturbed theory (that is, the CFT). We won't develop the whole problem here, and we refer to *e.g.* [26] for further details. In general, a correlation function will have both ultraviolet and infrared divergencies. Consider the action $S = S^{\text{CFT}} + \lambda \int \Phi(x) d^2x$, and perturb it with only one field $\Phi(x)$, satisfying $\Phi \xrightarrow{\lambda \rightarrow 0} \phi(x)$. Consider then a generic field $\Psi(x)$, such that $\Psi \xrightarrow{\lambda \rightarrow 0} \psi(x)$, where this time $\psi(x)$ may be *any* field of the CFT. For a generic set of fields X , we have, using (2.158):

$$\langle X\Psi(0) \rangle_\lambda \simeq \langle X\psi(0) \rangle_0 - \lambda \int_{\epsilon < |x| < R} d^2x \langle X\psi(0)\phi(x) \rangle_0 + O(\lambda^2) \quad (2.163)$$

where we have introduced, respectively, the ultraviolet and infrared cutoffs R , ϵ . If we want to cure the ultraviolet divergence at the first order in λ , notice that the integral diverges for $x \rightarrow \infty$ only if the OPE

$$\phi(x) \psi(0) = \sum_k C_{\phi\psi}^k |x|^{2(\Delta_k - \Delta_\psi - \Delta_\phi)} B_k(0) \quad (2.164)$$

contains the fields B_k of the CFT with conformal fields Δ_k such that:

$$\gamma_k \equiv \Delta_k - \Delta_\psi - \Delta_\phi + 1 \leq 0 \quad (2.165)$$

Then, the renormalized operator is defined by:

$$\Psi(x) = \psi(x) + \lambda \sum_k b_k e^{2\gamma_k} B_k(x) + O(\lambda^2) \quad (2.166)$$

Notice that Ψ , after the renormalization procedure, is not just a function of its limit field ψ : the renormalization procedure induces a *mixing* between the fields out of the fixed point and the fields of the CFT.

2.6.2 The Callan-Symanzik equation

We now discuss the variation of a correlation function of generic fields $A_i(x_i)$, defined as

$$\langle A_1(x_1) \dots A_n(x_n) \rangle = \int \mathcal{D}\phi A_1(x_1) \dots A_n(x_n) e^{-S[\phi]} \quad (2.167)$$

(where the normalization constant $1/Z$ has been absorbed in $\exp(-S[\phi])$) under the renormalization group flow, that is under a change of the cutoff $a \rightarrow ba \equiv e^t a$. The dilation factor is $b = e^t$, so every point of the flow is parametrized by t , which plays a role similar to time in classical mechanics. Accordingly, the coupling constants $g \equiv g(t)$ will depend on t . It is important to realize that the action

$$S(g, a) = \int d^2x \mathcal{L}_g \quad (2.168)$$

depends both on g and implicitly on the cutoff a . Let's now perform a dilation of the coordinates:

$$x^\mu \rightarrow x'^\mu = x^\mu + \epsilon^\mu \quad (2.169)$$

where $\epsilon^\mu = \epsilon x^\mu$. The fields will change as $A_i(x) \rightarrow A_i(x) + \delta A_i(x)$, and the variation of the action is given by (2.34):

$$\delta S = \int d^2x T_{\mu\nu}(x) \partial^\mu \epsilon^\nu(x) = \epsilon \int d^2x \Theta(x) \quad (2.170)$$

2. Conformal field theory

where the trace of the stress tensor energy is $\Theta(x) = T^\mu_\mu(x)$, and we absorbed a factor $1/(2\pi)$ in its definition. Thanks to (2.168), this can be written as:

$$\Theta(x) = \frac{d\mathcal{L}_g}{dt} \quad (2.171)$$

because the coordinates change as $x'^\mu = e^{-t}x^\mu$, and for infinitesimal transformation we have $\epsilon = dt$, apart for a sign.

Varying all the terms in (2.167), we obtain:

$$\sum_{i=1}^n \langle A_1(x_1) \dots \delta A_i(x_i) \dots A_n(x_n) \rangle - \epsilon \int d^2x \langle \Theta(x) A_1(x_1) \dots A_n(x_n) \rangle = 0 \quad (2.172)$$

It can be shown ([17]) that, under a dilation, the variations of the fields are:

$$\delta A_i(x) = \epsilon \left(\frac{1}{2} x^\mu \partial_\mu + \hat{D} \right) A_i(x) \quad (2.173)$$

where \hat{D} is the operator that implements the internal transformation of the fields. Its eigenvalues are the scaling dimensions of the fields.

Now, the fields of the theory are defined as

$$\phi_i(x) = \frac{\partial \mathcal{L}_g}{\partial g_i} \quad (2.174)$$

and if \mathcal{L}_g is a local Lagrangian, then the fields are local as well. Thanks to this last equation we can write:

$$\Theta(x) = \sum_a \frac{\partial \mathcal{L}_g}{\partial g_a} \frac{\partial g_a}{\partial t} = \sum_a \frac{\partial g_a}{\partial t} \phi_a(x) \quad (2.175)$$

If we consider only homogeneous and isotropic interactions, then the ϕ_i are scalar fields, and from the point of view of the differential geometry, these will span the tangent space at a given point (g_0, g_1, \dots) of the manifold of the coupling constants. This means that they form a basis for the set of scalar fields, and since Θ belongs to this space, we have:

$$\Theta(x) = \sum_a \beta^a(g) \phi_a(x) \quad (2.176)$$

where the coefficients $\beta^a(g)$ are the *beta functions* of the theory. Comparing with (2.175):

$$\beta^a(g) = \frac{\partial g_a}{\partial t} \quad (2.177)$$

so the beta functions express the variation of the coupling constants under the RG flow. Furthermore, since at a fixed point the coupling constants g^* don't vary for definition, it follows that:

$$\beta^a(g^*) = 0 \quad (2.178)$$

Now, the fields $A_i(x)$ may depend on the coupling constants as well, and we express their variation under a RG flow with an operator \hat{B}_i as:

$$\hat{B}_k A_i(x) = \frac{\partial}{\partial g_k} A_i(x) \quad (2.179)$$

If we take the partial derivative of $\langle A_1(x_1) \dots A_n(x_n) \rangle$ with respect to g_a we have, using (2.174):

$$\begin{aligned} \frac{\partial}{\partial g_a} \langle A_1(x_1) \dots A_n(x_n) \rangle &= \sum_{i=1}^n \left\langle A_1(x_1) \dots \hat{B}_a A_i(x_i) \dots A_n(x_n) \right\rangle \\ &\quad - \int d^2x \langle \phi_a(x) A_1(x_1) \dots A_n(x_n) \rangle \end{aligned} \quad (2.180)$$

Multiplying both sides by $\beta^a(g)$, summing over a and using (2.176), we finally obtain the *Callan-Symanzik equation*:

$$\begin{aligned} \sum_{i=1}^n \left\langle \left(\frac{1}{2} x_i^\mu \frac{\partial}{\partial x_i^\mu} + \hat{\gamma}^{(i)}(g) \right) A_1(x_1) \dots A_n(x_n) \right\rangle \\ - \sum_a \beta^a(g) \frac{\partial}{\partial g_a} \langle A_1(x_1) \dots A_n(x_n) \rangle = 0 \end{aligned} \quad (2.181)$$

where we defined $\hat{\gamma}(g) = \hat{D} + \beta^a(g) \hat{B}_a$. Comparing this equation with (2.172), we can interpret $\hat{\gamma}$ as an operator whose eigenvalues are the *anomalous dimensions* of the fields.

Let's see how to determine the first terms of the beta functions. We will perform infinitesimal transformations in the RG flow, and we'll take advantage of the invariance of the partition function under this transformation (remember that theories belonging to the same flow describe the same physics). If we set $g_i = \lambda_i a^{2(1-\Delta_i)}$, and impose the ultraviolet cutoff a , we have:

$$\begin{aligned} Z &= \int \mathcal{D}\varphi \exp \left[-S^* - \sum_i g_i \int \frac{d^2x}{a^{2(1-\Delta_i)}} \varphi_i(x) \right] \\ &= Z^* \left[1 - \sum_i g_i \int \frac{d^2x}{a^{2(1-\Delta_i)}} \langle \varphi_i(x) \rangle \right. \\ &\quad \left. + \frac{1}{2} \sum_{i,j} g_i g_j \int_{|x_1-x_2|>a} \langle \varphi_i(x_1) \varphi_j(x_2) \rangle \frac{d^2x_1}{a^{2(1-\Delta_i)}} \frac{d^2x_2}{a^{2(1-\Delta_j)}} + \dots \right] \end{aligned} \quad (2.182)$$

If we perform the infinitesimal scale transformation $a \rightarrow (1+dt)a$, the problem is now to understand how the g_i will transform so to leave Z invariant. To the first order, this task is simple:

$$g_i \rightarrow (1+dt)^{2(1-\Delta_i)} g_i \simeq g_i + 2(1-\Delta_i) g_i dt \quad (2.183)$$

2. Conformal field theory

At second order, we must pay attention to the transformation of the cutoff in the integral (see [26] for further details). Taking derivatives of the coupling constants, the beta functions have the following *universal behaviour*:

$$\frac{dg_k}{dt} \equiv \beta_k(g) = 2(1 - \Delta_k)g_k - \pi \sum_{i,j} \mathbf{C}_{ijk} g_i g_j + O(g^3) \quad (2.184)$$

The higher order terms can be computed, in principle, iterating the above procedure. However, we won't discuss this here, since the calculations are rather involved.

2.6.3 Zamolodchikov's c theorem

We know that the RG procedure reduces the degrees of freedom of the theory: if we move along the flow, we lose informations about the previous action S . Two theories that belong to the same RG flow are equivalent: if we compute the correlation functions of observables evaluated in points \vec{x}_i such that $|\vec{x}_i - \vec{x}_j| \rightarrow \infty$ for all i and j , these tend to the same limit. But, moving along the flow, we are not able anymore to evaluate correlation functions below the ultraviolet cutoff. So in this sense the flow is *irreversible* ([37]). The quantity that somehow describes how large is the space of the degrees of freedom is the central charge c : if at the end of the RG flow we encounter another CFT (with coupling constants \vec{g}) we then expect that its central charge c^{ir} is less than c^{uv} , because some degrees of freedom are "averaged out" in the flow. Let's denote S^{CFT} the action at the beginning of the flow, and S^* the action at the end of the flow. Notice that the degrees of freedom of S^* remain infinite, but they live in a space that is "less infinite" than the space of the degrees of freedom of S^{CFT} . We now demonstrate the *c-theorem*, that formalize these qualitative facts:

"For every 2D unitary field theory, that is invariant under rotations and translations, renormalizable, and whose stress tensor is conserved, there exist a function $C(g)$ of the coupling constants such that:

1. It decreases along the RG flow:

$$\frac{\partial C}{\partial g_i} \leq 0$$

2. It is stationary at the CFT points:

$$\left. \frac{dC}{dg_i} \right|_{g^*} = 0 \implies \beta(g^*) = 0$$

3. If $g = g^*$, we have:

$$\langle T(z, \bar{z}) T(0, 0) \rangle = \frac{c^{\text{uv}}/2}{z^4}$$

where the central charge of the new CFT is given by $c^{\text{uv}} = \lim_{g \rightarrow g^*} C(g)$."

To begin the demonstration, we remind that the components T , \bar{T} and Θ of the stress tensor have, respectively, spin 2, -2 and 0. The question is: what is the form of the correlator $\langle T(z, \bar{z}) T(0) \rangle$ out of the fixed point? If we require rotational invariance, the spin of the correlator should not change if we make a dilation of the system (*i.e.* if we move along the RG flow): then it will have the same spin of the fixed point, that is the CFT. On the other hand, the dilations may change the theory: if we look at the system at different scales, it might behave in a different way. This means that the correlator may depend on a function $F(m z \bar{z})$ that doesn't change the spin, whose argument contain the mass scale m ; this function depends on the coupling constants g as well. So, we have the off-critical correlators:

$$\begin{aligned}\langle T(z, \bar{z}) T(0, 0) \rangle &= \frac{F(m z \bar{z})}{z^4} \\ \langle T(z, \bar{z}) \Theta(0, 0) \rangle &= \frac{G(m z \bar{z})}{z^3 \bar{z}} \\ \langle \Theta(z, \bar{z}) \Theta(0, 0) \rangle &= \frac{H(m z \bar{z})}{z^2 \bar{z}^2}\end{aligned}\tag{2.185}$$

Now, we have to use the conservation law $\partial_\mu T^{\mu\nu} = 0$, whose form in complex coordinates we remind here:

$$\begin{cases} \partial_{\bar{z}} T + \frac{1}{4} \partial_z \Theta = 0 \\ \partial_z \bar{T} + \frac{1}{4} \partial_{\bar{z}} \Theta = 0 \end{cases}\tag{2.186}$$

If we derive (2.185) with respect to z or \bar{z} , and use (2.186), we obtain the differential equations:

$$\begin{cases} \dot{F} + \frac{1}{4}(\dot{G} - 3G) = 0 \\ \dot{G} - G + \frac{1}{4}(\dot{H} - 2H) = 0 \end{cases}\tag{2.187}$$

where $\tau = m^2 z \bar{z} = (mR)^2$ and

$$\dot{F} = \frac{dF}{d \log \tau}.$$

If we define

$$C(R, g) = 2F - G - \frac{3}{8}H\tag{2.188}$$

we have

$$\dot{C}(R, g) = -\frac{3}{4}H\tag{2.189}$$

Since, by hypothesis, our field theory theory is unitary, it is $H > 0$, and so $\dot{C} < 0$. From (2.185) we argue that, if $g = g^*$, then $H, G = 0$ and $F = c/2$ so

2. Conformal field theory

that $C(R, g^*) = c^{\text{uv}}$, and point 3 is demonstrated. Now, we need to use the Callan-Symanzik equation (2.181), which in our case reduces to:

$$\left(\frac{1}{2} R \frac{\partial}{\partial R} - \sum_a \beta^a \frac{\partial}{\partial g_a} \right) C(R, g) = 0 \quad (2.190)$$

This is because, for example, $\hat{\gamma}(g)(T(z, \bar{z})T(0, 0)) = \hat{\gamma}(g)(z^4)$, so we must have $\hat{\gamma}(g)(F(m z \bar{z})) = 0$: applying this reasoning to all the correlation functions of (2.185), we obtain $\hat{\gamma}(g)(C(R, g)) = 0$. If we use (2.176), we can express C as in (2.188) and equal the functions that depend only on R , obtaining:

$$\beta^a \frac{\partial}{\partial g^a} C(1, g) = -\frac{3}{4} G_{ab}(g) \beta^a(g) \beta^b(g) \quad (2.191)$$

where we have set $\tau = 1$ and

$$G_{ab}(z\bar{z}, g) = (m z \bar{z})^2 \langle \phi_a(z, \bar{z}) \phi_b(0, 0) \rangle, \quad G_{ab}(g) \equiv G_{ab}(1, g)$$

Again for the unitarity of the theory, $G_{ab}(g)$ is positive definite, and if the coupling constants remain small $\beta^a(g)$ is positive thanks to (2.184), so we must have

$$\frac{\partial C}{\partial g_i} \leq 0, \quad \forall i$$

and point 1 is demonstrated. Point 2 trivially follows from (2.191).

It is now easy to evaluate the difference $\Delta c = c^{\text{lr}} - c^{\text{uv}}$. From (2.185) and (2.189), we have:

$$\begin{aligned} \Delta c &= - \int_0^\infty \dot{C} d(\log \tau) = \frac{3}{4} \int_0^\infty H(m z \bar{z}) \frac{d\tau}{\tau} \\ &= \frac{3}{4} \int_0^\infty d(r^2) r^2 \langle \Theta(r) \Theta(0) \rangle = \frac{3}{2} \int_0^\infty dr r^3 \langle \Theta(r) \Theta(0) \rangle \end{aligned} \quad (2.192)$$

The c -theorem is very important in the context of conformal perturbation theory, and has a wide number of applications. We will discuss one of these in section 3.2, when we deal with entanglement entropy out of the critical point.

Chapter 3

Entanglement entropy in 1-D quantum chains

This chapter is dedicated to the evaluation of the entanglement entropy in one dimensional quantum systems. Typically, what one calculates is the entropy of one part of the system, which may be a finite interval, an infinite interval, or the union of more intervals, with respect to the rest of the system. The most important measures of entanglement are the Von Neumann entropy (to whom we will sometimes refer simply as entanglement entropy) and the Renyi entropy. For a definition of entanglement and the discussion of its measurement, see appendix A. In section 3.1 we will focus on systems at their critical point, for which we can apply the methods of conformal field theory developed in chapter 2, and we'll evaluate entanglement entropies in some cases. Section 3.2 is devoted to the entropy of non critical systems, while section 3.3 deals with corrections to the Renyi entropies. The corner transfer matrix method is developed in section 3.4, and it will then be applied to the XYZ model, which is the topic of section 3.5. Finally, in the last section we describe the entanglement spectrum, *i.e.* the eigenvalues of the reduced density matrix. The contents of section 3.1 are elaborated from [7], which was the first article that proposed the evaluation of entanglement entropies through the use of CFT. An alternative derivation can be found in [10].

3.1 The path integral approach

Let's start considering a lattice quantum theory in 1+1 dimensions, initially on the infinite line, described by a quantum Hamiltonian \hat{H} . We will always consider a continuous time, but for the moment let focus on a discrete lattice, whose "nearest neighbour" sites, identified by the couple (x, τ) , are separated by the lattice spacing a . Our theory is defined by a complete set of commuting observables, denoted by $\{\hat{\phi}_x\}$, evaluated at the points (x, τ) . We will denote their eigenvectors as $\otimes_x |\{\phi_x\}\rangle$, and for brevity we will refer to these objects

3. Entanglement entropy in 1-D quantum chains

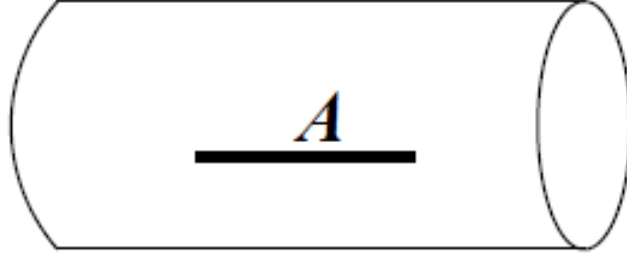


Figure 3.1: The cylindric surface with an open cut.

simply as $|\{\phi_x\}\rangle$. If the system, at an inverse temperature $\beta = 1/T$ in natural units, is canonical (*i.e.* it is isolated), then the density matrix is given by $\hat{\rho} = e^{-\beta\hat{H}}$. Using the eigenbasis $|\{\phi_x\}\rangle$, the matrix representation becomes:

$$\rho_{\{\phi'_x\},\{\phi''_x\}} = Z(\beta)^{-1} \langle\{\phi'_x\}| e^{-\beta\hat{H}} |\{\phi''_x\}\rangle. \quad (3.1)$$

Now, we switch to the path integral formalism and express the density matrix as:

$$\rho = Z^{-1} \int [d\phi_{x,\tau}] \prod_x \delta(\phi_{x,0} - \phi'_x) \prod_x \delta(\phi_{x,\beta} - \phi''_x) e^{-S_E} \quad (3.2)$$

where $S_E = \int_0^\beta L_E d\tau$, L_E is the euclidean Lagrangian, and with $\phi_{x,\tau}$ we denote the observable evaluated at (x, τ) .

It is clear that $\text{Tr} \rho$ is obtained by setting $\{\phi'_x\} = \{\phi''_x\}$, and integrating over these observables. The key point is that this is equivalent to *sewing* together the edges of the lattice along $\tau = 0$ and $\tau = \beta$, which reduces the space we are evaluating the observables to a *cylinder* of circumference β . In other words, calculating Z means performing a path integral of e^{-S_E} on a cylindrical geometry. Suppose then to have a subsystem A of the infinite line consisting, for simplicity, in the interval (x_1, x_2) (The case for A consisting in several intervals is similar). It is then natural to compute $\text{Tr} \rho_A$ as a path integral where we sewn together the points $x \notin A$. This will leave an open cut for (x_1, x_2) , along the line $\tau = 0$ (see Fig. 3.1). If we want to calculate ρ_A^n (with $n \in \mathbb{N}$), a smart trick is to make n copies, labelled by $1 \leq k \leq n$, of the above construction, and sewing them together cyclically along the cuts, that is by letting $\phi'_{x,k} = \phi''_{x,k+1}$, for all $x \in A$, and for $1 \leq k < n$ (See Fig. 3.1). With an abuse of notation, we denoted with $\phi_{x,k}$ the observable evaluated in the k -th copy. It is clear that our observables $\{\phi_x\}$ are now defined in a more complicated geometry, which we denote \mathcal{R}_n , that has *Riemann sheets* labelled by k , and is, roughly speaking, "n" times larger than the previous one (we are in fact raising ρ_A to the n -th power). The branch point of this structure are x_1 and x_2 , of order n . Clearly, we now have to divide our path integral by Z^n to recover ρ_A^n .

We can further calculate $\text{Tr } \rho_A^n$ by simply sewing together the first and the last sheet, that is by letting $\phi'_{x,n} = \phi''_{x,1}$, $\forall x \in A$. If we denote the path integral on this n -sheeted geometry by

$$Z_n(A) = \int [d\phi]_{\mathcal{R}_n} \exp \left[- \int_{\mathcal{R}_n} \mathcal{L}[\phi] d^2x \right], \quad (3.3)$$

then we have:

$$\text{Tr } \rho_A^n = \frac{Z_n(A)}{Z^n} \quad (3.4)$$

But we can express $\text{Tr } \rho_A^n$ in another way, that is $\text{Tr } \rho_A^n = \sum_{\lambda} \lambda^n$, where λ are the eigenvalues of ρ_A . Noting that this is analytic for all $\text{Re}(n) > 1$ ([7]), we have that the entropy $S_A = - \sum_{\lambda} \lambda \log \lambda$ can be written as:

$$S_A = - \lim_{n \rightarrow 1} \frac{\partial}{\partial n} \frac{Z_n(A)}{Z^n} \quad (3.5)$$

Clearly, if $a \rightarrow 0$ (continuum limit), the lattices points (x, τ) assume real values. This means that the set of observables $\{\hat{\phi}_x\}$ become now a field $\phi(x, \tau)$, and the density matrix involves now path integrals of fields over n -sheeted Riemann surface. We just mention that S_E should now go over into the euclidean action for a quantum field theory, which describes a CFT if it's relativistic invariant and massless (for further details, see again [7]).

3.1.1 The case of a single interval

As an example, we calculate the entropy of a single interval A of length l , which we now denote by (v, u) , in an infinitely long 1-d quantum system, at zero temperature. First, we map the n -sheeted Riemann surface \mathcal{R}_n to the z -plane \mathbf{C} . This can be done in two steps: we use the conformal mappint $w \rightarrow \zeta = (w - u)/(w - v)$ to map the branch points to $(0, \infty)$, and then we obtain the z -plane using:

$$\zeta \rightarrow z = \zeta^{\frac{1}{n}} = \left(\frac{w - u}{w - v} \right)^{\frac{1}{n}}. \quad (3.6)$$

The stress tensors $T(w)$ and $T(z)$ of the two geometries are related by (2.60), which we remind here:

$$T(w) = \left(\frac{dz}{dw} \right)^2 T(z) + \frac{c}{12} \{z, w\} \quad (3.7)$$

If we suppose that $\langle T(z) \rangle_{\mathbf{C}} = 0$, then we have:

$$\langle T(w) \rangle_{\mathcal{R}_n} = \frac{c}{12} \{z, w\} = \frac{c}{24} \left(1 - \frac{1}{n^2} \right) \frac{(v - u)^2}{(w - u)^2 (w - v)^2} \quad (3.8)$$

3. Entanglement entropy in 1-D quantum chains

Notice that $\langle T(w) \rangle_{\mathcal{R}_n} = 0$ if $n = 1$, since in that case we no longer have branch points and the geometry is translational invariant.

Now, a correlation function involves a local interaction between fields. This means that, whatever is the geometry, if we put $T(w)$ (the stress tensor of the n -sheeted geometry) in a correlation function it will assume the form:

$$T(w) = \frac{c}{12} \{z, w\} = \frac{c}{24} \left(1 - \frac{1}{n^2}\right) \frac{(v-u)^2}{(w-u)^2(w-v)^2} + \text{reg.} \quad (3.9)$$

If we are working in the plane, (3.9) must be compatible with the Ward identity:

$$\begin{aligned} & \langle T(w) \Phi_1(u) \Phi_2(v) \rangle_{\mathbf{C}} \\ &= \left(\frac{\Delta_1}{(w-u)^2} + \frac{\Delta_2}{(w-v)^2} + \frac{1}{w-u} \frac{\partial}{\partial u} + \frac{1}{w-v} \frac{\partial}{\partial v} \right) \langle \Phi_1(u) \Phi_2(v) \rangle_{\mathbf{C}} \end{aligned} \quad (3.10)$$

where $\Phi_1(u)$ and $\Phi_2(v)$ are two primary fields of conformal dimensions Δ_1 and Δ_2 . The compatibility is ensured if Φ_1 and Φ_2 have the same conformal dimension, equal to:

$$\Delta_n = \bar{\Delta}_n = \frac{c}{24} \left(1 - \frac{1}{n^2}\right). \quad (3.11)$$

and we refer to them simply as ϕ_n . Notice also that:

$$\langle T(w) \rangle_{\mathcal{R}_n} \equiv \frac{\int [d\phi] T(w) e^{-S_{E, \mathcal{R}_n}}}{\int [d\phi] e^{-S_{E, \mathcal{R}_n}}} = \frac{\langle T(w) \phi_n(u) \phi_n(v) \rangle_{\mathbf{C}}}{\langle \phi_n(u) \phi_n(v) \rangle_{\mathbf{C}}} \quad (3.12)$$

since $T(w)$ behaves like a c-number when inserted in an arbitrary correlation function (see again (3.9)), and can then be "pulled out" from it, leaving in (3.12) a fraction of two equal objects. Now, let's consider the effect of an infinitesimal conformal transformation $w \rightarrow w' = w + \alpha(w)$ on the \mathbf{C} coordinates, and denote the infinitesimal variation in real coordinates as α^μ . This transformation will act identically on each sheet of \mathcal{R}_n . If we evaluate the variation of $\log(Z_n/Z^n)$, we only need to study the variation of Z_n , because we obviously require that the partition function doesn't change under a conformal transformation (we are considering the critical point of the theory). We then

have:

$$\begin{aligned}
 \delta \log\left(\frac{Z_n}{Z^n}\right) &= \frac{1}{Z_n} \delta Z_n \\
 &= \frac{n}{Z_n} \int_{\mathcal{R}_n} [d\phi] (-\delta S_{E, \mathcal{R}_n}) e^{-S_{E, \mathcal{R}_n}} \\
 &= -\frac{n}{Z_n} \int_{\mathcal{R}_n} [d\phi] \int d^2x T^{\mu\nu} \partial_\mu \alpha_\nu e^{-S_{E, \mathcal{R}_n}} \\
 &= \frac{n}{2\pi i Z_n} \oint dw \alpha(w) \int_{\mathcal{R}_n} [d\phi] T(w) e^{-S_{E, \mathcal{R}_n}} \\
 &\quad - \frac{n}{2\pi i Z_n} \oint d\bar{w} \bar{\alpha}(\bar{w}) \int_{\mathcal{R}_n} [d\phi] \bar{T}(\bar{w}) e^{-S_{E, \mathcal{R}_n}} \\
 &= \frac{1}{2\pi i} \oint dw \alpha(w) \langle T(w) \rangle_{\mathcal{R}_n} - \frac{1}{2\pi i} \oint d\bar{w} \bar{\alpha}(\bar{w}) \langle \bar{T}(\bar{w}) \rangle_{\mathcal{R}_n}
 \end{aligned} \tag{3.13}$$

where the factor n in the second line comes from the fact that $T(w)$ has to be inserted in each sheet. We also notice the use of the Gauss theorem in the 4-th line, after writing $T^{\mu\nu} \partial_\mu \alpha_\nu = \partial_\mu (T^{\mu\nu} \alpha_\nu) - (\partial_\mu T^{\mu\nu}) \alpha_\nu$. On the other hand, let's set $G_\phi(u, v) \equiv \langle \phi_n(u) \phi_n(v) \rangle$. If we use the *same* coordinate transformation to compute the variation of $\log(G_\phi(u, v))^n$, this time on the \mathbf{C} geometry, we find:

$$\begin{aligned}
 \delta \log(G_\phi(u, v))^n &= \frac{n}{G_\phi(u, v)} \delta(G_\phi(u, v)) \\
 &= \frac{n}{G_\phi(u, v)} \frac{1}{Z_{\mathbf{C}}} \int_{\mathbf{C}} [d\phi] \phi_n(u) \phi_n(v) (-\delta S_E) e^{-S_E} \\
 &= -\frac{n}{G_\phi(u, v)} \frac{1}{Z_{\mathbf{C}}} \int_{\mathbf{C}} [d\phi] \phi_n(u) \phi_n(v) \left(\int d^2x T^{\mu\nu} \partial_\mu \alpha_\nu \right) e^{-S_E} \\
 &= \frac{1}{2\pi i} \frac{n}{G_\phi(u, v)} \frac{1}{Z_{\mathbf{C}}} \oint dw \alpha(w) \int_{\mathbf{C}} [d\phi] \phi_n(u) \phi_n(v) T(w) e^{-S_E} \\
 &\quad - \frac{1}{2\pi i} \frac{n}{G_\phi(u, v)} \frac{1}{Z_{\mathbf{C}}} \oint d\bar{w} \bar{\alpha}(\bar{w}) \int_{\mathbf{C}} [d\phi] \phi_n(u) \phi_n(v) \bar{T}(\bar{w}) e^{-S_E} \\
 &= \frac{n}{2\pi i G_\phi(u, v)} \oint dw \langle \phi_n(u) \phi_n(v) T(w) \rangle_{\mathbf{C}} \\
 &\quad - \frac{n}{2\pi i G_\phi(u, v)} \oint d\bar{w} \langle \phi_n(u) \phi_n(v) \bar{T}(\bar{w}) \rangle_{\mathbf{C}} \\
 &= \frac{1}{2\pi i} \oint dw \alpha(w) \langle T(w) \rangle_{\mathcal{R}_n} - \frac{1}{2\pi i} \oint d\bar{w} \bar{\alpha}(\bar{w}) \langle \bar{T}(\bar{w}) \rangle_{\mathcal{R}_n}
 \end{aligned} \tag{3.14}$$

where in the last passage we used (3.12). We have thus shown that:

$$\delta\left(\frac{Z_n}{Z^n}\right) \equiv \delta\left(\log \text{Tr} \rho_A^n\right) = \delta \log(G_\phi(u, v))^n \tag{3.15}$$

3. Entanglement entropy in 1-D quantum chains

for every infinitesimal conformal transformation. We remember here that, from conformal invariance, the two point correlation function G_ϕ has the form

$$G_\phi(u, v) = \langle \phi_n(u) \phi_n(v) \rangle = \frac{1}{(u - v)^{2\Delta_n} (\bar{u} - \bar{v})^{\bar{\Delta}_n}} \quad (3.16)$$

So, for a finite conformal transformation of the coordinates, we have $\log \text{Tr} \rho_A^n = \log(G_\phi(u, v))^n + \text{const}$, from which follows the main result of this section:

$$\text{Tr} \rho_A^n = c_n \left(\frac{v - u}{a} \right)^{-(c/12)(n-1/n)} \left(\frac{\bar{v} - \bar{u}}{a} \right)^{-(c/12)(n-1/n)} \quad (3.17)$$

where a is a constant that has been inserted to make the result dimensionless.

Let's now calculate entanglement entropies (Von Neumann entropies) in a few cases. If u and v are the edges of the interval A considered at the beginning of the section, then they have the same imaginary part: $v - u = \bar{v} - \bar{u} \equiv l$, and if we now use (3.5), we obtain the entropy of a single interval of length l in an infinitely long 1+1 quantum system:

$$S_A = \frac{c}{3} \log l \quad (3.18)$$

We can now easily obtain the entanglement entropy in other physical situations, by simply making conformal mappings $z \rightarrow z' = w(z)$: this is because the entropy is calculated as derivatives of correlation functions, and these change as:

$$\langle \Phi(z_1, \bar{z}_1) \Phi(z_2, \bar{z}_2) \dots \rangle = \prod_j |w'(z_j)|^{2\Delta_n} \langle \Phi(w_1, \bar{w}_1) \Phi(w_2, \bar{w}_2) \dots \rangle \quad (3.19)$$

Let's first consider the transformation

$$w \rightarrow w' = \frac{\beta}{2\pi} \log w, \quad (3.20)$$

which maps the \mathbf{C} geometry into an infinitely long cylinder of circumference β . Using (3.19) and (3.16), we have that the two-point correlation function changes as ([17])

$$\begin{aligned} \langle \Phi(w_1, \bar{w}_1) \Phi(w_2, \bar{w}_2) \rangle &= \left(\frac{2\pi}{L} \right)^{2\Delta_n + 2\bar{\Delta}_n} \left(2 \sinh \left[\frac{\pi(w_1 - w_2)}{\beta} \right] \right)^{-2\Delta_n} \\ &\quad \times \left(2 \sinh \left[\frac{\pi(\bar{w}_1 - \bar{w}_2)}{\beta} \right] \right)^{-2\bar{\Delta}_n} \end{aligned} \quad (3.21)$$

In we consider the points v and w as being part of the \mathbf{C} geometry, these are then mapped in the cylinder, and they still have the same imaginary part

thanks to (3.20): this means that they lie on a line parallel to the axis of the cylinder. Physically, we can interpret β as an inverse temperature (see chapter 1), so we get an expression for $\text{Tr} \rho_A^n$ in a thermal mixed state at a *finite temperature* $T = \beta^{-1}$. The new interval has length $u' - v' = \bar{u}' - \bar{v}' \equiv l$, where u' and v' are the transformed of u and v under (3.20) (denoting the transformed length as l is just an abuse of notation). We can now evaluate the entropy through (3.5), which gives:

$$S_A(\beta) \sim \frac{c}{3} \log \left(\frac{\beta}{\pi a} \sinh \left(\frac{\pi l}{\beta} \right) \right) + c'_1 \quad (3.22)$$

where again the constant a is inserted *ad hoc* to make the result dimensionless. It is natural, in most cases, to interpret a as the lattice spacing, since it's the only dimensionful quantity of the problem. As a check of the validity of this reasoning, we note that if $\beta \rightarrow \infty$, we recover the previous result (3.18): $S_A \sim (c/3) \log(l/a)$.

If instead we now consider the transformation

$$w \rightarrow w' = \frac{L}{2\pi} \log(iw) \quad (3.23)$$

we still have a mapping on the infinite cylinder, but this time u' and v' are aligned *perpendiculary* to its axis, that is they have the same *real* part. The difference with (3.21) is that we now have the replacements $\sinh \rightarrow \sin$ and $\beta \rightarrow L$, so we obtain the entropy for an interval of length l in a system of finite length L , at zero temperature:

$$S_A \sim \frac{c}{3} \log \left(\frac{L}{\pi a} \sin \left(\frac{\pi l}{L} \right) \right) + c'_1 \quad (3.24)$$

Notice that in this case we are imposing *periodic boundary conditions* on the quantum system, because its two edges are sewn together: the whole system of length L is placed perpendicularly to the axis of the cylinder, so the two edges coincide.

If in the last case just considered we impose instead *open boundary conditions*, the entropy behaves in the following way:

$$S_A \sim \frac{c}{6} \log \left(\frac{L}{\pi a} \sin \left(\frac{\pi l}{L} \right) \right) + c'_2 \quad (3.25)$$

We won't demonstrate this relation here (see [7]), but the treatment is quite similar to the former case. As a last remark, the constant c'_1 (and c'_2) is nonuniversal, because it depends on the integration constant c_n of equation (3.17). It is related to the boundary entropy (see [1] for further details).

3.1.2 The case of n disjoint intervals

In the general case, we wish to compute the bipartite entanglement of a set of n disjoint intervals with respect to the rest of the system. We won't develop the whole procedure here because it's very similar to what we have done in the case of a single interval, and we refer to [7] and [8] for further details. The basic idea is that $T(z)$ of the \mathcal{R}_n geometry can be expressed, when inserted in a correlator, as a c-function (see equation (3.9)). This suggests that, roughly speaking, $T(z)$ can be "pulled out" from every correlator, and we can generalize (3.12) as:

$$\langle T(w) \rangle_{\mathcal{R}_n} = \frac{\langle T(w) \phi_1(w_1) \dots \phi_1(w_n) \rangle_{\mathbf{C}}}{\langle \phi_1(w_1) \dots \phi_n(w_n) \rangle_{\mathbf{C}}} \quad (3.26)$$

This time, the transformation from the n -sheeted geometry to the complex plane is given by:

$$z = \prod_i (w - w_i)^{\alpha_i} \quad (3.27)$$

where we set $\sum_i \alpha_i = 0$ to avoid singularities at infinity. Then, performing the same reasoning of the previous section, we have that $(Z_n)/(Z^n)$ transforms in the same way as $\left(\langle \phi_1(z_1) \dots \phi_n(z_n) \rangle_{\mathbf{C}} \right)^n$. This correlator, as well as the α_i , can be determined by imposing the compatibility between

$$\langle T(w) \rangle_{\mathcal{R}_n} = \frac{c}{12} \{z, w\} \quad (3.28)$$

(where we used $\langle T(w) \rangle_{\mathbf{C}} = 0$), and the Ward Identity

$$\left\langle T(w) \prod_i \phi_i(w_i) \right\rangle_{\mathbf{C}} = \sum_i \left[\frac{\Delta_i}{(w - w_i)^2} + \frac{1}{w - w_i} \frac{\partial}{\partial w_i} \right] \left\langle \prod_k \phi_k(w_k) \right\rangle_{\mathbf{C}} \quad (3.29)$$

We just report the final result. If the whole system is infinite, and if the intervals j on the cylinder are (u_j, v_j) , then the entropy is:

$$S_A = \frac{c}{3} \left[\sum_{j \leq k} \log \left(\frac{v_k - u_j}{a} \right) - \sum_{j < k} \log \left(\frac{u_k - u_j}{a} \right) - \sum_{j < k} \log \left(\frac{v_k - v_j}{a} \right) \right] + N c'_1 \quad (3.30)$$

3.2 Entanglement Entropy in a non critical model

For our subsequent developments, it is necessary to evaluate the entropy in a off-critical point. For this purpose, we shall start with an infinite non-critical model in 1+1 dimensions, in the scaling limit $a \rightarrow 0$, and with the correlation length ξ fixed, satisfying $\xi \gg a$. The two subsystem consists in two half-infinite chains, covering respectively the positive and the negative axis. We

3.2. Entanglement Entropy in a non critical model

are still working in the \mathcal{R}_n geometry, but now we can't change it by conformal transformation, because the system is not at criticality anymore.

The argument ([7]) now parallels that of Zamolodchikov's c -theorem. Consider the expectation values $\langle T \rangle$, $\langle \bar{T} \rangle$, $\langle \Theta \rangle$. If we are out from criticality, not only $\langle T \rangle$, $\langle \bar{T} \rangle \neq 0$ in general (except for \mathcal{R}_1 , see section 3.1.1), but also $\langle \Theta \rangle \neq 0$: in fact, the expectation value of T_μ^μ is a measure of the breaking of scale invariance. Thanks to the rotational invariance of \mathcal{R}_n , we can write (in a similar fashion of section 2.6.3):

$$\langle T(z, \bar{z}) \rangle = \frac{F_n(z\bar{z})}{z^2} \quad (3.31a)$$

$$\langle \Theta(z, \bar{z}) \rangle_n - \langle \Theta(z, \bar{z}) \rangle_1 = \frac{G_n(z\bar{z})}{z\bar{z}} \quad (3.31b)$$

$$\langle \bar{T}(z, \bar{z}) \rangle_n = \frac{F_n(z\bar{z})}{\bar{z}^2} \quad (3.31c)$$

Notice that for $\langle T(z, \bar{z}) \rangle$ and $\langle \bar{T}(z, \bar{z}) \rangle_n$ we have the same function F_n , because T and \bar{T} are complex conjugated if put in a correlation function. Notice as well that we have set the mass scale m to 1 (see (2.185)).

Now, as we did for the c -theorem, we take advantage of (2.38), and end with:

$$(z\bar{z}) \left(F_n' + \frac{1}{4} G_n' \right) = \frac{1}{4} G_n \quad (3.32)$$

where ' means ∂_{R^2} , setting $R^2 = z\bar{z}$. If $|z| \ll \xi$, we expect that (see section 3.1):

$$\begin{cases} F_n \rightarrow \frac{c}{24} \left(1 - \frac{1}{n^2} \right) \\ G_n \rightarrow 0 \end{cases}$$

which are the CFT values. On the other hand, if $|x| \gg \xi$, we expect both F_n and G_n to approach zero, because \mathcal{R}_n is then indistinguishable from the \mathbb{C} -plane if we are far from the branch point $z = 0$.

Denoting

$$C_n(R^2) \equiv \left(F(R^2) + \frac{1}{4} G(R^2) \right),$$

then

$$R^2 \frac{\partial}{\partial(R^2)} C_n(R^2) = \frac{1}{4} G_n(R^2) \quad (3.33)$$

and if we integrate this equation, using the boundary conditions, we obtain:

$$\int_0^\infty \frac{G_n(R^2)}{R^2} d(R^2) = -\frac{c}{6} \left(1 - \frac{1}{n^2} \right) \quad (3.34)$$

3. Entanglement entropy in 1-D quantum chains

If instead we integrate over all the n -sheeted surface, we have to multiply the right hand side by n , and using the fact that $d^2x = d\theta \frac{d(R^2)}{2}$:

$$\int_{\mathcal{R}_n} \left(\langle \Theta \rangle_n - \langle \Theta \rangle_1 \right) d^2x = -\pi n \frac{c}{6} \left(1 - \frac{1}{n^2} \right) \quad (3.35)$$

Performing an infinitesimal scale transformation $x^\mu \rightarrow x^\mu + \epsilon^\mu$, where $\epsilon^\mu = \epsilon x^\mu$, the change of the free energy $F = -\log Z$ is:

$$\begin{aligned} \delta(-\log Z) &= \frac{\delta Z}{Z} \\ &= -\frac{1}{Z} \int [d\phi] (-\delta S) e^{-S} = \frac{1}{2\pi} \int d^2x \langle T^{\mu\nu}(x) \rangle \partial_\mu \epsilon_\nu \\ &= \frac{\epsilon}{2\pi} \int d^2x \langle T^\mu_\mu \rangle \end{aligned} \quad (3.36)$$

Now, ϵ is an adimensional quantity, and the only dimensionful parameter of the renormalized theory is the mass scale m . We thus expect that the change in the coordinates ϵ due to a dilation is *proportional* to the change in the scale (*i.e.* in the mass scale):

$$\epsilon = \frac{\delta m}{m} \quad (3.37)$$

where we obviously divided by m to for dimensional reasons. Thus, the left hand side of (3.35) is equal to

$$-(2\pi) m \frac{\partial}{\partial m} \left(\log Z_n - n \log Z \right) \quad (3.38)$$

and, integrating over m , gives:

$$\frac{Z_n}{Z^n} = c_n (ma)^{(c/12)(n-1/n)} \quad (3.39)$$

where c_n is the integration constant, and a makes the result dimensionless. Using (3.5), we finally arrive at the desired result:

$$\boxed{S_A \sim -\frac{c}{6} \log(ma) = \frac{c}{6} \log\left(\frac{\xi}{a}\right)} \quad (3.40)$$

As a final comment, remind that we had to impose $\xi \gg a$, so we could use the field theory approach. For lattice integrable models (such as the XYZ model of section 3.5), it is indeed possible to obtain this last equation without this restriction.

3.3 Corrections to Entanglement Entropy

In this section we want to give an idea about the main corrections to the entanglement entropy, and to understand why these emerge. We will review the main points of the articles [9], [11] and [12].

3.3.1 Corrections to Scaling

Before proceeding, let's compute the Renyi entropies using another approach, based on scaling intuitions. From (3.17), these have the form:

$$S_A^{(n)} = \frac{c}{6} \left(1 + \frac{1}{n}\right) \log l + \text{cost} \quad (3.41)$$

If we remind that the free energy is given by $F = -\log Z$, it is then useful to write:

$$\begin{aligned} \log(\text{Tr } \rho_A^n) &= \log\left(\frac{Z_n}{Z_1^n}\right) = \log Z_n - n \log Z_1 \\ &= -(F_n - nF_1) \end{aligned} \quad (3.42)$$

so that we can write the Renyi entropies as:

$$S_A^{(n)} = \frac{1}{1-n} \log(\text{Tr } \rho_A^n) = \frac{F_n - nF_1}{n-1} \quad (3.43)$$

From renormalization group theory, we know that the systems belonging to the same RG flow behave in a universal way if their correlation functions (the observable quantities) are evaluated at far distanced point. This means that these universal effects should be independent of the *cutoff* ϵ imposed to the systems. Our only dimensionful quantity is now ϵ (we are still at criticality, so the mass scale is equal to 0), and in a similar fashion of (3.36), we can then write:

$$-\epsilon \frac{\partial F}{\partial \epsilon} = \frac{1}{2\pi} \int \langle \Theta(z) \rangle d^2z \quad (3.44)$$

Now, we would like to apply (3.35) to our case. This is possible because $\langle \Theta \rangle \neq 0$: it is true that we are at the critical point, but the n -sheeted surface doesn't preserve the translational invariance of $\langle \Theta \rangle$. Pay attention that now we have two branch points instead of one: in section 3.2 the branch cut of the n -sheeted geometry was $A = [0, \infty)$, while now the branch cut is, say, $A' = [x_1, x_2]$. Thus, each branch point gives a contribution equal to (3.35):

$$\frac{1}{2\pi} \int_{\mathcal{R}_n} (\langle \Theta \rangle_n - \langle \Theta \rangle_1) d^2x = -n \frac{c}{12} \left(1 - \frac{1}{n^2}\right) \quad (3.45)$$

In conclusion, we have:

$$-\epsilon \frac{\partial(F_n - nF_1)}{\partial \epsilon} = -\frac{c}{6} \left(n - \frac{1}{n}\right) \quad (3.46)$$

and then:

$$(F_n - nF_1) = \frac{c}{6} \left(1 + \frac{1}{n}\right) \log\left(\frac{\epsilon}{a}\right) + \text{cost} \quad (3.47)$$

3. Entanglement entropy in 1-D quantum chains

If we postulate that the entropy obeys scaling hypothesis, we argue that the Entropy of an interval l should depend on the *ratio* l/ϵ , and then we must have $a = l$. This is how we recover (3.41) from scaling arguments.

Let's now perturb the action of the fixed point with an *irrelevant operator* $\Phi(z)$, that is with scaling dimension $x = 2\Delta > 2$:

$$S = S^* + \lambda \int \Phi(z) d^2 z \quad (3.48)$$

where $S^* = S^{\text{CFT}}$ and λ is, as usual, the coupling constant, which can be expressed as $\lambda = g/\epsilon^{2-x}$. Notice that, on the contrary of what we did for Conformal Perturbation Theory (see section 2.6.1), we are perturbing the action with irrelevant operators, because we want to evaluate corrections at the critical point. In fact, from RG reasoning, the points lying on a flow that points to S^* (*i.e.* on a critical surface, as in our case) are all characterized by $\xi = \infty$. But now the theory is not of the superrenormalizable type anymore, so we'll have an infinite number of divergencies, that all need to be cured to obtain finite results.

The change in the free energy is given by:

$$\begin{aligned} -\delta F_n &= -(F_n - F_n^*) \\ &= \frac{1}{Z_n} \left[\int [d\phi] \exp\{S^* + \lambda \int_{\mathcal{R}_n} \Phi(z) d^2 z\} - \int [d\phi] \exp\{-S^*\} \right] \\ &= \sum_{N=1}^{\infty} \frac{(-\lambda)^N}{N!} \int_{\mathcal{R}_n} \dots \int_{\mathcal{R}_n} \langle \Phi(z_1) \dots \Phi(z_n) \rangle_{\mathcal{R}_n} d^2 z_1 \dots d^2 z_N \end{aligned} \quad (3.49)$$

and if A is the interval $(0, l)$ in the n -sheeted geometry, then we can map \mathcal{R}_n in $\mathbf{C}' = \mathbf{C}/\{0\}$ by the coordinate transformation:

$$\zeta = \left(\frac{z}{z-l} \right)^{1/n} \quad z = lf(\zeta) \equiv l \frac{\zeta^n}{\zeta^n - 1} \quad (3.50)$$

where the interval A is mapped in $(0, \infty)$. The correlation functions of the two geometry are related by:

$$\langle \Phi(z_1) \dots \Phi(z_n) \rangle_{\mathcal{R}_n} = \prod_{j=1}^N |lf'(\zeta_j)|^{-x} \langle \Phi(\zeta_1) \dots \Phi(\zeta_N) \rangle_{\mathbf{C}'} \quad (3.51)$$

3.3. Corrections to Entanglement Entropy

Then we have, up to the second order:

$$\begin{aligned}
\delta F_n^{(2)} &= -\frac{1}{2}g^2\left(\frac{l}{\epsilon}\right)^{4-2x} \int_{\mathcal{C}'} \int_{\mathcal{C}'} \frac{|f'(\zeta_1)|^{2-x}|f'(\zeta_2)|^{2-x}}{|\zeta_1 - \zeta_2|^{2x}} d^2\zeta_1 d^2\zeta_2 \\
&= -\frac{1}{2}g^2\left(\frac{nl}{\epsilon}\right)^{4-2x} \int_{\mathcal{C}'} \int_{\mathcal{C}'} \frac{|\zeta_1\zeta_2|^{(2-x)(n-1)}}{|\zeta_1^n - 1|^{4-2x}|\zeta_2^n - 1|^{4-2x}|\zeta_1 - \zeta_2|^{2x}} d^2\zeta_1 d^2\zeta_2 \\
&\equiv -\frac{1}{2}g^2\left(\frac{nl}{\epsilon}\right)^{4-2x} I(x, \epsilon)
\end{aligned} \tag{3.52}$$

where we used the fact that $\langle \Phi \rangle_{\mathcal{C}'} = 0$. Now, as we have several potential sources of ultraviolet divergence, we need to impose an ultraviolet cutoff ϵ (the integral always converges in the infrared for $x > 2$). As said before, because the theory is not renormalizable, we might need ultraviolet cutoffs at every order. Let's take n to have the behaviour $n - 1 \ll 1$ and $n > 1$, and let's look to the case $\zeta_1 \rightarrow \zeta_2$: the integral will converge only if $2x < 2$, that is $x < 1$. But, with our hypothesis, we have $x > 2$, so we need to regularize this integral. If $n \simeq 1$, then:

$$z_1 - z_2 \simeq \frac{\zeta_2 - \zeta_1}{(\zeta_1 - 1)(\zeta_2 - 2)} \tag{3.53}$$

If $\zeta_1 \rightarrow 1$ or $\zeta_2 \rightarrow 1$, the integral converges in the ultraviolet region if $x > 3/2$, and if we consider the contribution coming from (3.53), the convergence is for $x > 2$, which is always satisfied by our hypothesis. So we shall not worry for ζ_1 or ζ_2 approaching 1. We then have the behaviour:

$$|z_1 - z_2| \sim |\zeta_1 - \zeta_2|$$

and we can impose an ultraviolet cutoff $|z_1 - z_2| > \epsilon$. If we now make the change of variables $z = \zeta_1 - \zeta_2$, $w = \zeta_1$, and denote the terms that make the integral convergent with B , then:

$$\begin{aligned}
I(x, \epsilon) &\sim \int_{\mathcal{C}'} \int_{\mathcal{C}'} \frac{B(\zeta_1, \zeta_2)}{|\zeta_1 - \zeta_2|^{2x}} d^2\zeta_1 d^2\zeta_2 \sim \int_{\mathcal{C}'} \int_{\mathcal{C}'} \frac{B'(z, w)}{|z|^{2x}} d^2z d^2w \\
&\sim \int_{\mathcal{C}'} \int_{\epsilon}^{\infty} \frac{B'(z, w)}{\rho^{2x}} \rho d\rho d^2y \sim \epsilon^{2-2x}
\end{aligned} \tag{3.54}$$

Fortunately, this divergence cancels out in the combination $F_n - nF_1$ (remember that $n \simeq 1$), so it is really a "fictitious" divergence of the entropy, and if we make an analytical continuation of the integral around the pole $x = 1$, the entropy remains finite for $x < 3$. What remains from $F_n - nF_1$ is the finite part of the integrals $I(x, \epsilon)$, that is our *first correction* to the entropy:

$$l^{4-2x} \tag{3.55}$$

Let's now study the case where n is larger and $x > 2$. $I(x, \epsilon)$ can now show divergencies for $\zeta_i \rightarrow 0$ and $\zeta_i \rightarrow \infty$, that means for z_1 or z_2 approaching

3. Entanglement entropy in 1-D quantum chains

the *branch points*. It is important to notice that these divergencies occur due to the existence of these branch points, because of the exponent $n - 1$, and $n \neq 1$. Consider, for example, the case $\zeta_i \rightarrow 0$, for $i = 1, 2$. we then have two integrals, each giving a contribute:

$$\int_{\epsilon}^{\infty} \rho^{(x/n)-x+1} d\rho$$

This diverges if

$$n > n_c(x) = \frac{x}{x-2}$$

and if does, $I(x, \epsilon)$ gives a multiplicative factor $\propto \epsilon^{2-x+(x/n)}$. But, for scaling hypothesis, $\delta F_n^{(2)}$ must depend on the ratio l/ϵ , and this gives our *second correction*:

$$l^{4-2x-(2-x+x/n)} = l^{2-x-x/n} \quad (3.56)$$

If both z_1 and z_2 are close to a branch point, we have a *third correction*:

$$l^{4-2x-2(2-x+x/n)} = l^{-2x/n} \quad (3.57)$$

Which of these 3 correction dominates depends on the value of n with respect to $n_c(x)$: if $n > n_c$, the first dominates, but for $n < n_c$ the other two are more relevant. If $n \approx n_c$, all of them may play a role, and if $n = n_c$, we expect multiplicative logarithmic factors.

Let's now discuss the appearance of corrections with $x < 2$. These are due to operators that live on the conical singularities, which have scaling dimension x/n with $x < 2$. To explain how this works, consider the n -sheeted geometry, where the branch points are, say, at 0 and ∞ : let now \mathcal{R}_n be the living space of the 2-d classical system that corresponds to the 1-d quantum chain. Every coordinate of the geometry corresponds to a site of the lattice, and we'll have a site positioned on the branch point. If each site, in 2-d, has 4 nearest neighbours, the site on the branch point will have instead $4n$ *nearest neighbours*: this breaks the selfduality of the system, and drives it out of criticality. The operator that concerns with the interaction between nearest neighbour sites is the *energy operator*, which has $x = 1$, so we expect that it will perturb the action S^* of the fixed point. In conclusion, the correct form of the perturbed action in the n -sheeted geometry is:

$$S = S^* + \sum_j \lambda_j \int_{\mathcal{R}_n} \Phi_j(z) d^2z + \sum_P \sum_k \lambda_k \Phi_k^{(n)}(P) \quad (3.58)$$

where $\Phi_k^{(n)}(P)$ is the relevant operator acting at the branch point P , with scaling dimension x_k/n . Each $\Phi_k^{(n)}$ should appear at most one in the perturbing expansion in λ_k , otherwise we can use the OPE to write higher powers of $\Phi_k^{(n)}$ in term of other localized operators. For $x < 2$ and $n \simeq 1$ we have another

3.3. Corrections to Entanglement Entropy

diverge, because the reasoning following (3.53) doesn't hold anymore. In fact, using (3.53), we have that $I(x, \epsilon)$ presents two terms $|\zeta_i - 1|^4$: regularizing the integral and collecting all the terms proportional to l , we have the correction

$$l^{-2x} \equiv l^{-2x_k/n} \quad (3.59)$$

Of course, this holds if $\langle \Phi^{(n)}(P) \rangle = 0$. But it may happen that $\langle \Phi^{(n)}(P) \rangle \neq 0$ if the branch point is at the end of a *finite system* (as we saw for the Casimir effect), and in this case the leading correction will be of the form

$$l^{-x_k/n} \quad (3.60)$$

In general, a correction at order λ^N to $F_n - nF_1$, for $x < 2$, will be of the form:

$$l^{-(Nx_k)/n} \quad (3.61)$$

We won't discuss the derivation of the s in the case $x \rightarrow 2$, which is much more difficult. The result, for $x \approx 2$, is:

$$F_n - nF_1 = -\frac{c}{6} \left(n - \frac{1}{n} \right) \log \left(\frac{l}{\epsilon} \right) + g^2 \left(n + \frac{1}{n} \right) \left(\frac{l}{\epsilon} \right)^{4-2x} \left(\frac{\pi^2}{4} + O(x-2) \right) + O(g^3) \quad (3.62)$$

Using (3.46), this can be recasted in the form:

$$\epsilon \frac{\partial(F_n - nF_1)}{\partial \epsilon} = -\frac{c_{\text{eff}}(g)}{6} \left(n - \frac{1}{n} \right) \quad (3.63)$$

where we have introduced the *effective charge*

$$c_{\text{eff}}(g) = c - 3\pi^2(2-x)g^2 + O(g^3) \quad (3.64)$$

Let's parametrize the beta function with the length l of the interval:

$$l \frac{dg(l)}{dl} = -\beta(g(l)) \quad (3.65)$$

We remind (see section 2.6.1) that $\beta(g)$ has the universal behaviour

$$-\beta(g) = (2-x)g - \pi b g^2 + O(g^3) \quad (3.66)$$

where g is the structure constant of $\langle \Phi(z)\Phi(w)\Phi(y) \rangle$, $\Phi(z)$ being the perturbing field with scaling dimension $x = 2$. If we suppose that $g/b > 0$, the perturbation is marginally relevant and $g(l)$ flows 0. Solving the differential equation (3.66), and substituting in (3.64):

$$c_{\text{eff}}(l) = c + \frac{2}{b^2 \left(\log \frac{l}{\epsilon} \right)^3} + O \left(\left(\log \frac{l}{\epsilon} \right)^4 \right) \quad (3.67)$$

Integrating (3.63) over ϵ , we obtain the final result:

$$c_{\text{eff}}(l) = c - \frac{1}{b^2 (\log l)^3} + O((\log l)^4) \quad (3.68)$$

and we notice the presence of *logarithmic corrections* to the entropy.

3.3.2 Correction for gapped systems

Now we discuss the corrections to the entropy for *gapped systems*, that is for systems whose correlation length ξ is finite. Suppose, like in section 3.2, that the infinite system is divided into two half-infinite intervals. In the case we've already considered, if we focus on relevant operators, the Renyi entropy of an interval with length l embedded in an infinite system behaves like:

$$S_n(l) \simeq \frac{c}{6} \left(1 + \frac{1}{n}\right) \log l + b_n l^{-2x/n} + c'_n \quad (3.69)$$

where again n is the order of the branch point of the n -sheeted geometry \mathcal{R}_n . Let's remind the reasoning at the beginning of section 3.3.1. Taking advantage of the cutoff ϵ of the system, we arrived at the relation

$$(F_n - nF_1) = \frac{c}{12} \left(1 + \frac{1}{n}\right) \log \left(\frac{\epsilon}{a}\right) + \text{const} \quad (3.70)$$

(this time we recover the factor $c/12$) and we said that it should be $a = l$, since by scaling the entropy should depend on ϵ/l . If the system is gapped, our main dimensionful quantities are now ϵ and ξ , so the entropy will depend on ϵ/ξ , and if this time we set $a = \xi$, we obtain:

$$S_n \simeq \frac{c}{12} \left(1 + \frac{1}{n}\right) \log \xi + C'_n \quad (3.71)$$

a result already derived in section 3.2. Now, what the authors of [12] did is to postulate corrections to (3.71) using the same scaling arguments to argue this relation. In equation (3.69), simply substitute l with ξ , so that:

$$\boxed{S_n \simeq \frac{c}{12} \left(1 + \frac{1}{n}\right) \log \xi + C'_n + B_n \xi^{-x/n}} \quad (3.72)$$

We notice that the last term has an exponent that is half the one in (3.69): this is because we have only one branch point (the other was sent to ∞). In general, there could be corrections of the form

$$\xi^{-(Nx)/n}, \quad \text{for } N = 1, 2, 3, \dots \quad (3.73)$$

as in the previous section (see (3.61)).

The authors of [12] then tested this formula in a few situations. We just report the calculations for the non-critical XXZ chain, whose Hamiltonian is:

$$H_{XXZ} = - \sum_j (\sigma_j^x \sigma_{j+1}^x + \sigma_j^y \sigma_{j+1}^y + \Delta \sigma_j^z \sigma_{j+1}^z) \quad (3.74)$$

in the ferromagnetic regime, that is for $\Delta < -1$. Furthermore, we remark again that the system is *infinite and bipartite*. Thus we can use the corner transfer matrix method (see section 3.4) to compute the reduced density matrix.

$$\rho_A = \frac{\hat{A}}{\text{Tr} \hat{A}^4} \quad (3.75)$$

3.3. Corrections to Entanglement Entropy

where the hat denotes the infinite-lattice limit. For our case (and other more, see [28] and chapter 3.5), we can write

$$\rho_A = \frac{e^{-H_{\text{CTM}}}}{\text{Tr} e^{-H_{\text{CTM}}}} = \frac{e^{H_{\text{CTM}}}}{Z} \quad (3.76)$$

where $H_{\text{CTM}} = \hat{A}^4 = \sum_{j=0}^{\infty} \epsilon_j n_j$ is an *effective hamiltonian*, written in terms of free-fermionic operators whose coefficients are

$$\epsilon_j = 2j\epsilon, \quad \epsilon = \text{arccosh} \Delta \quad (3.77)$$

and the partition function is

$$Z = \text{Tr} e^{-H_{\text{CTM}}} = \prod_{j=0}^{\infty} (1 + e^{-2j\epsilon}) \quad (3.78)$$

Noting that $\text{Tr} e^{-nH_{\text{CTM}}} = \prod_{j=0}^{\infty} (1 + e^{-2jn\epsilon})$, the Renyi entropies of the XXZ model are then given by:

$$S_n \equiv \frac{1}{1-n} \log \left(\text{Tr} \rho_A^n \right) = \frac{1}{1-n} \left(\log \left(\text{Tr} e^{-nH_{\text{CTM}}} \right) - \log Z^n \right) \quad (3.79)$$

that is:

$$S_n = \frac{1}{1-n} \left[\sum_{j=0}^{\infty} \log(1 + e^{-2nj\epsilon}) - n \sum_{j=0}^{\infty} \log(1 + e^{-2j\epsilon}) \right] \quad (3.80)$$

If we are interested in the critical regime $\xi \gg 1$, then ([3]) the correlation length is given by

$$\log \xi \simeq \frac{\pi^2}{2\epsilon} + O(\epsilon^0) \quad (3.81)$$

and $\epsilon \ll 1$. We are then looking to terms of the form $\epsilon^{-\alpha} \propto e^{-\alpha\pi^2/2\epsilon}$. Now, because the asymptotic expansion of the entropy around $\epsilon = 0$ vanishes (we have $\epsilon^k S_n \xrightarrow{\epsilon \rightarrow 0} 0, \forall k$), a nice trick is to use the Poisson resummation formula.

Given a function $f(x)$, and denoting $\hat{f}(y) = \int_0^{\infty} f(x) \cos(yx) dx$, this formula states that

$$\sum_{j=-\infty}^{\infty} f(|\epsilon j|) = \frac{2}{\epsilon} \sum_{k=-\infty}^{\infty} \hat{f}\left(\frac{2\pi k}{\epsilon}\right) \quad (3.82)$$

If we apply it to $f_n(x) = \log(1 + e^{-2nx})$, and denoting $\text{csch} x = 1/\sinh x$, the entropies become (see [12] for details):

$$S_n = \frac{\pi^2}{24\epsilon} \left(1 + \frac{1}{n}\right) + \frac{\log 2}{2} + \frac{1}{1-n} \sum_{k=1}^{\infty} \left(\frac{n}{2k} \text{csch} \frac{\pi^2 k}{\epsilon} - \frac{1}{2k} \text{csch} \frac{\pi^2 k}{\epsilon n} \right) \quad (3.83)$$

3. Entanglement entropy in 1-D quantum chains

That is, the entropy is equal to (3.71) with $c = 1$, plus corrections. If we use the fact that $\epsilon \simeq 0$, we can write

$$\operatorname{csch} \frac{\pi^2 k}{\epsilon n} \simeq 2 \exp\left(-\frac{\pi^2 k}{\epsilon n}\right)$$

Then, each of these terms in (3.83) gives rise to corrections of the form:

$$\exp\left(-\frac{\pi^2 k}{\epsilon n}\right) \simeq \xi^{-2k/n} \quad (3.84)$$

which agree with (3.73) if we set the scaling dimension x equal to 2. Notice that a multiplicative logarithmic correction is absent in the gapped phase.

3.3.3 Parity effects in gapless spin chains

We now mention a last, but important, correction to the entanglement entropy, which appears very often in DMRG simulations (see chapter 4 for numerical examples). Suppose the system is infinite, that is $L = \infty$. This correction introduces *oscillations* to the entropy, and if we denote with $S^{\text{CFT}}(l)$ the entropy at the CFT point (eventually including the corrections already discussed), it obeys the universal scaling law:

$$\boxed{S_n(l) - S^{\text{CFT}}(l) = f_n \cos(2k_F l) |2l \sin k_F|^{-p_n}} \quad (3.85)$$

where $p_n = 2K/n$, K is the Luttinger liquid parameter (see e.g. [30]), k_F is the Fermi momentum, and f_n is a nonuniversal constant. If the system has instead a finite length, we must perform the replacement:

$$l \rightarrow \frac{L}{\pi} \sin \frac{\pi l}{L} \quad (3.86)$$

in a similar fashion for the case without corrections, and $f_n \rightarrow F_n(l/L)$, a universal scaling function. If again the system is in zero magnetic field and at zero temperature, we have half filling of the Fermi levels, so that $k_F = (\pi/2)$ and the entropy correction reduces to:

$$S_n(l) - S^{\text{CFT}}(l) = f_n (-1)^l l^{-p_n} \quad (3.87)$$

We won't demonstrate (3.85) since it is a very technical demonstration, and we refer to [11] for details.

3.4 The Corner Transfer Matrix method

Here we want to show a method, first developed in [28], to evaluate reduced density matrices in the *thermodynamic limit*, using the Corner Transfer Matrices (CTMs, see the appendix B). This will be a useful tool for the calculation

3.4. The Corner Transfer Matrix method

of entanglement entropies of system out of criticality, in the thermodynamic limit. Consider a quantum spin chain with L sites and Hamiltonian H . We want to evaluate the entropy in the ground state $|\Phi\rangle$, so we'll need the density matrix

$$\rho = |\Phi\rangle \langle \Phi| \quad (3.88)$$

Let's denote with $\vec{\sigma} = \{\sigma_1, \sigma_2, \dots, \sigma_L\}$ the spin configuration of the chain, and its corresponding quantum state with $|\vec{\sigma}\rangle$. Then we have the matrix notation:

$$\rho(\vec{\sigma}, \vec{\sigma}') = \langle \vec{\sigma} | \rho | \vec{\sigma}' \rangle = \Phi(\vec{\sigma}) \Phi(\vec{\sigma}') \quad (3.89)$$

where $\Phi(\vec{\sigma}) = \langle \vec{\sigma} | \Phi \rangle$. Then we divide the system in two parts of length l and $L - l$. If we set the spins of the former as $\vec{\sigma}_1 = \{\sigma_1, \sigma_2, \dots, \sigma_l\}$ and the spins of the latter as $\vec{\sigma}_2 = \{\sigma_{l+1}, \sigma_{l+2}, \dots, \sigma_L\}$, we'll denote

$$\Phi(\vec{\sigma}_1, \vec{\sigma}_2) = \left(\langle \vec{\sigma}_1 | \otimes \langle \vec{\sigma}_2 | \right) |\Phi\rangle \quad (3.90)$$

The reduced density matrix of the part with length l is then:

$$\begin{aligned} \rho_1(\vec{\sigma}_1, \vec{\sigma}'_1) &= \sum_{\vec{\sigma}_2} \left(\langle \vec{\sigma}_1 | \otimes \langle \vec{\sigma}_2 | \right) |\rho\rangle \langle \rho| \left(|\vec{\sigma}'_1\rangle \otimes |\vec{\sigma}_2\rangle \right) \\ &= \sum_{\vec{\sigma}_2} \Phi(\vec{\sigma}_1, \vec{\sigma}_2) \Phi(\vec{\sigma}'_1, \vec{\sigma}_2) \end{aligned} \quad (3.91)$$

Let's now take advantage of the correspondence between this quantum chain of Hamiltonian H , and a classical spin model on a lattice whose row-to-row transfer matrix is $T = \exp(-\beta H)$ (see chapter 1). There we saw that the partition function of a classical model could be written (in "operatorial form") as

$$Z = \langle \vec{\sigma}_1 | T^N | \vec{\sigma}_N \rangle \quad (3.92)$$

where in this case $\vec{\sigma}_i$ is the spin configuration of the i -th line. Notice an important point: thanks to this correspondence, we can apply the operator T to states that belong to \mathcal{H} , the Hilbert space associated to H . Suppose that this transfer matrix commutes with the Hamiltonian of the quantum system:

$$[H, T] = 0 \quad (3.93)$$

so that they share the *same eigenvectors*. This means that the lowest eigenvalue of H (the energy of the ground state $|\Phi\rangle$) is equal to the highest eigenvalue of T . Let's consider the partition function

$$Z = \langle \vec{\sigma} | T^N | \vec{\alpha} \rangle \quad (3.94)$$

where the "start" spin configuration $\vec{\alpha}$ is arbitrary and the "final" configuration $\vec{\sigma}$ is fixed. The lattice of the classical system has N rows and L columns. Denote with $\{|\varphi_i\rangle\}$ the basis of eigenvector of H , where $|\varphi_0\rangle \equiv |\Phi\rangle$ (the ground

3. Entanglement entropy in 1-D quantum chains

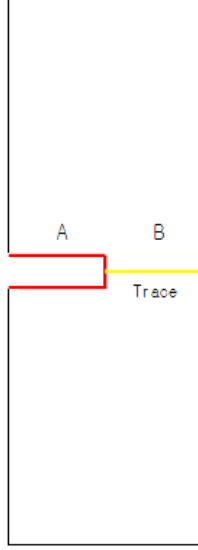


Figure 3.2: The infinite strip with a perpendicular cut, whose partition function in the reduced matrix of the system.

state), and with $\{E_i\}$ the corresponding eigenvalues. We can then expand $|\vec{\alpha}\rangle$ in this basis as:

$$|\vec{\alpha}\rangle = a_0 |\Phi\rangle + \sum_i a_i |\phi_i\rangle \quad (3.95)$$

and applying T^N , we obtain:

$$T^N |\vec{\alpha}\rangle = e^{-N\beta E_0} a_0 |\Phi\rangle + \sum_i e^{-N\beta E_i} a_i |\phi_i\rangle \quad (3.96)$$

If we send $N \rightarrow \infty$, we are considering a classical spin model on a half-infinite vertical *strip* of width L . In this limit, the partition function becomes:

$$\begin{aligned} Z &= \langle \vec{\sigma} | T^N |\vec{\alpha}\rangle = \langle \vec{\sigma} | \left[e^{-N\beta E_0} (a_0 |\Phi\rangle + \sum_i e^{-N\beta(E_0 - E_i)} |\phi_i\rangle) \right] \\ &\xrightarrow{N \rightarrow \infty} e^{-N\beta E_0} a_0 \langle \vec{\sigma} | \Phi \rangle \end{aligned} \quad (3.97)$$

and we have then established the important relation:

$$\boxed{Z \propto \langle \vec{\sigma} | \Phi \rangle \equiv \Phi(\vec{\sigma})} \quad (3.98)$$

which says that $\Phi(\vec{\sigma})$ can be interpreted as the partition function of an half-infinite vertical strip whose initial configuration is arbitrary and whose end configuration is $\vec{\sigma}$. Similarly, $\rho(\vec{\sigma}, \vec{\sigma}')$ can be regarded as the partition function of two such strips, one extending from $-\infty$ to 0, and the other from 0 to ∞ , with end configurations $\vec{\sigma}$ and $\vec{\sigma}'$ respectively. Finally, the reduced density matrix $\rho(\vec{\sigma}_1, \vec{\sigma}_2)$ is obtained by identifying the two spin configurations $\vec{\sigma}_2$ and

3.4. The Corner Transfer Matrix method

summing, that is by joining the two strips between sites $l + 1$ and L : it then represents the partition function of an infinite strip with a perpendicular cut in it ([28]). The situation is described in Fig. 3.2. Let now $L \rightarrow \infty$, and let be l equal to half-infinite chain. The system is then divided in four blocks, which can indeed be described by *corner transfer matrices*. These are denoted with A, B, C and D , see again Fig. 3.2 and appendix B. Then, the reduced density matrix $\rho_1(\vec{\sigma}_1, \vec{\sigma}_2)$ is given by:

$$\rho_1(\vec{\sigma}_1, \vec{\sigma}_2) = \frac{(ABCD)_{\vec{\sigma}_1, \vec{\sigma}_2}}{Z} \quad (3.99)$$

where the partition function is $Z = \text{Tr } ABCD$. If, at last, we want to evaluate entanglement entropies, we simply need the object:

$$\text{Tr } \rho_1^n = \frac{\text{Tr } (ABCD)^n}{Z^n} \quad (3.100)$$

Let's consider some applications of this method. For many models, we have that the reduced density matrix can be expressed as:

$$\rho_1 = e^{-H_{\text{CTM}}} \equiv e^{-\epsilon \mathcal{O}} \quad (3.101)$$

where \mathcal{O} is an operator with integer eigenvalue. For example, the quantum Ising chain with transverse field, with Hamiltonian:

$$H = - \sum_{n=1}^{L-1} (\sigma_n^x + \lambda \sigma_n^z \sigma_{n+1}^z) - \delta \sigma_L^x \quad (3.102)$$

is associated, with a proper choice of the parameters λ and δ , to the two-dimensional Ising model in zero magnetic field:

$$H = -J \sum_{i \text{ nn } j} \sigma_i \sigma_j \quad (3.103)$$

Since this classical lattice is isotropic, all the CTMs are equal and we'll refer to them simply as A . Then we have:

$$\rho_1 = A^4 = e^{-H_{\text{CTM}}} \quad (3.104)$$

Furthermore, the term $\delta \sigma_L^x$ can be neglected for $L \rightarrow \infty$. For this model, we have that H_{CTM} can be diagonalized in terms of free fermions (see again [28] for details):

$$H_{\text{CTM}} = \sum_{j=0}^{\infty} \epsilon_j n_j \quad (3.105)$$

3. Entanglement entropy in 1-D quantum chains

where $n_j = c_j^\dagger c_j$ gives the occupation number of fermions. The model is critical for $\lambda = 1$, and between the two phases there is a difference in the spectrum of the free fermions:

$$\epsilon_j = \begin{cases} (2j+1)\epsilon & \lambda < 1 \\ 2j\epsilon & \lambda > 1 \end{cases} \quad \epsilon = \pi \frac{I(k)}{I(k')} \quad (3.106)$$

Here $I(k)$ is the complete elliptic integral of the first kind, $k' = \sqrt{1-k^2}$ where $0 \leq k \leq 1$, and k is related to λ by:

$$k = \begin{cases} \lambda, & \lambda < 1 \\ \frac{1}{\lambda}, & \lambda > 1 \end{cases}$$

Another interesting example of the use of CTMs is the XYZ model, which will be treated in the next section.

3.5 The XYZ model

This is the main section of this chapter, since it describes the model which we will work on, the XYZ model.

3.5.1 The definition of the model

Let's begin by defining the quantum spin- $\frac{1}{2}$ ferromagnetic XYZ chain:

$$\hat{H}_{XYZ} = - \sum_n \left(J_x \sigma_n^x \sigma_{n+1}^x + J_y \sigma_n^y \sigma_{n+1}^y + J_z \sigma_n^z \sigma_{n+1}^z \right) \quad (3.107)$$

where σ_n^α are the Pauli matrices, and J_α ($\alpha = x, y, z$) are a measure of the anisotropy of the model (in this section we will follow [22]). In Fig. 3.3 we plot the phase diagram of the XYZ model in the $\left(\frac{J_y}{J_x}, \frac{J_z}{J_x}\right)$ plane. This is divided into 12 regions named $I_{a,b,c,d}$, $II_{a,b,c,d}$, $III_{a,b,c,d}$: regions of the diagram having the same latin number share the same description, since are connected by simmetries transformations which leave the Hamiltonian unchanged.

Consider first the $J_x = J_y$ line. Here we recover the XXZ model, and thanks to its equivalence with the six vertex model, we know that for $|\frac{J_z}{J_y}| < 1$ we have a critical paramagnetic phase, while for $|\frac{J_z}{J_y}| > 1$ the phase is ferromagnetic. Clearly, the same physics holds for $J_y = -J_x$. In fact, if we operate the parity transformation

$$\mathbf{P}_x = \prod_n \sigma_{2n}^x \quad (3.108)$$

to the hamiltonian, we only need to make the replacements

$$\begin{cases} J_y \rightarrow -J_y \\ J_z \rightarrow -J_z \end{cases} \quad (3.109)$$

Note that J_z changes sign under this transformation, so the ferromagnetic and antiferromagnetic phases are reversed. If we look at the lines $J_z = \pm J_x$, we are observing a XYX model, which is a rotated XXZ model because if this time we rotate the system around the x axis by 90° through

$$\mathbf{R}_x = \prod_n \exp\left(i\frac{\pi}{2}\sigma_n^x\right) \quad (3.110)$$

we need the replacements:

$$\begin{cases} J_y \rightarrow J_z \\ J_z \rightarrow J_y \end{cases} \quad (3.111)$$

Finally, along the diagonals $J_y = \pm J_z$ we have a XYY model of the form:

$$\hat{H}_{XYY} = - \sum_n \left(J_x \sigma_n^x \sigma_{n+1}^x + J_y (\sigma_n^y \sigma_{n+1}^y \pm \sigma_n^z \sigma_{n+1}^z) \right) \quad (3.112)$$

where the paramagnetic phase is for $|\frac{J_y}{J_x}| > 1$ and the Ising phase is for $|\frac{J_y}{J_x}| < 1$. The XYZ model presents four *tri-critical* point at $(\frac{J_y}{J_x}, \frac{J_z}{J_x}) = (\pm 1, \pm 1)$. Two of these are conformal points: $C_1 = (1, -1)$ and $C_2 = (-1, 1)$. These correspond to an antiferromagnetic Heisenberg chain at the Kosterlitz-Thouless transition (see *e.g.* [25], and there the correlation length diverges. The other two, denoted as $E_1 = (1, 1)$ and $E_2 = (-1, -1)$, correspond to an Heisenberg ferromagnet at its first order phase transition.

Sutherland ([33]) showed that the J_α constants of the XYZ model are related to the parameters Γ and Δ of the eight vertex model in zero magnetic field by the relations

$$J_x : J_y : J_z = 1 : \Gamma : \Delta \quad (3.113)$$

and this implies that we can set, without loss of generality, $J_x = 1$. The *principal regime* (PR) of the eight vertex model corresponds to $\Delta \leq 1$ and $|\Gamma| \leq 1$ and describes an anti-ferroelectric phase. In this regime, we have the following parametrization in terms of Jacobi elliptic functions (see [3], and appendix B for a definition):

$$\Gamma = \frac{1 + k \operatorname{sn}^2(i\lambda; k)}{1 - k \operatorname{sn}^2(i\lambda; k)} \quad \Delta = -\frac{\operatorname{cn}(i\lambda; k) \operatorname{dn}(i\lambda; k)}{1 - k \operatorname{sn}^2(i\lambda; k)} \quad (3.114)$$

with the restrictions

$$0 \leq k \leq 1, \quad 0 \leq \lambda \leq I(k') \quad (3.115)$$

and where

$$I(k') = \int_0^{\frac{\pi}{2}} \frac{d\theta}{\sqrt{1 - k'^2 \sin^2 \theta}} \quad (3.116)$$

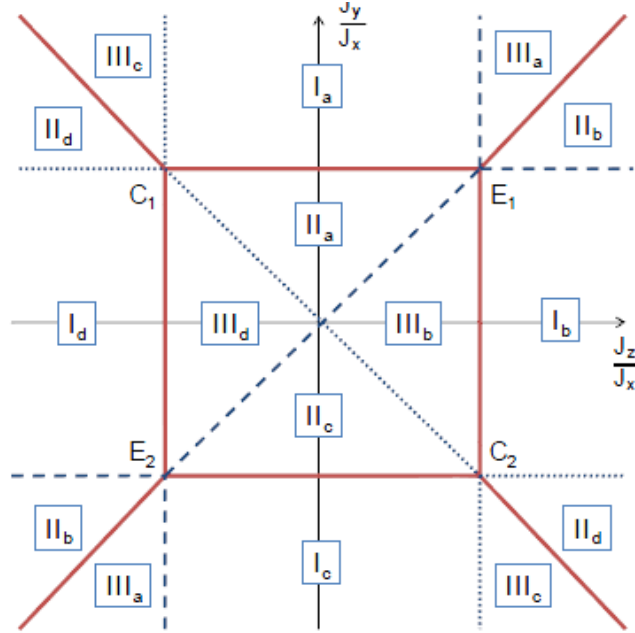


Figure 3.3: The phase diagram of the XYZ model. The critical lines of the model are represented by red lines.

is the complete elliptic integral of first kind, with argument $k' = \sqrt{1 - k^2}$. Accordingly, we refer as the principal regime for the XYZ model when the parameters obey

$$|J_y| < J_x < -J_z \quad (3.117)$$

corresponding to the region I_a of figure 3.3. If these parameters are out of the PR, we only need to use new J'_β that are functions of the old ones, and take advantage of

$$J'_x : J'_y : J'_z = 1 : \Gamma : \Delta$$

to recover J_α as functions of Γ and Δ .

3.5.2 Von Neumann and Renyi entropies

We now want to evaluate the entanglement entropy of a subsystem with length l such that

$$\frac{l}{L} = \frac{1}{2}$$

where L is the length of the chain, in its ground state. We will do this in the *thermodynamic limit*, that is for $L \rightarrow \infty$, and we will take advantage of the CTMs method developed in section 3.4. We know (see appendix B) that for the eight vertex model in zero field the four CTMs are symmetric and satisfy the relations $A = C$ and $B = D$. The Hilbert space of the quantum chain can be divided in two parts describing the two half-infinite chains, that

is $\mathcal{H} = \mathcal{H}_R \otimes \mathcal{H}_L$, and for the density matrix of the ground state $\rho = |0\rangle\langle 0|$ we have the expression in term of CTMs:

$$\rho_R(\vec{\sigma}, \vec{\sigma}') = \left[\text{Tr}_{\mathcal{H}_L}(\rho) \right]_{\vec{\sigma}, \vec{\sigma}'} = (ABCD)_{\vec{\sigma}, \vec{\sigma}'} = (AB)_{\vec{\sigma}, \vec{\sigma}'}^2 \quad (3.118)$$

We now use the diagonal CTMs $A_d(u)$ and $B_d(u)$ (defined respectively in (B.39) and (B.40)) to write:

$$\rho_R = \begin{pmatrix} 1 & 0 \\ 0 & x^2 \end{pmatrix} \otimes \begin{pmatrix} 1 & 0 \\ 0 & x^4 \end{pmatrix} \otimes \begin{pmatrix} 1 & 0 \\ 0 & x^6 \end{pmatrix} \otimes \dots \quad (3.119)$$

where

$$x = e^{-\epsilon} \quad \epsilon \equiv \pi \frac{\lambda}{2I(k)} \quad (3.120)$$

Using $A_d(u)$ or $A(u)$ doesn't make any difference here, because the entropies we want to evaluate are traces over functions of ρ_R . Notice that we can write our reduced density matrix as:

$$\rho_R = e^{-\epsilon \hat{O}} \quad (3.121)$$

where \hat{O} has integer eigenvalues (compare with (3.101)). If we denote the normalized reduced density matrix $\rho'_R = \rho_R/Z$, where the partition function is

$$Z = \text{Tr}_{\mathcal{H}_R} \rho_R = \prod_{j=1}^{\infty} (1 + x^{2j}) \quad (3.122)$$

the Von Neumann entropy is then given by

$$S = -\text{Tr}_{\mathcal{H}_R} \rho'_R \log \rho'_R = -\epsilon \frac{\partial \ln Z}{\partial \epsilon} + \ln Z \quad (3.123)$$

Thus, we obtain an exact analytic expression for the entanglement entropy of the XYZ model as:

$$S = 2\epsilon \sum_{j=1}^{\infty} \frac{j}{1 + e^{2j\epsilon}} + \sum_{j=1}^{\infty} \log(1 + e^{-2j\epsilon}) \quad (3.124)$$

As an important remark, note that this formula has been deduced for *open boundary conditions*, see the discussion in appendix B. To compute the Renyi entropies, whose definition we remind here

$$S_\alpha = \frac{1}{1 - \alpha} \log \text{Tr} \rho_R^\alpha \quad (3.125)$$

we need instead

$$\rho_R^\alpha = \begin{pmatrix} 1 & 0 \\ 0 & x^{2\alpha} \end{pmatrix} \otimes \begin{pmatrix} 1 & 0 \\ 0 & x^{4\alpha} \end{pmatrix} \otimes \begin{pmatrix} 1 & 0 \\ 0 & x^{6\alpha} \end{pmatrix} \otimes \dots \quad (3.126)$$

3. Entanglement entropy in 1-D quantum chains

and noting that $\text{Tr } \rho_R^\alpha = \text{Tr } \rho_R^\alpha / (Z^\alpha)$, we have:

$$S_\alpha = \frac{\alpha}{\alpha - 1} \sum_{j=1}^{\infty} \log(1 + e^{-2j\epsilon}) + \frac{1}{1 - \alpha} \sum_{j=1}^{\infty} \log(1 + e^{-2j\alpha\epsilon}) \quad (3.127)$$

As a check of the validity of these equations, let's consider the non critical XXZ chain for $J_z \rightarrow -1^-$ (that is, J_z approaches -1 from below). In this limit, we have

$$\begin{cases} \Gamma = 1 \\ \Delta \rightarrow -1^- \end{cases} \quad \begin{cases} k = 0 \\ \lambda \rightarrow 0^+ \end{cases}$$

and from (3.120), using the fact that $I(k) \xrightarrow[k \rightarrow 0]{} \pi/2$, it is $\epsilon \approx \lambda$, and then $\epsilon \approx 0$. This allows us to approximate the summations in (3.124) with an integral. Using the Euler-MacLaurin formula, the entropy behaves as:

$$\begin{aligned} S &\approx \int_1^\infty dx \left(\frac{x\epsilon}{1 + e^{x\epsilon}} + \log(1 + e^{-x\epsilon}) \right) \\ &\approx \int_0^\infty dx \left(\frac{x\epsilon}{1 + e^{x\epsilon}} + \log(1 + e^{-x\epsilon}) \right) - \frac{\log 2}{2} + O(\epsilon) = \frac{\pi^2}{12\epsilon} - \frac{\log 2}{2} + O(\epsilon) \end{aligned} \quad (3.128)$$

From our approximations, we have as well

$$-\Delta \simeq \cosh \lambda$$

so that:

$$\epsilon \approx \lambda \approx \sqrt{2\sqrt{-\Delta - 1}} \quad (3.129)$$

We know from [3] that the XXZ chain is equivalent to the six vertex model (which means, again, that the Hamiltonian of the former and the transfer matrix of the latter commute). For $\epsilon \ll 1$, the correlation function behaves like

$$\log \xi \simeq \frac{\pi^2}{2\epsilon} \quad (3.130)$$

and at last, substituting properly all the terms in (3.128), we find:

$$S \sim \frac{1}{6} \log \frac{\xi}{a} + U \quad (3.131)$$

where $U = -\log(2)/6$. This agrees with Cardy, Calabrese prediction for the entropy of a system out of criticality (see equation (3.40)), with $c = 1$. Notice that this result was already obtained in section 3.3.2 by other means.

3.5.3 The essential critical points

We now study the behaviour of the Von Neumann entropy in the (J_y, J_z) plane. For this purpose, it is useful to switch from (λ, k) to the new parameters (u, l) , linked to the previous ones by a *Landen transformation*, that is:

$$l = \frac{2\sqrt{k}}{1+k} \quad u = (1+k)\lambda \quad (3.132)$$

In this way, we can reparametrize the two constants Γ and Δ as (see [3]):

$$\Gamma = \frac{1 + k \operatorname{sn}^2(i\lambda; k)}{1 - k \operatorname{sn}^2(i\lambda; k)} = \frac{1}{\operatorname{dn}(iu; l)} \quad (3.133a)$$

$$\Delta = -\frac{\operatorname{cn}(i\lambda; k) \operatorname{dn}(i\lambda; k)}{1 - k \operatorname{sn}^2(i\lambda; k)} = -\frac{\operatorname{cn}(iu; l)}{\operatorname{dn}(iu; l)} \quad (3.133b)$$

It is possible to express (l, u) as functions of (J_y, J_z) . Following [22], and working for example in the principal regime

$$J_y > 1 \quad -1 < J_z < 1 \quad (3.134)$$

one can obtain the following relations:

$$l = \sqrt{\frac{1 - J_z^2}{J_y^2 - J_z^2}} \quad u = K(l') + F(\arcsin J_z; l') \quad (3.135)$$

where $l' = \sqrt{1 - l^2}$ and

$$F(\phi, k) = \int_0^\phi \frac{d\theta}{\sqrt{1 - k^2 \sin^2 \theta}} = \operatorname{sn}^{-1}(\sin \phi; k) \quad (3.136)$$

is the incomplete elliptic integral of the first type. Furthermore, we have:

$$I(l) = (1+k)I(k) \quad (3.137)$$

which allows us to write

$$\epsilon = \pi \frac{\lambda}{2I(k)} = \pi \frac{u}{2I(l)} \quad (3.138)$$

Since the entanglement entropy S , whose expression is given in equation (3.124), depends only on ϵ , we have thus obtained a way to express it as a function of (J_y, J_z) . In figure 3.4 we plot S in the (J_y, J_z) plane for $-2 < J_y < 2$ and $-2 < J_z < 2$.

This is a contour plot: regions of similar colour have similar value of the entropy, and the lines dividing regions of different colors are lines of constant entropy. The brighter is the colour, the bigger is the entropy. From this figure

3. Entanglement entropy in 1-D quantum chains

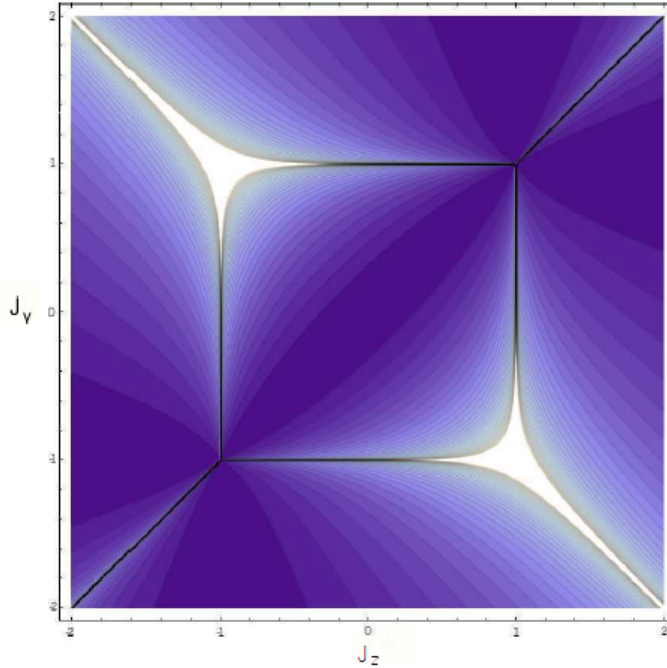


Figure 3.4: Curves of constant entropy of the XYZ model in the (J_y, J_z) plane.

is evident the phase diagram of the model, and the most interesting points are easily recognized as the four tri-critical points C_1 , C_2 and E_1 , E_2 , for $J_y = \pm 1$ and $J_z = \pm 1$ (see section 3.5.1). We emphasize the fact that C_1 and C_2 are conformal, while E_1 and E_2 are not, since the latter points have low energy excitations following the quadratic dispersion relation $\epsilon(q) = 1 - \cos q$: conformal field theories are also relativistically invariant field theories, so they require a linear dispersion relation for the energy. This implies that the entropy at E_1 doesn't follow the behaviour predicted by Cardy and Calabrese ([7]) at criticality.

Let's first study the conformal point $C_1 \rightarrow (J_y, J_z) = (1, -1)$ (the point C_2 has a similar treatment). We use the following parametrization

$$\begin{cases} \Gamma = 1 - \rho \cos \phi \\ \Delta = -1 - \rho \sin \phi \end{cases} \quad 0 \leq \phi \leq \frac{\pi}{2} \quad (3.139)$$

which leads to:

$$\begin{cases} l = (\tan \phi + 1)^{-1/2} + O(\rho) \\ \text{snh}(z; l) = \sqrt{2 \cos \phi + 2 \sin \phi} \sqrt{\rho} + O(\rho^{3/2}) \end{cases} \quad (3.140)$$

where we defined

$$z = iu$$

The point C_1 is reached for $\rho \rightarrow 0$. In this limit l is not defined, since it depends on the path followed towards C_1 , that is on ϕ . Solving (3.133), we

find that $\text{sn}(u; l) \simeq u + O(u^2)$, and then:

$$z = \sqrt{2 \cos \phi + 2 \sin \phi \sqrt{\rho}} + O(\rho^{3/2}) \quad (3.141)$$

It follows from (3.138) that $\epsilon \sim \sqrt{\rho}$, which means that S diverges in any neighbourhood of C_1 .

For the point $E_1 \rightarrow (J_y, J_z) = (1, 1)$ we use instead the following parametrization:

$$\begin{cases} \Gamma = -1 - \rho \cos \phi \\ \Delta = -1 - \rho \sin \phi \end{cases} \quad 0 \leq \phi \leq \frac{\pi}{2} \quad (3.142)$$

which implies:

$$\begin{cases} l = (\tan \phi + 1)^{-1/2} + O(\rho) \\ \text{snh}(z; l) = -\sqrt{2 \cos \phi + 2 \sin \phi \sqrt{\rho}} + O(\rho^{3/2}) \end{cases} \quad (3.143)$$

In this case, using (3.133), it turns out that we must use the following expansion:

$$\text{sn}(iu) = u - 2iI' + O((u - 2iI')^2)$$

Clearly, we now have $z \sim 2I'$, and then

$$\epsilon \sim \frac{I(l')}{I(l)}$$

The fact that l is still not defined for $\rho \rightarrow 0$ implies that ϵ can take any positive values in the neighbourhood of E_1 , depending on the value of ϕ ; the same holds true for the entropy. For this reason the point E_1 is called an *essential singularity* for the Renyi entropies: the value of S is direction dependent, since E_1 is an accumulation point for isoentropic lines (see also figure 3.5), and it seems that S can assume all the values between 0 to ∞ , as we'll see below.

Let's now explain qualitatively why the entropy at E_1 has this singular behaviour. The isotropic point E_1 can be described by the Hamiltonian:

$$\hat{H}_{XXX} = - \sum_{n=1}^N \vec{\sigma}_n \cdot \vec{\sigma}_{n+1} \quad (3.144)$$

(we take for the moment a finite number of sites N in the chain), which commutes with the generators

$$S^2 = \frac{1}{4} \sum_{n=1}^N \vec{\sigma}_n \cdot \vec{\sigma}_n, \quad S^z = \frac{1}{2} \sum_{n=1}^N \sigma_n^z, \quad S^\pm = \frac{1}{2} \sum_{n=1}^N \sigma_n^\pm \quad (3.145)$$

The ground state is then $N + 1$ degenerated, spanned by the basis corresponding to ferromagnetic states alligned along different directions. Its precise form depends on how the symmetry $SU(2)$, satysfied by the Hamiltonian (3.144), is

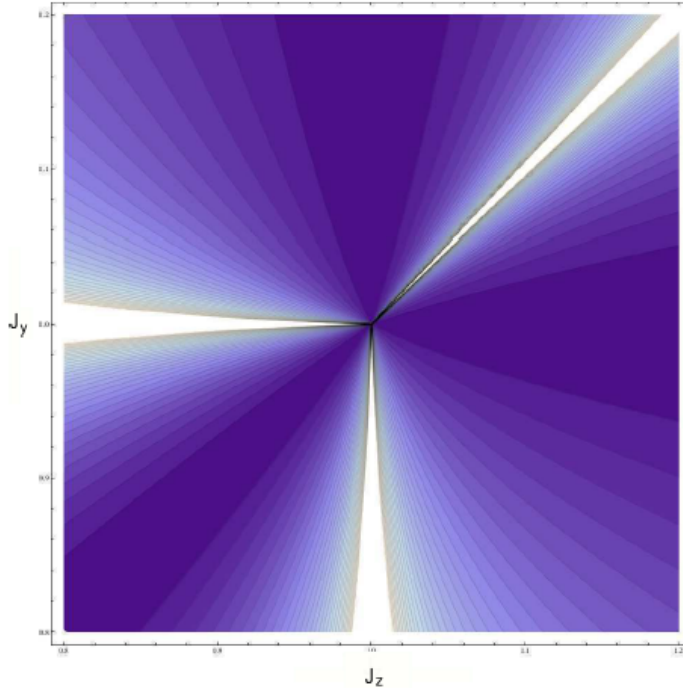


Figure 3.5: Curves of constant entropy of the XYZ model in the vicinity of E_1 .

broken. If the ground state consists in one of these (classical) basis states, the entropy is 0, but a superposition of such states have an entanglement entropy that may grow with the number of basis states, and in the limit $N \rightarrow \infty$ this entropy can even diverge. In fact, two of the isoentropic lines approaching E_1 are the Ising ferromagnetic line ($J_z = 1$) for which $S = 0$, and the XXZ line that implies $S \rightarrow \infty$ in the thermodynamic limit. The situation is different for the points C_1 and C_2 , since there the order is antiferromagnetic: the antiferromagnetic states (Neel states) *are not* eigenstates of the Hamiltonian describing C_1 or C_2 .

In the next chapter we will test the validity of formula (3.124) for the entanglement entropy in the vicinity of the essential singularity.

3.5.4 Unusual corrections to the entanglement entropy

In section 3.3 we analyzed all the possible corrections to the formula

$$S = \frac{c}{6} \ln l \tag{3.146}$$

for the entanglement entropy of an interval of length l , embedded in an infinitely long spin chain at criticality with open boundary conditions. For

gapped systems, by simply scaling arguments, we found instead the behaviour:

$$S_\alpha = \frac{c + \bar{c}}{12} \left(1 + \frac{1}{\alpha}\right) \ln \xi + C'_\alpha + \sum_{n=1}^{\infty} B_{n,\alpha} \xi^{-(nx)/\alpha} \quad (3.147)$$

Using the same scaling arguments, we can add all the corrections found at criticality (see section 3.3.1) by simply making the substitution $l \rightarrow \xi$.

On the other hand, we have the formula of the Renyi entropies for the XYZ model, given by (3.127). We now want to show (following [19]) that this formula gives rise to corrections which can not be predicted by the reasonings presented in section 3.3.

Using the q -Pochhammer symbol, defined by

$$(a; q)_n \equiv \prod_{k=0}^{n-1} (1 - aq^k) \quad (3.148)$$

we can write the partition function of the XYZ model, whose expression is given in (3.122), as

$$Z = (-x^2; x^2)_\infty \quad (3.149)$$

where x is defined in (3.120). Furthermore, using (3.126), we find a similar expression for the density matrix:

$$\text{Tr} \rho_R^\alpha = \frac{(-x^{2\alpha}; x^{2\alpha})_\infty}{(-x^2; x^2)_\infty^\alpha} \quad (3.150)$$

It can be shown (see [19]) that this partition function has the following alternative form:

$$Z = x^{-1/12} \chi_{1,2}^{\text{Ising}}(i\epsilon/\pi) \quad (3.151)$$

where $\chi_{1,2}^{\text{Ising}}$ is a Virasoro character (see section 2.5) of the Ising model (whose central charge is $c = 1/2$). It's interesting that the partition function of a $c = 1$ model can be expressed as a function of Virasoro characters of the $c = 1/2$ conformal field theory, but we won't discuss this aspect further.

We now want to study the behaviour of the entanglement entropy approaching to the critical line. It is then convenient to switch to the variable

$$\tilde{x} \equiv e^{-i\pi^2/\mu\tau} = e^{-\pi^2/\epsilon} \quad (3.152)$$

through a modular transformation, and then take the limit $\tilde{x} \rightarrow 0$. It is known (see for example [22]) that the elliptic parameter k , defined in section 3.5.1, can be written as

$$k \equiv k(x) = 4 \frac{x^{1/2} (-1; x^2)_\infty^4}{(-x; x^2)_\infty^4} \quad (3.153)$$

This changes, under a modular transformation, as:

$$k(\tilde{x}) = \frac{(x; x^2)_\infty^4}{(-x; x^2)_\infty^4} \quad (3.154)$$

3. Entanglement entropy in 1-D quantum chains

Taking advantage of these last two expressions, and denoting $k' = \sqrt{1 - k^2}$, we obtain

$$(-x^{2\alpha}; x^{2\alpha})_\infty = \frac{(\tilde{x}^{1/\alpha}; \tilde{x}^{2/\alpha})_\infty}{\sqrt{2}x^{\alpha/12}\tilde{x}^{1/(24\alpha)}} \quad (3.155)$$

from which follows:

$$\text{Tr } \rho_R^\alpha = 2^{(\alpha-1)/2} \tilde{x}^{(\alpha^2-2)/(24\alpha)} \frac{(\tilde{x}^{1/\alpha}; \tilde{x}^{2/\alpha})_\infty}{(\tilde{x}; \tilde{x}^2)_\infty^\alpha} \quad (3.156)$$

Using the expansion

$$\ln(1 - x) = -\sum_{m=1}^{\infty} \frac{x^m}{m} \quad (3.157)$$

the divisor function

$$\sigma_{-1}(n) \equiv \frac{1}{n} \sum_{\substack{j < k=1 \\ j \cdot k=n}}^{\infty} (j + k) + \sum_{\substack{j=1 \\ j^2=n}}^{\infty} \frac{1}{j} \quad (3.158)$$

and the definition (3.125), we can now write the Renyi entropies as:

$$\begin{aligned} S_\alpha &= -\frac{1+\alpha}{24\alpha} \ln \tilde{x} - \frac{1}{2} \ln 2 \\ &\quad - \frac{1}{1-\alpha} \sum_{n=1}^{\infty} \sigma_{-1}(n) (\tilde{x}^{n/\alpha} - \alpha \tilde{x}^n - \tilde{x}^{2n/\alpha} + \alpha \tilde{x}^{2n}) \end{aligned} \quad (3.159)$$

Since \tilde{x} has meaning only within Baxter's parametrization of the model, if we want to gain generality we must measure the entropy as a function of a universal parameter, such as the correlation length. In the scaling limit, obtained for $\tilde{x} \rightarrow 0$, one can show that:

$$\tilde{x} \simeq \left(\frac{\xi}{a_0}\right)^2 + O(\xi^{-1}) \quad (3.160)$$

where a_0 is a short distance cutoff, such as the lattice spacing. At last, keeping only the dominant term of this last expression, we end up with the final formula:

$$\begin{aligned} S_\alpha &= \frac{1+\alpha}{12\alpha} \ln \frac{\xi}{a_0} - \frac{1}{2} \ln 2 \\ &\quad - \frac{1}{1-\alpha} \sum_{n=1}^{\infty} \sigma_{-1}(n) \left[\left(\frac{\xi}{a_0}\right)^{-2n/\alpha} - \left(\frac{\xi}{a_0}\right)^{-4n/\alpha} \right] \\ &\quad + \frac{\alpha}{1-\alpha} \sum_{n=1}^{\infty} \sigma_{-1}(n) \left[\left(\frac{\xi}{a_0}\right)^{-2n} - \left(\frac{\xi}{a_0}\right)^{-4n} \right] \end{aligned} \quad (3.161)$$

Notice that the leading term of this formula is correctly predicted by (3.147), while the other ones have a more difficult interpretation. Indeed, using (3.147)

for a scalar field, the scaling dimension reduces to $x = 2h$ and (3.161) would indicate $h = 2$, meaning that a marginal operator is dragging the system out of criticality. But this is in contrast with what we deduced in section 3.3.1, since a marginal operator would give rise to logarithmic corrections.

Furthermore, depending on the path used to reach the critical line, the expansion of \tilde{x} in term of ξ/a_0 is different. Substituting these different expansions in (3.159) gives rise to many kind of terms, such as ξ^{-2h} , $\xi^{-2h/\alpha}$, $\xi^{-2(1+1/\alpha)}$, or even $1/\ln \xi$. For some of these terms a theoretical explanation is still lacking, which may be possible by applying a reasoning similar to that of [9] for the XYZ model.

3.6 The entanglement spectrum

We saw in section A.3 that the reduced density matrix of a subsystem can be written as:

$$\rho_A = \text{Tr}_B |\Psi\rangle_C \langle \Psi|_C = \sum_i |\lambda_i|^2 |\tilde{i}\rangle_A \langle \tilde{i}|_A \quad (3.162)$$

That is, the eigenvectors $|\tilde{i}\rangle_A$ of ρ_A have eigenvalues $|\lambda_i|^2$, which have a meaning of probabilities: the subsystem has classical probability $|\lambda_i|^2$ to be in the state $|\tilde{i}\rangle_A$. The set $\{|\lambda_i|^2\}$ is called the *entanglement spectrum* (ES).

We won't focus here on the ES at criticality (see [13] for details), but we will be more concerned to it's connection with critical exponents: the *Schmidt gap*, that is the difference between the greatest and the second greatest eigenvalue, can be related to critical exponents of the theory, as we'll see in section 3.6.1. We then evaluate the ES for the XY model in section 3.6.2, and we will generalize its derivation in the following chapter.

3.6.1 ES and critical exponents

The Schmidt gap is defined as the difference between the two largest eigenvalues of the reduced density matrix:

$$\Delta\lambda \equiv \lambda_0 - \lambda_1 \quad (3.163)$$

It is known (see for example [14]) that $\Delta\lambda$ closes in the thermodynamic limit, since it has the form:

$$\Delta\lambda \propto \frac{1 - q^{\alpha_1}}{l^{c/12}} \quad (3.164)$$

Here q and α_1 depend on the model under consideration, and l is the length of the subsystem under consideration, which diverges in the thermodynamic limit.

In the article [14], the authors make the ansatz that the Schmidt gap scales with the universal critical exponents. In particular, in the thermodynamic limit

3. Entanglement entropy in 1-D quantum chains

$\Delta\lambda$ scale as

$$\Delta\lambda \propto |g - g_c|^\beta \quad (3.165)$$

and its finite-size scaling is

$$\Delta\lambda \simeq L^{\beta/\nu} f(|g - g_c|L^{1/\nu}) \quad (3.166)$$

This means that the Schmidt gap should have the same behaviour of the order parameter. Indeed, near criticality an order parameter has the following behaviour:

$$Q(L, g) \simeq L^{\beta_Q/\nu} f_Q(|g - g_c|L^{1/\nu}) \quad (3.167)$$

where ν is the critical exponent associated to the divergence of the correlation length, β_Q is the order parameter critical exponent and f_Q is a universal scaling function.

One way to recover the two exponents β and ν is to take advantage of the universality of the function f : we then require that the left hand side of

$$\Delta\lambda L^{\beta/\nu} \simeq f(|g - g_c|L^{1/\nu}) \quad (3.168)$$

keeps the same values varying L and g , but leaving the combination $|g - g_c|L^{1/\nu}$ fixed.

Consider for example the transverse-field Ising model, whose Hamiltonian is:

$$H = -J \sum_i \sigma_i^x \sigma_{i+1}^x - B_z \sum_i \sigma_i^z \quad (3.169)$$

This model has $c = \frac{1}{2}$, so we expect that

$$\beta = \frac{1}{8} \quad \nu = 1 \quad (3.170)$$

In [14] the authors used numerical simulations to evaluate $\Delta\lambda$ as a function of L and g . Since the model is critical for $J = B_z$, a reasonable choice for the parameter g is:

$$g \equiv \frac{J}{B_z} \quad g_c = 1 \quad (3.171)$$

Using the method explained above, and taking advantage of the ansatz (3.168), they found that

$$\begin{cases} \beta = 0.124 \pm 0.002 \\ \nu = 1.00 \pm 0.01 \end{cases} \quad (3.172)$$

which is in perfect agreement with (3.170).

In the next chapter we want to test these conjectures about the Schmidt gap to the XYZ model, approaching the critical line $J_x = J_y = 1$.

3.6.2 ES for the XY model

In some relevant cases the Renyi entropy can determine completely the entanglement spectrum. Let's follow [23] and consider the XY model, already defined in section 2.3.3. We impose *periodic boundary conditions* on the system. Here we change the notation:

$$H = - \sum_{j=-\infty}^{\infty} \left[(1 + \gamma) \sigma_j^x \sigma_{j+1}^x + (1 - \gamma) \sigma_j^y \sigma_{j+1}^y + h \sigma_j^z \right] \quad (3.173)$$

We restrict to $\gamma \geq 0$ and $h \geq 0$, since the Hamiltonian is invariant for $\gamma \rightarrow \gamma$ and $h \rightarrow -h$. If $h = 2$ the system undergoes a second order phase transition. For $h < 2$ we have the *ordered phase*, since the ground state is doubly degenerate, while $h > 2$ is the *disordered phase*.

The so called zeta-function for a density matrix is

$$\zeta_{\rho_A}(\alpha) \equiv \text{Tr} \rho_A^\alpha = \sum_{n=0}^{\infty} g_n \lambda^n \quad (3.174)$$

Here g_n is the multiplicities of the eigenvalue λ_n . In term of the Renyi entropy, this is:

$$\zeta_{\rho_A}(\alpha) = \exp \left[(1 - \alpha) S(\rho_A, \alpha) \right] \quad (3.175)$$

since the Renyi entropy is defined as (see appendix A)

$$S(\rho_A, \alpha) = \frac{1}{1 - \alpha} \log \text{Tr}(\rho_A^\alpha) \quad (3.176)$$

First, let's define the two quantities:

$$\tau_0 \equiv \frac{I(k')}{I(k)} \quad q \equiv e^{-\pi \tau_0} \quad (3.177)$$

where $I(k)$ is the complete elliptic integral of the first kind,

$$k = \begin{cases} (\sqrt{(h/2)^2 + \gamma^2 - 1})/\gamma & \text{if } 4(1 - \gamma^2) < h^2 < 4 \\ \sqrt{(1 - h^2/4 - \gamma^2)/(1 - h^2/4)} & \text{if } h^2 < 4(1 - \gamma^2) \\ \gamma/(\sqrt{(h^2/4 + \gamma^2 - 1)}) & \text{if } h > 2 \end{cases} \quad (3.178)$$

and $k' = \sqrt{1 - k^2}$. The Renyi entropy for the XY model is given by:

$$S(\rho, \alpha) = \begin{cases} \frac{1}{12} \frac{\alpha}{1 - \alpha} \log \frac{k^2 k'^2}{16q} + \frac{2}{1 - \alpha} \log \prod_{m=0}^{\infty} \left[1 + q^{(2m+1)\alpha} \right] & \text{for } h > 2 \\ \frac{1}{6} \frac{\alpha}{1 - \alpha} \log \frac{16qk'}{k^2} + \frac{2}{1 - \alpha} \log \prod_{m=1}^{\infty} (1 + q^{2m\alpha}) & \text{for } h < 2 \end{cases} \quad (3.179)$$

It's now easy to obtain the entanglement spectrum. Defining

$$q_\alpha \equiv q^\alpha \quad (3.180)$$

3. Entanglement entropy in 1-D quantum chains

we have that, using (3.179), the zeta functions are:

$$\zeta_{\rho_A}(\alpha) = \begin{cases} \exp\left[\alpha\left(\frac{\pi\tau_0}{12} + \frac{1}{6}\log\frac{kk'}{4}\right)\right] \prod_{m=0}^{\infty} (1 + q_{\alpha}^{2m+1})^2 & h > 2 \\ 2 \exp\left[\alpha\left(-\frac{\pi\tau_0}{6} + \frac{1}{6}\log\frac{k'}{4k^2}\right)\right] \prod_{m=1}^{\infty} (1 + q_{\alpha}^{2m})^2 & h < 2 \end{cases} \quad (3.181)$$

We need the following relations from partition theory, that is

$$\prod_{n=0}^{\infty} (1 + q^{2n+1}) = \sum_{n=0}^{\infty} p_{\mathcal{O}}(n) q^n \quad (3.182a)$$

$$\prod_{n=1}^{\infty} (1 + q^{2n}) = \sum_{n=0}^{\infty} p_{\mathcal{D}}(n) q^n \quad (3.182b)$$

where:

- $p_{\mathcal{O}}(n)$ is the number of partitions of n into distinct *odd* integers;
- $p_{\mathcal{D}}(n)$ is the number of partition of n into distinct positive integers.

If we focus on the case $h > 2$, we take advantage of (3.182a). The zeta function becomes:

$$\zeta_{\rho_A}(\alpha) = \exp\left[\alpha\left(\frac{\pi\tau_0}{12} + \frac{1}{6}\log\frac{kk'}{4}\right)\right] \sum_{n=0}^{\infty} a_n q_{\alpha}^n \quad (3.183)$$

with

$$a_0 = 1 \quad a_n = \sum_{j=0}^n p_{\mathcal{O}}(j) p_{\mathcal{O}}(n-j) \quad (3.184)$$

Thanks to (3.180), we conclude that

$$\zeta_{\rho_A}(\alpha) = \sum_{n=0}^{\infty} a_n \lambda_n^{\alpha} \quad \lambda_n = \exp\left(-\pi\tau_0 n + \frac{\pi\tau_0}{12} + \frac{1}{6}\log\frac{kk'}{4}\right) \quad (3.185)$$

that is, comparing to (3.174), the eigenvalues of the reduced density matrix for the case $h < 2$ are λ_n defined in (3.185), with multiplicities $g_n = a_n$.

If instead $h < 2$ we use (3.182b), so that:

$$\zeta_{\rho_A}(\alpha) = 2 \exp\left[\alpha\left(-\frac{\pi\tau_0}{6} + \frac{1}{6}\log\frac{k'}{4k^2}\right)\right] \sum_{n=0}^{\infty} b_n q_{\alpha}^{2n} \quad (3.186)$$

where

$$b_0 = 1 \quad b_n = \sum_{j=0}^n p_{\mathcal{D}}(j) p_{\mathcal{D}}(n-j) \quad (3.187)$$

the eigenvalues of ρ_A are now given by

$$\lambda_n = \exp\left(-2\pi\tau_0 n - \frac{1}{6}\pi\tau_0 + \frac{1}{6}\log\frac{k'}{4k^2}\right) \quad (3.188)$$

Table 3.1: Values of a_n and b_n .

(a) $h > 2$		(b) $h < 2$	
n	g_n	n	g_n
0	1	0	2
1	2	1	4
2	1	2	6
3	2	3	12
4	4	4	18
5	4	5	28
6	5	6	44
7	6	7	64

with degeneracies

$$g_n = 2b_n \tag{3.189}$$

In table 3.1 we list some values of the degeneracies in the two cases $h > 2$ and $h < 2$.

3. Entanglement entropy in 1-D quantum chains

Chapter 4

Numerical simulations

4.1 Entanglement spectrum for the XYZ model

In this section we want to compute the entanglement spectrum in the case of the XYZ model, for an infinite system splitted in two half infinite chains with open boundary conditions. The approach is the same of section 3.6.2. We remind that the Renyi entropies for this model are given by:

$$S_\alpha = \frac{\alpha}{\alpha - 1} \sum_{j=1}^{\infty} \log(1 + e^{-2j\epsilon}) + \frac{1}{1 - \alpha} \sum_{j=1}^{\infty} \log(1 + e^{-2j\alpha\epsilon}) \quad (4.1)$$

For this case we must use again the relation (3.182b), which we report here:

$$\prod_{n=1}^{\infty} (1 + q^{2n}) = \sum_{n=0}^{\infty} p_{\mathcal{D}}(n) q^n \quad (4.2)$$

The zeta function is then:

$$\begin{aligned} \zeta_{\rho_A}(\alpha) &\equiv \exp\left[(1 - \alpha)S(\alpha)\right] \\ &= \exp\left[-\sum_{j=1}^{\infty} \log(1 + e^{-2j\alpha\epsilon})\right] \sum_{n=1}^{\infty} p_{\mathcal{D}}(n) e^{-2n\alpha\epsilon} \end{aligned} \quad (4.3)$$

Remind that $p_{\mathcal{D}}(n)$ is the partition of n into distinct positive integers. We plot some of its values in table 4.1.

In conclusion, the zeta function gives us the *entanglement spectrum of the XYZ model*, for a half infinite chain with open boundary conditions:

$$\boxed{\zeta_{\rho_A}(\alpha) = \sum_{n=0}^{\infty} p_{\mathcal{D}}(n) \lambda_n^\alpha \quad \lambda_n = \exp\left(-2n\epsilon - \sum_{j=1}^{\infty} \log(1 + e^{-2j\epsilon})\right)} \quad (4.4)$$

4. Numerical simulations

Table 4.1: values of $p_{\mathcal{D}}(n)$

n	$p_{\mathcal{D}}(n)$
0	1
1	1
2	1
3	2
4	2
5	3
6	4
7	5
8	6

As a check of the consistency of this equation, notice that the eigenvalues sum up to 1, as to be expected for a reduced density matrix:

$$\begin{aligned} \sum_{n=0}^{\infty} p_{\mathcal{D}}(n) \lambda_n &= \exp\left(-\sum_{j=1}^{\infty} \log(1 + e^{-2j\epsilon})\right) \sum_{n=0}^{\infty} p_{\mathcal{D}}(n) e^{-2n\epsilon} \\ &= \frac{1}{\prod_{j=1}^{\infty} (1 + e^{-2j\epsilon})} \sum_{n=0}^{\infty} p_{\mathcal{D}}(n) e^{-2n\epsilon} = 1 \end{aligned} \quad (4.5)$$

4.2 Check of known results

Now we discuss the numerical simulations performed. These are based on the DMRG algorithm, described in appendix C, where we also give a brief description of the program in C++ that realizes the algorithm. This DMRG program always evaluates entropies with logarithms *in base 2*: if not specified, we will work from now on with logarithms in this base. We further assume that the lattice spacing is $a = 1$. Let's report again the Hamiltonian of the XYZ model for the sake of clarity:

$$H_{XYZ} = - \sum_n \left(J_x \sigma_n^x \sigma_{n+1}^x + J_y \sigma_n^y \sigma_{n+1}^y + J_z \sigma_n^z \sigma_{n+1}^z \right) \quad (4.6)$$

As a first check of the validity of the program we performed a simulation of the XXZ model in its ferromagnetic regime, using the following parameters:

$$\begin{cases} J_x = 1 \\ J_y = 1 \\ J_z = 0.4 \end{cases} \quad (4.7)$$

The plot of the Von Neumann entropy S as a function of the number of sites L of the system is given in figure 4.1: periodic boundary conditions (PBC) are

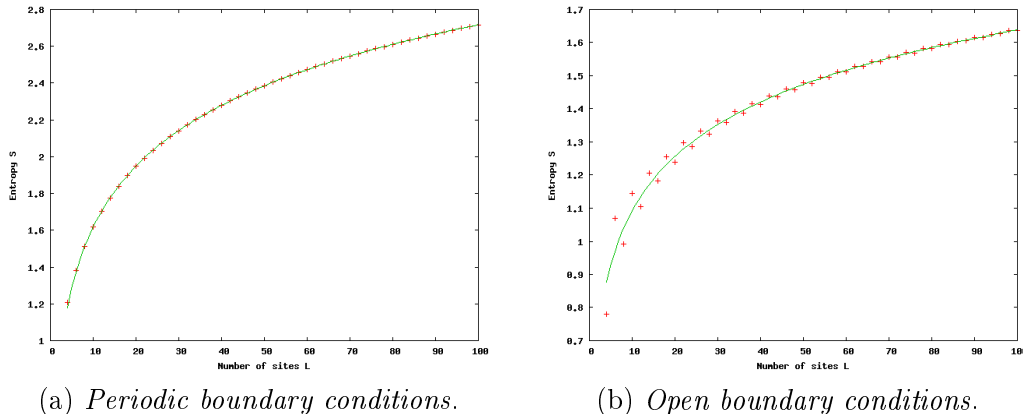


Figure 4.1: The XXZ model with parameters given by (4.7). The plots show the entropy S as a function of the number of sites L . The points represent numerical data, while the continuous lines are the best fit of the form (4.8).

implemented in figure 4.1a, while open boundary conditions (OBC) are used in figure 4.1b. Numerical data are extrapolated from $L = 4$ to $L = 100$, and the number of sites L is always *even*: this is a peculiarity of the DMRG algorithm (see again appendix C). We also have $M_{\min} = M_{\max} = 400$, where M_{\min} and M_{\max} are respectively the minimum and maximum states used by the DMRG program to construct the approximated wave function ψ_{dmrg} at each passage; furthermore, we used no sweeps in the algorithm (see section C.1.3 for further details).

Now, the form of S as a function of L must be compatible with Cardy and Calabrese formula for the entanglement entropy in the case of zero temperature, and for a subsystem with length $L/2$ (see section 3.1.1). We then tried to fit the numerical results with the following function:

$$S = \frac{c}{\kappa} \log_2 L + b \quad (4.8)$$

Remember that $a = 1$, and that the logarithms are evaluated in base 2. Here $\kappa = 3$ for PBC and $\kappa = 6$ for OBC. The constant b includes a nonuniversal term, the contribute of the boundary entropy and $-(c/\kappa) \log_2 \pi$. We made the fits in the following range:

$$\text{OBC: } L \in [50, 90] \quad \text{PBC: } L \in [30, 90] \quad (4.9)$$

Notice that for OBC we have *oscillations* of the entropy, encountered in section 3.3.3: this is why we performed the fit for larger values of L , where the oscillations are weaker. Thus, the best fit of (4.8) for both cases is:

$$\text{OBC: } \begin{cases} c = 0.98 \pm 0.02 \\ b = 0.55 \pm 0.02 \end{cases} \quad \text{PBC: } \begin{cases} c = 0.9942 \pm 0.0003 \\ b = 0.5157 \pm 0.0006 \end{cases} \quad (4.10)$$

4. Numerical simulations

Since the XXZ model has central charge $c = 1$, the fit is satisfactory, and this is a good check for the validity of the DMRG program.

We then moved away from criticality and used the following values for the parameters:

$$(a) \begin{cases} J_x = 1 \\ J_y = 1.1 \\ J_z = 0.4 \end{cases} \quad (b) \begin{cases} J_x = 1 \\ J_y = 1.2 \\ J_z = 0.4 \end{cases} \quad (c) \begin{cases} J_x = 1 \\ J_y = 1.3 \\ J_z = 0.4 \end{cases} \quad (4.11)$$

In these and all the subsequent simulations we used the following parameters for the DMRG program:

$$M_{\min} = 50, \quad M_{\max} = 200, \quad D = 10^{-8} \quad 4 < L < 90 \quad (4.12)$$

The Von Neumann entropy computed by the DMRG algorithm must now agree with the formula for the XYZ model of section 3.5.2, that is (using base 2 for the logarithms):

$$S = \frac{1}{\log 2} \left[2\epsilon \sum_{j=1}^{\infty} \frac{j}{1 + e^{2j\epsilon}} + \sum_{j=1}^{\infty} \log(1 + e^{-2j\epsilon}) \right] \quad (4.13)$$

While comparing the values given by the two methods, we faced the following problem: the entropy obtained by numerical simulations was always greater of about 1 than the one given by the exact formula. The origin of this fact is due to the *double degeneracy* of the ground state (see [16]). While using corner transfer matrices, we kept only one ground state. Instead, the DMRG program can't distinguish between the two degenerated ground states, say, $|\psi_1\rangle$ and $|\psi_2\rangle$, so it picks up the combination:

$$|\psi\rangle = \alpha |\psi_1\rangle + \beta |\psi_2\rangle \quad (4.14)$$

The reduced density matrices are then evaluated from this pure state, whose density matrix is:

$$\rho \equiv |\psi\rangle \langle \psi| = |\alpha|^2 |\psi_1\rangle \langle \psi_1| + |\beta|^2 |\psi_2\rangle \langle \psi_2| + \left(\alpha\beta^* |\psi_1\rangle \langle \psi_2| + \beta\alpha^* |\psi_2\rangle \langle \psi_1| \right) \quad (4.15)$$

Suppose now that $|\psi_1\rangle$ and $|\psi_2\rangle$ live in spaces which are orthonormal, or almost. This means that if we take the partial trace of ρ , the terms living inside the round brackets give a negligible contribute, so we ignore them. Let's denote the density matrices of the two states $|\psi_1\rangle$ and $|\psi_2\rangle$ with ρ_1 and ρ_2 respectively. Thanks to eq. (A.40), we can write:

$$S(\rho) = S(|\alpha|^2 \rho_1 + |\beta|^2 \rho_2) = H(\alpha, \beta) + |\alpha|^2 S(\rho_1) + |\beta|^2 S(\rho_2) \quad (4.16)$$

where we used the expression for the Shannon entropy:

$$H(\alpha, \beta) = -|\alpha|^2 \log_2 |\alpha|^2 - |\beta|^2 \log_2 |\beta|^2 \quad (4.17)$$

Table 4.2: Values of S

(a) $h = 0$		(b) $h = 0.001$	
L	S	L	S
80	1.172616969688	80	0.172618694316
82	1.172616589206	82	0.172618700352
84	1.172617320654	84	0.172618685142
86	1.172616704045	86	0.172618692224
88	1.172616579468	88	0.172618698385
90	1.172616573404	90	0.172618687172

If now we set

$$\alpha = \beta = \frac{1}{\sqrt{2}}$$

and we suppose that $S(\rho_1) = S(\rho_2)$, which is quite reasonable if we interpret the entanglement entropy as the thermodynamical entropy (see for example [15]), then:

$$S(\rho) = 1 + S(\rho_1) \tag{4.18}$$

This is how the term 1 is justified, when all the entropies are evaluated using basis 2 for the logarithms. Otherwise the difference is, of course, log 2.

To remove the degeneracy of the two ground states, we used a weak *magnetic field*. The degeneracy is broken if the field is oriented along the y axis, since it is the variation of the J_y parameter that moves the system out of criticality. We then used the Hamiltonian:

$$H' = H_{XYZ} + -h \sigma_0^y \tag{4.19}$$

It was enough to apply the field at only one site. Figure 4.2a represents numerical data from a simulation with no magnetic field; in figure 4.2b we switched on a magnetic field $h = 0.001$ while figure 4.2c involves a field $h = 0.000001$. The values for the parameters of the model in these simulations are given by case (c) of (4.11). The figures involve lines connecting the numerical data, instead of a set of points: this makes the situation visibly clearer. The value of the entropy given by (4.13) is then

$$S = 0.17261871484 \tag{4.20}$$

and this must be compared with the values in table 4.2, for the simulations with $h = 0$ and $h = 0.001$.

For the case of $h = 0.001$, notice that first S increases with L , and then it drops towards its correct value (4.20). This means that for small L the two ground states are not degenerate yet. Increasing L their energy value

4. Numerical simulations

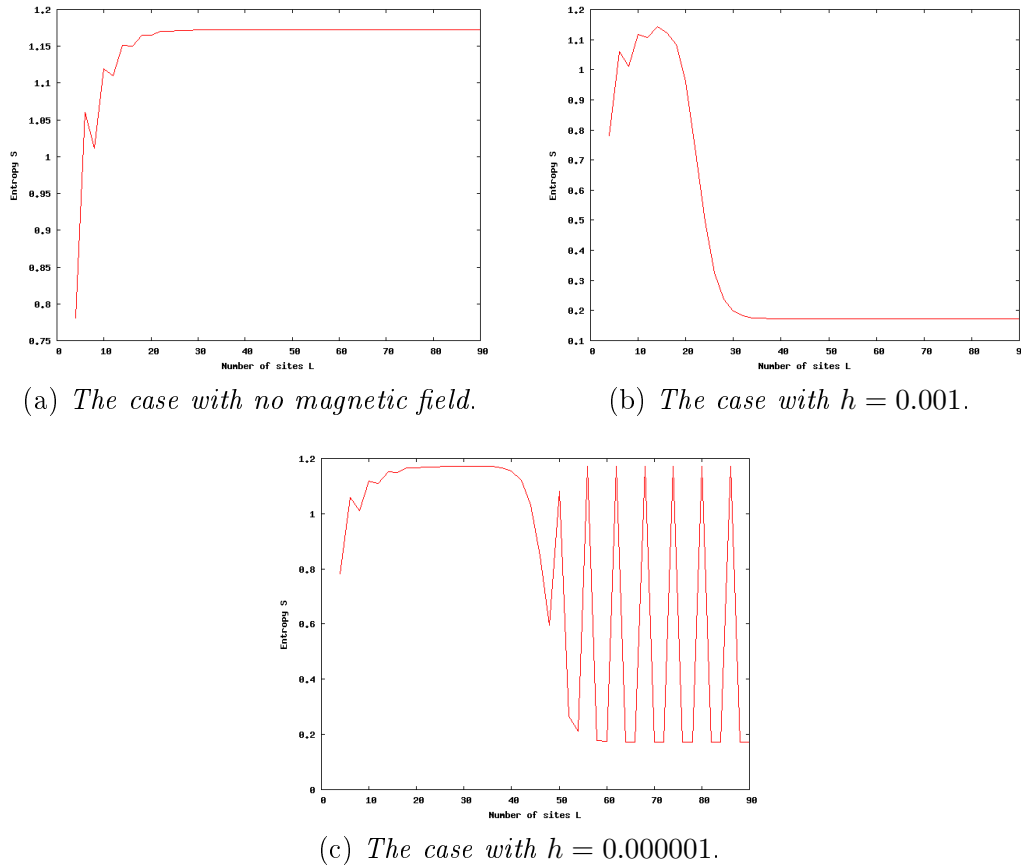


Figure 4.2: XYZ model with parameters given by case (c) of (4.11). The plots show the entropy S as a function of the number of sites L .

tend to coincide, but the magnetic field split these values: the DMRG will take as the ground state that state with lower energy. Furthermore, in the case $h = 0.000001$ the field is so weak that the program couldn't split the two ground states at every passage. This represents somehow a limit of the weakness of h , so we always worked with stronger fields.

4.3 The Essential critical point

After the numerical checks discussed in the previous section, we proceeded to study the *essential critical point* of the XYZ model (see section 3.5.3), that is the point $(J_y, J_z) = (1, 1)$. From now on we will always set $J_x = 1$, and we first consider the case:

$$J_y > 1 \quad -1 < J_z < 1 \quad (4.21)$$

We will use the parameters (u, l) , see section 3.5.3.

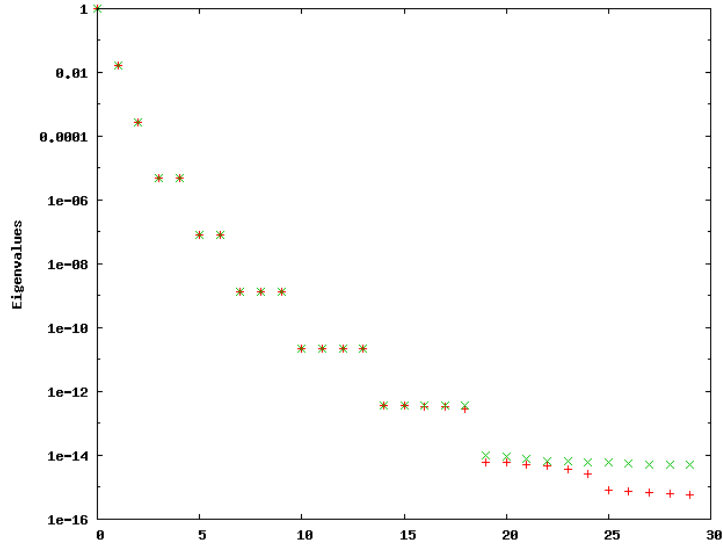


Figure 4.3: Comparing the entanglement spectrum obtained from two simulations for $J_z = 0.5$ and $J_y = 1.3343958$. The red dots are for the simulation with $D = 10^{-8}$, while the green dots are relative to the simulation with $D = 10^{-10}$. The x -coordinate merely represents a label for the eigenvalues plotted.

4.3.1 Lines of constant l

First, we performed simulations on lines of constant l , precisely for the values

$$l = 0.25, 0.35, 0.4, 0.45, 0.5, 0.6, 0.7$$

and for each of these values we performed 7 simulations for various J_z , that is:

$$J_z = 0.5, 0.6, 0.7, 0.8, 0.9, 0.95, 0.98$$

The idea is to study the behaviour of the entanglement entropy and the entanglement spectrum by approaching the essential critical point along these lines, represented in figure 4.4.

In appendix C we scheduled all the numerical results obtained from these simulations. Here we just plot some significant graphics, such as the Von Neumann entropy and the Schmidt gap for various l , as a function of J_z (see figure 4.5). It is very remarkable that the entropy obtained by these simulations is in astonishing agreement with the values evaluated from the exact formula: in some cases they coincide up to the twelfth decimal. As for the entanglement spectrum, the agreement between exact and numerical data is better for the first eigenvalues, and gets worse for smaller eigenvalues. Part of this fact is that the "machine precision" is about 10^{-15} : as can be noticed from figure 4.3, eigenvalues of this order and smaller tend to form a "continuum" (see also section C.2).

In table 4.3 we list the eigenvalues of the reduced density matrix evaluated from (4.4), as well as those calculated by two simulations relative to the same

4. Numerical simulations

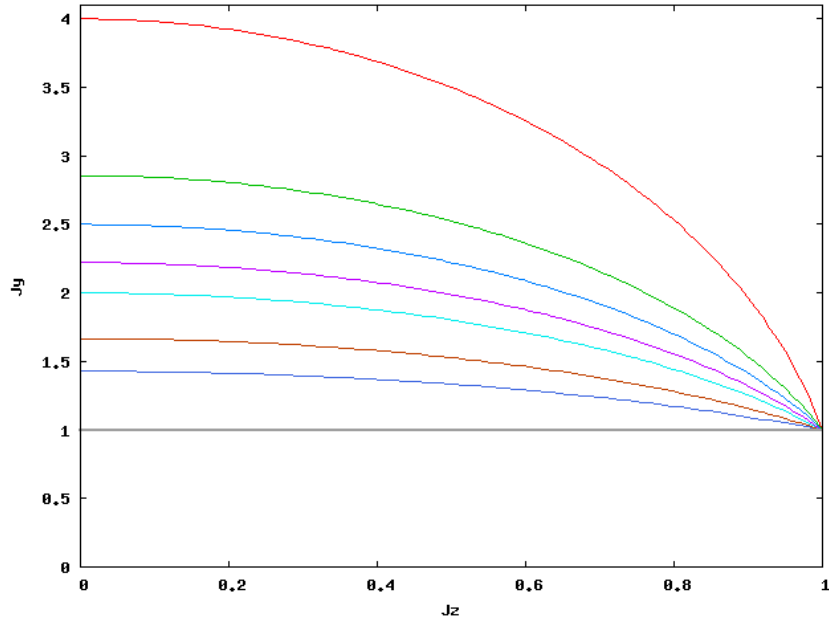


Figure 4.4: Lines of constant l in the (J_y, J_z) plane, from $l = 0.25$ (red) to $l = 0.7$ (light blue). The bold black line represents the critical XXZ line.

point $(J_y, J_z) = (1.3343958, 0.5)$, corresponding to $l = 0.7$. The first has

$$M_{\min} = 50, \quad M_{\max} = 200, \quad D = 10^{-8} \quad (4.22)$$

while for the second

$$M_{\min} = 50, \quad M_{\max} = 400, \quad D = 10^{-10} \quad (4.23)$$

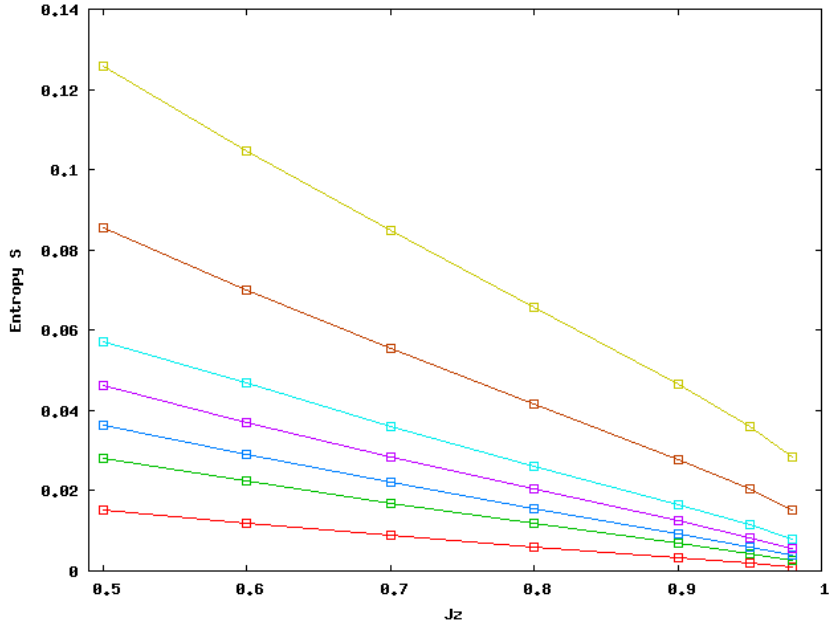
Notice that by increasing the precision, groups of eigenvalues tend to assume the same value, and the agreement with the formula for the entanglement spectrum (4.4) is much better: see also figure 4.3.

4.3. The Essential critical point

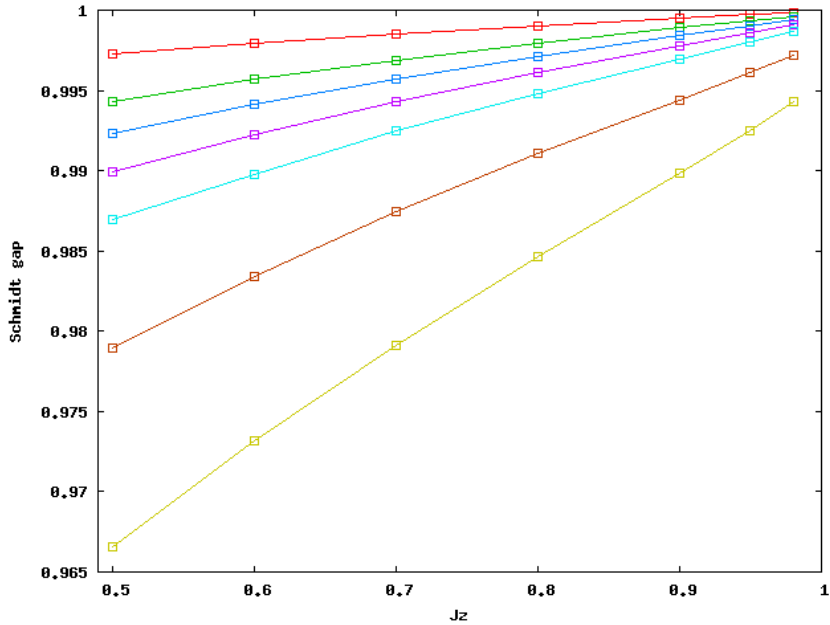
Table 4.3: The values of the entanglement spectrum for $J_z = 0.5$ and $J_y = 1.3343958$. We compare the first 30 eigenvalues of the two simulations with $D = 10^{-8}$ and $D = 10^{-10}$ with the exact relation for the entanglement spectrum (4.4).

(a) $D = 10^{-8}$.	(b) $D = 10^{-10}$.	(c) Formula (4.4).
$9.831296568968 \cdot 10^{-01}$	$9.831311792830 \cdot 10^{-01}$	$9.831359753752 \cdot 10^{-01}$
$1.657962648369 \cdot 10^{-02}$	$1.657962659151 \cdot 10^{-02}$	$1.657962659366 \cdot 10^{-02}$
$2.796005039061 \cdot 10^{-04}$	$2.796005492151 \cdot 10^{-04}$	$2.796005495284 \cdot 10^{-04}$
$4.715191452217 \cdot 10^{-06}$	$4.715212769425 \cdot 10^{-06}$	$4.715212785703 \cdot 10^{-06}$
$4.715179631467 \cdot 10^{-06}$	$4.715212549797 \cdot 10^{-06}$	$4.715212785703 \cdot 10^{-06}$
$7.951446139730 \cdot 10^{-08}$	$7.951783458651 \cdot 10^{-08}$	$7.951783947476 \cdot 10^{-08}$
$7.950376571850 \cdot 10^{-08}$	$7.951778901702 \cdot 10^{-08}$	$7.951783947476 \cdot 10^{-08}$
$1.338552392480 \cdot 10^{-09}$	$1.340996253781 \cdot 10^{-09}$	$1.340997126133 \cdot 10^{-09}$
$1.337775725778 \cdot 10^{-09}$	$1.340994809357 \cdot 10^{-09}$	$1.340997126133 \cdot 10^{-09}$
$1.336512880107 \cdot 10^{-09}$	$1.340961571140 \cdot 10^{-09}$	$1.340997126133 \cdot 10^{-09}$
$2.253191380502 \cdot 10^{-11}$	$2.261475451018 \cdot 10^{-11}$	$2.261471519064 \cdot 10^{-11}$
$2.243414875683 \cdot 10^{-11}$	$2.261463477196 \cdot 10^{-11}$	$2.261471519064 \cdot 10^{-11}$
$2.231616133352 \cdot 10^{-11}$	$2.261388463525 \cdot 10^{-11}$	$2.261471519064 \cdot 10^{-11}$
$2.172088861992 \cdot 10^{-11}$	$2.260829765861 \cdot 10^{-11}$	$2.261471519064 \cdot 10^{-11}$
$3.682638141387 \cdot 10^{-13}$	$3.813197078716 \cdot 10^{-13}$	$3.813769121405 \cdot 10^{-13}$
$3.645046952995 \cdot 10^{-13}$	$3.811791843748 \cdot 10^{-13}$	$3.813769121405 \cdot 10^{-13}$
$3.445858752500 \cdot 10^{-13}$	$3.807374734025 \cdot 10^{-13}$	$3.813769121405 \cdot 10^{-13}$
$3.335553660803 \cdot 10^{-13}$	$3.803414101681 \cdot 10^{-13}$	$3.813769121405 \cdot 10^{-13}$
$2.854555380192 \cdot 10^{-13}$	$3.763069961364 \cdot 10^{-13}$	$3.813769121405 \cdot 10^{-13}$
$6.189419079311 \cdot 10^{-15}$	$1.026766160278 \cdot 10^{-14}$	$6.431579964094 \cdot 10^{-15}$
$5.861904932748 \cdot 10^{-15}$	$9.210305292276 \cdot 10^{-15}$	$6.431579964094 \cdot 10^{-15}$
$5.320737390903 \cdot 10^{-15}$	$7.796748051580 \cdot 10^{-15}$	$6.431579964094 \cdot 10^{-15}$
$4.644028724437 \cdot 10^{-15}$	$6.390375353193 \cdot 10^{-15}$	$6.431579964094 \cdot 10^{-15}$
$3.606257376956 \cdot 10^{-15}$	$6.339236379522 \cdot 10^{-15}$	$6.431579964094 \cdot 10^{-15}$
$2.685535888280 \cdot 10^{-15}$	$6.270108610732 \cdot 10^{-15}$	$6.431579964094 \cdot 10^{-15}$

4. Numerical simulations



(a) Entanglement entropy.



(b) Schmidt gap.

Figure 4.5: Plots of the entanglement entropy and the Schmidt gap as functions of J_z , along the lines of constant l . These lines are: $l = 0.25$ (red), $l = 0.35$ (green), $l = 0.4$ (blue) and $l = 0.45$ (purple), $l = 0.5$ (light blue), $l = 0.6$ (light brown) and $l = 0.7$ (yellow). The boxes refer to the value computed by the DMRG, while the lines are for visible clarity.

4.3.2 Circles surrounding the essential critical point

We then studied the behaviour of the entanglement entropy *around* the essential singularity. We achieved this by performing numerical simulations on circles parametrized by:

$$\begin{cases} J_y = 1 + r \sin \alpha \\ J_z = 1 - r \cos \alpha \end{cases} \quad (4.24)$$

The values of r used are:

$$r = 0.96, 0.97, 0.98 \quad (4.25)$$

and for each radius we performed 24 simulations. We chose the points on the circles for equally distant values of α , whose range was $\alpha \in [\pi/48, \pi/2]$, and where each value of α is separated from its neighbour by $\pi/48$.

The values of the entanglement entropies obtained by the simulations are reported in appendix 4. In figure 4.6 we show the lines of constant radius given by (4.25), while in figure 4.7 we plot the entropies evaluated by the DMRG program as a function of the angle α of equation (4.24).

We didn't use the same DMRG parameters for all the simulations. Case by case, finding a balance between the precision of the output and a quick execution of the simulations, we chose between three set of DMRG parameters:

$$\begin{aligned} (a) : & \begin{cases} M_{\min} = 50, & M_{\max} = 200 \\ D = 10^{-8} \\ L_{\max} = 90 \end{cases} \\ (b) : & \begin{cases} M_{\min} = 10, & M_{\max} = 100 \\ D = 0.25 \cdot 10^{-7} \\ L_{\max} = 180 \end{cases} \\ (c) : & \begin{cases} M_{\min} = 10, & M_{\max} = 100 \\ D = 0.25 \cdot 10^{-7} \\ L_{\max} = 220 \end{cases} \end{aligned} \quad (4.26)$$

and for each one we performed 5 sweeps at each passage. The agreement between the entanglement entropies calculated by the DMRG program and those evaluated by the exact formula (4.13) is still good, see appendix 4 for further comments.

4. Numerical simulations

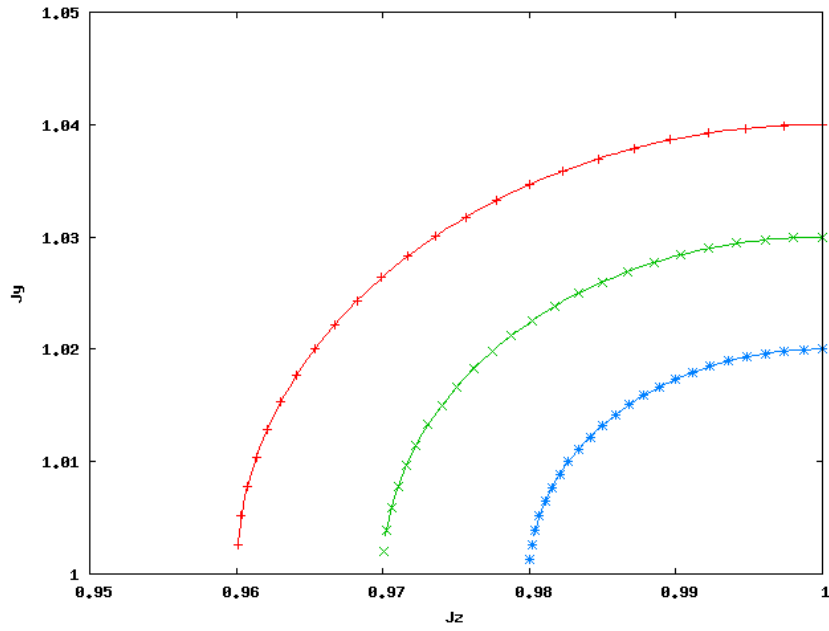


Figure 4.6: The lines of constant r where we performed the simulations. The dots denote the values of J_y and J_z used for the simulations.

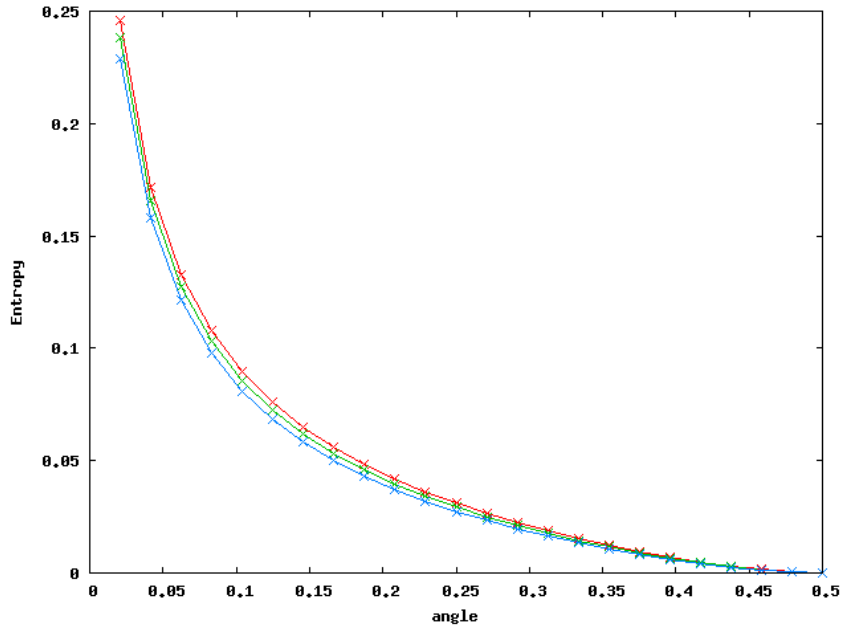


Figure 4.7: Plots of the entropies, obtained by numerical simulations, as a function of the angle α . These corresponds to $r = 0.04$ (red), $r = 0.03$ (green) and $r = 0.02$ (blue).

4.4 Study of the Schmidt gap

We now wish to study the Schmidt gap along a different line, that is for μ constant, where

$$\mu \equiv \pi \frac{\lambda}{I(k')} \quad (4.27)$$

From formula (4.4), the Schmidt gap is:

$$\Delta\lambda = \frac{1 - e^{-2\epsilon}}{\prod_{j=1}^{\infty} (1 + e^{-2j\epsilon})} \quad (4.28)$$

Our goal is to find the critical exponents of the Sine-Gordon model from the behaviour of the Schmidt gap near its critical point, that is approaching the line of the XXZ model. In table 4.4 we report the values of $\Delta\lambda$ obtained using the analytic expression (4.28), for the line

$$\mu = 2.1 \quad (4.29)$$

These lines of constant μ (represented in figure 4.8) correspond to the Sine-Gordon model (see [22] for further details). To understand the notation, consider the first value of J_y in the tables:

$$1.0 \dots 01 \quad (4.30)$$

With this we mean that "... " represents a number of zeroes. For example, for $\dots = 9$, (4.30) represents the number

$$1.000000000001$$

Following section 3.6.1, and noticing that we are working in the thermodynamic limit, it is then natural to assume the following "ansatz":

$$\Delta\lambda = a (J_y - 1)^\beta \quad (4.31)$$

The best fits for the three cases of table 4.4 are:

$$\begin{aligned} \text{(a): } & \begin{cases} a = 1.221 \pm 0.002 \\ \beta = 0.1023 \pm 0.0003 \end{cases} \\ \text{(b): } & \begin{cases} a = 0.959 \pm 0.002 \\ \beta = 0.08983 \pm 0.00007 \end{cases} \\ \text{(c): } & \begin{cases} a = 0.920 \pm 0.002 \\ \beta = 0.08829 \pm 0.00007 \end{cases} \end{aligned} \quad (4.32)$$

and in figures 4.9, 4.10, 4.11 we plot the numerical data with the fit functions. The agreement with numerical data is good in each of the three cases, but notice that the exponent β changes as we consider different sets of data.

4. Numerical simulations

Table 4.4: Schmidt gap as a function of J_y , evaluated on the line $\mu = 2.1$.

(a) No "...".		(b) "... = 9.		(c) "... = 10.	
J_y	$\Delta\lambda$	J_y	$\Delta\lambda$	J_y	$\Delta\lambda$
1.0001	0.473689	1.0...01	0.080190	1.0...01	0.065488
1.0002	0.509419	1.0...02	0.085284	1.0...02	0.0695889
1.0003	0.531567	1.0...03	0.088426	1.0...03	0.072105
1.0004	0.547852	1.0...04	0.090731	1.0...04	0.073952
1.0005	0.560812	1.0...05	0.092565	1.0...05	0.075423
1.0006	0.571615	1.0...06	0.094093	1.0...06	0.076645
1.0007	0.580899	1.0...07	0.095406	1.0...07	0.077698
1.0008	0.589052	1.0...08	0.096559	1.0...08	0.078620
1.0009	0.596329	1.0...09	0.097590	1.0...09	0.079444
1.0010	0.602905	1.0...10	0.098521	1.0...10	0.080190
1.0015	0.628796	1.0...11	0.099372	1.0...11	0.080870
1.002	0.647712	1.0...12	0.100156	1.0...12	0.081496
1.0025	0.662684	1.0...13	0.100884	1.0...13	0.082078
1.003	0.675100	1.0...14	0.101562	1.0...14	0.082620
1.0035	0.685721	1.0...15	0.102198	1.0...15	0.083128
1.004	0.695007	1.0...16	0.102797	1.0...16	0.083607
1.0045	0.703260	1.0...17	0.103363	1.0...17	0.084059
1.005	0.710690	1.0...18	0.103900	1.0...18	0.084487
1.0055	0.717446	1.0...19	0.104410	1.0...19	0.084895
1.006	0.723643	1.0...20	0.104897	1.0...20	0.085284
1.0065	0.729364				
1.007	0.734679				
1.0075	0.739641				
1.008	0.744293				
1.0085	0.748672				
1.009	0.752808				
1.0095	0.756727				
1.01	0.760449				

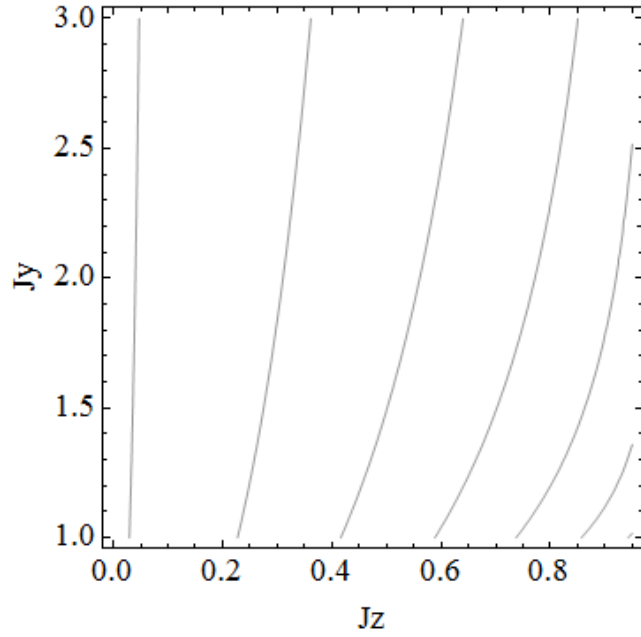


Figure 4.8: Lines of constant μ , where we plotted J_y as a function of J_z . Here are represented the lines from $\mu = 1.6$ to $\mu = 2.6$, and μ increases by steps of 0.2.

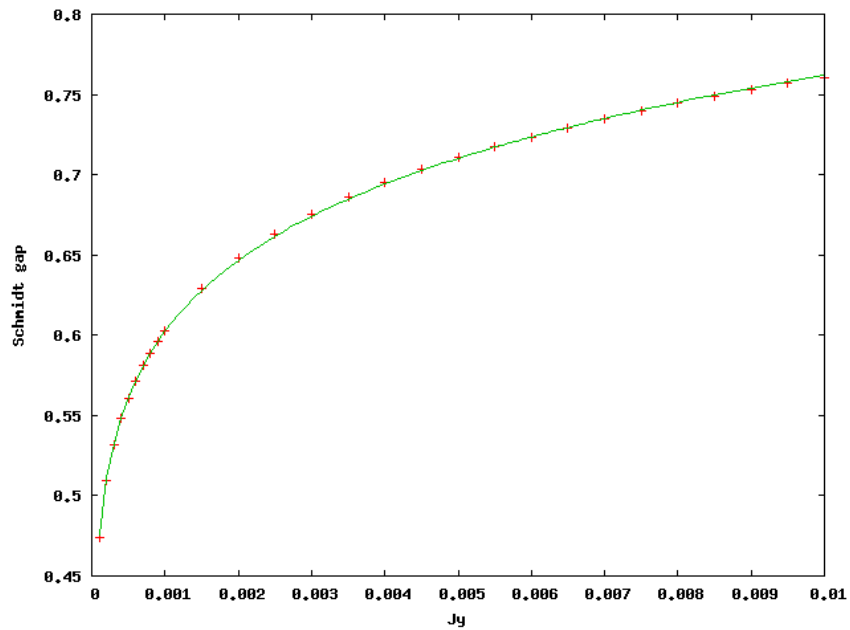


Figure 4.9: Plot of the Schmidt gap as a function of $(J_y - 1)$ and the fitting function (4.31): case (a).

4. Numerical simulations

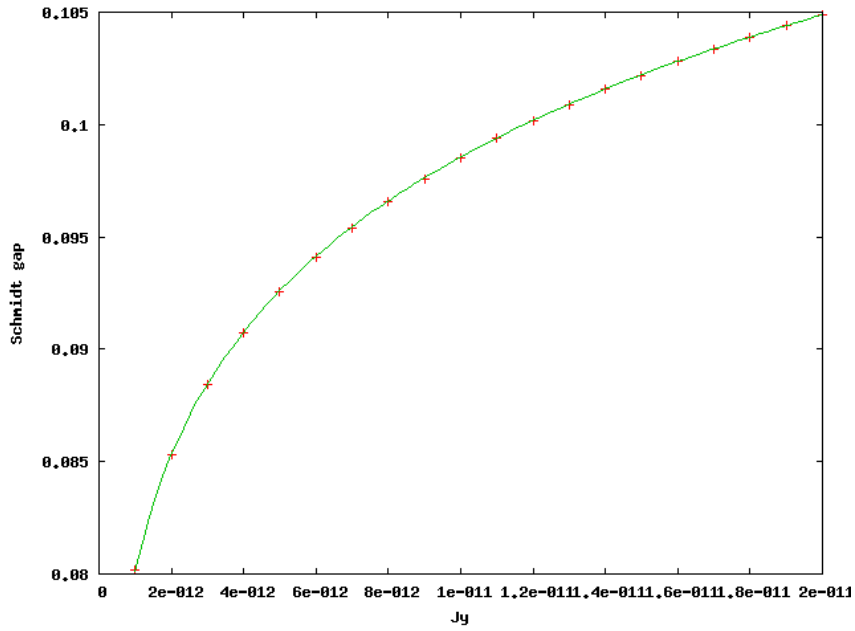


Figure 4.10: Plot of the Schmidt gap as a function of $(J_y - 1)$ and the fitting function (4.31): case (b).

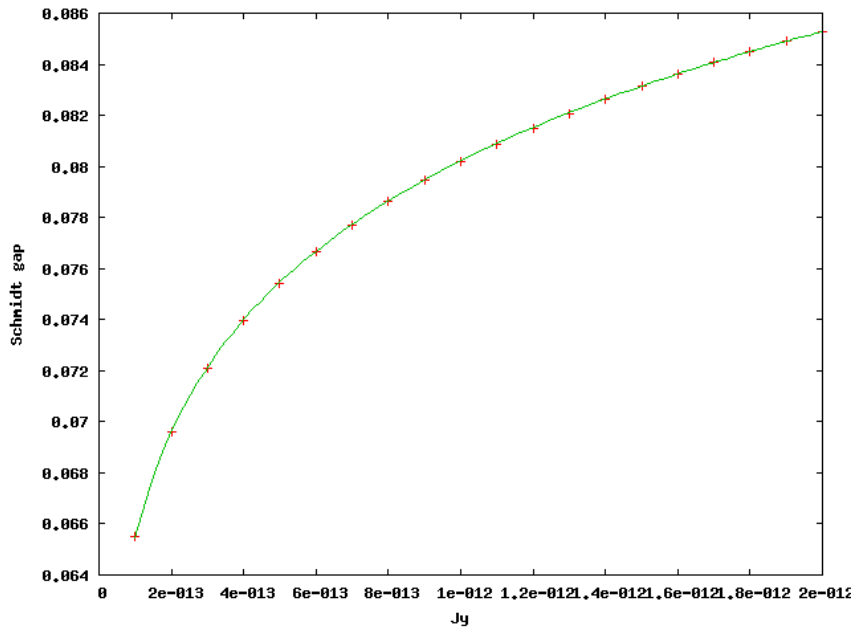


Figure 4.11: Plot of the Schmidt gap as a function of $(J_y - 1)$ and the fitting function (4.31): case (c).

4.5 Studying the FSS of the entanglement spectrum

Our last task is to study, at least numerically, the behaviour of the Von Neumann entropy and of the entanglement spectrum as functions of the number of sites L of the system. This is always splitted in two halves (with respect to which we calculate the entanglement) and it's described by one of the two degenerated ground states.

We remind that, applying a small field h to just one site, the system is described by the Hamiltonian

$$H' = H_{XYZ} + h\sigma_0^y \quad (4.33)$$

and the entropy (as a function of L) follows the path of figure 4.2b. This field, as we discussed in section 4, is needed to split the degenerated ground states. On the other hand, without magnetic fields the entropy behaves like in figure 4.2a. This suggests that the true behaviour of the entropy should simulate this last situation: the entropy should be a *monotonically increasing* function of L , apart from the oscillations explained in section 3.3.3, which saturates to the value S_{exact} given by equation (3.128). We then performed simulations corresponding to the parameters

$$\begin{cases} J_x = 1 \\ J_y = 1.1 \\ J_z = 0.4 \end{cases} \quad (4.34)$$

and we tried to eliminate the "hunch" of figure 4.2b using the following approaches.

- Varying the intensity of the field h in equation (4.33), from $h = 0.001$ to $h = 100$. The result is that the convergence to the value of the exact formula has different speeds for different values of h . Furthermore the "hunch" remains, even if it's much less pronounced: see figure 4.12.
- Using a staggered field, that is

$$H' = H_{XYZ} + h \sum_i (-1)^i \sigma_i^y \quad (4.35)$$

for values of h from $h = 0.001$ to $h = 1$. Here the convergence is really fast, and the hunch remains still. The final value of the entropy differs significantly from S_{exact} by increasing the value of h . For values near $h \simeq 1$ the entropy follows a path completely different from the cases with smaller values of h , and it doesn't even converge.

4. Numerical simulations

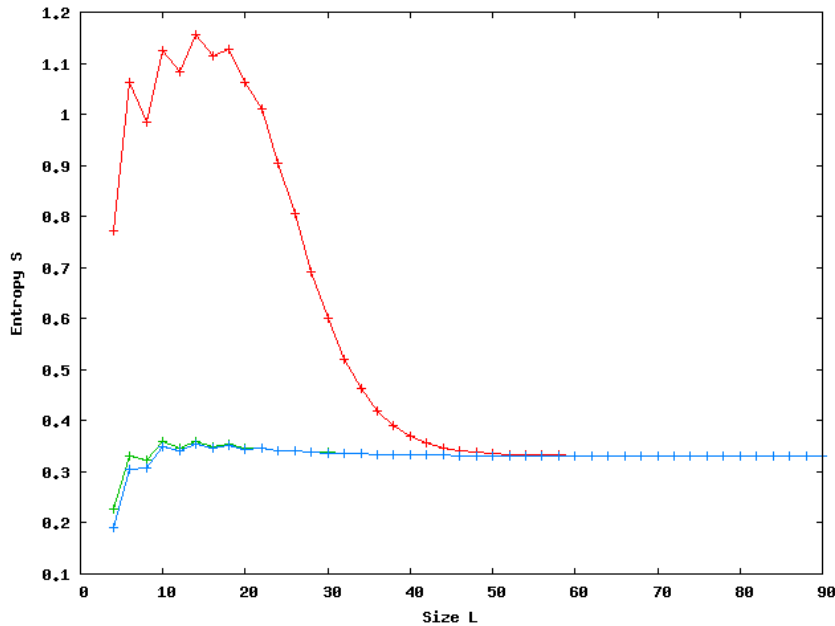


Figure 4.12: The entropy as a function of L , for the following values of the magnetic field at one edge: $h = 0.01$ (red), $h = 1$ (green), $h = 100$ (blue).

- Using a magnetic field only at the edges, that is

$$\begin{cases} (a) : H' = H_{XYZ} + h\sigma_0^y - h\sigma_{L-1}^y \\ (b) : H' = H_{XYZ} + h\sigma_0^y + h\sigma_{L-1}^y \end{cases} \quad (4.36)$$

where $L - 1$ represents the last site of the chain. For case (a) the problem remains. Eventually, for h sufficiently large, the hunch disappears, and the entropy becomes a monotonically *decreasing* function of L . For case (b) we found that for $h \approx 0.25$ the hunch disappears and the entropy becomes a monotonically *increasing* function of L , apart from the oscillations.

Therefore, we performed numerical simulations using fields at the edges with the same magnitude and direction, in the neighbourhood of $h \simeq 0.25$. The Hamiltonian of the system is then:

$$H' = H_{XYZ} + h\sigma_0^y + h\sigma_{L-1}^y \quad (4.37)$$

In figure 4.13 we plotted the entropy, as a function of L , for some values of h . From $h = 1$ to $h = 10$ the behaviour of the entropy is the same: somehow this represents a saturation for the effects of these fields, or perhaps we need much stronger fields to check a different behaviour.

The main problem with this approach is that the entropy as a function of L depends also on the field h , even if, as we've already discussed, this

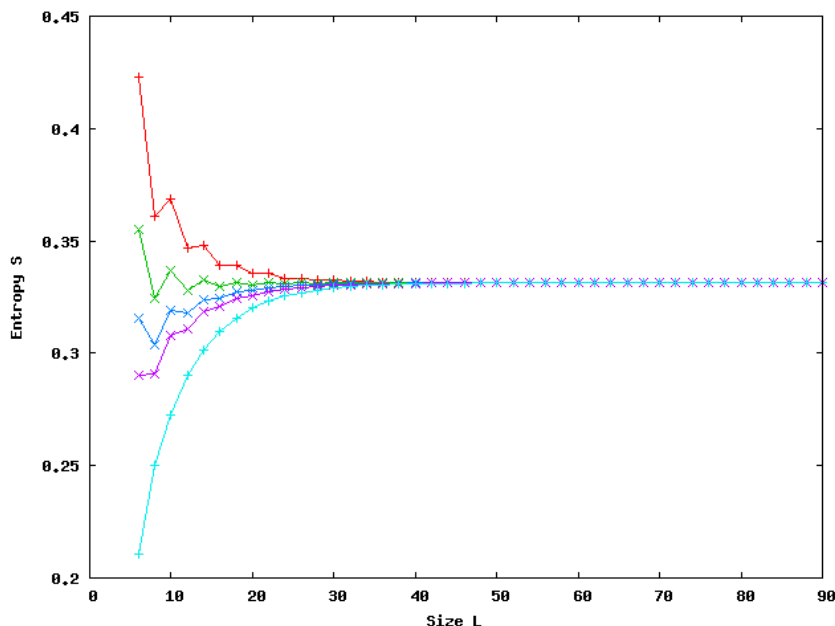


Figure 4.13: The entropy as a function of L , for the following values of the magnetic field at the two edges: $h = 0.15$ (red), $h = 0.2$ (green), $h = 0.25$ (blue), $h = 0.3$ (fuchsia), $h = 10$ (light blue).

dependence is much weaker for $h > 1$. We would like to describe the scaling of the entropy and of the entanglement spectrum in a way which is independent of the magnetic field applied.

For this purpose we turned back to the case without magnetic field, that is $h = 0$, and we noticed the following: for $L \rightarrow \infty$, with respect to (4.4) (the formula for the entanglement spectrum in the limit $L \rightarrow \infty$) the entanglement spectrum degeneracies are doubled and each value is halved. This can be explained quite easily. Suppose that the ground state is

$$|\psi\rangle = \frac{1}{\sqrt{2}} |\psi_1\rangle + \frac{1}{\sqrt{2}} |\psi_2\rangle \quad (4.38)$$

where

$$|\psi_1\rangle = \sum_i \alpha_i |a_i\rangle \quad |\psi_2\rangle = \sum_i \beta_i |b_i\rangle \quad (4.39)$$

and furthermore

$$\langle a_i | b_j \rangle = 0, \quad \forall i, j \quad (4.40)$$

This last requirement is reasonable since orthonormal states belong to orthonormal spaces. For the same reasons of section 4.2, we have:

$$\rho = \rho_1 + \rho_2 \quad (4.41)$$

4. Numerical simulations

We denote the eigenvalues of ρ_1 and ρ_2 with $\{\lambda_i^{(1)}\}$ and $\{\lambda_i^{(2)}\}$ respectively. Thanks to (4.40), if $|\phi_j\rangle$ is an eigenstate of ρ_1 , then:

$$\rho_2 |\phi_j\rangle = 0 \quad (4.42)$$

It is natural to suppose that the entanglement spectrum is the same for ρ_1 and ρ_2 . Then the entanglement spectrum is doubled, and to recover $\sum \lambda_i = 1$ we must halve each eigenvalue.

In figure 4.15 we report the plot of the first and the second eigenvalue λ_0 and λ_1 . In figure 4.16, instead, we report λ_2 and λ_3 . Notice that each eigenvalue has parity effects similar to those discussed for the entropy in section 3.85. Indeed, from numerical data we infer that if

$$L \bmod 4 = 0 \quad (4.43a)$$

there is no degeneration between any of the eigenvalues, while if

$$L \bmod 4 = 2 \quad (4.43b)$$

the eigenvalue λ_0 and λ_1 coincide up to 6 or 7 digits, and the same holds for λ_2 and λ_3 . Moreover, as can be seen from these two figures, the value for (4.43a) tend to approach the values for (4.43b) in the limit $L \rightarrow \infty$. This suggests that, if we want to describe the eigenvalues of just one of the degenerated ground states, we should take those satisfying condition (4.43b).

In figure 4.17 we plotted the Schmidt gap for these values of L (a), as well as the Schmidt gap in the case of equation (4.37) (b). For case b we found that a fit using the function

$$\Delta\lambda(L) = a + b \cdot \exp cL \quad (4.44)$$

is very satisfactory, with parameters given by:

$$\begin{cases} a = 0.89143 \pm 0.00005 \\ b = 0.153 \pm 0.002 \\ c = -0.185 \pm 0.002 \end{cases} \quad (4.45)$$

For case a, instead, we didn't find any satisfactory function fitting these data, trying with the following ansatz:

$$\Delta\lambda = a + b \cdot \exp cL \quad \Delta\lambda = a + b \cdot L^c \quad (4.46)$$

Besides these facts, we still need to understand which approach is better to describe the scaling of the quantities we are studying.

4.5. Studying the FSS of the entanglement spectrum

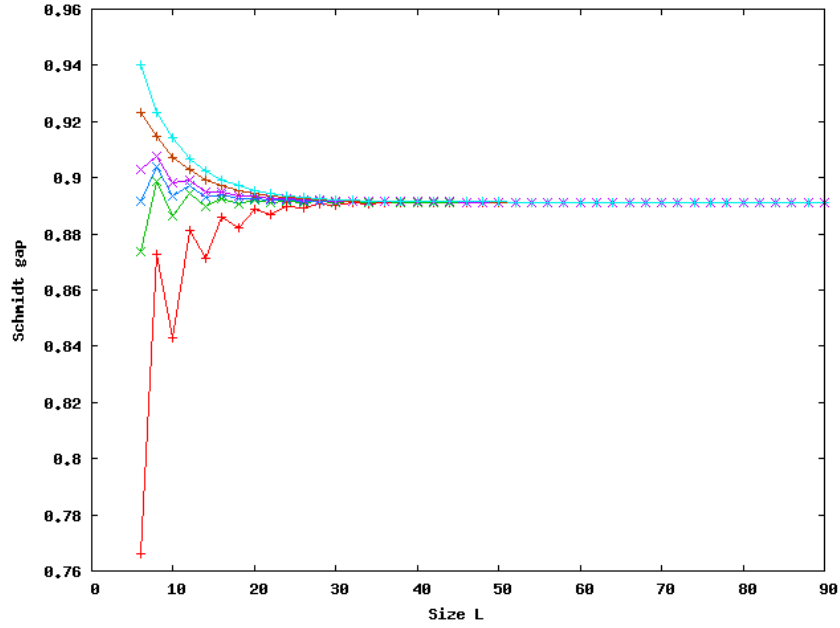


Figure 4.14: The Schmidt gap as a function of L , for the following values of the magnetic field at the two edges: $h = 0.1$ (red), $h = 0.2$ (green), $h = 0.25$ (blue), $h = 0.3$ (fuchsia), $h = 0.5$ (purple), $h = 10$ (light blue).

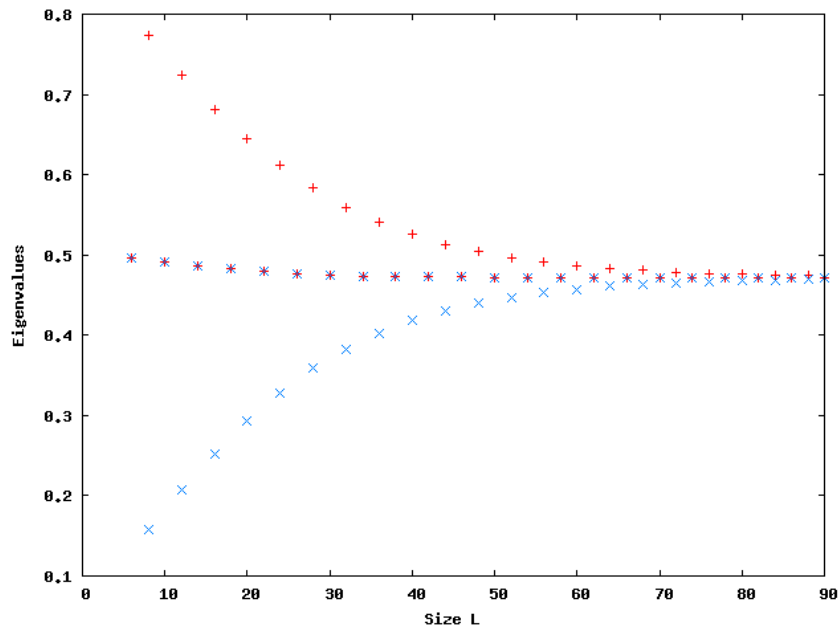


Figure 4.15: The eigenvalues λ_0 (red) and λ_1 (blue) as a function of L , with no magnetic field. Notice that they both have an oscillating behaviour.

4. Numerical simulations

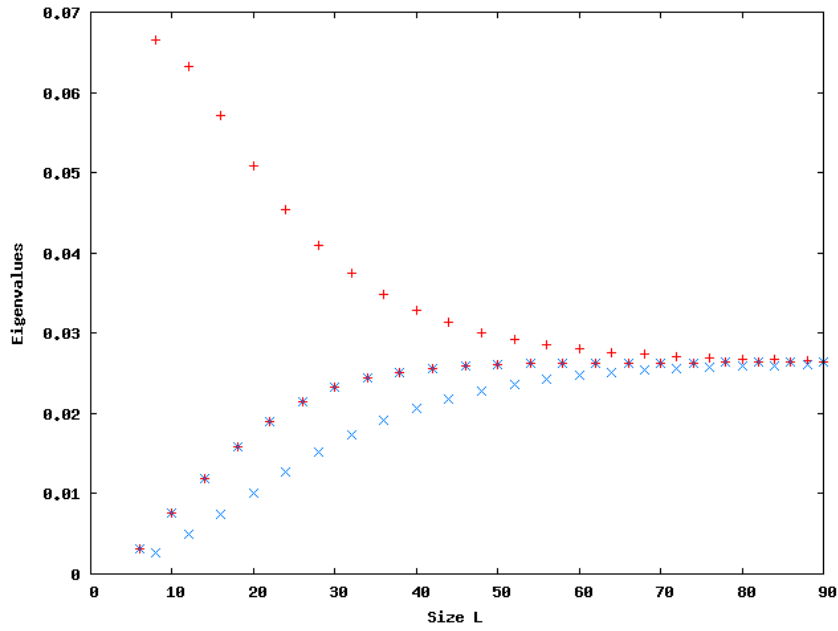


Figure 4.16: The eigenvalues λ_2 (red) and λ_3 (blue) as a function of L , with no magnetic field. Notice that they both have an oscillating behaviour.

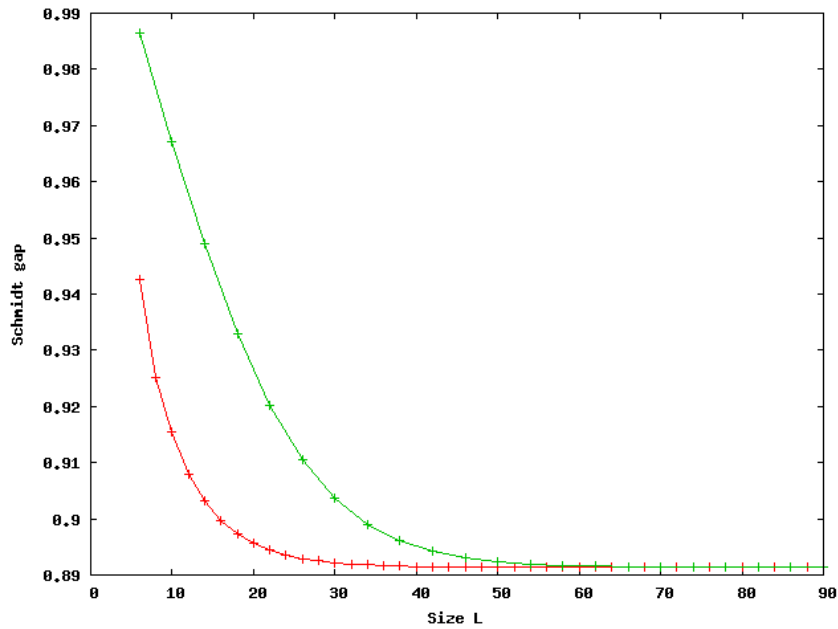


Figure 4.17: The Schmidt gap as a function of L for $h = 10$ (red) and no magnetic field (green).

4.5. Studying the FSS of the entanglement spectrum

As a last task of this section, we tried to get closer to the critical line, using the following parameters:

$$\begin{cases} J_x = 1 \\ J_y = 1.005 \\ J_z = 0.4 \end{cases} \quad (4.47)$$

The simulations without a magnetic field didn't provide sensible results, since the algorithm doesn't converge for parameters so close to the critical line. We saw that, empirically, these simulations converge for values of the entropy given by formula (4.13) smaller than $S \approx 0.5$, while in this case the entropy has a theoretical value of

$$S = 0.874061 \quad (4.48)$$

Instead, the application of a magnetic field as in case (4.37) brings to a result which is at least convergent, even if not very precise (the agreement with (4.13) is up to 2 figures for $L \rightarrow \infty$). We performed the simulations with such a magnetic field without sweeps, and with DMRG parameters:

$$M_{\min} = 10, \quad M_{\max} = 100, \quad D = 0.25 \cdot 10^{-7}, \quad L_{\max} = 600 \quad (4.49)$$

Notice that we needed a huge number of sites in the chain, compared to the previous simulations, to obtain the convergence of the algorithm.

The behaviour of the entropy as a function of L (the size of the system) is similar to the one in figure 4.13. In figures 4.18 and 4.19 we show the results for $h = 10$. This time the best fit for the Schmidt gap, whose shape is in figure 4.19, is not an exponential anymore, while it is of the form

$$\Delta\lambda(L) = a + b \cdot L^c \quad (4.50)$$

obtaining the following best fit values, which are quite acceptable:

$$\begin{cases} a = 0.652 \pm 0.001 \\ b = 1.03 \pm 0.03 \\ c = -0.67 \pm 0.01 \end{cases} \quad (4.51)$$

Furthermore, an ansatz of the same kind for the entropy

$$S(L) = d + e \cdot L^f \quad (4.52)$$

is also quite compatible with numerical data, with the following values of the coefficients:

$$\begin{cases} d = 0.940 \pm 0.004 \\ e = -2.35 \pm 0.07 \\ f = -0.60 \pm 0.01 \end{cases} \quad (4.53)$$

We tried to add terms of the form L^{nf} to the ansatz (4.52), but this provided a slightly worse agreement with numerical data. Perhaps, these terms acquire

4. Numerical simulations

more importance further from to the critical line, where the best fit becomes an exponential. In figures 4.18 and 4.19 we also plotted the best fits for the Schmidt gap and the Entanglement entropy.

We remind here, from section 3.6.1, the ansatz of the function describing the Schmidt gap, which represents the behaviour of an order parameter:

$$\Delta\lambda \simeq L^{\beta/\nu} f(|g - g_c|L^{1/\nu}) \quad (4.54)$$

where for example, in the case of the Sine-Gordon model, we have

$$g - g_c = J_y - 1$$

The best fit (4.50) would suggest the following form for the universal function f :

$$f(|g - g_c|L^{1/\nu}) = \alpha |g - g_c|^{-\beta} \cdot L^{-\beta/\nu} + \gamma |g - g_c|^\delta L^{\delta/\nu} \quad (4.55)$$

if, of course, we are near enough to the critical line. The constants α , γ and δ should be determined from the simulations. In this way we would have

$$\Delta\lambda = \alpha |g - g_c|^{-\beta} + \gamma |g - g_c|^\delta L^{(\beta+\delta)/\nu} \quad (4.56)$$

Indeed, to better understand if this form is sensible we need to perform further simulations along a given line of constant μ , and check that the shape of the Schmidt gap doesn't change when we get closer to the critical line. A determination of the exponent β may come from the method discussed in section 3.6.1, since we have an exact formula for the Schmidt gap. But as we saw there, the exponent β changes as we approach the critical line. A numerical study of the Schmidt gap seems then the best way to evaluate β and ν for the Sine-Gordon model.

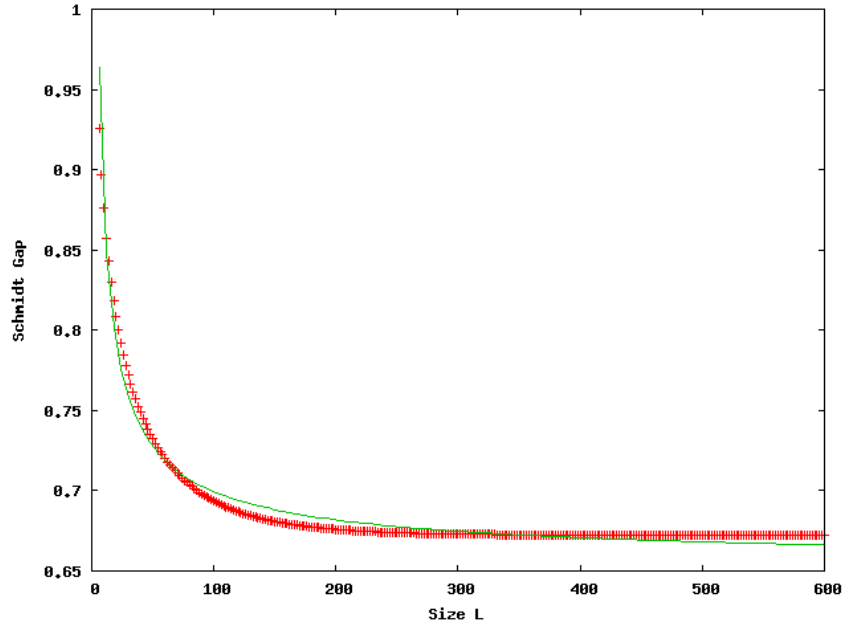


Figure 4.18: The Schmidt gap for the parameters given in (4.47) as a function of L (red crosses), and the best fit (4.50) (green line). The magnetic field is $h = 10$.

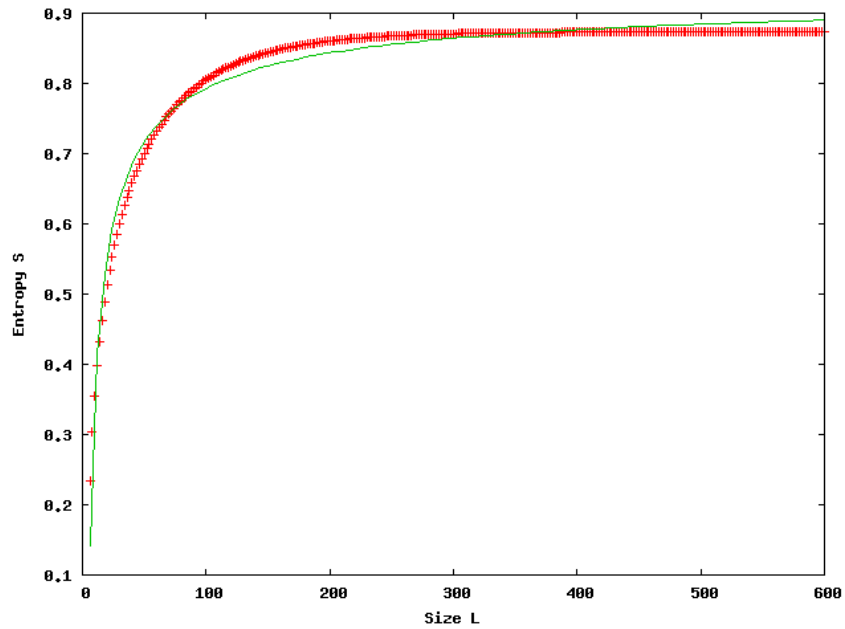


Figure 4.19: The entropy for the parameters given in (4.47) as a function of L (red crosses), and the best fit (4.52) (green line). The magnetic field is $h = 10$.

4.6 Conclusions and outlook

In this thesis we wanted to better understand the behaviour of the Entanglement entropies and the Entanglement Spectrum for a XYZ chain. If we denote with L the length of this chain, formulas for the Entanglement entropies already existed in the case $L \rightarrow \infty$, and turned out to be in excellent agreement with numerical data. As for the Entanglement Spectrum, we derived a formula for $L \rightarrow \infty$ which also agreed greatly with numerical data. Indeed, the agreement got worse as we approached the critical XXZ line. Numerical simulations which may give a very accurate accordance with theoretical results, approaching the XXZ line, would probably require a huge amount of memory and several days of computer working: these could be a possible task for the future.

A further task would be to test these formulas near the antiferromagnetic points. Indeed, in every neighborhood of such points the Entanglement entropy diverges, as we described in section 3.5: this implies that the convergence of the numerical algorithms is difficult to obtain however we move towards such points. Moreover, since the correlation length is greater near the antiferromagnetic points, the convergence of the Entanglement entropy is eventually reached for very high values of L : one then needs to find a compromise between the realization of this convergence and the precision of numerical data.

As we pointed out, a formula for the Entanglement entropy and the Entanglement spectrum for finite size systems is still lacking. The main problem in the numerical study of the behaviour of the Entanglement entropy as a function of L is the double degeneracy of the ground state: this requires necessarily the use of magnetic fields to split the degenerated ground states. We showed that, with a smart application of these fields, one can obtain an Entanglement entropy which is monotonically increasing with L . But with this approach, for example, the oscillations of the entropy disappear. On the other hand, the use of no magnetic fields gives results which can hardly be represented by fitting functions, and near the critical line simulations without magnetic fields don't converge at all. It would be interesting to understand in an analytical way which approach is the best, and then eventually obtain a plausible function for the entropy as a function of L , which might be explained analytically. Moreover, near the antiferromagnetic point the oscillations of the entropy are much more pronounced, so it may be easier to understand analytically their origin near these points, if one could manage to achieve the convergence of the entropy.

At last, finding the correct behaviour of the Schmidt gap as a function of L would allow us to compute the critical exponents of the Sine-Gordon model, that is to check if the conjecture in [14], about the behaviour of the Schmidt gap as an order parameter, is correct even for the XYZ model.

Appendix A

Entanglement

Entanglement is one of the most striking evidence of the quantum behaviour of Nature. It has no classical counterpart, as for the concept of spin, and from a point of view generally accepted it represents the non-locality of the quantum theory.

Suppose we have a physical system C , composed by two subparts A and B and described by a pure state $|\Psi\rangle_C$ (entanglement for mixed states will not be treated here). We say that the system C is *separable* with respect to the partition $A|B$ if we can write

$$|\Psi\rangle_C = |\psi\rangle_A \otimes |\psi\rangle_B \quad (\text{A.1})$$

where obviously $|\psi\rangle_A \in \mathcal{H}_A$, the Hilbert space of the subsystem A , and the same for B . If this is not possible, we say that $|\Psi\rangle_C$ is *entangled*. What we defined is the bipartite entanglement, but let's define the *multipartite* entanglement in an analogous way. A system C composed by subparts A_1, A_2, \dots, A_n is separable with respect to this partition if it can be written as:

$$|\Psi\rangle_C = |\psi\rangle_{A_1} \otimes |\psi\rangle_{A_2} \cdots \otimes |\psi\rangle_{A_n} \quad (\text{A.2})$$

otherwise $|\Psi\rangle_C$ is said to be entangled. To give an example of an entangled state, suppose that a spinless particle (for example a π_+), at rest, decays in two fermions α and β with spin $\frac{1}{2}$, and opposite momentum. The two subparts of the system are the two particles respectively. Let's denote the eigenstates of $\frac{\hbar}{2}\sigma_z$ with $|0\rangle$ and $|1\rangle$ (σ_z is a Pauli matrix, and in the following we will set $\hbar = 1$). Then these two fermions may be described by the following spin wave function:

$$|\Psi\rangle_C = \frac{|1\rangle|0\rangle - |0\rangle|1\rangle}{\sqrt{2}} \quad (\text{A.3})$$

that is, a singlet state with spin 0 by definition. This function can't by no means reduced to the form (A.1), so the state $|\Psi\rangle_C$ is entangled with respect to the partition $\alpha|\beta$. In general, a physical state described by a bidimensional Hilbert space, that is which is spanned by two base vectors $|0\rangle$ and $|1\rangle$, is called a *qubit*.

A. Entanglement

Consider now a less trivial example. Suppose again $|\Psi\rangle_C = |\psi\rangle_A \otimes |\psi\rangle_B$, where $|\psi\rangle_A$ is a qubit, and:

$$|\psi\rangle_B = \frac{|0\rangle_{B'} |1\rangle_{B''} - |1\rangle_{B'} |0\rangle_{B''}}{\sqrt{2}} \quad (\text{A.4})$$

We see that $|\Psi\rangle_C$ is separable with respect to the separation $A|B'B''$, but is not with respect to $AB'|B''$.

A.1 EPR paradox and Bell inequality

We want to describe why entanglement is a genuine quantum effect, and its consequences on our vision of the world. We know that Albert Einstein has always been skeptical about quantum theory of nature. In 1935, A. Einstein, B. Podolsky and E. Rose (EPR) proposed a paradox that aimed to demolish the internal consistency of quantum mechanics. In their article ([18]), they asked which properties should have a physical theory to be successful. They required that such a theory must:

- agree with experiments;
- have elements of *reality* (realism): if, without perturbing the system, we can predict with certainty the value of a physical quantity, then "there exists an element of physical reality corresponding to this physical quantity".
- be *complete* (completeness): "every element of the physical reality must have a counterpart in the physical theory".

While quantum mechanics agrees very well with experimental data, the question is if this theory satisfy reality and completeness, that is if it's (in one word) complete. We now describe an experiment, similar to the one proposed by EPR but with the same consequences, that gives a negative answer to this question. This is based on the existence of entangled states.

Let's then turn back to our state (A.3), composed by two travelling particles α and β with spin $\frac{1}{2}$ and opposite momentum:

$$|\Psi\rangle_C = \frac{|0\rangle |1\rangle - |1\rangle |0\rangle}{\sqrt{2}} \quad (\text{A.5})$$

The two particles will travel far away from each other, and at some time they will be separated by a space-like interval. Suppose we have two observers called Alice and Bob (in the same fashion of information theory). Alice can perform measurements on α , while Bob on β . Now, Alice measures $s_z(\alpha)$, the spin component along z of particle α . This will alter the wave function:

A.1. EPR paradox and Bell inequality

if Alice measures, say, $\frac{1}{2}$, then $|\Psi\rangle_C$ collapses to $|1\rangle|0\rangle$ (neglecting a phase factor). This means that $s_z(\beta) = -\frac{1}{2}$ without uncertainty. In EPR view, $s_z(\beta)$ is an element of reality, since we can predict its value without uncertainty before making any measurements. But why this is so? Indeed, we apparently "perturbed" the system. The fact is that the two particles are separated by a space-like interval, so these cannot be in any kind of cause-effect relationship, if we accept Special Relativity. This is the hypothesis of *locality* and implies that $s_z(\beta)$ must be in its value $\frac{1}{2}$ *before* we start performing the measures.

But let's denote with $|1\rangle_x$ and $|0\rangle_x$ the eigenstates of $\frac{1}{2}\sigma_x$. If we expand $|1\rangle$ and $|0\rangle$ in term of this new base, we have:

$$|\Psi\rangle_C = \frac{|0\rangle_x |1\rangle_x - |1\rangle_x |0\rangle_x}{\sqrt{2}} \quad (\text{A.6})$$

Alice could as well have performed a measurement of $s_x(\alpha)$, and it follows that $s_x(\beta)$ is another element of realism. On the other hand, remember that spin operators along different axis satisfy the commutation relation:

$$[\sigma^z, \sigma^x] = 2i\sigma^y \quad (\text{A.7})$$

So, quantum mechanics tells us that the the spin components of two different axis can not be determined simultaneously, while we just showed that this is possible since they must have definite values. This is the EPR paradox. If we require quantum theory to be *complete* and *local*, then it's not consistent.

If quantum mechanics is not satisfactory to describe reality, it should be possible to find a theory which is complete, local, and agrees with experiment. Various attempt have been made to find such a theory (see for example the hidden variable theory), and finally in 1964 Alexander Bell proposed an experiment to discern between these.

Let's take for the moment the point of view of a theory that is complete and local. We start again from a pion π_+ at rest, decaying in two particles α and β having opposite momentum. Suppose Alice measures two physical properties of the particle α , which we denote with Q and R , and Bob measures the properties S and T of the particle β . Let the possible values of these physical quantities (which we denote with q , r , s and t) be ± 1 . These are elements of reality, so they are known before performing any measurements. If we repeat this experiments many times, we can evaluate the probabilities $p(q, r, s, t)$ of the system to have definite values of these quantities. Consider now the particular combination $QS + RS + RT - QT$, which can only assume the values ± 2 . If we denote with $\mathbf{E}(\cdot)$ the mean value of a quantity, we have:

$$\begin{aligned} \mathcal{B} &\equiv \mathbf{E}(QS) + \mathbf{E}(RS) + \mathbf{E}(RT) - \mathbf{E}(QT) = \mathbf{E}(QS + RS + RT - QT) \\ &= \sum_{q,r,s,t} p(q, r, s, t) (qs + rs + rt - qt) \leq 2 \sum_{q,r,s,t} p(q, r, s, t) = 2 \end{aligned} \quad (\text{A.8})$$

A. Entanglement

and this defines the *Bell inequality* for a complete and local physical theory:

$$\boxed{\mathcal{B} \leq 2} \quad (\text{A.9})$$

Let's now turn to quantum mechanics, and choose the properties described above to be the following:

$$Q = \sigma_\alpha^z \quad S = \frac{-\sigma_\beta^z - \sigma_\beta^x}{\sqrt{2}} \quad (\text{A.10})$$

$$R = \sigma_\beta^x \quad T = \frac{\sigma_\beta^z - \sigma_\beta^x}{\sqrt{2}} \quad (\text{A.11})$$

which have the same possible values ± 1 . If we compute the expectation value of these quantities over the state $|\Psi\rangle_C$ given by (A.5), we find that:

$$\langle QS \rangle = \frac{1}{\sqrt{2}}, \quad \langle RS \rangle = \frac{1}{\sqrt{2}}, \quad \langle RT \rangle = \frac{1}{\sqrt{2}}, \quad \langle QT \rangle = -\frac{1}{\sqrt{2}} \quad (\text{A.12})$$

and so:

$$\mathcal{B} \equiv \langle QS \rangle + \langle RS \rangle + \langle RT \rangle - \langle QT \rangle = 2\sqrt{2} > 2 \quad (\text{A.13})$$

that is, quantum mechanics *violates* the Bell inequality.

In the last decades, various experiments showed that Bell inequality is violated up to 30 standard deviations: this is a striking evidence of the validity of quantum theory of nature. We then have to reject some of the commonsense intuitions: quantum mechanics is either not complete or not local, and philosophical debates about which point of view is more correct are still open. If we accept non-locality, it seems that entanglement violates special relativity, because a perturbation on the subsystem α propagates *instantaneously* on β . Now, if Alice, after measuring $s_z(\alpha)$, wants to know if $s_z(\beta)$ assumed a definite value, she has to *communicate* her results to Bob: otherwise Bob, measuring $s_z(\beta)$, may think to be the first who perturbed the wave function. But no signal can travel faster than light, and in this way the relationship of cause-effect is preserved.

A.2 Reduced density matrices

It is known (see *e.g.* [25] or [27]) that quantum mechanics can be reformulated in terms of density matrices. If a system is in a pure state $|\Psi\rangle$, its density matrix is defined as $\rho \equiv |\Psi\rangle\langle\Psi|$. If, instead, a system is not in a fixed state, but has (classical) probabilities p_i to be in the states $|\psi_i\rangle$, then its density matrix is $\rho \equiv \sum_i p_i |\psi_i\rangle\langle\psi_i|$: we will refer to this as a mixed state. Given a density matrix, we can discern these two situations by simply calculating ρ^2 : if $\rho^2 = \rho$ the system is in a pure state, otherwise it's in a mixed state. Notice that this last situation can not be described by a wave function: in some sense, the density matrix is a more general object than the $|\psi_i\rangle$ themselves.

A.3. Schmidt decomposition

Suppose we have a system C divided in two subparts A and B . In the case $\rho_C \equiv \rho_{AB} = \rho_A \otimes \rho_B$, we can describe the subsystem A through:

$$\rho_A = \text{Tr}_B \rho_C \quad (\text{A.14})$$

This is the *reduced density matrix* for the system A , and this definition is valid even in the more complex case $\rho_{AB} \neq \rho_A \otimes \rho_B$. To see this, suppose \mathcal{M} is an observable on the system A . If we denote with $\tilde{\mathcal{M}}$ the same observable performed on the larger system AB , it is easy to see that:

$$\tilde{\mathcal{M}} = \mathcal{M} \otimes \mathbb{I}_B \quad (\text{A.15})$$

In fact, we have the decomposition $\mathcal{M} = \sum_m p_m P_m$, where P_m are projectors on A , with eigenvectors $|m\rangle$. We then have to find in AB the vectors whose eigenvalues are p_m , and these are clearly $|m\rangle \otimes |\psi\rangle$, with $|\psi\rangle$ arbitrary. From this reasoning the validity of (A.15) follows.

Now, physical consistency requires that any prescription to associate a state ρ_A to the subsystem A must have the property that measurements averages be the same whether computed via ρ_A or ρ_{AB} , that is:

$$\text{Tr}_A (\mathcal{M} \rho_A) = \text{Tr}_{AB} (\tilde{\mathcal{M}} \rho_{AB}) = \text{Tr}_{AB} ((\mathcal{M} \otimes \mathbb{I}_B) \rho_{AB}) \quad (\text{A.16})$$

and this relation is satisfied only for $\rho_A = \text{Tr}_B \rho_{AB}$. This is because (A.16) is valid for all observables, so let's take $\{\mathcal{M}_i\}$ to be an orthonormal basis with respect to the scalar product $(\mathcal{P}, \mathcal{Q}) \equiv \text{Tr} (\mathcal{P} \mathcal{Q})$. We have the decomposition:

$$\rho_A = \sum_i \mathcal{M}_i \text{Tr}_A (\mathcal{M}_i \rho_A) = \sum_i \mathcal{M}_i \text{Tr}_{AB} ((\mathcal{M}_i \otimes \mathbb{I}_B) \rho_{AB}) \quad (\text{A.17})$$

Thus, ρ_A is uniquely defined by (A.16) if we know ρ_{AB} , and this is equal to $\text{Tr}_B \rho_{AB}$ since it satisfies (A.16).

A.3 Schmidt decomposition

A useful tool to determine whether a state is entangled or not is the *Schmidt decomposition*. Suppose $\{|i\rangle_A\}$ and $\{|j\rangle_B\}$ are orthonormal bases of \mathcal{H}_A and \mathcal{H}_B respectively, and let the dimensions of \mathcal{H}_A and \mathcal{H}_B be d_A and d_B . Then, a pure state belonging to $\mathcal{H}_C = \mathcal{H}_A \otimes \mathcal{H}_B$ can be expanded as:

$$|\Psi\rangle_C = \sum_{i,j} M_{ij} |i\rangle_A |j\rangle_B \quad (\text{A.18})$$

A theorem of linear algebra states that any rectangular matrix \mathbf{M} with $d_A \times d_B$ lines and rows can be decomposed as:

$$\mathbf{M} = \mathbf{U} \mathbf{\Lambda} \mathbf{V}^\dagger \quad (\text{A.19})$$

A. Entanglement

where \mathbf{U} is a $d_A \times d_A$ unitary matrix, \mathbf{V} is a $d_B \times d_B$ unitary matrix, and $\mathbf{\Lambda}$ is a $d_A \times d_B$ matrix whose non zero elements, lying in the diagonal, are all real and positive. If we switch to the orthonormal vectors:

$$\begin{cases} |\tilde{i}\rangle_A = \sum_j (\mathbf{U}^\top)_{ij} |j\rangle_A \\ |\tilde{i}\rangle_B = \sum_j (\mathbf{F}^\dagger)_{ij} |j\rangle_B \end{cases} \quad (\text{A.20})$$

(note that (\mathbf{U}^\top) and (\mathbf{F}^\dagger) are unitary matrices as well), then (A.18) becomes:

$$|\Psi\rangle_C = \sum_{i,k,l,j} U_{i,k} \Lambda_{k,l} V_{l,j}^\dagger |i\rangle_A |j\rangle_B = \sum_{k,l} \Lambda_{k,l} |\tilde{i}\rangle_A |\tilde{i}\rangle_B \quad (\text{A.21})$$

If, at last, we write $\Lambda_{k,l} = \delta_{k,l} \lambda_k$, we obtain the Schmidt decomposition of the pure state $|\Psi\rangle_C$:

$$|\Psi\rangle_C = \sum_i \lambda_i |\tilde{i}\rangle_A |\tilde{i}\rangle_B \quad (\text{A.22})$$

Notice that in equation (A.20) the two set of states are orthonormal, but only the states corresponding to the Hilbert space with lower dimension are a basis. Furthermore, the state $|\Psi\rangle_C$ is separable if $\lambda_i = 1$ for some i : this implies that $\lambda_j = 0$ for $j \neq i$ because $\sum_j |\lambda_j|^2 = 1$.

If we take the partial trace of $|\Psi\rangle_C$ with respect to the subsystem B , we have:

$$\rho_A = \text{Tr}_B |\Psi\rangle_C \langle \Psi|_C = \sum_i |\lambda_i|^2 |\tilde{i}\rangle_A \langle \tilde{i}|_A \quad (\text{A.23})$$

But in an analogous way:

$$\rho_B = \text{Tr}_A |\Psi\rangle_C \langle \Psi|_C = \sum_i |\lambda_i|^2 |\tilde{i}\rangle_B \langle \tilde{i}|_B \quad (\text{A.24})$$

that is, the two reduced density matrix ρ_A and ρ_B share the same eigenvalues. We will find this property very important when defining the Von Neumann entropy of a pure state. The numbers λ_i are the *Schmidt numbers* for the state $|\Psi\rangle_C$, and they quantify the amount of entanglement between the two systems A and B . Since the set $\{|\lambda_i|^2\}$ is formed by real numbers, it represents a better way to describe the entanglement: it is called the *entanglement spectrum*. Notice also the following: if the system $|\Psi\rangle_C$ is separable, then ρ_A and ρ_B describe *pure* states, because only one Schmidt number is non-zero. Otherwise, if the system is entangled, ρ_A and ρ_B always describe *mixed* states.

A.4 Information theory and Shannon entropy

Information theory is the study of the quantification of information. For example, if we have a source sending information, the goal of information theory is to evaluate the smallest amount of memory needed to store all the output.

A.4. Information theory and Shannon entropy

The key concept of classical information theory is the *Shannon entropy*, which is associated to a probability distribution $X = (p_1, p_2, \dots, p_n)$, and is defined by:

$$H(X) \equiv H(p_1, \dots, p_n) = - \sum_i p_i \log_2 p_i \quad (\text{A.25})$$

where the logarithm is taken in base 2. We use the convention $0 \log_2 0 = 0$. This gives us the first hint on $H(X)$: if an event has probability 0, then it will never give us any kind of information.

To understand the meaning of Shannon entropy, suppose we have a source that is producing bits X_1, X_2, \dots , each being 0 with probability p , and equal to 1 with probability $1-p$ (that is, these variables are independent). Let's then study the limit $n \rightarrow \infty$, where n is the number of bits emitted by the source. In this limit we know that, for a given output, the number of 0 bits is equal to pn , and the number of 1 bits is $(1-p)n$. The outputs (x_1, \dots, x_n) satisfying this condition are called *typical sequences*, and for $n \rightarrow \infty$ this is true for all outputs. If n is finite, the probability to find a typical sequence is given by:

$$p(x_1, \dots, x_n) = p(x_1) p(x_2) \dots p(x_n) = p^{np} (1-p)^{(1-p)n} \quad (\text{A.26})$$

If we take the logarithm on both sides, we get:

$$-\log_2 p(x_1, \dots, x_n) = -np \log_2 p - n(1-p) \log_2 (1-p) = nH(X) \quad (\text{A.27})$$

where $X = (p, 1-p)$ is the probability distribution for each bit. Finally:

$$p(x_1, \dots, x_n) = 2^{-nH(X)} \quad (\text{A.28})$$

Now, we want to store the information we obtained from the source, that is we search a method to record the output of the source using the least number of bits possible. Recall that j bits can describe 2^j numbers. If $n \rightarrow \infty$, the number of sequences which are not typical tends to 0, so let's focus on the typical ones. Since the probability for each of these sequences is given by (A.28), if we label each sequence with a number, we then need $nH(x)$ bits to store the informations in output from the source. Clearly, this very simple "algorithm" of data compression has some lacks, the most obvious one is that it doesn't consider the untypical sequences. But this gives us an idea of the meaning of Shannon entropy: it is the mean number of bits we need to store our information. In other words, $H(X)$ quantifies how much information we gain, on average, when we learn the value of X ([27]), and this is equivalent to say that $H(X)$ measures the amount of *uncertainty* about X before we learn its value.

Clearly, the reasoning above is valid for an arbitrary probability distribution $X = (p_1, \dots, p_k)$, where, for the sake of clarity, p_i is the probability for the outcome of the variable labelled v_i . Now a typical sequence (x_1, \dots, x_n) will

A. Entanglement

have np_1 outputs of v_1 , and in general np_i outputs of v_i , and its probability to appear is:

$$p(x_1, \dots, x_n) = 2^{-nH(X)} \quad (\text{A.29})$$

If we assume that all the outputs are typical sequence (a good approximation indeed in the limit $n \rightarrow \infty$), we just need $nH(X)$ bits to store all the information in output.

Let's define the *relative entropy* between two probability distributions $X = \{p(x)\}$ and $Y = \{q(x)\}$ as:

$$H(p(x) \parallel q(x)) \equiv \sum_x p(x) \log \frac{p(x)}{q(x)} = -H(X) - \sum_x p(x) \log q(x) \quad (\text{A.30})$$

This gives us a measure of the closeness between X and Y . It has the important property $H(p(x) \parallel q(x)) \geq 0$, with equality if $p(x) = q(x)$ for all x . If we set $q(x) = 1/d$ for all x , where d is the number of outcomes from a source, we have:

$$H(p(x) \parallel q(x)) = \log d - H(X) \quad (\text{A.31})$$

It's then easy to see that the Shannon entropy has the boundaries

$$0 \leq H(X) \leq \log d \quad (\text{A.32})$$

where the equality $H(X) = \log d$ is for $p(x) = 1/d$ for all x . This corresponds to the maximum uncertainty of the output given by a source, so we'll need the maximum possible amount of bits to store it.

The *joint entropy* of a pair of random variables X and Y is defined as:

$$H(X, Y) \equiv \sum_{x,y} p(x, y) \log p(x, y) \quad (\text{A.33})$$

and it simply represents the amount of information we gain from the two events X and Y combined together. If these are independent variables, then it's simply $H(X, Y) = H(X) + H(Y)$, otherwise we have:

$$H(X, Y) \leq H(X) + H(Y) \quad (\text{A.34})$$

Other kind of entropies can be defined, see again [27] for further details.

A.5 Measuring the entanglement

A.5.1 The Von Neumann entropy

The Von Neumann entropy is the generalization of the classical case to the quantum context, with density operators replacing probability distributions. Suppose that a state is described by

$$\rho = \sum_i \lambda_i |\psi_i\rangle \langle \psi_i| \quad (\text{A.35})$$

A.5. Measuring the entanglement

If $\{|\psi_i\rangle\}$ is a set of orthogonal vectors belonging to a Hilbert space \mathcal{H} , the Von Neumann entropy of ρ is defined as:

$$S(\rho) = -\text{Tr } \rho \log \rho \quad (\text{A.36})$$

where the trace is over \mathcal{H} . Clearly, thanks to (A.35) we have:

$$S(\rho) = -\sum_i \lambda_i \log \lambda_i \quad (\text{A.37})$$

Here we state some properties of $S(\rho)$:

- $S(\rho)$ is positive; $S(\rho) = 0$ only for pure states and has its maximal value $\log d$ when the states $|\psi_i\rangle$ are all equally probable, in which case $\rho = \mathbb{I}/d$:

$$0 \leq S(\rho) \leq \log d$$

- If a composite system C is in a pure state $|\Psi\rangle_C = |\psi\rangle_A \otimes |\psi\rangle_B$ then we have:

$$S(\rho_A) = S(\rho_B) \quad (\text{A.38})$$

where ρ_A and ρ_B are the reduced density matrices of the two subsystems A and B respectively. This property follows from (A.23) and (A.24).

- The entropy is *concave*: if a state is a classical superposition of states ρ_j , with probabilities p_j , then:

$$S\left(\sum_j p_j \rho_j\right) \geq \sum_j p_j S(\rho_j) \quad (\text{A.39})$$

This means, in the point of view of classical information theory, that the information we have about $\rho = \sum_j p_j \rho_j$ is greater than the average of the $S(\rho_j)$, because $S(\rho)$ takes into account not only our ignorance about the whole system ρ , but also our lack of knowledge on the ρ_j themselves. In the special case where the ρ_j live in orthogonal spaces, we have:

$$S\left(\sum_j p_j \rho_j\right) = H(\{p_j\}) + \sum_j p_j S(\rho_j) \quad (\text{A.40})$$

- $S(\rho)$ satisfies *subadditivity*: if $\rho = \rho_{AB}$, where A and B are two subsystems, then

$$S(\rho_{AB}) \leq S(\rho_A) + S(\rho_B) \quad (\text{A.41})$$

where the equality is for $\rho_{AB} = \rho_A \otimes \rho_B$.

- If we apply a unitary transformation $\rho \rightarrow U\rho U^{-1}$ on our system, the entropy remains invariant:

$$S(U\rho U^{-1}) = S(\rho) \quad (\text{A.42})$$

A. Entanglement

Let's turn to the problem of measuring the entanglement. This hasn't been solved yet, in the sense that it is still lacking a formula which measures, in a satisfactory way, bipartite and multipartite entanglement in every possible cases. Let's approach the problem in the case of bipartite entanglement of a pure state. Suppose we have, as usual, a system C described by a density matrix $\rho = |\Phi\rangle\langle\Phi|$ and divided in two subsystems A and B . We then require that a measure $E(\rho)$ of the entanglement of the system C satisfies the following reasonable properties:

1. $E(\rho) = 0$ for separable states
2. If Θ is an operator that realizes LOCC, then

$$E(\Theta(\rho)) \leq E(\rho) \quad (\text{A.43})$$

A "local operation" (LO) is an operation acting locally on only one of the subsystems, and it shouldn't increase $E(\rho)$ since entanglement exists only as an interaction between the two subsystems. Furthermore, entanglement is a quantum effect, so if A and B perform operations between themselves through a classic channel ("channel communication", CC), we expect this not to increase the entanglement of the total system as well.

3. $E(\rho)$ is a *convex function*, that is:

$$E(\lambda\rho_1 + (1 - \lambda)\rho_2) \leq \lambda E(\rho_1) + (1 - \lambda)E(\rho_2) \quad (\text{A.44})$$

for $0 \leq \lambda$. In fact, it is reasonable to assume that entanglement doesn't increase under a classical mixing of two or more states, since this is a quantum effect, and it is not concerned with classical statistics.

4. given two states described by ρ and σ , we have:

$$E(\rho \otimes \sigma) \leq E(\rho) + E(\sigma) \quad (\text{A.45})$$

which means that putting together two non interacting systems should not increase the overall entanglement. Of course, for a single state ρ we expect that

$$E(\rho^{\otimes N}) = NE(\rho)$$

We now want to show that the entropy

$$S(\rho_A) = -\text{Tr} \rho_A \log \rho_A \quad (\text{A.46})$$

gives a measure of the entanglement between A and B , in the case of a pure state $|\Phi\rangle$. First of all notice that $S(\rho_A) = S(\rho_B)$, thanks to (A.23) and (A.24). This states the reasonable fact that A is entangled to B in the same measure

that B is entangled of A . As a consequence, we can euristically define the entropy of the pure state $|\Phi\rangle_C$ as:

$$\boxed{E(|\Phi\rangle_C) \equiv S(\rho_A) = S(\rho_B)} \quad (\text{A.47})$$

Furthermore, $S(\rho_A) = 0$ if ρ_A describes a pure state, which implies that $|\Psi\rangle_C$ is separable (see section A.3): when the entropy is 0, we have no entanglement between the two parts. If instead $S(\rho_A)$ takes its maximum value $\log d$, we expect $|\Psi\rangle_C$ to be maximally entangled. This is the case where we have the maximum uncertainty about the mixed state ρ_A , that is we have the least amount of information possible to know which pure state A is going to take, since $\rho_A = \mathbb{I}_A/d$ (if A is the part with lower dimensional Hilbert space). Anyway, the most important problem of Von Neumann entropy is that it is *concave*, so it doesn't satisfy property 3 for a measure of entanglement at all. This means that we can take $S(\rho_A) = -\text{Tr} \rho_A \log \rho_A$ to measure entanglement of a system C only if ρ_C is in a *pure state*, in which case we always have $\lambda = 1$ in property 3, and (A.44) becomes an equality.

We will deal with Von Neumann entropy in the context of conformal field theory (see chapter 3), but due to this last discussion we will always refer to the entropy of a pure and bipartite state.

A.5.2 The Renyi entropies

Let's now derive Shannon Entropy in a more abstract way. We already know that $H(X) \equiv H(p_1, p_2, \dots, p_n)$ quantifies our uncertainty about the probability distribution X before we know its value. Actually, the form

$$H(X) = - \sum_i p_i \log p_i \quad (\text{A.48})$$

can be derived from a set of axioms that Shannon entropy should satisfy. These axioms are ([29]):

1. $H(p_1, \dots, p_n)$ is a symmetric function of its arguments;
2. $H(p, 1 - p)$ is a continuous function of p , for $0 \leq p \leq 1$;
3. $H\left(\frac{1}{2}, \frac{1}{2}\right) = 1$;
4. $H(tp_1, (1 - t)p_1, \dots) = tH(p_1, \dots) + p_1H(t, 1 - t)$ for $0 \leq t \leq 1$.

Suppose we have two sets of probability distributions $X = (p_1, p_2, \dots, p_n)$ and $Y = (q_1, q_2, \dots, q_n)$, and denote with $X * Y$ the direct product of these two distributions, whose elements are given by $p_i q_j$. It follows from (A.48) that:

$$H(X * Y) = H(X) + H(Y) \quad (\text{A.49})$$

A. Entanglement

This equation expresses the property of *additivity* for Shannon entropy: if we have two independent events, the information we gain on the combined experiment is equal to the sum of the information we gain performing the two experiments separately. It can be shown that axiom 4 implies (A.49), but the opposite is not true. Anyway, (A.49) is the only important property we need for a measure of information, so if we try to find an expression satisfying axioms 1, 2, 3 and (A.48), we end up with several functions. One class of such functions are the so called *Renyi entropies*:

$$H_\alpha(X) = \frac{1}{1-\alpha} \log_2 \left(\sum_i p_k^\alpha \right) \quad (\text{A.50})$$

and these can also be regarded as a measure of the entropy of the distribution X . An important property of the Renyi entropies is that for $\alpha \rightarrow 1$ we recover the Shannon entropy, as can be easily seen by taking this limit in (A.50).

The quantum equivalent take also the name of Renyi entropies, and these are given by:

$$S_\alpha(\rho) = \frac{1}{1-\alpha} \log(\text{Tr } \rho^\alpha) \quad (\text{A.51})$$

As a final remark, note that Von Neumann and Renyi entropies are defined with logarithms in base 2. When evaluating these objects in statistical systems (as in chapter 3), we will take, for convenience, the natural logarithms instead.

Appendix B

Corner Transfer Matrix

In this section we focus on the definition and some properties of the Corner Transfer Matrices (CTMs). We also give an overview of the eight vertex model, and describe its CTMs. The presentation is concise, since these topics are very wide. The book which best covers them is ([3]), and all the details can be found there.

B.1 Definitions

We know that, in the context of classical models, a row-to-row transfer matrix describes the interaction between two rows, or equivalently it adds a row on the lattice, from the point of view of Baxter's book. This transfer matrix is composed by the two operators

$$[P_i(K)]_{\vec{\sigma}, \vec{\sigma}'} = \exp(K \sigma_i \sigma_{i+1}) \delta_{\sigma_1, \sigma'_1} \cdots \delta_{\sigma_N, \sigma'_N} \quad (\text{B.1})$$

and

$$[Q_i(L)]_{\vec{\sigma}, \vec{\sigma}'} = \delta_{\sigma_1, \sigma'_1} \cdots \delta_{\sigma_{i-1}, \sigma'_{i-1}} \exp(L \sigma_i \sigma'_i) \delta_{\sigma_{i+1}, \sigma'_{i+1}} \cdots \delta_{\sigma_N, \sigma'_N} \quad (\text{B.2})$$

where the $\delta_{\alpha, \beta}$ are Kronecker deltas, also denoted with $\delta(\alpha, \beta)$. Suppose we are building the Boltzmann weight of a lattice with M rows and N columns, and that we have already constructed k rows. Then $[P_i(K)]_{\vec{\sigma}, \vec{\sigma}'}$ adds an interaction between sites σ_i and σ_{i+1} (on the same row k) with Boltzmann weight $\exp(K \sigma_i \sigma_{i+1})$. On the contrary, $[Q_i(L)]_{\vec{\sigma}, \vec{\sigma}'}$ first creates a *new spin* σ_i in a new row $k + 1$, and then produces an interaction between σ_i and the old spin σ'_i (on row k), with Boltzmann weight $\exp(L \sigma_i \sigma'_i)$. With the expression "old spin" we mean a site over which we are not going to apply these operators anymore, because it became now a "bulk" spin. Combining (B.1) and (B.2) (for i ranging from 1 to N) in a smart way, we then obtain the row-to-row transfer matrix of the model.

In the same fashion, a corner transfer matrix adds an entire quadrant to the lattice. We will just need four of these objects: in the thermodynamic

B. Corner Transfer Matrix

limit, they will cover the entire plain. CTMs can be defined in general for models with short-range interaction, but for the sake of clarity we will restrict ourselves to a square lattice model with interactions round faces (also known as IRF models). The eight vertex model enters in this class, because it's equivalent to a model with diagonal and nearest neighbour interactions. Let's associate to each site of the lattice a spin σ_i , whose possible values are $\sigma_i = \pm 1$ for simplicity. The IRF models, by definition, have interactions between spins that lay on the same face, so the Hamiltonian H can be written as a sum of terms ϵ involving only spins on the same face, that is:

$$H = \sum_{\text{faces}} \epsilon(\sigma_i, \sigma_j, \sigma_k, \sigma_l) \quad (\text{B.3})$$

Here the subscripts (i, j, k, l) refers to the sites surrounding counterclockwise a given face, see Fig. B.1a. Let's denote with $\{\sigma\}$ the set of all the spins of the lattice, and $\beta = 1/(kT)$. Thanks to the form (B.3) of the energy, the partition function is:

$$\begin{aligned} Z &\equiv \sum_{\{\sigma\}} e^{-\beta H(\{\sigma\})} \\ &= \sum_{\{\sigma\}} \prod_{\text{faces}} w(\sigma_i, \sigma_j, \sigma_k, \sigma_l) \end{aligned} \quad (\text{B.4})$$

where the sum is over all the spin configurations of the lattice, the product is over all the faces of the lattice, and the Boltzmann weight are:

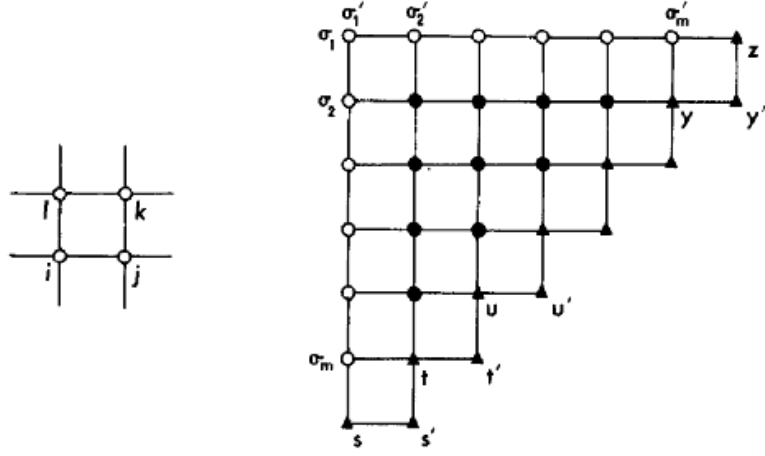
$$w(\sigma_i, \sigma_j, \sigma_k, \sigma_l) = e^{-\beta \epsilon(\sigma_i, \sigma_j, \sigma_k, \sigma_l)} \quad (\text{B.5})$$

Consider now the lattice in Fig. B.1b, which has the shape of a quadrant of the lattice in Fig. B.2, and let's evaluate its partition function. Label the left-hand spins with $\vec{\sigma} = \{\sigma_1, \sigma_2, \dots, \sigma_m\}$, and the top ones with $\vec{\sigma}' = \{\sigma'_1, \sigma'_2, \dots, \sigma'_m\}$. It is clear from the figure that $\sigma_1 = \sigma'_1$, and with the numbers (j) , $(j)'$ we indicate the boundary spins. The CTM of this quadrant is then defined as its partition function:

$$A_{\vec{\sigma}, \vec{\sigma}'} = \begin{cases} \sum_{\{\sigma\}} \prod_{\text{faces}} w(\sigma_i, \sigma_j, \sigma_k, \sigma_l) & \text{if } \sigma_1 = \sigma'_1 \\ 0 & \text{if } \sigma_1 \neq \sigma'_1 \end{cases} \quad (\text{B.6})$$

Note that $A_{\vec{\sigma}, \vec{\sigma}'}$ is a function of $\vec{\sigma}$ and $\vec{\sigma}'$: we are not summing over this indices, as well as over the boundary conditions, which we suppose to be fixed to their ground state values. Let's now define the corner transfer matrices $B_{\vec{\sigma}, \vec{\sigma}'}$, $C_{\vec{\sigma}, \vec{\sigma}'}$ and $D_{\vec{\sigma}, \vec{\sigma}'}$ as in Fig. B.2, where the spins $\vec{\sigma}'$ of each CTM can be reached from $\vec{\sigma}$ circling counterclockwise on the lattice. The matrices product

$$A_{\vec{\sigma}, \vec{\sigma}'} B_{\vec{\sigma}', \vec{\sigma}''} C_{\vec{\sigma}'', \vec{\sigma}'''} D_{\vec{\sigma}''', \vec{\sigma}}$$



(a) A Boltzmann weight.

(b) The CTM A.

Figure B.1

is then the Boltzmann weight of the entire lattice (with fixed boundaries) and the partition function is:

$$Z = \sum_{\vec{\sigma}, \vec{\sigma}', \vec{\sigma}'', \vec{\sigma}'''} A_{\vec{\sigma}, \vec{\sigma}'} B_{\vec{\sigma}', \vec{\sigma}''} C_{\vec{\sigma}'', \vec{\sigma}'''} D_{\vec{\sigma}''', \vec{\sigma}} \quad (\text{B.7})$$

where the summation is subjected to the condition $\sigma_1 = \sigma'_1 = \sigma''_1 = \sigma'''_1$. But this can be ignored thanks to the definition (B.6), and so we have:

$$Z = \text{Tr } ABCD \quad (\text{B.8})$$

Let's now define other classes of CTMs. Denote with \vec{s} the spins in the ground state of the model. If we set

$$\alpha = A_{\vec{s}, \vec{s}'} \quad \beta = B_{\vec{s}', \vec{s}''} \quad (\text{B.9})$$

$$\gamma = C_{\vec{s}'', \vec{s}'''} \quad \delta = D_{\vec{s}''', \vec{s}} \quad (\text{B.10})$$

then we have the *normalized* CTMs M_n (where M is one of the four matrices):

$$A_n = \alpha^{-1} A \quad B_n = \beta^{-1} B \quad (\text{B.11})$$

$$C_n = \gamma^{-1} C \quad D_n = \delta^{-1} D \quad (\text{B.12})$$

normalized in the sense that their ground state elements $(M_n)_{\vec{s}, \vec{s}}$ are unity. We can also define the *diagonal* CTMs M_d as:

$$A_n = \alpha' P A_d Q^{-1} \quad B_n = \beta' Q B_d R^{-1} \quad (\text{B.13})$$

$$C_n = \gamma' R C_d T^{-1} \quad D_n = \delta' T D_n P^{-1} \quad (\text{B.14})$$

where the factors α' , β' , γ' and δ' ensures that the maximum values of the diagonal matrices M_d are unity.

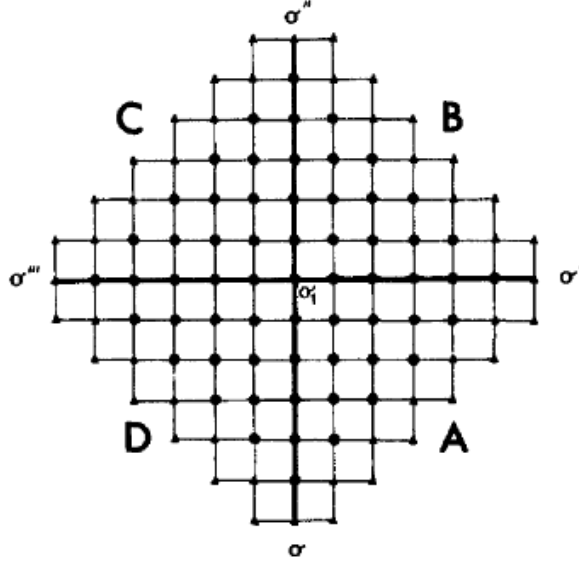


Figure B.2: The lattice with partition function (B.7)

All these sets of CTMs have the property that they do not change the expectation value of the observables. For example, the mean value of the spin, say, σ_1 over the lattice is:

$$\begin{aligned} \langle \sigma_1 \rangle &= \frac{1}{Z} \sum_{\{\sigma\}} \sigma_1 \prod_{\text{faces}} w(\sigma_i, \sigma_j, \sigma_k, \sigma_l) \\ &= \frac{\text{Tr}(SABCD)}{\text{Tr}(ABCD)} \end{aligned} \quad (\text{B.15})$$

where $S = \begin{pmatrix} 1 & 0 \\ 0 & -1 \end{pmatrix}$. Thanks to the cyclicity of the traces, we can make the substitution $M \rightarrow M_n \rightarrow M_d$ without affecting the result.

Now, if the model is isotropic and reflection-symmetric, and is ferromagnetic (so the boundary spins can be chosen to be equal), then all the CTMs are equal and symmetric. If otherwise we have the symmetry:

$$w(a, b, c, d) = w(c, b, a, d) = w(a, d, c, b) \quad (\text{B.16})$$

(where a, b, c and d are the value of the spins surrounding a face) the CTMs are still symmetric, and satisfy $C = A, B = D$. Thanks to the symmetry of the CTMs, we can set

$$M_n = \mu' P M_d P^{-1} \quad (\text{B.17})$$

where P is an orthonormal matrix that diagonalize all the CTMs.

To conclude this section, let's define the *face operators* as:

$$(U_i)_{\vec{\sigma}, \vec{\sigma}'} = \delta_{\sigma_1, \sigma'_1} \cdots \delta_{\sigma_{i-1}, \sigma'_{i-1}} w(\sigma_i, \sigma_{i+1}, \sigma'_i, \sigma'_{i+1}) \delta_{\sigma_{i+1}, \sigma'_{i+1}} \cdots \delta_{\sigma_m, \sigma'_m} \quad (\text{B.18})$$

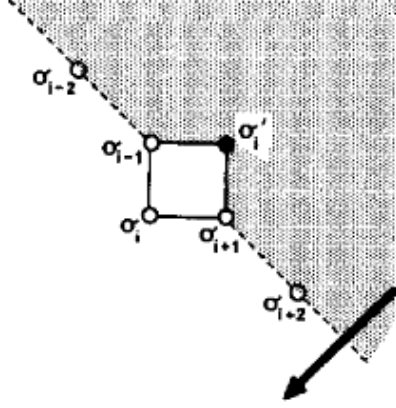


Figure B.3: The effect of the face operator (B.18) on the preexistent sites of the lattice. The old site is σ'_i .

These operators create a new face to the lattice: first they add a new spin σ_i , going in the NE to SW direction (see Fig. B.3), and then they link it with the rest of the lattice through an interaction round faces with Boltzmann weight $w(\sigma_i, \sigma_{i+1}, \sigma'_i, \sigma_{i-1})$. Since our CTM A is built by faces of spins, we expect that it can be written in term of these operators. To do this, we need to define face operators involving boundary spins, and we have two types of these faces. One contains one boundary of spin s , and will be "created" by the operator

$$(U_m^s)_{\vec{\sigma}, \vec{\sigma}'} = \delta_{\sigma_1, \sigma'_1} \dots \delta_{\sigma_{m-1}, \sigma'_{m-1}} w(\sigma_m, s, \sigma'_m, \sigma_{m-1}) \quad (\text{B.19})$$

The other will contain three boundary spins, whose value is s , t and z respectively, and its associated face operator is:

$$(U_{m+1}^{stz})_{\vec{\sigma}, \vec{\sigma}'} = \delta_{\sigma_1, \sigma'_1} \dots \delta_{\sigma_m, \sigma'_m} w(s, t, z, \sigma_m) \quad (\text{B.20})$$

We will label the boundary spins with numbers (j) and $(j)'$, which means that they lay in the same row of σ_j , and the prime indicates the spin on the right. There is only one spin at "row" 1, denoted in a obvious way as (1). Paying now attention to the positions of all the face operators, the CTM A is easy to construct. It is given by:

$$A = \mathcal{F}_2^{(m+1)(m+1)'(m)} \mathcal{F}_3^{(m)(m)'(m-1)} \dots \mathcal{F}_{m+1}^{(2)(2)'(1)} \quad (\text{B.21})$$

where

$$\mathcal{F}_j^{(m+3-j)(m+3-j)'(m+2-j)} = U_{m+1}^{(m+3-j)(m+3-j)'(m+2-j)} U_m^{(m+1)} U_{m-1} U_{m-2} \dots U_j \quad (\text{B.22})$$

As a simple case, for $m = 2$ we have:

$$A = U_3^{(3)(3)'(2)} U_2^{(2)} U_3^{(2)(2)'(1)} \quad (\text{B.23})$$

B.2 The eight vertex model

Consider a lattice with sites and edges, and let's synthesize the interaction between two adjacent sites in a graphical way with an *arrow*, that can point towards one or the other site respectively. For the sake of clarity, consider an ice cube, which is modeled in the following way. Each site contains an Oxygen atom, and the Hydrogen atoms are placed on the edges. Suppose that each edge can host only one Hydrogen atom. We then have two situations: the *H* atom, due to electrical attraction, may seat nearer to one or the other *O* atom, and these possibilities will be represented with an arrow that points towards one or the other site. Here, the arrow is simply describing the electric dipole between two opposite charges. If we further require that only 0 or 2 Hydrogen atoms

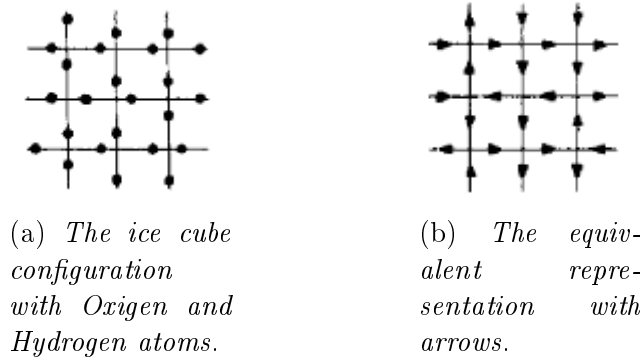


Figure B.4: A modelization of the ice cube

can lie in the neighbour of an Oxygen atom, we have then defined the ice type model, known as well as the *six vertex model*, because only six vertex configurations are allowed. The *eight vertex model* is a generalization of this, and the allowed vertex configurations are represented in Fig. B.5. We will here focus on the "zero field" eight vertex model: if we denote with $w(a, b, c, d)$ the Boltzmann weight of a vertex configuration, only four of these are independent, and are denoted as

$$\begin{cases} w(+, +|+, +) = w(-, -|-,-) \equiv a \\ w(+, -|-+, +) = w(-, +|+, -) \equiv b \\ w(+, -|+, -) = w(-, +|-, +) \equiv c \\ w(+, +|-, -) = w(-, -|+, +) \equiv d \end{cases} \quad (\text{B.24})$$

Moreover, if ϵ_α (for $\alpha = a, b, c, d$) is the energy of a vertex, these weights can be written as:

$$a = e^{-\beta\epsilon_a} \quad (\text{B.25})$$

and so on. Let's now define the *Jacobi elliptic functions* $\text{sn}(u, k)$, $\text{cn}(u, k)$ and $\text{dn}(u, k)$ as a generalization of the trigonometric functions, such that they

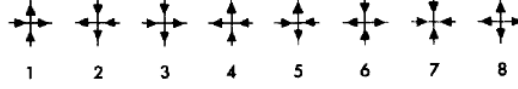


Figure B.5: The vertex configurations allowed by the eight vertex model.

satisfy:

$$\operatorname{sn}^2 u + \operatorname{cn}^2 u = 1 \quad \operatorname{sn}^2 u + k^2 \operatorname{dn}^2 u = 1 \quad (\text{B.26})$$

These are real if $0 \leq k \leq 1$, and if it's clear the value of k from the context, we simply write, for example, $\operatorname{sn} u$. Denoting with $f(u)$ one of the elliptic functions, these have the important property:

$$\begin{cases} f(u + 2I(k)) = \pm f(u) \\ f(u + 2iI(k')) = \pm f(u) \end{cases} \quad (\text{B.27})$$

where the sign \pm depends on which one we are considering. This means that elliptic functions are *double periodic* on the complex plane, with periods $4I$ and $4I'$, where

$$I(k) = \int_0^{\frac{\pi}{2}} \frac{d\theta}{\sqrt{1 - k'^2 \sin^2 \theta}} \quad (\text{B.28})$$

is the complete elliptic integral of first kind, of argument k , and $k' = \sqrt{1 - k^2}$. Let's define in a similar fashion the function $\operatorname{snh} u = -i \operatorname{sn} iu$, which is the analog of the iperbolic function $\sinh u = -i \sin iu$. A series expansion of all these functions can be found in chapter 15 of [3]. The Boltzmann weights of the eight vertex model can then be parametrized in terms of entire functions as:

$$\begin{cases} a = \rho \operatorname{snh}(\lambda - u) \\ b = \rho \operatorname{snh} u \\ c = \rho \operatorname{snh} \lambda \\ d = \rho k \operatorname{snh} \lambda \operatorname{snh} u \operatorname{snh}(\lambda - u) \end{cases} \quad (\text{B.29})$$

We now want to give a sketch, without proving every passage (the demonstration is quite lengthy), of the derivation of the CTMs for the eight vertex model. First, note that this model can be described as a "IRF model". To see this, replace the arrows with spins, the arrow pointing left/right corresponding to spins having value $\sigma = +1, -1$ respectively: we can then consider the Boltzmann weight $w(a, b, c, d)$ of a vertex as a Boltzmann weight of a face. Since these weights satisfy (B.16), the CTMs will be symmetric and $A = C$, $B = D$. Furthermore, this implies that:

$$A_n(\lambda - v) = B_n(v) \quad (\text{B.30})$$

Using (B.17), let's write

$$A_d(u) = \frac{P^{-1} A_n(u) P}{a_1(u)} \quad (\text{B.31})$$

B. Corner Transfer Matrix

with $a_1(u)$ the highest eigenvalue of $A_n(u)$. Thanks to these symmetry properties, the diagonal matrix $A_d(u)$ satisfies

$$A_d(u)A_d(v) = X_d(u + v - \lambda) \quad (\text{B.32})$$

where X_d is another diagonal matrix. Due to the dependence on $u + v$ of X_n , if we take $\frac{\partial}{\partial \log x}$ and $\frac{\partial}{\partial \log y}$ separately on this equation, and then compare the results, we have that the elements of $A_d(u)$ must have the form:

$$[A_d(u)]_{r,r} = m_r \exp(-\alpha_r u) \quad (\text{B.33})$$

and it can be shown, by other means, that the m_r must all be equal to 1. Now, the CTMs are functions of the Boltzmann weights of the faces of the lattices, and these are double periodic thanks to (B.29). Because they are real quantities, we have $u \in i\mathbb{R}$, so $A_d(u)$ is periodic along the complex line, with period $4iI$. We then have:

$$[A_d(u)]_{r,r} = \exp\left(-\frac{\pi n_r u}{2I}\right) \quad (\text{B.34})$$

The integers n_r can be determined in the limit $k \rightarrow 0$, while leaving the other parameters fixed. The Boltzmann weight will tend to:

$$\begin{cases} w(a, b, a, b) \rightarrow \frac{1}{2}\rho \exp\left(\frac{\pi\lambda}{2I}\right) \\ w(a, b, -a, -b) \rightarrow 0 \\ w(a, b, a, -b) \rightarrow \frac{1}{2}\rho \exp\left(\frac{\pi(u-\lambda)}{2I}\right) \\ w(a, b, -a, b) \rightarrow 0 \end{cases} \quad (\text{B.35})$$

and so the face operators (B.18) will be diagonal:

$$(U_i)_{\vec{\sigma}, \vec{\sigma}'} = \delta(\sigma_1, \sigma'_1) \dots \delta(\sigma_m, \sigma'_m) \frac{1}{2}\rho \exp\left(\frac{2\lambda - \pi u(1 - \sigma_{i-1}\sigma_{i+1})}{4I}\right) \quad (\text{B.36})$$

Thanks to (B.21), $A(u)$ is diagonal as well, and to recover $A_d(u)$ we simply need to divide all the elements of $A(u)$ by $\exp(\lambda/(2I))$ (we have to normalize the maximum entry by 1). Performing the matrix products in (B.21), and omitting the Kronecker deltas for clarity, we have:

$$\begin{aligned} [A_d(u)]_{\vec{\sigma}, \vec{\sigma}'} &= \exp\left[-\pi u \sum_{i=2}^{m+1} \frac{(i-1)(1 - \sigma_{i-1}\sigma_{i+1})}{4I}\right] \\ &\equiv s^{\sum_{i=2}^{m+1} (i-1)(1 - \sigma_{i-1}\sigma_{i+1})/2} \end{aligned} \quad (\text{B.37})$$

where we defined $s = \exp\left(-\frac{\pi u}{2I}\right)$. With respect to the top spins of Fig. B.1b, the spin σ_{m+1} is (1), while σ_{m+2} is (2)'. It is important to notice that this

formula for $A_d(u)$, in the limit $m \rightarrow \infty$, is valid only in the *ferromagnetic ordered phase*: this means that $A_d(u)$ will have a finite value only if there exist j such that

$$\sigma_i = 1 \text{ for } i > j \quad \text{OR} \quad \sigma_i = -1 \text{ for } i > j \quad (\text{B.38})$$

Furthermore, this makes evident that the boundary conditions are effectively *open boundary conditions*.

We are now ready to put these CTMs in their final form: this is an infinite tensor product of matrices. For A_d and C_d , we have

$$A_d(u) = C_d(u) = \begin{pmatrix} 1 & 0 \\ 0 & s \end{pmatrix} \otimes \begin{pmatrix} 1 & 0 \\ 0 & s^2 \end{pmatrix} \otimes \begin{pmatrix} 1 & 0 \\ 0 & s^3 \end{pmatrix} \otimes \dots \quad (\text{B.39})$$

Remembering (B.30), and setting $t = \exp\left(-\frac{\pi(\lambda-u)}{2l}\right)$, we have instead for B_d and D_d :

$$B_d(u) = D_d(u) = \begin{pmatrix} 1 & 0 \\ 0 & t \end{pmatrix} \otimes \begin{pmatrix} 1 & 0 \\ 0 & t^2 \end{pmatrix} \otimes \begin{pmatrix} 1 & 0 \\ 0 & t^3 \end{pmatrix} \otimes \dots \quad (\text{B.40})$$

This notations means the following. The matrix elements of $A_d(u)$ are labelled with $(\vec{\sigma}, \vec{\sigma}')$ as above. The first matrix of (B.39) concerns with σ_1 and σ'_1 , and in general the n -th matrix deals with σ_n and σ'_n . Then, label the elements of these 2×2 matrices with (σ_1, σ'_1) (where the value +1 stands for the first row and the first column), and select the element corresponding to these spin values (σ_1, σ'_1) . Do this for all the 2×2 matrices, and take the product of all the elements selected: this will give the value $[A_d(u)]_{\vec{\sigma}, \vec{\sigma}'}$. The reader may convince himself that this infinite matrix product is equivalent to (B.37).

B. Corner Transfer Matrix

Appendix C

Numerical data

This section involves the description of the DMRG algorithm, first introduced by White in [34], which is actually the most powerful one for the realization of numerical simulations. We then briefly describe the C++ program that implements the algorithm and we report the data obtained by the simulations.

C.1 The DMRG algorithm

C.1.1 Density-Matrix approach

In the standard renormalization group approach (see chapter 1) one starts with a spin chain, and breaks it into identical blocks, denoted by B . Let H_B be the Hamiltonian describing a single block, which doesn't involve interactions with other blocks. Consider, for example, the Heisenberg model, whose Hamiltonian is

$$H = \sum_i \vec{S}_i \cdot \vec{S}_{i+1} \quad (\text{C.1})$$

If at the beginning each B is made by just one spin, we have $H_B = 0$. The next step consists in embodying two neighbour blocks in a bigger block $B' = BB$, and taking into account the interactions between these blocks. In the Heisenberg model, for example, only the neighbour spins interact, and if each block consists in a number n of spins then, eventually, only the neighbouring spins, set in the edges of the two blocks respectively, may interact through (C.1). This means that, instead of diagonalizing the Hamiltonian of the whole spin chain, we are studying "smaller" systems which are ensembled together step by step: the idea is then to find a proper number of states that best describe the Hamiltonian $H_{B'}$, instead of keeping all the states, otherwise the number of states would be too large to perform any kind of calculations.

The main problem of this approach is how to consider the interaction of the blocks with the rest of the system: in each step the Hamiltonians $B' = BB$ of each pair of blocks do not involve the rest of the system in which they

C. Numerical data

are embedded, and this rebounds in important numerical errors after each step. Some temptatives to fix this inconvenient have been made, such as the "combination of boundary conditions" (CBC) approach (see [36]). This consist in varying the boundary conditions of each block of spins in a suitable manner, so to simulate the quantum fluctuations of the whole spin chain: the authors spoke about a complete set of boundary conditions to be found case by case. But in more than one cases it's impossible to find a satisfactory set of such boundary conditions.

The best way to describe a system as being part of a universe is to consider its density matrix. If the system is isolated we simply talk of density matrix, while if this is embedded in a larger environment we invoke the more general concept of *reduced density matrix* (see appendix A), which describes completely the interaction between the system and the environment. This is the basic idea of the DMRG algorithm.

The density matrix approach assumes the knowledge of the wave function of the whole spin chain (which typically describes the ground state), also called *target state*. Consider a subsystem of our spin chain, formed by two blocks BB . Denote with $\{|i\rangle\}$ a base of BB (whose dimension is l), and let $\{|j\rangle\}$ describe the rest of the spin chain. Then we can write

$$|\psi\rangle = \sum_{i,j} \psi_{i,j} |i\rangle |j\rangle \quad (\text{C.2})$$

We need to define a procedure for producing a set of states

$$|u^\alpha\rangle \quad \alpha = 1, \dots, M \quad (\text{C.3})$$

that describe the subsystem BB in the best way. Here M is the maximum number of states we use to describe BB , also denoted *DMRG states*. Of course, we can't reproduce exactly $|\psi\rangle$ if $M < l$, but we may construct a wave function

$$|\bar{\psi}\rangle = \sum_{\alpha,j} a_{\alpha,j} |u^\alpha\rangle |j\rangle \quad (\text{C.4})$$

which best represents $|\psi\rangle$ if the quantity

$$S \equiv \|\psi - \psi_{\text{dmrg}}\|^2 \quad (\text{C.5})$$

is minimized. It can be shown (see [34]) that the set of states $\{|u^\alpha\rangle\}$ minimizing S are eigenstates of the reduced density matrix ρ describing BB , and corresponds to the M largest eigenvalues of ρ . This is a general result, no matter if $|\psi\rangle$ is in a pure or mixed state.

We know that the set of eigenvalues $\{w_\alpha\}$ of ρ satisfies

$$\sum_{\alpha} w_{\alpha} = 1$$

This suggests the following: a good way to determine how large should be the number M of DMRG states is by requiring that the quantity

$$D = 1 - \sum_{\alpha=1}^M w_{\alpha} \tag{C.6}$$

should be reasonably small.

Once we have constructed the wave function of BB , we then consider bigger blocks B' that englobe the previous B , and repeat the procedure until we eventually cover the whole size of the system. Furthermore, each eigenstate of the reduced density matrix describes how the block BB is entangled with the spin chain, that is it describes the connection between BB and the rest of the systems: this is why we need to consider smaller blocks B and add them together.

C.1.2 Density-Matrix algorithm

Indeed, if we want to reproduce this reasoning in a numerical algorithm, we can't use the wave function describing the whole system, because typically it is not known. What we can do is to diagonalize a *larger systems*, called superblock, containing the two blocks B . A density-matrix algorithm is defined mainly by the form of this systems, the target space used, and the manner in which the blocks are enlarged. Let's define the blocks B_i^L and B_i^R , where the

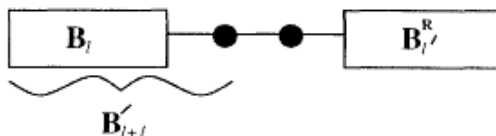


Figure C.1: Spin-block configuration.

superscripts L and R denote the left or the right block respectively, and the subscript counts the number of spins contained by the blocks. In our case, we won't double the blocks, that is $B' = BB$, but instead we add a single site to each block: $B' = B + \text{site}$. We won't explain here all the advantages of this choice, see [35] for further details. Figure C.1 shows the spin-block configuration at each passage of the algorithm. The superblock is then composed by B_i^L , B_i^R and the two spins in figure. As described in [34], the passage of the DMRG algorithm are the following:

1. Make four initial blocks, each consisting of a single site, representing the initial four site system.
2. Diagonalize the superblock Hamiltonian to find the target state.

C. Numerical data

3. Form the reduced density matrix for the two-block system, formed by $B_2^L = B_1^L + \text{site}$ and $B_2^R = B_1^R + \text{site}$ (in general $B_{i+i}^{L/R} = B_i^{L/R} + \text{site}$).
4. Diagonalize the reduced density matrix and keep the m largest eigenvalues with associated eigenvectors: these will describe the block B_{i+i}^L . We take as the block B_{i+1}^R the *reflection* of block B_{i+1}^L .
5. Add two spins as in figure C.1, and go to step 2.

In principle this process could continue to infinity, but in practice, after a certain number of iteration which depend on the correlation length of the system, the main properties of the system (such as the energy or the entanglement entropy) don't vary appreciably anymore, and at that point one can stop the process: this means that the chain obtained is simulating nicely the infinite chain.

C.1.3 The DMRG program

Here we just give a few notions of the program used to implement the DMRG simulations.

Among other data, the input of the DMRG program requires:

- A number M_{\min} that imposes the minimum number of DMRG states to be taken in the construction of ψ_{dmrg} ;
- A number M_{\max} which instead represents the maximum number of DMRG states;
- The number D of condition (C.6).
- The length of the spin chain L_{\max} , that is the number of spins.
- Two numbers describing how many sweeps (see below) should the program perform, and at which length of the subsystem the program begins to perform these sweeps.

The program starts from a number of spins $L = 4$, and adds two spins after each step, until L_{\max} is reached: this implies that L_{\max} must be even. Initially the two blocks B^L and B^R consist in one spin, as described in the previous section.

Before adding to the superblock $B_i^L B_i^R$ the two spins, the program may eventually perform some *sweeps*. These consists in removing one spin from, say, B_i^L and attach it to B_i^R , so to create the superblock $B_{i-1}^L B_{i+1}^R$: again we calculate the reduced density matrix and the states describing the left block, which is our reference block. This operation is repeated until B^L has approximately 10 spins, and then the operation is reversed, removing spins from B^R and attaching them to B^L . When the two blocks B^L and B^R have

again the same number of spins, the "sweep" is completed. This improves the precision of the final data, even if the reason for this fact is still not clear.

At each passage of the algorithm, the new wave function ψ_{dmrg} , describing B^L , must satisfy

$$1 - \sum_{\alpha=1}^M w_{\alpha} < D \tag{C.7}$$

where w_{α} , as already explained, are the eigenvalues of the reduced density matrix ρ describing B^L .

After each step, the program makes one of the following choices. To construct ψ_{dmrg} we use a number of states M which possibly satisfy the condition (C.6). If $M < M_{\text{min}}$, then the wave function is built using exactly $M = M_{\text{min}}$ states. If there doesn't exist any value $M < M_{\text{max}}$ such that (C.6) is true, then the algorithm takes $M = M_{\text{max}}$ states. Otherwise, the algorithm takes the first value M , between the two edges, that satisfy (C.6). If, at last, we have $M_{\text{min}} = M_{\text{max}}$, then $M = M_{\text{min}} = M_{\text{max}}$ at each passage.

At last, one can ask the program to send in output several quantities, for example energies, entanglement entropies, entanglement spectrum, and mean values of various quantities, such as the spin along a certain direction.

C.2 Simulations for constant l

Here we report (from table C.2 to table C.15) all the data obtained by the simulations performed for constant l , in the sector

$$J_y > 1 \quad -1 < J_z < 1 \tag{C.8}$$

and we remind the definition of l (see (3.135)):

$$l = \sqrt{\frac{1 - J_z^2}{J_y^2 - J_z^2}} \tag{C.9}$$

We performed simulations according to the following values of l :

$$l = 0.25, 0.35, 0.4, 0.45, 0.5, 0.6, 0.7 \tag{C.10}$$

The number of "DMRG states" used to construct ψ_{dmrg} lied between $N_{\text{min}} = 50$ and $N_{\text{max}} = 200$; furthermore, $D = 10^{-8}$ and $L_{\text{max}} = 90$. All the entropies are evaluated with logarithms in base 2, because this is the basis used by the DMRG program. We always applied, to one site of the spin chain, a magnetic field along the y axis, of magnitude

$$h = 0.0001$$

This is to split the two existing ground states (see discussion in section 4.2).

The tables relative to a certain value of l are gathered together. For each value of l , we have:

C. Numerical data

- A table where we plotted all the values (J_y, J_z) used to perform the numerical simulations. Here J_z is treated as the independent variable, and J_y is computed according to (C.9).
- The Schmidt gap as a function of J_z , that is the difference between the largest and the next-largest eigenvalues.
- Two tables, representing respectively the value of the entanglement entropy $S(J_z, l)$ computed by the program, and the entanglement entropy computed by the exact formula (3.124). We remark the very good agreement between numerical and exact data, even though we applied a (small but nonzero) magnetic field.
- The entanglement spectrum for each couple (J_y, J_z) , always specified in the relative table. We kept only the eigenvalues greater than 10^{-16} , because the "machine precision" is about 10^{-15} . Even the eigenvalues of this order are not reliable: indeed, we can hardly find degenerations of eigenvalues at order 10^{-15} . Below this value the DMRG saves a huge number of eigenvalues that form a "continuum" down to about 10^{-20} : these values are certainly not reliable, so we do not report them.

C.3 Simulations around the circles

In this section we show (from table C.16 to table C.21) the results obtained by the simulations performed on the circles parametrized by

$$\begin{cases} J_y = 1 + r \sin \alpha \\ J_z = 1 - r \cos \alpha \end{cases} \quad (\text{C.11})$$

for the values

$$r = 0.96, 0.97, 0.98 \quad (\text{C.12})$$

For each value of r we have two tables. The first one depicts the values of J_y and J_z used for the numerical simulations. The other one shows the values of the entanglement entropy obtained from the exact formula and from the numerical simulations, as well as the DMRG parameters (see section 4.3.2) used in each simulation, under the column "type".

Notice the following: in certain simulations we used values of (J_y, J_z) which were very close to the critical line. This implied that the value of the entropy may have converged, in some case, only for a huge number of spins in the chain: for this reason, we used such high values for L_{\max} . Let's explain this in a better way.

In column "type" of the tables we put in round brackets the number L of sites corresponding to the value of the entanglement entropy S_{DMRG} reported. In fact the DMRG program, increasing the number of sites, gives at some point

Table C.1: $r = 0.02$: Values of the entropies.

L	S_{DMRG}
200	0.228886240228
202	0.228879294565
204	0.228875349080
206	0.228875295600
208	0.228869337533
210	0.228866288713
212	0.228867026761
214	0.228861814841
216	0.228859443283
218	0.228860778550
220	0.228856130471

a value of S_{DMRG} that best represents the value of S in the limit $L \rightarrow \infty$. As we saw in section 4.2 (see figure 4.2b), first the entropy increases, it reaches a maximum, and then decreases monotonically towards a value S_{theor} , that may be predicted theoretically. But for a certain value of L this entropy starts to *oscillate*: there is a number of digits that don't vary, while the others may increase or decrease randomly. In the case of the simulations for constant l we didn't mention these oscillations because they were negligible (typically at order 10^{-12}). This situation is represented in table C.1, where we plotted the values of the entropies given by the DMRG program as a function of the size L of the spin chain, corresponding to:

$$r = 0.98 \qquad J_y = 1.002610523844 \qquad J_z = 0.9801711028 \qquad (\text{C.13})$$

Here the entropy decreases up to the value $L = 210$, after which it starts oscillating. In each simulation performed, we took the value of the entropy corresponding to the size L before which S_{DMRG} begins its oscillations, in this case to $L = 210$. If there is no value under round brackets, we took the value of S_{DMRG} corresponding to L_{max} .

For the parameters (C.13) the agreement between theoretical and numerical results is good, up to 4 digits, but not excellent (see the tables below); the agreement improves by moving away from the critical line.

C. Numerical data

Table C.2: $l = 0.25$

(a) J_z and J_y values for simulation

J_z	J_y
0.5	3.5
0.6	3.2557641
0.7	2.9410882
0.8	2.5298221
0.9	1.9621417
0.95	1.5692355
0.98	1.2625371

(b) Schimdt gap as a function of J_z .

J_z	S
0.5	0.997255524040
0.6	0.997923911443
0.7	0.998514687860
0.8	0.999040766679
0.9	0.999512774952
0.95	0.999732097652
0.98	0.999861072803

(c) Von Neumann Entropy $S(J_z, l)$ from numerical data.

J_z	S
0.5	0.015057025216
0.6	0.011803444757
0.7	0.008800369296
0.8	0.005984089290
0.9	0.003276682161
0.95	0.001917026574
0.98	0.001059845581

(d) Von Neumann Entropy $S(J_z, l)$ from the exact formula.

J_z	S
0.5	0.01505702507
0.6	0.01180344476
0.7	0.008800369295
0.8	0.00598408929
0.9	0.003276682161
0.95	0.001917026575
0.98	0.0010598455812

C.3. Simulations around the circles

Table C.3: $l = 0.25$ entanglement spectrum.

$J_y = 3.5$ $J_z = 0.5$	$J_y = 3.2557641$ $J_z = 0.6$	
$9.986268179140 \cdot 10^{-01}$ $1.371293874288 \cdot 10^{-03}$ $1.883032625348 \cdot 10^{-06}$ $2.585741295973 \cdot 10^{-09}$ $2.585734088540 \cdot 10^{-09}$ $3.550628872635 \cdot 10^{-12}$ $3.550535618713 \cdot 10^{-12}$ $4.935291161068 \cdot 10^{-15}$ $4.914771109798 \cdot 10^{-15}$ $4.876814878059 \cdot 10^{-15}$ $1.017995958292 \cdot 10^{-15}$	$9.989614158338 \cdot 10^{-01}$ $1.037504391023 \cdot 10^{-03}$ $1.077534463610 \cdot 10^{-06}$ $1.119108764941 \cdot 10^{-09}$ $1.119104057236 \cdot 10^{-09}$ $1.162259098212 \cdot 10^{-12}$ $1.162068952302 \cdot 10^{-12}$ $1.989709123934 \cdot 10^{-15}$ $1.476791191750 \cdot 10^{-15}$ $1.370261818168 \cdot 10^{-15}$	
$J_y = 2.9410882$ $J_z = 0.7$	$J_y = 2.5298221$ $J_z = 0.8$	
$9.992570677514 \cdot 10^{-01}$ $7.423798909343 \cdot 10^{-04}$ $5.515376522404 \cdot 10^{-07}$ $4.097547438435 \cdot 10^{-10}$ $4.097539503194 \cdot 10^{-10}$ $3.044138339756 \cdot 10^{-13}$ $3.044100003982 \cdot 10^{-13}$ $1.490815921691 \cdot 10^{-15}$ $1.269093176625 \cdot 10^{-15}$	$9.995202682129 \cdot 10^{-01}$ $4.795015343334 \cdot 10^{-04}$ $2.300320728298 \cdot 10^{-07}$ $1.103535732268 \cdot 10^{-10}$ $1.103533240164 \cdot 10^{-10}$ $5.294409472305 \cdot 10^{-14}$ $5.291598120734 \cdot 10^{-14}$ $1.121229590792 \cdot 10^{-15}$	
$J_y = 1.9621417$ $J_z = 0.9$	$J_y = 1.5692355$ $J_z = 0.95$	$J_y = 1.2625371$ $J_z = 0.98$
$9.997563577880 \cdot 10^{-01}$ $2.435828359919 \cdot 10^{-04}$ $5.934705201648 \cdot 10^{-08}$ $1.445923431165 \cdot 10^{-11}$ $1.432202335705 \cdot 10^{-11}$ $3.746302224271 \cdot 10^{-15}$ $3.600001111242 \cdot 10^{-15}$	$9.998660398519 \cdot 10^{-01}$ $1.339422003252 \cdot 10^{-04}$ $1.794291548702 \cdot 10^{-08}$ $2.403620163220 \cdot 10^{-12}$ $2.403413731795 \cdot 10^{-12}$ $1.732850402985 \cdot 10^{-15}$ $1.125728349574 \cdot 10^{-15}$	$9.999305339887 \cdot 10^{-01}$ $6.946118527233 \cdot 10^{-05}$ $4.825189638050 \cdot 10^{-09}$ $3.351287444326 \cdot 10^{-13}$ $3.349898223094 \cdot 10^{-13}$ $1.292905818465 \cdot 10^{-15}$

C. Numerical data

Table C.4: $l = 0.35$

(a) J_z and J_y values for simulation

J_z	J_y
0.5	2.5243710
0.6	2.3631525
0.7	2.1571429
0.8	1.8917652
0.9	1.5365612
0.95	1.3032338
0.98	1.1329895

(b) Schimdt gap as a function of J_z .

J_z	S
0.5	0.994330825351
0.6	0.995676342233
0.7	0.996868040435
0.8	0.997931843444
0.9	0.998890885049
0.95	0.999341843291
0.98	0.999614496856

(c) Von Neumann Entropy $S(J_z, l)$ from numerical data.

J_z	S
0.5	0.028186351065
0.6	0.022324583995
0.7	0.016888389693
0.8	0.011764003266
0.9	0.006803580126
0.95	0.004283919290
0.98	0.002657537920

(d) Von Neumann Entropy $S(J_z, l)$ from the exact formula.

J_z	S
0.5	0.02818635107
0.6	0.022324583995
0.7	0.016888389692
0.8	0.011764003266
0.9	0.006803580125
0.95	0.004283919290
0.98	0.002657537926

Table C.5: $l = 0.35$ entanglement spectrum.

$J_y = 2.5243710$ $J_z = 0.5$	$J_y = 2.3631525$ $J_z = 0.6$
$9.971613724005 \cdot 10^{-01}$	$9.978358242419 \cdot 10^{-01}$
$2.830547049683 \cdot 10^{-03}$	$2.159482009034 \cdot 10^{-03}$
$8.034804413615 \cdot 10^{-06}$	$4.673476768618 \cdot 10^{-06}$
$2.280762987760 \cdot 10^{-08}$	$1.011417434011 \cdot 10^{-08}$
$2.280762770168 \cdot 10^{-08}$	$1.011416407772 \cdot 10^{-08}$
$6.474159048802 \cdot 10^{-11}$	$2.188843117780 \cdot 10^{-11}$
$6.473759435556 \cdot 10^{-11}$	$2.188754769074 \cdot 10^{-11}$
$1.837217259306 \cdot 10^{-13}$	$4.735210216564 \cdot 10^{-14}$
$1.836981652180 \cdot 10^{-13}$	$4.714040491190 \cdot 10^{-14}$
$1.834211149953 \cdot 10^{-13}$	$4.653287860726 \cdot 10^{-14}$
$1.113095438047 \cdot 10^{-15}$	$1.094521271613 \cdot 10^{-15}$
$J_y = 2.1571429$ $J_z = 0.7$	$J_y = 1.8917652$ $J_z = 0.8$
$9.984327902256 \cdot 10^{-01}$	$9.989653859560 \cdot 10^{-01}$
$1.564749790587 \cdot 10^{-03}$	$1.033542512345 \cdot 10^{-03}$
$2.452285148175 \cdot 10^{-06}$	$1.069316452747 \cdot 10^{-06}$
$3.843230792317 \cdot 10^{-09}$	$1.106325257348 \cdot 10^{-09}$
$3.843224585259 \cdot 10^{-09}$	$1.106319817135 \cdot 10^{-09}$
$6.023015789257 \cdot 10^{-12}$	$1.144592978417 \cdot 10^{-12}$
$6.022838130864 \cdot 10^{-12}$	$1.144514305291 \cdot 10^{-12}$
$9.455276287559 \cdot 10^{-15}$	$1.684518948997 \cdot 10^{-15}$
$9.436505637753 \cdot 10^{-15}$	$1.593455630160 \cdot 10^{-15}$
$9.401174444697 \cdot 10^{-15}$	$1.451946651526 \cdot 10^{-15}$
$1.391490191667 \cdot 10^{-15}$	$1.345167869953 \cdot 10^{-15}$
$1.080836738172 \cdot 10^{-15}$	

C. Numerical data

$J_y = 1.5365612$ $J_z = 0.9$	$J_y = 1.3032338$ $J_z = 0.95$	$J_y = 1.1329895$ $J_z = 0.98$
$9.994452885872 \cdot 10^{-01}$	$9.996708674640 \cdot 10^{-01}$	$9.998072298313 \cdot 10^{-01}$
$5.544035383758 \cdot 10^{-04}$	$3.290241728504 \cdot 10^{-04}$	$1.927329756937 \cdot 10^{-04}$
$3.075338715282 \cdot 10^{-07}$	$1.082925469446 \cdot 10^{-07}$	$3.715306057973 \cdot 10^{-08}$
$1.705918443487 \cdot 10^{-10}$	$3.564192217792 \cdot 10^{-11}$	$7.165017677871 \cdot 10^{-12}$
$1.705914104591 \cdot 10^{-10}$	$3.564134169096 \cdot 10^{-11}$	$7.152991029390 \cdot 10^{-12}$
$9.459428583036 \cdot 10^{-14}$	$1.176507359572 \cdot 10^{-14}$	$2.068557389183 \cdot 10^{-15}$
$9.441708583341 \cdot 10^{-14}$	$1.169915475431 \cdot 10^{-14}$	$1.293343211254 \cdot 10^{-15}$
$1.499302365054 \cdot 10^{-15}$		$1.082761637969 \cdot 10^{-15}$
		$1.002461901748 \cdot 10^{-15}$

Table C.6: $l = 0.4$

(a) J_z and J_y values
for simulation

J_z	J_y
0.5	2.2220486
0.6	2.0880613
0.7	1.9176809
0.8	1.7
0.9	1.4133294
0.95	1.2295833
0.98	1.0990405

(b) Schimdt gap as a func-
tion of J_z .

J_z	S
0.5	0.992339295357
0.6	0.994127727340
0.7	0.995714002160
0.8	0.997132661462
0.9	0.998416346970
0.95	0.999025043655
0.98	0.999399087058

(c) Von Neumann Entropy
 $S(J_z, l)$ from numerical
data.

J_z	S
0.5	0.036466907924
0.6	0.029050441639
0.7	0.022156694159
0.8	0.015641641310
0.9	0.009310347139
0.95	0.006070799703
0.98	0.003950623534

(d) Von Neumann Entropy
 $S(J_z, l)$ from the exact for-
mula.

J_z	S
0.5	0.036466907925
0.6	0.029050441639
0.7	0.022156694159
0.8	0.015641641306
0.9	0.009310347134
0.95	0.006070799703
0.98	0.003950623538

Table C.7: $l = 0.4$ entanglement spectrum.

$J_y = 2.2220487$ $J_z = 0.5$	$J_y = 2.0880613$ $J_z = 0.6$
$9.961622554925 \cdot 10^{-01}$	$9.970595278442 \cdot 10^{-01}$
$3.822960135817 \cdot 10^{-03}$	$2.931800504524 \cdot 10^{-03}$
$1.467132900076 \cdot 10^{-05}$	$8.620803425263 \cdot 10^{-06}$
$5.630397998235 \cdot 10^{-08}$	$2.534900971208 \cdot 10^{-08}$
$5.630396895427 \cdot 10^{-08}$	$2.534900551681 \cdot 10^{-08}$
$2.160767128637 \cdot 10^{-10}$	$7.453701390712 \cdot 10^{-11}$
$2.160650072096 \cdot 10^{-10}$	$7.453146469155 \cdot 10^{-11}$
$8.291186369418 \cdot 10^{-13}$	$2.191308968230 \cdot 10^{-13}$
$8.290538029931 \cdot 10^{-13}$	$2.190916077495 \cdot 10^{-13}$
$8.288295325350 \cdot 10^{-13}$	$2.189705577742 \cdot 10^{-13}$
$3.302762641646 \cdot 10^{-15}$	$1.183995157659 \cdot 10^{-15}$
$3.227250135354 \cdot 10^{-15}$	$1.092868781349 \cdot 10^{-15}$
$3.214457083321 \cdot 10^{-15}$	
$3.176086051042 \cdot 10^{-15}$	
$J_y = 1.9176809$ $J_z = 0.7$	$J_y = 1.7$ $J_z = 0.8$
$9.978546949978 \cdot 10^{-01}$	$9.985653000769 \cdot 10^{-01}$
$2.140692837682 \cdot 10^{-03}$	$1.432638614902 \cdot 10^{-03}$
$4.592417963133 \cdot 10^{-06}$	$2.055402290997 \cdot 10^{-06}$
$9.852086920929 \cdot 10^{-09}$	$2.948865651242 \cdot 10^{-09}$
$9.852080324518 \cdot 10^{-09}$	$2.948857497220 \cdot 10^{-09}$
$2.113539697132 \cdot 10^{-11}$	$4.230533233792 \cdot 10^{-12}$
$2.113406695691 \cdot 10^{-11}$	$4.230280213367 \cdot 10^{-12}$
$4.529126900855 \cdot 10^{-14}$	$6.129311827700 \cdot 10^{-15}$
$4.513596095192 \cdot 10^{-14}$	$6.092005240754 \cdot 10^{-15}$
$4.495545450041 \cdot 10^{-14}$	$5.812802086164 \cdot 10^{-15}$
$1.126674743995 \cdot 10^{-15}$	$1.066647490466 \cdot 10^{-15}$
$1.041978269571 \cdot 10^{-15}$	

C. Numerical data

$J_y = 1.4133294$ $J_z = 0.9$	$J_y = 1.2295833$ $J_z = 0.95$	$J_y = 1.0990450$ $J_z = 0.98$
$9.992078594938 \cdot 10^{-01}$	$9.995124028940 \cdot 10^{-01}$	$9.996994981474 \cdot 10^{-01}$
$7.915125235778 \cdot 10^{-04}$	$4.873592393429 \cdot 10^{-04}$	$3.004110895427 \cdot 10^{-04}$
$6.269887336760 \cdot 10^{-07}$	$2.376348926239 \cdot 10^{-07}$	$9.027389696354 \cdot 10^{-08}$
$4.966597917868 \cdot 10^{-10}$	$1.158689931863 \cdot 10^{-10}$	$2.712624487109 \cdot 10^{-11}$
$4.966562765108 \cdot 10^{-10}$	$1.158665573207 \cdot 10^{-10}$	$2.712208599514 \cdot 10^{-11}$
$3.933175030477 \cdot 10^{-13}$	$5.636367946705 \cdot 10^{-14}$	$8.201008467041 \cdot 10^{-15}$
$3.931925349418 \cdot 10^{-13}$	$5.632120798273 \cdot 10^{-14}$	$7.804607993945 \cdot 10^{-15}$
$1.686352084125 \cdot 10^{-15}$	$1.241852454706 \cdot 10^{-15}$	$1.166710551867 \cdot 10^{-15}$
$1.539495830403 \cdot 10^{-15}$	$1.028671542729 \cdot 10^{-15}$	$1.033782687658 \cdot 10^{-15}$
$1.076733444892 \cdot 10^{-15}$		

Table C.8: $l = 0.45$

(a) J_z and J_y values for simulation

J_z	J_y
0.5	1.9883922
0.6	1.8762979
0.7	1.7345081
0.8	1.5549205
0.9	1.3222222
0.95	1.1764274
0.98	1.0751537

(b) Schimdt gap as a function of J_z .

J_z	S
0.5	0.989911349885
0.6	0.992222020234
0.7	0.994275206310
0.8	0.996115791867
0.9	0.997789055296
0.95	0.998590329137
0.98	0.999091134481

(c) Von Neumann Entropy $S(J_z, l)$ from numerical data.

J_z	S
0.5	0.046086065287
0.6	0.036942408348
0.7	0.028423477633
0.8	0.020350684902
0.9	0.012470791065
0.95	0.008404969492
0.98	0.005705035306

(d) Von Neumann Entropy $S(J_z, l)$ from the exact formula.

J_z	S
0.5	0.046086065289
0.6	0.036942408349
0.7	0.028423477633
0.8	0.020350684901
0.9	0.012470791054
0.95	0.008404969494
0.98	0.005705035309

Table C.9: $l = 0.45$ entanglement spectrum.

$J_y = 1.9883922$ $J_z = 0.5$	$J_y = 1.8762979$ $J_z = 0.6$
$9.949428234119 \cdot 10^{-01}$	$9.961033889771 \cdot 10^{-01}$
$5.031473526758 \cdot 10^{-03}$	$3.881368742800 \cdot 10^{-03}$
$2.544440266064 \cdot 10^{-05}$	$1.512395547718 \cdot 10^{-05}$
$1.286735510126 \cdot 10^{-07}$	$5.893127259518 \cdot 10^{-08}$
$1.286735229992 \cdot 10^{-07}$	$5.893126438684 \cdot 10^{-08}$
$6.507061662705 \cdot 10^{-10}$	$2.296283674744 \cdot 10^{-10}$
$6.506959436862 \cdot 10^{-10}$	$2.296125219709 \cdot 10^{-10}$
$3.290303618027 \cdot 10^{-12}$	$8.946081001084 \cdot 10^{-13}$
$3.290048656720 \cdot 10^{-12}$	$8.945446654387 \cdot 10^{-13}$
$3.288951348558 \cdot 10^{-12}$	$8.941882998576 \cdot 10^{-13}$
$1.666823245044 \cdot 10^{-14}$	$3.592287370945 \cdot 10^{-15}$
$1.656560935294 \cdot 10^{-14}$	$3.513354380212 \cdot 10^{-15}$
$1.651195975213 \cdot 10^{-14}$	$3.483055467363 \cdot 10^{-15}$
$1.635335272919 \cdot 10^{-14}$	$3.452257071555 \cdot 10^{-15}$
$1.100986948690 \cdot 10^{-15}$	$1.259353421478 \cdot 10^{-15}$
$J_y = 1.7345081$ $J_z = 0.7$	$J_y = 1.5549205$ $J_z = 0.8$
$9.971334829858 \cdot 10^{-01}$	$9.980560027119 \cdot 10^{-01}$
$2.858276675630 \cdot 10^{-03}$	$1.940210844783 \cdot 10^{-03}$
$8.193231587479 \cdot 10^{-06}$	$3.771750395338 \cdot 10^{-06}$
$2.348584194880 \cdot 10^{-08}$	$7.332242644488 \cdot 10^{-09}$
$2.348583818047 \cdot 10^{-08}$	$7.332235102405 \cdot 10^{-09}$
$6.732163303422 \cdot 10^{-11}$	$1.425368281414 \cdot 10^{-11}$
$6.731645513891 \cdot 10^{-11}$	$1.425273955645 \cdot 10^{-11}$
$1.929120540914 \cdot 10^{-13}$	$2.770648493557 \cdot 10^{-14}$
$1.928921816871 \cdot 10^{-13}$	$2.765574578027 \cdot 10^{-14}$
$1.927627131534 \cdot 10^{-13}$	$2.749995745531 \cdot 10^{-14}$
$1.165291681496 \cdot 10^{-15}$	$1.232206770708 \cdot 10^{-15}$
$1.064852930109 \cdot 10^{-15}$	

C. Numerical data

$J_y = 1.3222222$ $J_z = 0.9$	$J_y = 1.1764274$ $J_z = 0.95$	$J_y = 1.0751537$ $J_z = 0.98$
$9.988939152620 \cdot 10^{-01}$	$9.992949158187 \cdot 10^{-01}$	$9.995454614904 \cdot 10^{-01}$
$1.104859965584 \cdot 10^{-03}$	$7.045866813828 \cdot 10^{-04}$	$4.543270094637 \cdot 10^{-04}$
$1.222067246410 \cdot 10^{-06}$	$4.967926541793 \cdot 10^{-07}$	$2.065068437844 \cdot 10^{-07}$
$1.351695785930 \cdot 10^{-09}$	$3.502777874374 \cdot 10^{-10}$	$9.386380784400 \cdot 10^{-11}$
$1.351672285343 \cdot 10^{-09}$	$3.502644583469 \cdot 10^{-10}$	$9.385442559898 \cdot 10^{-11}$
$1.495097912390 \cdot 10^{-12}$	$2.467604561651 \cdot 10^{-13}$	$4.253642235830 \cdot 10^{-14}$
$1.494289554576 \cdot 10^{-12}$	$2.459143096335 \cdot 10^{-13}$	$4.205163741897 \cdot 10^{-14}$
$2.076479470705 \cdot 10^{-15}$	$1.527917692312 \cdot 10^{-15}$	$1.085230073819 \cdot 10^{-15}$
$1.757506452574 \cdot 10^{-15}$	$1.284035410656 \cdot 10^{-15}$	
$1.663862761799 \cdot 10^{-15}$		

Table C.10: $l = 0.5$

(a) J_z and J_y values for simulation		(b) Schimdt gap as a function of J_z .	
J_z	J_y	J_z	S
0.5	1.8027756	0.5	0.986957398455
0.6	1.7008007	0.6	0.989739720936
0.7	1.5905973	0.7	0.992482335847
0.8	1.4422205	0.8	0.994822301380
0.9	1.2529964	0.9	0.996961709197
0.95	1.1368817	0.95	0.997997670619
0.98	1.0577334	0.98	0.998656427614

(c) Von Neumann Entropy $S(J_z, l)$ from numerical data.		(d) Von Neumann Entropy $S(J_z, l)$ from the exact formula.	
J_z	S	J_z	S
0.5	0.057261457250	0.5	0.057261457258
0.6	0.046749794225	0.6	0.046749794230
0.7	0.035885277318	0.7	0.035885277318
0.8	0.026074132763	0.8	0.026074132763
0.9	0.016448944937	0.9	0.016448944913
0.95	0.011435840724	0.95	0.011435840714
0.98	0.008056897255	0.98	0.008056897276

Table C.11: $l = 0.5$ entanglement spectrum.

$J_y = 1.8027756$ $J_z = 0.5$	$J_y = 1.7008007$ $J_z = 0.6$
$9.934571566189 \cdot 10^{-01}$	$9.948565656764 \cdot 10^{-01}$
$5.031473526758 \cdot 10^{-03}$	$3.881368742800 \cdot 10^{-03}$
$2.544440266064 \cdot 10^{-05}$	$1.512395547718 \cdot 10^{-05}$
$1.286735510126 \cdot 10^{-07}$	$5.893127259518 \cdot 10^{-08}$
$1.286735229992 \cdot 10^{-07}$	$5.893126438684 \cdot 10^{-08}$
$6.507061662705 \cdot 10^{-10}$	$2.296283674744 \cdot 10^{-10}$
$6.506959436862 \cdot 10^{-10}$	$2.296125219709 \cdot 10^{-10}$
$3.290303618027 \cdot 10^{-12}$	$8.946081001084 \cdot 10^{-13}$
$3.290048656720 \cdot 10^{-12}$	$8.945446654387 \cdot 10^{-13}$
$3.288951348558 \cdot 10^{-12}$	$8.941882998576 \cdot 10^{-13}$
$1.666823245044 \cdot 10^{-14}$	$3.592287370945 \cdot 10^{-15}$
$1.656560935294 \cdot 10^{-14}$	$3.513354380212 \cdot 10^{-15}$
$1.651195975213 \cdot 10^{-14}$	$3.483055467363 \cdot 10^{-15}$
$1.635335272919 \cdot 10^{-14}$	$3.452257071555 \cdot 10^{-15}$
$1.100986948690 \cdot 10^{-15}$	$1.259353421478 \cdot 10^{-15}$
$J_y = 1.5905974$ $J_z = 0.7$	$J_y = 1.4422205$ $J_z = 0.8$
$9.962340502308e \cdot 10^{-01}$	$9.974077822292 \cdot 10^{-01}$
$2.858276675630 \cdot 10^{-03}$	$1.940210844783 \cdot 10^{-03}$
$8.193231587479 \cdot 10^{-06}$	$3.771750395338 \cdot 10^{-06}$
$2.348584194880 \cdot 10^{-08}$	$7.332242644488 \cdot 10^{-09}$
$2.348583818047 \cdot 10^{-08}$	$7.332235102405 \cdot 10^{-09}$
$6.732163303422 \cdot 10^{-11}$	$1.425368281414 \cdot 10^{-11}$
$6.731645513891 \cdot 10^{-11}$	$1.425273955645 \cdot 10^{-11}$
$1.929120540914 \cdot 10^{-13}$	$2.770648493557 \cdot 10^{-14}$
$1.928921816871 \cdot 10^{-13}$	$2.765574578027 \cdot 10^{-14}$
$1.927627131534 \cdot 10^{-13}$	$2.749995745531 \cdot 10^{-14}$
$1.165291681496 \cdot 10^{-15}$	$1.232206770708 \cdot 10^{-15}$
$1.064852930109 \cdot 10^{-15}$	

C. Numerical data

$J_y = 1.2529964$ $J_z = 0.9$	$J_y = 1.1368817$ $J_z = 0.95$	$J_y = 1.0577334$ $J_z = 0.98$
$9.984796971875 \cdot 10^{-01}$	$9.989983330885 \cdot 10^{-01}$	$9.993279694942 \cdot 10^{-01}$
$1.104859965584 \cdot 10^{-03}$	$7.045866813828 \cdot 10^{-04}$	$4.543270094637 \cdot 10^{-04}$
$1.222067246410 \cdot 10^{-06}$	$4.967926541793 \cdot 10^{-07}$	$2.065068437844 \cdot 10^{-07}$
$1.351695785930 \cdot 10^{-09}$	$3.502777874374 \cdot 10^{-10}$	$9.386380784400 \cdot 10^{-11}$
$1.351672285343 \cdot 10^{-09}$	$3.502644583469 \cdot 10^{-10}$	$9.385442559898 \cdot 10^{-11}$
$1.495097912390 \cdot 10^{-12}$	$2.467604561651 \cdot 10^{-13}$	$4.253642235830 \cdot 10^{-14}$
$1.494289554576 \cdot 10^{-12}$	$2.459143096335 \cdot 10^{-13}$	$4.205163741897 \cdot 10^{-14}$
$2.076479470705 \cdot 10^{-15}$	$1.527917692312 \cdot 10^{-15}$	$1.085230073819 \cdot 10^{-15}$
$1.757506452574 \cdot 10^{-15}$	$1.284035410656 \cdot 10^{-15}$	
$1.663862761799 \cdot 10^{-15}$		

Table C.12: $l = 0.6$

(a) J_z and J_y values for simulation

J_z	J_y
0.5	1.5275252
0.6	1.5275252
0.7	1.3808210
0.8	1.2806248
0.9	1.1566234
0.95	1.0832051
0.98	1.0346013

(b) Schimdt gap as a function of J_z .

J_z	S
0.5	0.978936153343
0.6	0.983408828653
0.7	0.987416103248
0.8	0.991048176714
0.9	0.994418085799
0.95	0.996092126131
0.98	0.997193269529

(c) Von Neumann Entropy $S(J_z, l)$ from numerical data.

J_z	S
0.5	0.085593499917
0.6	0.070103300982
0.7	0.055558246072
0.8	0.041638245770
0.9	0.027813561503
0.95	0.020457791044
0.98	0.015348864455

(d) Von Neumann Entropy $S(J_z, l)$ from the exact formula.

J_z	S
0.5	0.085593500056
0.6	0.070103301050
0.7	0.055558246080
0.8	0.041638245770
0.9	0.027813561502
0.95	0.020457791042
0.98	0.015348864911

C.3. Simulations around the circles

Table C.13: $l = 0.6$ entanglement spectrum.

$J_y = 1.5275252$ $J_z = 0.5$	$J_y = 1.4621141$ $J_z = 0.6$
9.894114364211 · 10 ⁻⁰¹	9.916694308714 · 10 ⁻⁰¹
1.047528307852 · 10 ⁻⁰²	8.260602218392 · 10 ⁻⁰³
1.109058875745 · 10 ⁻⁰⁴	6.881078142452 · 10 ⁻⁰⁵
1.174202965767 · 10 ⁻⁰⁶	5.731933051471 · 10 ⁻⁰⁷
1.174202275905 · 10 ⁻⁰⁶	5.731930325391 · 10 ⁻⁰⁷
1.243157412417 · 10 ⁻⁰⁸	4.774623043901 · 10 ⁻⁰⁹
1.243121450238 · 10 ⁻⁰⁸	4.774522878739 · 10 ⁻⁰⁹
1.315288692702 · 10 ⁻¹⁰	3.975001527535 · 10 ⁻¹¹
1.315163007884 · 10 ⁻¹⁰	3.974539777383 · 10 ⁻¹¹
1.314337781050 · 10 ⁻¹⁰	3.973613275351 · 10 ⁻¹¹
1.391422790559 · 10 ⁻¹²	3.307951448204 · 10 ⁻¹³
1.388900142074 · 10 ⁻¹²	3.299048004016 · 10 ⁻¹³
1.385367107157 · 10 ⁻¹²	3.289507383443 · 10 ⁻¹³
1.378581361617 · 10 ⁻¹²	3.283929044340 · 10 ⁻¹³
1.448429323560 · 10 ⁻¹⁴	2.882063188926 · 10 ⁻¹⁵
1.443068554062 · 10 ⁻¹⁴	2.761445848185 · 10 ⁻¹⁵
1.398654917759 · 10 ⁻¹⁴	2.702644910514 · 10 ⁻¹⁵
1.378848851191 · 10 ⁻¹⁴	2.560610080195 · 10 ⁻¹⁵
1.181408216888 · 10 ⁻¹⁴	2.365066363748 · 10 ⁻¹⁵
1.101291556910 · 10 ⁻¹⁵	1.101291556910 · 10 ⁻¹⁵
$J_y = 1.3808210$ $J_z = 0.7$	$J_y = 1.2806248$ $J_z = 0.8$
9.936880068405 · 10 ⁻⁰¹	9.955139814368 · 10 ⁻⁰¹
6.271903592402 · 10 ⁻⁰³	4.465804722463 · 10 ⁻⁰³
3.958664525370 · 10 ⁻⁰⁵	2.003328147817 · 10 ⁻⁰⁵
2.498606844544 · 10 ⁻⁰⁷	8.986786276503 · 10 ⁻⁰⁸
2.498605980016 · 10 ⁻⁰⁷	8.986778680528 · 10 ⁻⁰⁸
1.577045995091 · 10 ⁻⁰⁹	4.031321542321 · 10 ⁻¹⁰
1.577033354227 · 10 ⁻⁰⁹	4.031196253264 · 10 ⁻¹⁰
9.950848457898 · 10 ⁻¹²	1.807986064053 · 10 ⁻¹²
9.946188316285 · 10 ⁻¹²	1.805969758786 · 10 ⁻¹²
9.944936784662 · 10 ⁻¹²	1.804812588495 · 10 ⁻¹²
6.269193126165 · 10 ⁻¹⁴	8.144327269268 · 10 ⁻¹⁵
6.252917825388 · 10 ⁻¹⁴	8.001642400590 · 10 ⁻¹⁵
6.247281353138 · 10 ⁻¹⁴	7.923541796429 · 10 ⁻¹⁵
6.210595770850 · 10 ⁻¹⁴	7.783237084407 · 10 ⁻¹⁵
1.066671190300 · 10 ⁻¹⁵	1.256211649377 · 10 ⁻¹⁵
1.027482821941 · 10 ⁻¹⁵	1.027482821941 · 10 ⁻¹⁵

C. Numerical data

$J_y = 1.1566234$ $J_z = 0.9$	$J_y = 1.0832051$ $J_z = 0.95$	$J_y = 1.0346014$ $J_z = 0.98$
$9.972051262866 \cdot 10^{-01}$	$9.980441415455 \cdot 10^{-01}$	$9.985951373483 \cdot 10^{-01}$
$2.787040488049 \cdot 10^{-03}$	$1.952015414536 \cdot 10^{-03}$	$1.401867818848 \cdot 10^{-03}$
$7.789364986407 \cdot 10^{-06}$	$3.817831283572 \cdot 10^{-06}$	$1.967995752375 \cdot 10^{-06}$
$2.177011358389 \cdot 10^{-08}$	$7.467065646671 \cdot 10^{-09}$	$2.762697880055 \cdot 10^{-09}$
$2.177009158659 \cdot 10^{-08}$	$7.466910540514 \cdot 10^{-09}$	$2.761540041283 \cdot 10^{-09}$
$6.084137238369 \cdot 10^{-11}$	$1.460392636017 \cdot 10^{-11}$	$3.878975338704 \cdot 10^{-12}$
$6.083986200895 \cdot 10^{-11}$	$1.460197038788 \cdot 10^{-11}$	$3.866218923669 \cdot 10^{-12}$
$1.696844061248 \cdot 10^{-13}$	$2.844642271624 \cdot 10^{-14}$	$5.335418400126 \cdot 10^{-15}$
$1.692667244087 \cdot 10^{-13}$	$2.824332864223 \cdot 10^{-14}$	$4.421481089779 \cdot 10^{-15}$
$1.676653119160 \cdot 10^{-13}$	$2.634910984739 \cdot 10^{-14}$	$1.030127608893 \cdot 10^{-15}$
$1.640253294719 \cdot 10^{-15}$	$1.067513977102 \cdot 10^{-15}$	
$1.169062738101 \cdot 10^{-15}$		

Table C.14: $l = 0.7$

(a) J_z and J_y values for simulation

J_z	J_y
0.5	1.3343958
0.6	1.2907836
0.7	1.2307837
0.8	1.1724734
0.9	1.0944200
0.95	1.0495140
0.98	1.0204001

(b) Schimdt gap as a function of J_z .

J_z	S
0.5	0.966550030413
0.6	0.973168128626
0.7	0.979149383523
0.8	0.984634250478
0.9	0.989823874642
0.95	0.992478629130
0.98	0.994273426958

(c) Von Neumann Entropy $S(J_z, l)$ from numerical data.

J_z	S
0.5	0.125660655013
0.6	0.104690856436
0.7	0.084869957704
0.8	0.065731010764
0.9	0.046424509528
0.95	0.035897741561
0.98	0.028365564586

(d) Von Neumann Entropy $S(J_z, l)$ from the exact formula.

J_z	S
0.5	0.125660657866
0.6	0.104690857496
0.7	0.084869936795
0.8	0.065731010809
0.9	0.046424509533
0.95	0.03589774157
0.98	0.02836555636

Table C.15: $l = 0.7$ entanglement spectrum.

$J_y = 1.3343958$ $J_z = 0.5$	$J_y = 1.2907837$ $J_z = 0.6$
$9.831296568968 \cdot 10^{-01}$	$9.864916108747 \cdot 10^{-01}$
$1.657962648369 \cdot 10^{-02}$	$1.332348224849 \cdot 10^{-02}$
$2.796005039061 \cdot 10^{-04}$	$1.799459376832 \cdot 10^{-04}$
$4.715191452217 \cdot 10^{-06}$	$2.430330839314 \cdot 10^{-06}$
$4.715179631467 \cdot 10^{-06}$	$2.430323122390 \cdot 10^{-06}$
$7.951446139730 \cdot 10^{-08}$	$3.282225512440 \cdot 10^{-08}$
$7.950376571850 \cdot 10^{-08}$	$3.281607874690 \cdot 10^{-08}$
$1.338552392480 \cdot 10^{-09}$	$4.426578863841 \cdot 10^{-10}$
$1.337775725778 \cdot 10^{-09}$	$4.423405340038 \cdot 10^{-10}$
$1.336512880107 \cdot 10^{-09}$	$4.420894303105 \cdot 10^{-10}$
$2.253191380502 \cdot 10^{-11}$	$5.960140429232 \cdot 10^{-12}$
$2.243414875683 \cdot 10^{-11}$	$5.931080676299 \cdot 10^{-12}$
$2.231616133352 \cdot 10^{-11}$	$5.868804645602 \cdot 10^{-12}$
$2.172088861992 \cdot 10^{-11}$	$5.542801482664 \cdot 10^{-12}$
$3.682638141387 \cdot 10^{-13}$	$7.835367645201 \cdot 10^{-14}$
$3.645046952995 \cdot 10^{-13}$	$7.622385122664 \cdot 10^{-14}$
$3.445858752500 \cdot 10^{-13}$	$7.038442798378 \cdot 10^{-14}$
$3.335553660803 \cdot 10^{-13}$	$6.892833188857 \cdot 10^{-14}$
$2.854555380192 \cdot 10^{-13}$	$6.372006793749 \cdot 10^{-14}$
$6.189419079311 \cdot 10^{-15}$	$1.624682579609 \cdot 10^{-15}$
$5.861904932748 \cdot 10^{-15}$	$1.329368786890 \cdot 10^{-15}$
$5.320737390903 \cdot 10^{-15}$	$1.226513533030 \cdot 10^{-15}$
$4.644028724437 \cdot 10^{-15}$	$1.055629801461 \cdot 10^{-15}$
$3.606257376956 \cdot 10^{-15}$	
$2.685535888280 \cdot 10^{-15}$	

C. Numerical data

$J_y = 1.2372616$ $J_z = 0.7$	$J_y = 1.1724734$ $J_z = 0.8$
$9.895192032876 \cdot 10^{-01}$	$9.922871541645 \cdot 10^{-01}$
$1.036981976427 \cdot 10^{-02}$	$7.652903686917 \cdot 10^{-03}$
$1.086721306049 \cdot 10^{-04}$	$5.902216298931 \cdot 10^{-05}$
$1.138845828824 \cdot 10^{-06}$	$4.552017664292 \cdot 10^{-07}$
$1.138842497468 \cdot 10^{-06}$	$4.552016763553 \cdot 10^{-07}$
$1.193451258575 \cdot 10^{-08}$	$3.510619821723 \cdot 10^{-09}$
$1.193403149078 \cdot 10^{-08}$	$3.510500586897 \cdot 10^{-09}$
$1.249718032540 \cdot 10^{-10}$	$2.706529127291 \cdot 10^{-11}$
$1.248057078748 \cdot 10^{-10}$	$2.706061419488 \cdot 10^{-11}$
$1.247406660143 \cdot 10^{-10}$	$2.699940350733 \cdot 10^{-11}$
$1.303719187720 \cdot 10^{-12}$	$2.080315773445 \cdot 10^{-13}$
$1.296660713881 \cdot 10^{-12}$	$2.066680101866 \cdot 10^{-13}$
$1.293839811332 \cdot 10^{-12}$	$2.051808792497 \cdot 10^{-13}$
$1.275460119601 \cdot 10^{-12}$	$2.008326080823 \cdot 10^{-13}$
$1.335936891060 \cdot 10^{-14}$	$1.778607640279 \cdot 10^{-15}$
$1.293735626207 \cdot 10^{-14}$	$1.739096258223 \cdot 10^{-15}$
$1.244754347454 \cdot 10^{-14}$	$1.674502168523 \cdot 10^{-15}$
$1.060571232444 \cdot 10^{-14}$	$1.566276156328 \cdot 10^{-15}$
$1.044273775056 \cdot 10^{-14}$	$1.410694278584 \cdot 10^{-15}$

$J_y = 1.0944200$ $J_z = 0.9$	$J_y = 1.0495140$ $J_z = 0.95$	$J_y = 1.0204001$ $J_z = 0.98$
$9.948988497066 \cdot 10^{-01}$	$9.962318679854 \cdot 10^{-01}$	$9.971249273000 \cdot 10^{-01}$
$5.074975065089 \cdot 10^{-03}$	$3.753238855869 \cdot 10^{-03}$	$2.851500341546 \cdot 10^{-03}$
$2.588742695534 \cdot 10^{-05}$	$1.414007379298 \cdot 10^{-05}$	$8.154372603602 \cdot 10^{-06}$
$1.320516908617 \cdot 10^{-07}$	$5.327183810878 \cdot 10^{-08}$	$2.331943545124 \cdot 10^{-08}$
$1.320511253743 \cdot 10^{-07}$	$5.327111677679 \cdot 10^{-08}$	$2.331863788055 \cdot 10^{-08}$
$6.735534359265 \cdot 10^{-10}$	$2.006858483946 \cdot 10^{-10}$	$6.668043891079 \cdot 10^{-11}$
$6.734996209253 \cdot 10^{-10}$	$2.006249046052 \cdot 10^{-10}$	$6.663472375819 \cdot 10^{-11}$
$3.435508329811 \cdot 10^{-12}$	$7.532220278431 \cdot 10^{-13}$	$1.904804928343 \cdot 10^{-13}$
$3.422959223799 \cdot 10^{-12}$	$7.467872179098 \cdot 10^{-13}$	$1.866852907652 \cdot 10^{-13}$
$3.417085354369 \cdot 10^{-12}$	$7.436498589340 \cdot 10^{-13}$	$1.842782773708 \cdot 10^{-13}$
$1.723824122505 \cdot 10^{-14}$	$2.799672543455 \cdot 10^{-15}$	$1.074447694899 \cdot 10^{-15}$
$1.654321141274 \cdot 10^{-14}$	$2.496918238966 \cdot 10^{-15}$	
$1.565786889779 \cdot 10^{-14}$	$2.228639310547 \cdot 10^{-15}$	
$1.471545345651 \cdot 10^{-14}$	$1.576338027746 \cdot 10^{-15}$	

Table C.16: $r = 0.04$: values for simulations.

α/π	J_y	J_z
1/48	1.002616125169	0.9600856431
2/48	1.005221047689	0.9603422055
3/48	1.007803612881	0.9607685888
4/48	1.0103527618	0.9613629669
5/48	1.01285757861	0.9621227948
6/48	1.01530733729	0.9630448187
7/48	1.01769154761	0.9641250903
8/48	1.02	0.9653589838
9/48	1.02222280932	0.9667412155
10/48	1.02435045716	0.9682658664
11/48	1.0263738326	0.9699264077
12/48	1.02828427125	0.9717157288
13/48	1.0300735923	0.9736261674
14/48	1.03173413361	0.9756495428
15/48	1.03325878449	0.9777771907
16/48	1.03464101615	0.98
17/48	1.03587490966	0.9823084524
18/48	1.0369551813	0.9846926627
19/48	1.03787720518	0.9871424214
20/48	1.03863703305	0.9896472382
21/48	1.03923141122	0.9921963871
22/48	1.03965779445	0.9947789523
23/48	1.03991435693	0.9973838748
24/48	1.04	1

C. Numerical data

Table C.17: $r = 0.04$: Values of the entropies.

α/π	type	$S_{\text{theor.}}$	S_{DMRG}
1/48	c (180)	0.246125579330	0.246118354635
2/48	c (144)	0.171810663637	0.171809858054
3/48	c (136)	0.132950275427	0.132949973342
4/48	b (126)	0.107823585477	0.107823539042
5/48	b (92)	0.089811885516	0.089812124370
6/48	b (88)	0.076057537202	0.076057561516
7/48	b (88)	0.065086724876	0.065086676452
8/48	b (90)	0.056050650089	0.056050637384
9/48	b (88)	0.048422100970	0.048422091959
10/48	a	0.041855187031	0.041855190188
11/48	a	0.036113531221	0.036113532521
12/48	a	0.031030619486	0.031030620012
13/48	a	0.026486614752	0.026486615016
14/48	a	0.022394204904	0.022394204970
15/48	a	0.018689719261	0.018689719351
16/48	a	0.015327503342	0.015327502988
17/48	a	0.012276454800	0.012276454666
18/48	a	0.009518146370	0.009518146313
19/48	a	0.007046304431	0.007046304418
20/48	a	0.004867729808	0.004867729812
21/48	a	0.003005190546	0.003005190549
22/48	a	0.001503795125	0.001503795131
23/48	a	0.000445582680	0.000445582504
24/48	a	0	0.000000000000

Table C.18: $r = 0.03$: values for simulations.

α/π	J_y	J_z
1/48	1.001962093877	0.9700642323
2/48	1.003915785767	0.9702566542
3/48	1.00585270966	0.9705764416
4/48	1.007764571353	0.9710222252
5/48	1.009643183959	0.9715920961
6/48	1.01148050297	0.972283614
7/48	1.01326866071	0.9730938178
8/48	1.015	0.9740192379
9/48	1.01666710699	0.9750559116
10/48	1.01826284287	0.9761993998
11/48	1.01978037445	0.9774448058
12/48	1.02121320344	0.9787867966
13/48	1.02255519422	0.9802196255
14/48	1.02380060021	0.9817371571
15/48	1.02494408837	0.983332893
16/48	1.02598076211	0.985
17/48	1.02690618225	0.9867313393
18/48	1.02771638598	0.988519497
19/48	1.02840790388	0.990356816
20/48	1.02897777479	0.9922354286
21/48	1.02942355841	0.9941472903
22/48	1.02974334584	0.9960842142
23/48	1.0299357677	0.9980379061
24/48	1.03	1

C. Numerical data

Table C.19: $r = 0.03$: Values of the entropies.

α/π	type	$S_{\text{theor.}}$	S_{DMRG}
1/48	c (186)	0.238108317085	0.238108886334
2/48	c (166)	0.165415130137	0.165413840331
3/48	b (156)	0.127547618706	0.127547360711
4/48	b (114)	0.103143815107	0.103144060800
5/48	b (104)	0.085704006231	0.085704003142
6/48	b (104)	0.072425388065	0.072425260363
7/48	b (96)	0.061863931007	0.061863957500
8/48	b (104)	0.053188706166	0.053188680546
9/48	b (96)	0.045883943986	0.045883946226
10/48	b (102)	0.039611412342	0.039611387625
11/48	b (96)	0.034140011525	0.034140002077
12/48	b (88)	0.029306922072	0.029306921755
13/48	a	0.024994897824	0.024994900918
14/48	a	0.021118410843	0.021118412466
15/48	a	0.017614954662	0.017614954953
16/48	a	0.014439531216	0.014439531357
17/48	a	0.011561248019	0.011561248171
18/48	a	0.008961456674	0.008961456798
19/48	a	0.006633202072	0.006633202173
20/48	a	0.004582055658	0.004582055685
21/48	a	0.002828828669	0.002828828720
22/48	a	0.001415586340	0.001415586375
23/48	a	0.000419424084	0.000419423689
24/48	a	0	0

Table C.20: $r = 0.02$: values for simulations.

α/π	J_y	J_z
1/48	1.001308062585	0.9800428215
2/48	1.002610523844	0.9801711028
3/48	1.00390180644	0.9803842944
4/48	1.005176380902	0.9806814835
5/48	1.006428789306	0.9810613974
6/48	1.007653668647	0.9815224093
7/48	1.008845773804	0.9820625452
8/48	1.01	0.9826794919
9/48	1.01111140466	0.9833706078
10/48	1.01217522858	0.9841329332
11/48	1.0131869163	0.9849632039
12/48	1.01414213562	0.9858578644
13/48	1.01503679615	0.9868130837
14/48	1.01586706681	0.9878247714
15/48	1.01662939225	0.9888885953
16/48	1.01732050808	0.99
17/48	1.01793745483	0.9911542262
18/48	1.01847759065	0.9923463314
19/48	1.01893860259	0.9935712107
20/48	1.01931851653	0.9948236191
21/48	1.01961570561	0.9960981936
22/48	1.01982889723	0.9973894762
23/48	1.01995717846	0.9986919374
24/48	1.02	1

C. Numerical data

Table C.21: $r = 0.02$: Values of the entropies.

α/π	type	$S_{\text{theor.}}$	S_{DMRG}
1/48	<i>c</i> (210)	0.228859204209	0.228866288713
2/48	<i>c</i> (196)	0.158056446596	0.158055094877
3/48	<i>b</i> (142)	0.121344050136	0.121344993672
4/48	<i>b</i> (140)	0.097779189906	0.097779097234
5/48	<i>b</i> (128)	0.081001414425	0.081001206766
6/48	<i>b</i> (120)	0.068272162287	0.068272029391
7/48	<i>b</i> (128)	0.058182329410	0.058182274384
8/48	<i>b</i> (114)	0.049921957210	0.049922003174
9/48	<i>b</i> (116)	0.042988718020	0.042988724461
10/48	<i>b</i> (112)	0.037053390331	0.037053375719
11/48	<i>b</i> (112)	0.031891093262	0.031891082204
12/48	<i>b</i> (106)	0.027343373370	0.027343371429
13/48	<i>b</i> (98)	0.023296056905	0.023296066110
14/48	<i>b</i> (106)	0.019665744513	0.019665741756
15/48	<i>b</i> (100)	0.016391331377	0.016391332607
16/48	<i>a</i>	0.013428628013	0.013428644089
17/48	<i>a</i>	0.010747029302	0.010747039849
18/48	<i>a</i>	0.008327672212	0.008327679276
19/48	<i>a</i>	0.006162853389	0.006162858145
20/48	<i>a</i>	0.004256762036	0.004256765029
21/48	<i>a</i>	0.002627988999	0.002627991009
22/48	<i>a</i>	0.001315131014	0.001315132137
23/48	<i>a</i>	0.000389638509	0.000389637826
24/48	<i>a</i>	0	0.000000000000

Bibliography

- [1] I. Affleck, A. Ludwig. *Universal non-integer “ground-state degeneracy” in critical quantum systems*. Phys. Rev. Lett. 67 161, 1991.
- [2] V. Alba, M. Haque and A. M. Laeuchli. *Boundary-locality and perturbative structure of entanglement spectra in gapped systems*. Phys. Rev. Lett. 108, 227201 (2012).
- [3] R. J. Baxter. *Exactly Solved Models in Statistical Mechanics*. Dover Publications, 2007.
- [4] D. Bianchini. *Entanglement entropy in restricted integrable spin-chains* - Master thesis.
- [5] J. Cardy. *Scaling and Renormalization in Statistical Physics*, Cambridge University Press, 1996.
- [6] J. Cardy. *Conformal Field Theory and Statistical Mechanics*. les Houches, July 2008.
- [7] J. Cardy and P. Calabrese. *Entanglement entropy and quantum field theory*. J. Stat. Mech. 0406:P06002, 2004.
- [8] J. Cardy and P. Calabrese. *Entanglement entropy and conformal field theory*. J. Phys. A42:504005, 2009.
- [9] J. Cardy and P. Calabrese. *Unusual Correction to Scaling in Entanglement Entropy*. J. Stat. Mech. 1004:P04023, 2010.
- [10] J. Cardy, O.A. Castro-Alvaredo and B. Doyon. *Form factors of branch-point twist fields in quantum integrable models and entanglement entropy*. J. Stat. Phys. 130:129-168, 2008.
- [11] P. Calabrese, M. Campostrini, F. Essler and B. Nienhuis. *Parity effects in the scaling of block entanglement in gapless spin chains*. Phys. Rev. Lett. 104:095701, 2010.
- [12] P. Calabrese, J. Cardy and I. Peschel. *Corrections to scaling for block entanglement in massive spin-chains*. J. Stat. Mech. 1009:P09003, 2010.

Bibliography

- [13] P. Calabrese, A. Lefevre. *Entanglement spectrum in one-dimensional systems*. Phys. Rev. A 78:032329, 2008.
- [14] G. De Chiara, L. Lepori, M. Lewenstein and A. Sanpera. *Entanglement Spectrum, Critical Exponents and Order Parameters in Quantum Spin Chains*. Phys. Rev. Lett. 109:237208, 2012.
- [15] C. Degli Esposti Boschi. *Introduzione alla Teoria dell'Informazione Quantistica* - Lecture notes. <https://www.bo.imm.cnr.it/users/degliesposti/TIQ.pdf>.
- [16] C. Degli Esposti Boschi, S. Evangelisti, E. Ercolessi, F. Ravanini. *Block Entropy of the XYZ Model: Exact Results and Numerical Study*. Talk given at the Italian Quantum Information Science Conference, Pisa, Italy, november 5-8, 2009.
- [17] P. Di Francesco, P. Mathieu and D. Senéchal. *Conformal field theory*. Springer, 1997.
- [18] A. Einstein, B. Podolsky and E. Rosen. *Can Quantum-Mechanical description of physical reality be considered complete?*. Phys. Rev. 45:777, 1935.
- [19] E. Ercolessi, S. Evangelisti, F. Franchini and F. Ravanini. *Correlation Length and Unusual Corrections to the Entanglement entropy*. Phys. Rev. B, 85 (2012).
- [20] E. Ercolessi, S. Evangelisti, F. Franchini and F. Ravanini. *Essential singularity in the Renyi entanglement entropy of the one-dimensional XYZ spin-1/2 chain*. Phys. Rev. B 83:012402, 2011.
- [21] E. Ercolessi, S. Evangelisti and F. Ravanini. *Exact entanglement entropy of the XYZ model and its sine-Gordon limit*. Phys. Lett. A 374:2101-2105, 2010.
- [22] S. Evangelisti. *Quantum Correlations in Field Theory and Integrable Systems* - Dissertation thesis. Alma Mater Studiorum Università di Bologna. Dottorato di ricerca in Fisica, 25 Ciclo. DOI 10.6092/unibo/amsdottorato/5161.
- [23] F. Franchini, A.R. Its, V. E. Korepin and L.A. Takhtajan. *Entanglement spectrum for the XY model in one dimension*. Quantum Information Processing 10: 325-341, 2011.
- [24] M. Hankel. *Conformal Invariance and Critical Phenomena*. Springer, 1999.

- [25] G. Morandi, F. Napoli, E. Ercolessi. *Statistical Mechanics: An Intermediate Course*. World Scientific, 2001.
- [26] G. Mussardo. *Statistical field theory: an introduction to exactly solved models in statistical physics*. Oxford University Press, 2010.
- [27] M. Nielsen and I. Chuang. *Quantum Computation and Quantum Information*. Cambridge University Press, 2000.
- [28] I. Peschel, M. Kaulke and O. Legeza. *Density-Matrix spectra for integrable models*. Ann. Physik (Leipzig) 8 (1999) 153.
- [29] A. Renyi. *On the measure of entropy and information*. Proceedings of the 4th Berkeley Symposium on Mathematics, Statistics and Probability, pages 547–561, 1960.
- [30] H.J. Schulz, G. Cuniberti and P. Pieri. *Fermi liquids and Luttinger liquids*. in ‘Field Theories for Low-Dimensional Condensed Matter Systems’. G. Morandi et al. Eds. Springer (2000). ISBN: 3540671773.
- [31] R. Soldati. *Introduction to Quantum Field Theory* - Lecture notes. <http://www.robertosoldati.com/archivio/news/107/primonew.pdf>.
- [32] R. Soldati. *Intermediate Quantum Field Theory* - Lecture notes. <http://www.robertosoldati.com/archivio/news/112/2semnote.pdf>.
- [33] B. Sutherland. J. Math. Phys., 11:3183, 1970.
- [34] S. R. White. *Density matrix formulation for quantum renormalization groups*. Phys. Rev. Lett. 69:2863, 1992.
- [35] S. R. White. *Density-matrix algorithms for quantum renormalization groups*. Phys. Rev. B 48:10345, 1993.
- [36] S. R. White and R. M. Noack. *Real-space quantum renormalization groups*. Phys. Rev. Lett. 68:3487, 1992.
- [37] A. B. Zamolodchikov. *“Irreversibility” of the flux of the renormalization group in a 2D field theory*. JETP Lett. 43 731, 1986.

Bibliography

Ringraziamenti

Questi ringraziamenti non sono certamente esaustivi, ma servono a ricordare le persone direttamente o indirettamente coinvolte nella realizzazione di questa tesi magistrale.

Vorrei per prima cosa ringraziare i miei relatori Francesco Ravanini ed Elisa Ercolessi, che con pazienza mi hanno guidato attraverso il meraviglioso mondo dei Sistemi Integrabili e che hanno contribuito in maniera fondamentale al compimento di questo lavoro.

Un ringraziamento va anche a tutti coloro che con i loro suggerimenti hanno contribuito anch'essi a questa tesi, tra cui Fabio Franchini, Fabio Ortolani, Davide Vodola e Piero Naldesi.

Grazie inoltre agli amici dell'ufficio di Fisica Teorica, tra cui Alessandro, Enrico e Mirko, per la compagnia e per essere sempre stati presenti nei momenti di sconforto; grazie anche a Tommaso e Stefano, per le discussioni di Fisica sempre interessanti.

Vorrei inoltre ringraziare Leonardo per avermi ospitato svariate volte in questi ultimi mesi: senza di lui questo percorso sarebbe stato certamente più difficile.

Infine, un ringraziamento speciale va alla mia famiglia, che nei momenti più difficili mi è sempre rimasta accanto e senza la quale il mio percorso universitario non sarebbe potuto esistere.